MECHANISIMS OF SIGNAL DIVERSITY IN MORMYRID ELECTRIC FISH

A Dissertation

Presented to the Faculty of the Graduate School

of Cornell University

In Partial Fulfillment of the Requirements for the Degree of

Doctor of Philosophy

by

Jason Raymond Gallant

August 2011

MECHANSIMS OF SIGNAL DIVERSITY IN MORMYRID ELECTRIC FISH

Jason Raymond Gallant, Ph. D.

Cornell University 2011

Mormyrid fishes are one of six independent lineages of vertebrates to have evolved electric organs from skeletal muscle. The physiological output of the electric organ is an electric signal called the electric organ discharge (EOD). EODs are especially diverse among mormyrids, particularly among a rapidly diverged, geographically restricted species flock *Paramormyrops*. Recent studies have implicated that EODs may be a contributing factor to the process of species divergence in *Paramormyrops.* In this dissertation, I have examined the genetic basis of differences between skeletal muscle and electric organ in mormyrids, and the population-level processes that contribute to their diverse physiological outputs of electric organs.

In Chapter 1, I provide a general overview of electric organs, with specific attention to the developmental and genetic mechanisms underlying their development. Chapter 1 concludes with a discussion of evolutionary processes responsible for signal diversification.

In Chapter 2, I describe the use of suppressive subtractive hybridization to identify genes differentially expressed in the electric organ *vs.* skeletal muscle in the mormyrid *Brienomyrus brachyistius*. This work provides a basis for future comparative work with other electric fishes.

In Chapter 3, I describe patterns of geographic variation in EOD signaling among a geographically widespread member of the *Paramormyrops* species flock, *P. kingsleyae*, and describe morphological correlates of this variation.

In Chapter 4, I use a population genetics approach to analyze data concerning signal variation, behavior, and anatomy in *Paramormyrops kingsleyae* to specifically test the hypothesis that the unique patterns of geographic variation and signal divergence detected in Chapter 3 are the result of geographic barriers and distance that reduce gene flow between local populations.

BIOGRAPHICAL SKETCH

Jason Gallant was born on November 28, 1983 in Hartford, Connecticut. Thanks to the early encouragement of his parents Roy and Lisa Gallant, Jason has had a longstanding passion for things in the natural world. Growing up in the quiet corner of Connecticut, in the woods of Ashford, his hometown, Jason was constantly surrounded by animal life. Jason spent his early days in the company of his sister, brother, and whatever he could capture in his butterfly net, along with numerous pets, including many tanks of tropical fish. Jason's curiosity about animal life was fueled by his entry into public school, where a litany of gifted early educators gave him the information and the enthusiasm necessary for a career in science. Through this, and the ever-present involvement of his parents, Jason was constantly challenged by a never-ending stream of science projects, which he pursued with a sometimes single-minded gusto. This lead to plenty of adventures with his father observing beaver dam-building behavior in the early hours of the morning, and weekend journeys with his mother composing a photo journal of the ecological process called succession. When high school finally came, Jason's science projects became more elaborate, perhaps the earliest evidence of how his career would proceed. The first, a scaled down version of the famous Miller-Urey experiment (built in consultation with Stanley Miller himself!), followed by the construction of a backyard radio telescope, and finally a genetic study of invasive plant hybridization under the advice of then graduate student Dr. Michael Moody, that won him a trip to a national science fair to present his work.

This early educational background provided the ladder up which Jason would climb to continue to his college education at Trinity College, in Hartford Connecticut, where he received his B.S. in 2005 with honors in Biology and a minor in Human Rights. Between his full course load, student research, and his dizzying involvement in numerous student organizations, including the presidency of his own senior class, Jason found his intellectual home in University life. During this time at Trinity, he met Dr. Kent Dunlap who introduced him to the world of weakly electric fish, which would be the beginning of the 10 years that he spent studying the

evolution of their electric signals. His research at Trinity culminated in his presentation of his honors thesis in Nyborg, Denmark at the International Congress of Neuroethology, where he met Dr. Carl Hopkins and was encouraged to join the department of Neurobiology and Behavior at Cornell University.

Jason's arrival at Cornell University marked a new, and needed time for focus on research, which Jason took to under the advisement of Dr. Carl Hopkins and Dr. David Deitcher. While at Cornell, Jason undertook several teaching positions which he enjoyed, including multiple assignments to the Writing in the Majors section of Introduction to Neurobiology and Behavior, which he helped design the curriculum for, to teaching his own course for First-Year Writing entitled "Imagining the Brain". Jason also worked for several years with Andy Moore and his 5th grade classroom, sharing his passion for biology, specifically electric fish, with hundreds of students.

During his time in Ithaca, he met his future wife, Maite Tapia, who has proven time and again to be his match, providing humor, love, a keen intellect, and much moral support up and through the final days of this thesis. After leaving Cornell, Jason and Maite plan to marry in Bruges, Belgium, and then move to Boston, Massachusetts where Jason will begin his postdoctoral work with Dr. Sean Mullen, on the comparative genetics of wing pattern diversity in mimetic butterflies.

To my family, and my family to be…

ACKNOWLEDGMENTS

"If I have seen a little further it is by standing on the shoulders of Giants."

– Isaac Newton

I have many giants to thank for helping me see the things this dissertation has taught me. I first wish to thank my co-advisors, Dr. Carl Hopkins and Dr. David Deitcher. Dr. Hopkins has instilled in me a deep desire to be a careful and thorough scientist above all else, and has also provided me with countless opportunities, assistance, and support through the years. Dr. Deitcher has been an excellent mentor, troubleshooter, and conversationalist during the more tedious execution of my research. I also wish to thank Dr. Joe Fetcho, who has gone above and beyond the call of duty as a Director of Graduate Studies and committee member during my years at Cornell. Dr. Fetcho has provided me with very frank but helpful and sincere, evaluation of all the numerous situations I have found myself in. I also wish to thank the two additional members of my special committee, Dr. Kerry Shaw and Dr. Amy McCune, who have kept open doors, and have shared their own wisdom in helping me complete this thesis. Their good advice and sharp intellects have helped guide me past several pitfalls, as well as help interpret the many things that I have learned through my research.

I wish to also especially thank Dr. Matthew Arnegard and Dr. Bruce Carlson, two intellectual giants in the field of electric fish research, who have contributed enormously to the work described in these pages. My time with them in the field was some of the most exciting to me scientifically. Their good humor and selfless generosity with their time and advice has without a doubt been one of my most valuable assets during tenure at Cornell. I also wish to thank the numerous people with whom I've worked in the Hopkins Lab, especially Catherine Cheng whose gifts for histology contributed greatly to the last chapter of this work. Also, Garry

Harned has taught me everything I have come to learn about histology, and has been an excellent friend and role model throughout my time in Ithaca. In addition, Dr. John Sullivan, Dr. Laurianne Dent, Dr. B. Scott Jackson, Brian Isett, Kevin Gardener, Farah Ismail, Jessica Thiesmeyer, Erica Sher, Josh Sperling, Natalie Trzcinski. In the Deitcher Lab, this includes Dr. Brandon Loveall, Jad Husseni, Kristy Lawton and Hannah Kim.

The work presented here has been funded by a number of funding agencies, including the National Institutes of Health (NIMH TG T32-MH015793 and NIH TG 2T32GM007469 to JRG; NIH R01-DC6206 to CDH), the National Science Foundation (0818305 to CDH), the Department of Neurobiology and Behavior, and the Cornell Center for Vertebrate Genomics. Permits to collect fishes in Gabon and export them for the studies in this dissertation were granted by the Centre National de la Recherche Scientifique et Technologique of Gabon. I am particularly grateful for the valuable assistance and logistical support we received from Jean-Danielle Mbega in the field, and his students working in these institutions, particularly Roger Afene and Marie-Francois Eva. Thanks must also be given to our friends at the Bongolo Hospital who provided us with logistic help and lodging during our stay in Bongolo.

The support staff in the Department of Neurobiology and Behavior is unparalleled at any institution I have been part of. I wish to thank above all Saundra Anderson for her tireless dedication to making our day-to-day operations run smoothly in the lab, as well as Terri Natoli and Stacey Coil for taking such great care of the graduate students. In addition, I wish to acknowledge the hard work suffered by Rich Moore, who has taken excellent care of our fish. I have enjoyed our conversations, ranging from hunting to boating to politics. I also wish to extend my thanks to Charles Dardia and John Friel at the Cornell Museum of Vertebrates for their assistance in organizing our collections of Mormyrids. Finally, I have made considerable

use of Cornell's excellent core facilities, including the Cornell Microscopy and Imaging Core Facility, the Core Laboratories Center for Genomics, the Evolutionary Genetics Core Facility (with a plethora of helpful advise from Steve Bogdanowicz), and the Cornell Computational Biology Service Unit's Center for High Performance Computing.

I would be remiss to not acknowledge my "personal" giants, who of course include all of the talented and gifted graduate students, postdocs, and faculty that make the department of Neurobiology and Behavior what it is. In particular, Dr. Sandeep Kishore, Dr. Martin von Arx, Dr. Boris Chagnaud, Dr. Andreas Huch, as well as Shane Peace, John Oltoff, without whom my time at Cornell would have been much less enjoyable. Finally, I wish to thank my parents for their unwavering support over all of these years as I have sought to achieve my goals, and Maite who has provided me with love, humor, and support

TABLE OF CONTENTS

LIST OF FIGURES:

LIST OF TABLES:

CHAPTER 1. A GENERAL INTRODUCTION TO ELECTRIC ORGANS: WHERE DO THEY COME FROM, AND WHY ARE THERE SO MANY DIFFERENT KINDS?

The electric organs of fishes offer another case of special difficulty; for it is impossible to conceive by what steps these wondrous organs have been produced. But this is not surprising, for we do not even know of what use they are. In the Gymnotus and torpedo they no doubt serve as powerful means of defense, and perhaps for securing prey; yet in the ray, as observed by Matteucci, an analogous organ in the tail manifests but little electricity, even when the animal is greatly irritated; so little, that it can hardly be of any use for the above purposes….It is generally admitted that there exists between these organs and ordinary muscle a close analogy, in intimate structure, in the distribution of the nerves, and in the manner in which they are acted on by various reagents… Beyond this we cannot at present go in the way of explanation; but as we know so little about the uses of these organs, and as we know nothing about the habits and structure of the progenitors of the existing electric fishes, it would be extremely bold to maintain that no serviceable transitions are possible by which these organs might have been gradually developed.
-Darwin, 1859, The Origin of Species

Following publication of *The Origin of Species,* nearly 100 years would pass before Lissman (1951) made the first electrical recording of the discharge of a "weakly electric" fish *Gymnarchus niloticus* and noted its importance as a solution to the difficulty posed to Darwin's model of natural selection. We now know that strongly discharging electric eels have likely evolved from weakly electric ancestors, and that electric organs evolved originally for electrolocation (Lissmann and Machin, 1958) and electrocommunication (Lissmann, 1958; Mörhes, 1957). From the subsequent work that followed these important discoveries, more difficult, but equally fascinating problems have emerged surrounding electric fish, resonant of standing problems in modern biology. The first is a remnant of Darwin's original difficulty: namely the steps by which novel physiological and anatomical features, such as electric organs, originate. The second problem is the result of an ensuing century of field collections, taxonomic, and phylogenetic work on electric fishes: why are there so many species of electric fish? In some taxa, electric fishes have undergone what may be considered "explosive" speciation, which is associated with considerable diversity in electric signals. Is species diversity in electric fish related to the evolution of diversity in electric organ physiology? It is these two problems that have motivated the work presented in the following pages of this dissertation.

Problem 1: Where Do Electric Organs Come From?

Electric organs are one of many unique physiological tissue types that have evolved from muscle in teleost fishes. Also present among teleosts are sonic muscles capable of high-frequency contraction (Rome, 2006), and heater organs for efficient thermogenesis (Block, 1994). In each case, a suite of anatomical and physiological adaptations is required to produce these "novel" structures from muscle (Block, 1994), though the molecular factors underlying the origins of these tissues remain poorly understood. If the goal is to extract common principles by which a "novel" tissue or physiological function is built, it may be advantageous to consider examples where a particular configuration has evolved multiple times: in this sense, electric fish are ideal.

Darwin (1859) recognized that the diversity of electric organs among fishes had not arisen from a common ancestor, but multiply through convergent evolution. We presently know of six independent origins of electric organs in fishes: torpedinoids, rajoids, mormyrids, gymnotiforms, siluriforms uranoscopids (Bass, 1986). In all but one family of gymnotiforms, the apteronotidae, electric organs are derived during development from skeletal muscle tissue (Bass, 1986; Bennett, 1971). There is considerable variation between lineages (reviewed by Bass, 1986; Bennett, 1971), particularly in the types of skeletal muscle that electric organs originate from (e.g. eye muscles, trunk musculature, pectoral fin musculature), in the voltage of electrical discharge (approx. 10 mv-600 V;), in their innervation (either in a restricted region of, or diffusely over, a single electrocyte face), and in the complexity of their anatomy (ranging from simple sac-like electrocytes to those with complex stalk-like protrusions). At the cellular level, the electrical discharge of marine fishes results from opening acetylcholine gated receptors at the neuro/electric organ synapse, whereas in freshwater forms, the electrical discharge is a

sodium-channel dependent spike in modified skeletal muscle membranes (Bennett, 1971).

Of all potential comparisons between groups of electric fish, comparisons between the gymnotiforms of South America and mormyrids of Africa may be the most fruitful, owing to the fact that the two groups have independently evolved electrogenesis with so many convergently evolved traits. Aside from the instances of convergence in electrosensory systems (Heiligenberg, 1986; Kawasaki, 2005; Zakon, 1986), both groups have independently evolved numerous similarities in their electric organs. Both groups have evolved electric organs that originate developmentally from a distinct group of fully differentiated skeletal myofibrils (Patterson and Zakon, 1997). The transition between skeletal muscle and electric organ is accompanied by a substantial change in cell size (Unguez and Zakon, 1998a, b), morphology (Denizot et al., 1982b), and physiology (Westby and Kirschbaum, 1977), which ultimately leads to the retention of electrical excitability without the generation of contractile force. Unlike other electric fish, both mormyrids and gymnotiforms have electric organs with two excitable faces, oriented in opposing polarity. One electrocyte face is typically innervated, though in some derived gymnotiforms, both faces can be innervated (Trujillo-Cenóz et al., 1984). This innervated face typically exhibits complex protrusions originating from the innervated membrane, termed "stalks" (Bass, 1986; Bennett, 1971). Unlike in marine electric fish, electrocyte faces in gymnotiforms and mormyrids produce sodium spikes (Bennett, 1971). Intriguingly, both groups have convergently co-opted the same sodium channel gene, *Scn4aa*, (which arose by fish specific whole-genome duplication c.a. 200-300 MYA), to produce EODs (Arnegard et al., 2010b).

Of course, there are also important differences between gymnotiforms and mormyrids. In gymnotiforms, the transition between skeletal muscle and electric organ is accompanied by the

down-regulation of sarcomeric proteins (Kim et al.; Patterson and Zakon, 1997; Unguez and Zakon; Zakon and Unguez, 1999). In mormyrids, histological work has suggested that sarcomeric proteins are retained (Bass, 1986; Bass et al., 1986). The gymnotiform electric organ can be regenerated upon injury (Cuellar et al., 2006; Kim et al., 2008; Kim et al., 2009; Kim et al., 2004; Patterson and Zakon, 1996, 1997; Unguez and Zakon, 1998a, b; Zakon and Unguez, 1999), whereas the mormyrid electric organ cannot. Finally, experimental manipulations of innervation in mormyrids and gymnotiforms has revealed that innervation appears to be essential in the development and maintenance of the ECs in gymnotiforms (Cuellar et al., 2006; Patterson and Zakon, 1997; Unguez and Zakon, 1998a, b; Zakon and Unguez, 1999), but does not appear necessary for the development of ECs in mormyrids (Szabo and Kirschbaum, 1983).

Some attempts have been made to determine potential mechanisms that may be involved in the developmental transition between skeletal muscle and electric organ in these groups, however all of the studies involving molecular biology have concerned gymnotiforms, thus limiting the potential for comparative study. One hypothesis has been that motor neurons innervating the electric organ facilitate the developmental transition between skeletal muscle and electric organ (Patterson and Zakon, 1997; Szabo and Kirschbaum, 1983; Unguez and Zakon, 1998b). A recent study by Cuellar et al (2006) has found that several sarcomeric genes are transcribed in the electric organ of gymnotiforms, however proteins are not translated. This has motivated the hypothesis that motor neuron activity in gymnotiform electric organ may suppress skeletal-muscle specific gene expression via through post-transcriptional regulation. The evidence for a similar mechanism in mormyrids seems weak, given that electric organs seem to persist, even in the absence of nerve input. In addition to the role of innervation, a variety of studies have hypothesized that transcription factors involved in the early development of muscle,

may somehow be involved in the transition to skeletal muscle (Kim et al., 2008). Intriguingly many are upregulated (e.g. *MyoD*, *myogenin*, *myf5*, and *MRF4*) whereas others (e.g. *MEF2c*, *Id1*, and *Id2*) are not (Kim et al., 2008). No data on transcription factor expression has been published in mormyrids.

Determination of genes that are expressed in the mormyrid electric organ is an important goal for future comparative studies into the mechanisms that underlie the evolution of novel physiological and anatomical structures. It is this goal that has motivated the study described in Chapter 2 of this dissertation. Considering the close developmental relationship between skeletal muscle and electric organ, as well as the focus of previous studies in gymnotiforms on changes in gene expression between the two tissues, I designed a study which took the approach of using suppressive subtractive hybridization (SSH), a simple PCR-based method that selectively enriches for differentially expressed mRNAs, to identify unique patterns of gene expression in the electric organ and skeletal muscle without *a priori* assumptions regarding gene identities. Using these results, we provide data on the localization of protein products of a subset of these differentially expressed genes in skeletal muscle and electric organ using immunohistochemistry and western blotting. The results of this study indicate that mormyrids, unlike gymnotiforms retain expression and translation of several sarcomeric proteins during the developmental transition from skeletal muscle to electric organ. Instead of expressing the same form in skeletal muscle and electric organ, mormyrids seem to express electric organ specific isoforms of these genes. We also show the differential expression of a critical transcription factor, myocyte enhancer factor 2A (*MEF2a*), which is upregulated in the electric organ.

Problem 2: Has Electric Organ Diversity Contributed to Species Diversity?

The process by which animal species diversity is generated is called *speciation*. Arguably, the most important insights into how speciation occurs have been granted by groups of organisms that have evolved exceptionally high species diversity over relatively short periods of time, so called "species radiations". Frequently associated with species radiations is matching diversity in communication systems, which have been described in nearly every known sensory modality (Allender et al., 2003; Boul et al., 2006; Diamond, 1986; Mendelson and Shaw, 2005; Mullen et al., 2007; Sullivan et al., 2002). This connection impressed upon Mayr (1963) "If we were to rank the various isolating mechanisms of animals according to their importance, we would have to place behavioral isolation far ahead of all others". Classic models of speciation presume that this association between species and signal diversity has evolved as an incidental by-product of divergent natural selection (Mayr, 1942) on ecological traits, or in other explanations to "reinforce" divergence resulting from natural selection (Dobzhansky, 1937).

However in some systems the signature of ecological divergence preceding signal divergence is low, (Allender et al., 2003; Arnegard et al., 2010a; Mendelson and Shaw, 2005) suggesting the intriguing alternative hypothesis that divergent courtship signaling behavior may itself contribute to the speciation process, through sexual selection (Panhuis et al., 2001). This seems plausible among several electric fish taxa, in which electrogenic diversity is pronounced, such as the South American gymnotiform genera *Brachyhypopomus* (Sullivan, 1997) and *Gymnotus* (Lovejoy et al., 2010) and the two African mormyrid genera *Campylomormyrus* (Feulner et al., 2008; Feulner, 2006; Feulner et al., 2007) and *Paramormyrops*, (Sullivan et al., 2004; Sullivan et al., 2000). Of particular note are the two mormyrid genera, which have undergone recent, rapid speciation in the freshwater drainage systems of West-Central Africa,

and are considered examples of "species flocks" (Feulner et al., 2008; Feulner, 2006; Feulner et al., 2007; Sullivan et al., 2004; Sullivan et al., 2000).

Perhaps most thoroughly studied of these radiations is that of the *Paramormyrops* (formerly the "Gabon-clade *Brienomyrus"*) of West-Central Africa. Recent estimates have suggested as many as 22 *Paramormyrops* species (Lavoué et al., 2008). In contrast to the low level of genetic divergence between these species that suggests the recency of their origin (Sullivan et al., 2002), *Paramormyrops* exhibit highly divergent electrical signals (Sullivan et al., 2004; Sullivan et al., 2002). A recent, detailed study of rates of divergence in EOD signals, feeding morphology, size, and trophic ecology in *Paramormyrops* by Arnegard et al. (2010a) has indicated that electric signal divergence within *Paramormyrops* greatly outpaces rates of diversification in ecological and morphological characteristics, suggesting that sexual selection is important driver of species divergence, rather than natural selection in this group. Because of the uniqueness of the electric signaling modality, and the relative "privacy" it affords, Arnegard et al. (2010a) notes that an opportunity for species radiation in *Paramormyrops* may have arisen due to their use of electric "signal space", which compared to other signaling modalities is comparatively private and relatively free from selective pressures.

EODs may vary in duration (0.5-8 ms), in polarity, in the number of phases, and in the rates of voltage change over time (Sullivan et al., 2002). Each EOD typically consists of two main peaks, a head-positive phase, P1, followed by a head negative phase, P2. P1 is sometimes preceded by a weak head negative phase, P0, which is absent in some specimens (Fig. 1-1). EOD variation within *Paramormyrops* and other mormyrids originates from changes in the electric organ anatomy and physiology (Bass, 1986; Bennett, 1971). In mormyrids, the electric organ is comprised of four axially oriented columns, each consisting of approximately 20-100

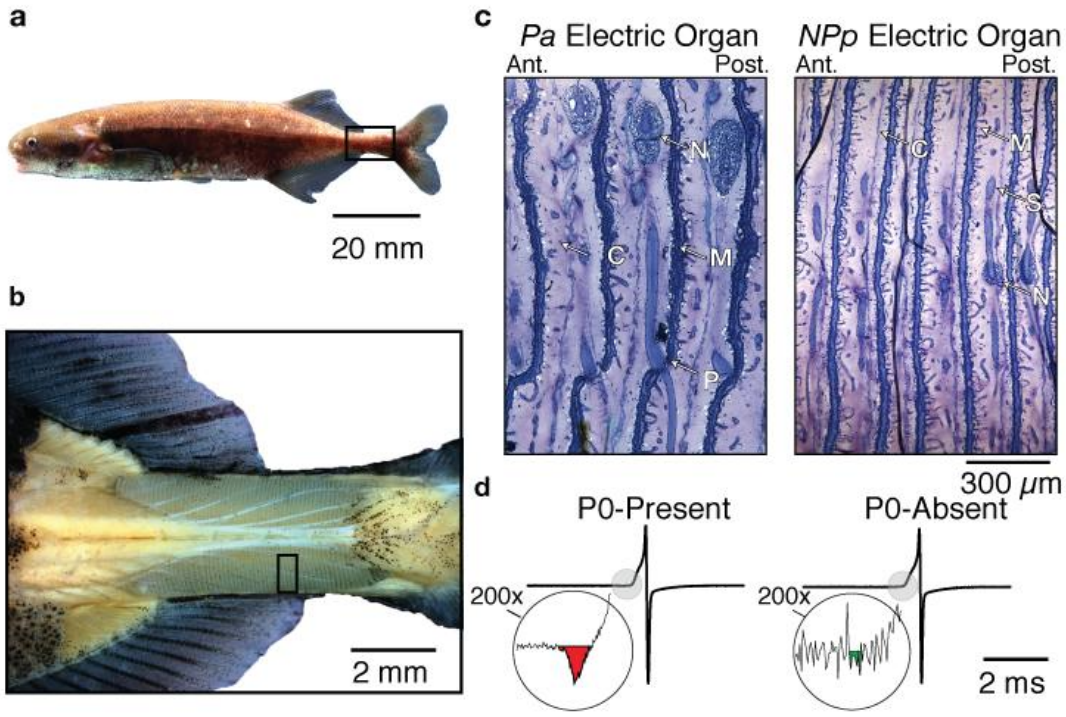

Figure 1-1: Paramormyrops kingsleyae and its divergent signaling types.

a. *Paramormyrops kingsleyae* from Biroundou Creek, in Gabon West Central Africa (see Table 3-1). **b.** The electric organ of *P. kingsleyae* is located in the caudal peduncle. When skin and scales are removed, the electric organ is clearly visible as a striated structure flanked by two groups of muscles. **c.** Two specimens are represented by sections of electric organs; *P. kingsleyae* that have either penetrating with anterior innervation (*Pa*) type electric organs or non-penetrating with posterior innervation (*NPp*) type electric organs. Anatomical features shown are **N**erve, **C**onnective tissue septa bounding each electrocyte, **M**icrostalklets, and **P**enetrations. Electrocytes are the dark longitudinal stripes present in each section. For A, B, C, anterior is left, posterior is right. **d.** EOD waveforms corresponding to *Pa* and *NPp* type anatomy (above) are shown at 1 and 200x. A small head negative component at the beginning of the EOD occurs only when *Pa* type electrocytes are present. Mormyrids lacking *NPp* type electrocytes also lack EODs with P0.

disc-shaped electrocytes (Bass, 1986). One of the best-understood sources of variation in mormyrid EODs is an anatomical change in electrocytes which results in either the presence or absence of phase P0 (Fig. 1-1; for reviews see also: Bass, 1986; Bennett, 1971; Bennett and Grundfest, 1961). Mormyrid electrocytes have protruding stalk systems that can originate on the posterior face, and pass through to the anterior face, where they are innervated (*P*enetrating with *a*nterior innervation or *Pa*; Fig 1-1c). Alternatively they can have stalks that remain on the posterior face, and are innervated on the posterior face (*N*on-*P*enetrating with *p*osterior innervation, or *NPp*; Fig 1-1c). The EOD waveform produced by these two electric organ types relates to the direction of current flow through the stalk and the relative order in which the anterior and posterior electrocyte faces depolarize (see Bass, 1986; Bennett, 1971). P0-present EODs are associated with *Pa* type electric organs, and P0-absent EODs are associated with *NPp* type electric organs (Fig. 1-1c).

Pa electrocytes evolved from NPp-type early in the history of Mormyridae, followed by seven reversals to NPp-type (Sullivan et al. 2000). In *Paramormyrops*, Pa-type were likely ancestral and there have been minimally five reversals to NPp in this genus alone (Sullivan et al. 2004). Stalk penetrations appear late in electrocyte ontogeny—Pa-type electrocytes pass through an NPp stage of development (Denizot et al., 1982a; Szabo, 1960; Hopkins 1999). Thus, these reversals from adult Pa-type to NPp-type electrocytes have been interpreted as paedomorphic (Sullivan et al. 2004). These multiple reversals from Pa to NPp type morphology characterize a large component of signal diversity in mormyrids, and particularly within the *Paramormyrops*.

If the evolution of signal diversity is a critical component to the speciation process, as has been suggested by Arnegard et al. (2010a), then instances in which signal diversity has evolved

prior to the evolution of reproductive isolation become of particular interest, because these cases may represent potential "incipient species". Study of such cases should provide insight into the population-level processes that might contribute to overall macroevolutionary patterns of species and signal evolution. Two of such monophyletic groups of *Paramormyrops* have been identified through phylogenetic work by Sullivan et al. (2004).

The first group is the *Paramormyrops* 'magnostipes' complex, which exhibits divergent courtship signals that are substantially differentiated in terms of their temporal features (Arnegard et al., 2006). These signal forms often occur in sympatry, particularly in two focal regions of Gabon in which the Hopkins lab has performed sampling over the past several decades: the Ivindo River in the North, and tributaries of the Ngounié River in the South. In several collection localities, signal types of the *P.* 'magnostipes' complex co-exist in sympatry. Arnegard et al. (2005) demonstrated that these sympatric forms are genetically identical across five microsatellite loci in every population sampled, suggesting substantial gene flow between divergent forms. Subsequent work has been demonstrated that the two forms overlap substantially in both trophic ecology and overall morphology; though there appears to be association with particular signal types and body size (Arnegard et al., 2006). It is presently unclear how such divergent EOD types may have evolved given the substantial gene flow between species, though it raises the possibility that divergence may have occurred in sympatry.

The second monophyletic group in which signal diversity appeared to exceed species diversity was what Sullivan et al. (2004) referred to as the *Paramormyrops* 'cabre' complex, which has subsequently been revised based on detailed morphometric and molecular analysis as the species *Paramormyrops kingsleyae* (Günther, 1896), the subject of the following chapters. *P. kingsleyae* is a geographically widespread species in West-Central Africa, exhibits a more

subtle form of variation in its EODs: some of the specimens have a P0-present signal, whereas other specimens had a P0-absent signal. Unlike the *P.* 'magnostipes complex' described above, this divergent signal character is subtle; at maximum the magnitude of peak P0 is only 2% of the peak-to-peak amplitude of an EOD. Despite this, variation in this character represents an important component of signal variation within *Paramormyrops* and other mormyrids, as discussed in detail above. Given the role of this character in signal evolution among mormyrids, there is considerable interest in determining the evolutionary forces that act upon this signal character. A strategy used by many to infer the evolutionary processes that contribute to signal evolution is to use patterns of intraspecific geographic variation (Endler, 1989; Foster et al., 1998; Lewontin, 1974; Mayr, 1963; McPhail, 1994; Verrell, 1998). Patterns of intraspecific variation may indicate key variables that influence the evolution of a trait interest within a species, potentially granting insight into how traits might evolve between species.

In Chapter 3 of this dissertation, I embark on a detailed description of the nature of intraspecific variation in EOD signals of *P. kingsleyae*, followed by a description of the biogeographic patterns that this variation takes. I examine the morphology of electric organs of *P. kingsleyae* from several independent populations, and demonstrate morphological correlates for the observed signal variation. Our results have shown that *P. kingsleyae* exhibit clinal variation in EOD signals with regard to duration, and the small head-negative phase, P0. While the majority of populations across Gabon had P0-present EODs, two populations isolated by major barriers to migration (a waterfall, Bongolo Falls in the South, or the Atlantic Ocean in a Northern Population), we found populations where every individual possessed P0-absent EODs. Two populations, Apassa and Bambomo creek, occurred along a watershed boundary between which streams either drained above or below Bongolo Falls, and were the only locations where

individuals with P0-present and P0-absent waveforms co-occurred. In the majority of specimens surveyed from populations across Gabon, individuals with P0-present EODs had electric organs with *Pa* type anatomy, whereas individuals with P0-absent EODs had electric organs with *NPp* type anatomy. However, in Bambomo creek, we discovered multiple individuals that contained both Pa type electrocyte and NPp type electrocytes in the electric organ. At the end of Chapter 3, I discuss some insights gained into potential mechanisms that might have contributed to the evolution of divergent signals among populations of *P. kingsleyae*. Given the rather small magnitude of the signal differences, it seems unlikely that the patterns of signal divergence have arisen due to the effects of selection, but rather are the results of substantial population structure (a signature of limited dispersal between populations).

In Chapter 4, the final chapter of this dissertation, I test this hypothesis specifically, using population genetics, behavior, and analysis of morphology and EOD signals. If this hypothesis is valid, we expect to find: (1) evidence of genetic structure, which is associated with physical barriers or large distances between populations, which correlates with detectable variation in EOD signals. (2) Evidence that P. kingsleyae individuals are incapable of discriminating between divergent EOD types (i.e. P0-absent vs. P0-present), and (3) Genetic, morphological, and/or physiological evidence that, in populations where individuals occur sympatrically, hybridization between signal forms occurs.

The results of this analysis demonstrate evidence supporting each of these predictions, supporting the overall hypothesis that signal variation, and in its morphological correlate have arisen as the result of limited dispersal between populations of *P. kingsleyae*, rather than the alternative hypothesis that selection against migration (i.e. "reinforcement" or recognition of cryptic species) has led to the current biogeographic distribution of signal types. Limited

dispersal seems to be imposed by a combination of habitat preferences of *P. kingsleyae* for the headwaters of streams, sheer distances between populations, and the existence of substantial barriers to migration (i.e. waterfalls). This result, taken with the lack of evidence of selective pressure acting on signals, seems to most strongly support the hypothesis that genetic drift may have influenced the evolution of divergent electric signals among *P. kingsleyae.*

Conclusions, Insights, and Future Directions

This dissertation work has contributed towards our greater understanding of two fundamental problems in electric fish. The first chapter develops a novel approach to identifying genes in electric organ tissues, and has demonstrated that the developmental mechanisms that govern the transition between skeletal muscle and electric organ may be complex. In gymnotiforms, previous research has shown that electric organ development is dependent on innervation, whereas the novel results presented in this dissertation suggest that in mormyrids these mechanisms are not used, identifying several genes isoforms, normally expressed in muscle, that contribute to the unique physiology and anatomy of the electric organ.

The second and third chapters attempt to gain insight into the causes of divergence between electric organ physiologies. This work has identified a major component of electric signals that is repeatedly lost within the *Paramormyrops* radiation, and within other genera of mormyrids, which is variable within populations of a single species, *Paramormyrops kingsleyae.* The influences of population structure on the distribution of this character imply that genetic drift might be sufficient to contribute to waveform variation in *P. kingsleyae*, suggesting that the genetic mechanisms underlying this component of EOD signal variation might be simple. This neutral variation could conceivably be the substrate upon which natural, or probably sexual selection could later act to cause divergence between *Paramormyrops* species.

Future work should focus on the identification of the genes that contribute to this character, which seems tantalizingly close given the divergent signals discovered in *P. kingsleyae*. Based on the methods developed in the second chapter of this dissertation, it may be possible to determine gene expression differences between *P. kingsleyae* signal types that contribute to this variation, or potentially that the sarcomeric genes described as differentially expressed, which have no known function in mormyrid electric organs, may contribute to structural features of the electrocyte. The advent of several new technologies, most excitingly RAD-tag sequencing (Miller et al., 2007), are making the possibility of quantitative trait mapping studies possible in non-model systems. Once genes linked to the loss or gain of penetrating stalks (and associated P0-absent and P0-present signals, respectively) are discovered, direct hypothesis testing would be possible in *P. kingsleyae* and other *Paramormyrops* concerning the evolutionary influences that shape signal evolution and speciation from the population to the generic levels.

References

Allender CJ, Seehausen O, Knight ME, Turner GF, Maclean N (2003) Divergent selection during speciation of Lake Malawi cichlid fishes inferred from parallel radiations in nuptial coloration. Proc Natl Acad Sci USA 100:13074-14079

Arnegard M, McIntyre PB, Harmon LJ, Zelditch ML, Crampton WGR, Davis JK, Sullivan JP, Lavoué S, Hopkins C (2010a) Sexual signal evolution outpaces ecomorphological and trophic divergence during electric fish species radiation. Am Nat 176:335-356

Arnegard M, Zwickl D, Lu Y (2010b) Old gene duplication facilitates origin and diversification of an innovative communication system—twice. Proc Natl Acad Sci USA

Arnegard ME, Bogdanowicz SM, Hopkins CD (2005) Multiple cases of striking genetic similarity between alternate electric fish signal morphs in sympatry. Evolution 59:324-343

Arnegard ME, Jackson BS, Hopkins CD (2006) Time-domain signal divergence and discrimination without receptor modification in sympatric morphs of electric fishes. J Exp Biol 209:2182-2198

Bass AH (1986) Electric organs revisited: evolution of a vertebrate communication and orientation organ. In: Bullock TH, Heiligenberg W (eds) Electroreception. Wiley, New York, pp 13-70

Bass AH, Denizot JP, Marchaterre M (1986) Ultrastructural features and hormone-dependent sex-differences of mormyrid electric organs. J Comp Neurol 254:511-528

Bennett M (1971) Electric organs. In: Hoar WS, Randall DJ (eds) Fish Physiology. Academic Press, New York, NY, pp 347-491

Bennett M, Grundfest H (1961) Studies on morpology and electrophysiology of electric organs III. Electrophysiology of electric organs in mormyrids. Bioelectrogenesis (C Chagas and A Paes de Carvalho, Eds):113-135

Block BA (1994) Thermogenesis in muscle. Annu Rev Phyiol 56:535-577

Boul KE, Chris Funk W, Darst CR, Cannatella DC, Ryan MJ (2006) Sexual selection drives speciation in an Amazonian frog. Proc Roy Soc B 274:399-406

Cuellar H, Kim JA, Unguez GA (2006) Evidence of post-transcriptional regulation in the maintenance of a partial muscle phenotype by electrogenic cells of *S. macrurus*. FASEB J 20:2540

Darwin C (1859) The Origin of Species. Vol. XI: The Harvard Classics. P.F. Collier & Sons, New York

Denizot JP, Kirschbaum F, Max Westby GW, Tsuji S (1982a) On the development of the adult electric organ in the mormyrid fish Pollimyrus isidori (with special focus on the innervation). J Neurocytol 11:913-934

Denizot JP, Kirschbaum F, Westby GW, Tsuji S (1982b) On the development of the adult electric organ in the mormyrid fish *Pollimyrus isidori* (with special focus on the innervation). J Neurocytol 11:913-934

Diamond J (1986) Biology of Birds of Paradise and Bowerbirds. Annual Review of Ecology and Systematics

Dobzhansky T (1937) Genetics and the Origin of Species. Columbia University Press, New York, NY

Endler JA (1989) Conceptual and other problems in speciation. In: Otte D, Endler JA (eds)

Speciation and its consequences. Sinauer Associates, Sunderland, MA, pp 625-648.
Feulner P, Kirschbaum F, Tiedemann R (2008) Adaptive radiation in the Congo River: An ecological speciation scenario for African weakly electric fish (Teleostei; Mormyridae; Campylomormyrus). J Physiol Paris 102:340-346
Feulner PGD (2006) Adaptive radiation, speciation, and reproductive isolation in African weakly electric fish. PhD Dissertation
Feulner PGD, Kirschbaum F, Mamonekene V, Ketmaier V, Tiedemann R (2007) Adaptive radiation in African weakly electric fish (Teleostei: Mormyridae: Campylomormyrus): a combined molecular and morphological approach. J Evol Biol 20:403-414
Foster SA, Scott RJ, Cresko WA (1998) Nested biological variation and speciation. Philosophical Transactions of the Royal Society of London B 353:207-218
Günther A (1896) Report on a collection of reptiles and fishes made by Miss M.H. Kingsley during her travels on the Ogowe River and in Old Calabar. Ann and Mag Nat Hist (Ser 6) 17:261-285
Heiligenberg W (1986) Jamming avoidance responses: model systems for neuroethology. In: Bullock TH, Heiligenberg W (eds) Electroreception. John Wiley & Sons, Inc., New York
Hopkins, C.D. (1999). Signal evolution in electric communication. In: Hauser, MD and Konishi, M (eds) The Design of Animal Communication. MIT Press, Cambridge, MA.
Kawasaki M (2005) Physiology of the tuberous electrosensory system. In: Bullock TH, Hopkins CD, Popper AN, Fay RR (eds) Electroreception. Springer, New York, pp 154-194
Kim HJ, Archer E, Escobedo N, Tapscott SJ, Unguez GA (2008) Inhibition of mammalian muscle differentiation by regeneration blastema extract of *Sternopygus macrurus*. Dev Dyn 237:2830-2843
Kim HJ, Güth R, Jonsson CB, Unguez GA (2009) *S. macrurus* myogenic regulatory factors (MRFs) induce mammalian skeletal muscle differentiation; evidence for functional conservation of MRFs. Dev Biol 53:993-1002
Kim JA, Jonsson CB, Calderone T, Unguez GA (2004) Transcription of MyoD and myogenin in the non-contractile electrogenic cells of the weakly electric fish, Sternopygus macrurus. Dev Genes and Evol 214:380-392
Lavoué S, Arnegard M, Sullivan JP, Hopkins C (2008) Petrocephalus of Odzala offer insights into evolutionary patterns of signal diversification in the Mormyridae, a family of weakly electrogenic fishes from Africa. J Comp Physiol Paris 102:322-339
Lewontin RC (1974) The genetic basis for evolutionary change. Columbia University Press, New York, NY
Lissmann H (1958) On the function and evolution of electric organs in fish. J Exp Biol 35:156-191
Lissmann HW (1951) Continuous electrical signals from the tail of a fish, *Gymnarchus niloticus* Cuv. Nature 167:201-202
Lissmann HW, Machin KE (1958) The mechanisim of object location of *Gymnarchus niloticus* and similar fish. J Exp Biol 35:451-486
Lovejoy NR, Lester K, Crampton WGR, Marques FPL, Albert JS (2010) Phylogeny, biogeography, and electric signal evolution of Neotropical knifefishes of the genus Gymnotus (Osteichthyes: Gymnotidae). Mol Phylo Evol 54:278-290
Mayr E (1942) Systematics and the origin of species: from the viewpoint of a zoologist. Columbia University Press, New York
Mayr E (1963) Animal Species and Evolution. Belknap Press, New York, NY

McPhail JD (1994) Speciation and the evolution of reproductive isolation in the sticklebacks (Gasterosteus) of southwestern British Columbia. In: Bell MA, Foster SA (eds) The evolutionary biology of the threespine stickleback. Oxford University Press, Oxford, UK
Mendelson TC, Shaw KL (2005) Sexual Behavior: rapid speciation in an arthropod. Nature 433:375-376
Miller MR, Dunham JP, Amores A, Cresko WA, Johnson EA (2007) Rapid and cost-effective polymorphisim identification and genotyping using restriction site associated DNA (RAD) markers. Genome Res 17:240-248
Mörhes FP (1957) Elektrische entladungen im dienste der revierabgrenzung bel fischen. Naturwissenschaften 44
Mullen SP, Mendelson TC, Schal C, Shaw KL (2007) Rapid evolution of cuticular hydrocarbons in a species radiation of acoustically diverse hawaiian crickets (gryllidae: trigonidiinae: laupala). Evolution 61:223-231
Panhuis TM, Butlin R, Zuk M, Tregenza T (2001) Sexual selection and speciation. Trends in Ecology and Evolution 16:364-371
Patterson JM, Zakon HH (1996) Differential expression of proteins in muscle and electric organ, a muscle derivative. J Comp Neurol 370:367-376
Patterson JM, Zakon HH (1997) Transdifferentiation of muscle to electric organ: Regulation of muscle-specific proteins is independent of patterned nerve activity. Dev Biol 186:115-126
Rome LC (2006) Design and function of superfast muscles: new insights into the physiology of skeletal muscle. Annu Rev Phyiol 68:193-221
Sullivan JP (1997) A phylogenetic study of the Neotropical hypopomid electric fishes (Gymnotiformes: Rhamphichthyoidea). Duke University, Durham, North Carolina
Sullivan JP, Lavoué S, Arnegard ME, Hopkins CD (2004) AFLPs resolve phylogeny and reveal mitochondrial introgression within a species flock of African electric fish (Mormyroidea: Teleostei). Evolution 58:825-841
Sullivan JP, Lavoue S, Hopkins CD (2000) Molecular systematics of the African electric fishes (Mormyroidea: teleostei) and a model for the evolution of their electric organs. J Exp Biol 203:665-683
Sullivan JP, Lavoué S, Hopkins CD (2002) Discovery and phylogenetic analysis of a riverine species flock of African electric fishes (Mormyridae: Teleostei). Evolution 56:597-616
Szabo T (1960) Development of the electric organ of Mormyridae. Nature 188:760-762
Szabo T, Kirschbaum F (1983) On the differentiation of electric organs in the absence of central connections or peripheral innervation. The Physiology of Excitable Cells. Alan R. Liss, New York, pp 451-460
Trujillo-Cenóz O, Echagüe JA, Macadar O (1984) Innervation pattern and electric organ discharge waveform in Gymnotus carapo teleostei Gymnotiformes. J Neurobiol 15: 273–281
Unguez GA, Zakon HH (1998a) Phenotypic conversion of distinct muscle fiber populations to electrocytes in a weakly electric fish. J Comp Neurol 399:20-34
Unguez GA, Zakon HH (1998b) Reexpression of myogenic proteins in mature electric organ after removal of neural input. J Neurosci 18:9924-9935
Verrell PA (1998) Geographic variation in sexual behavior: sex signals and speciation. In: Foster SA, Endler JA (eds) The Evolution of Geographic Variation in Behavior. Oxford University Press, Oxford, UK

Westby GW, Kirschbaum F (1977) Emergence and development of the electric organ discharge in the mormyrid fish, *Pollimyrus isidori* I. The larval discharge. J Comp Physiol A 122:251-271

Zakon HH (1986) The electroreceptive periphery. In: Bullock TH, Heiligenberg W (eds) Electroreception. Wiley, New York, pp 103-156

Zakon HH, Unguez GA (1999) Development and regeneration of the electric organ. J Exp Biol 202: 1427–1434

CHAPTER 2. DIFFERENTIAL EXPRESSION OF GENES AND PROTEINS BETWEEN ELECTRIC ORGAN AND SKELETAL MUSCLE IN THE MORMYRID ELECTRIC FISH *BRIENOMYRUS BRACHYISTIUS**

Abstract

Electric organs (EOs) have evolved independently in vertebrates six times from skeletal muscle (SM). The transcriptional changes accompanying this developmental transformation are not presently well understood. Mormyrids and gymnotiforms are two highly convergent groups of weakly electric fish that have independently evolved electric organs: while much is known about development and gene expression in gymnotiforms, very little is known about development and gene expression in mormyrids. This lack of data limits prospects for comparative work. We report here on the characterization of 28 differentially expressed genes between SM and EO tissues in the mormyrid *Brienomyrus brachyistius*, which were identified using suppressive subtractive hybridization (SSH). Forward and reverse SSH was performed on tissue samples of EO and SM resulting in one cDNA library enriched with mRNAs expressed in EO, and a second library representing mRNAs unique to SM. Nineteen expressed sequence tags (ESTs) were identified in EO and nine were identified in SM using BLAST searching of *Danio rerio* sequences available in NCBI databases. We confirmed differential expression of all 28 ESTs using RT-PCR. In EO these ESTs comprise four classes of proteins: (1) ion pumps, including the alpha and beta subunits to Na^{+}/K^{+} ATPase, and a plasma membrane Ca^{+2} ATPase, (2) Ca^{+2} binding proteins S100, several parvalbumin isoforms, calcyclin binding protein, and neurogranin (3) sarcomeric proteins troponin I, myosin heavy chain, and actin-related protein complex subunit 3 Arcp3, and (4) the transcription factors enhancer of rudimentary homolog ERH and Myocyte Enhancer Factor 2A, MEF2a. Immunohistochemistry and western blotting were used to demonstrate the translation of seven proteins (myosin heavy chain, Na^{+}/K^{+} ATPase, plasma membrane Ca^{+2} ATPase, MEF2, troponin, and parvalbumin) and their cellular localization in EO and SM. Our findings suggest that several isoforms of muscle specific genes and the proteins they encode are expressed in mormyrid electric organ, unlike gymnotiforms, which may post-transcriptionally repress several sarcomeric proteins. In spite of the similarity of the physiology and function of EOs in mormyrids and gymnotiforms, this study indicates that the mechanisms of development in the two groups may be considerably different.

* Currently under review for publication in the *Journal of Experimental Biology*

Introduction

Darwin (1859) considered strongly discharging electric fishes as a case of special difficulty for his theory of natural selection, noting of their electric organs (EOs) that it was "impossible to conceive by, what steps these wondrous organs have been produced." Nearly 100 years would pass before Lissman (1951) recorded the first "weakly electric" discharges from the fish *Gymnarchus niloticus* and noted its importance as a solution to Darwin's difficulty. We now know that strongly discharging electric eels have evolved from weakly electric ancestors, and that EOs evolved originally for the purposes of electrolocation (Lissmann and Machin 1958) and electrocommunication (Mörhes 1957; Lissmann 1958). Today's remnants of Darwin's difficulty are an enduring and pervasive problem in biology; namely the steps by which novel physiological and anatomical features, such as electric organs, originate.

In his consideration of EOs, Darwin (1859) recognized that the diversity of electric organs among fishes had not arisen from a single common ancestor, but multiply through convergent evolution. We presently know of six independent origins of electric organs in fishes: torpedinoids, rajoids, mormyrids, gymnotiforms, siluriforms, and uranoscopids (Bass, 1986). In all but one family of gymnotiforms, the Apteronotidae[1], consisting of 64 species (Albert 2003), electric organs are derived during development from skeletal muscle tissue (Bass 1986; Bennett 1971). There is considerable variation between lineages (reviewed by Bass 1986; Bennett), particularly in the types of skeletal muscle (SM) that EOs originate from (e.g. eye muscles, trunk musculature, pectoral fin musculature), in the voltage of electrical discharge (approximately 10 mv in "weakly electric" mormyrids and gymnotiforms to 600 V in the

[1] We note here that the exceptional Apteronotidae have a myogenic larval organ which appears early in development, but is later replaced with a neurogenic adult electric organ. See Kirschbaum (1983).

strongly electric gymnotiform *Electrophorus electricus*), in their innervation (either in a restricted region in the case of most mormyrids, or diffusely over as in *E. electricus*, a single electrocyte face), and in the complexity of the electrocyte anatomy (ranging from simple sac-like electrocytes in *Torpedo* to those with complex stalk-like protrusions, as in mormyrids). In addition, the electrical discharge of marine species, including elasmobranchs and teleosts, is the result of acetylcholine receptors-mediated post-synaptic potentials, whereas in freshwater species, the electrical discharge results from activation of voltage gated sodium channels restricted to the EO plasma membrane.

Despite this considerable diversity, two groups of freshwater teleosts, the gymnotiforms of South America and mormyrids of Africa exhibit several convergently evolved traits. Gymnotiforms and mormyrids have convergently evolved two classes of tuberous electroreceptors one type that encodes EOD amplitude and a second that encodes timing information (Zakon 1986; Kawasaki 2005). Mormyrid and gymnotiforms have similar electrosensory behaviors, most famously the jamming avoidance response (Heiligenberg 1986). Both groups also have similar electromotor discharge patterns: both groups have independently evolved short "pulse type" electric organ discharges (EODs) with long intervals in between and essentially continuous, quasi-sinusoidal "wave type" discharges (Zupanc and Bullock 2005). Unlike many other electric fish, the electrocytes that comprise the EOs of both mormyrids and gymnotiforms produce spikes on both cell faces, and have complex anatomical features such as protrusions from the innervated membrane, termed "stalks" (Bennett 1971; Bass 1986). Convergence between mormyrids and gymnotiforms EOs has even been demonstrated at the molecular level; gymnotiforms and mormyrids have utilized the same sodium channel *Scn4aa* for producing EOD discharges (which arose by fish specific whole-genome duplication c.a. 200-

300 MYA). *Scn4aa* has been modified by positive selection leading to amino acid substitutions that affect sodium channel inactivation kinetics convergently, likely contributing to electric signal variation (Arnegard et al. 2010b).

It is notable that teleost fishes have evolved a wide variety of highly specialized muscle tissues aside from EOs, including sonic muscles capable of high-frequency contraction (e.g. plainfin midshpimen and toadfishes, Rome 2006), and heater organs for efficient thermogenesis (e.g. billfishes and swordfishes Block 1994). In each case, a suite of anatomical and physiological adaptations is required to produce these "novel" structures from muscle (Block 1994), though the molecular factors underlying the origins of these tissues remains poorly understood in all of these cases. It may be considerably advantageous; therefore, to consider electric organs as a model for such molecular and developmental processes due to the repeated evolution of EOs, particularly among gymnotiforms and mormyrids that exhibit remarkably similar electric organs.

Several studies over the past two decades have contributed to our understanding of gene expression and development in gymnotiform EOs, in particular with regard to the role of innervation (Cuellar et al. 2006; Kim et al. 2008; Kim et al. 2009; Kim et al. 2004; Unguez and Zakon 1998a, b; Zakon and Unguez 1999; Patterson and Zakon 1996, 1997). Comparative studies between gymnotiforms and mormyrids, however, are presently limited because no studies have described gene expression in the mormyrid EO, which is the focus of the present study. We were therefore motivated to consider a study design that would allow for the simultaneous identification of such genes and determination of their protein expression patterns. Considering the close developmental relationship between SM and EO, as well as the focus of previous studies in gymnotiforms on changes in gene expression between the two tissues, we took the

approach of using suppressive subtractive hybridization (SSH), a simple PCR-based method that selectively enriches for differentially expressed mRNAs, to identify unique patterns of gene expression in the EO and SM without *a priori* assumptions regarding their identities. Next, we provide data on the localization of protein products in SM and EO using immunohistochemistry and western blotting. Finally, we further examine the differential expression of a myogenic regulatory factor (detected using SSH), myocyte enhancer factor 2A (*MEF2a*). Following the presentation of our results, compare our results with previous findings in gymnotiforms, which indicates important differences in the developmental mechanisms underlying EO development. We conclude by briefly considering avenues for future comparative work between mormyrids and gymnotiforms.

Materials and Methods

RNA Isolation, Subtractive Hybridization, and Expressed Sequence Tag (EST) Identification

All specimens used were adult *Brienomyrus brachyistius* (Osteoglossiformes: Mormyridae; Gill 1862). Fish were housed in groups, and kept at 12h dark 12h light and fed live blackworms daily. All methods described are in accordance with Cornell's Animal Research and Education Committee policies. SM and EO tissues were collected from 10 adult *B. brachyistius* electric organs. Electric organs were dissected by removing skin and muscle from the caudal peduncle, excision of the electric organ and spinal column, and finally removal of the spinal cord by inserting a fine pin into the vertebral column. Trunk skeletal muscle was dissected from the same 10 individuals (approx. 2cm x 1 cm x 0.5cm, caudal to operculum, dorsal to lateral line; skin removed). Tissue was immediately frozen in liquid nitrogen, pulverized using mortar and pestle, and total RNA was extracted using TRIZOL solution (Invitrogen Corporation) according to the manufacturer's instructions. Extracted RNA was resuspended in RNAase free water

(water was treated with diethylpyrocarbonate then autoclaved), and then stored at -80˚C in aliquots until use.

Total RNA was PolyA+ purified using a FastTrack MAG mRNA isolation kit (Invitrogen Corporation). PolyA+RNA was reverse transcribed to cDNA using SuperScript III RT (Invitrogen Corporation) using oligo dT priming. Subtractive hybridization was then performed following the method of Rebrikov (2003), using EO as the tester and SM as the driver (EO library). A second library was also constructed using SM as the tester with EO as the driver (SM library). This SSH protocol resulted in two pools of PCR products representing mRNAs enriched in EO and SM respectively.

PCR products from EO and SM libraries were subsequently cloned into chemically competent *E. coli* using the TOPO TA cloning system (Invitrogen Corporation), resulting in many hundreds of colonies for each library. We randomly selected 130 colonies from the EO library and 36 colonies from the SM library for sequencing. These colonies were grown overnight in LB broth containing 50µg/ml ampicillin, and DNA was isolated and purified using a PureLink Miniprep kit (Invitrogen Corporation). Isolated and purified DNA was then submitted for Sanger sequencing via Cornell Core Laboratory Services, and resulting expressed sequence tags (ESTs) were assigned unique numbers. EST sequences were edited automatically to remove contaminating cloning vector sequence, and then identified by performing searches against entries for *Danio rerio* sequences in the NCBI nr database with BLASTx and BLASTn search strategies using default parameters: Matrix BLOSUM62; gap opening cost 11; gap extension cost 1; no low-complexity filtering. For DNA sequences: match reward 1, mismatch penalty -3, non-affine gapping costs wordsize 28. The e-value threshold for matches was set to 1e-6. Sequences with significant matches to database entries are listed in Tables 2-1 and 2-2. All edited

sequences were deposited in the NCBI dbEST database (Boguski et al, 1993), and are listed with their accession numbers in Appendix 1.

Reverse-Transcription PCR (RT-PCR)

To independently confirm differential expression of identified ESTs (Table 2-1, 2-2), primers were designed for reverse-transcription PCR (RT-PCR). RT-PCR reactions were performed using the RT-PCR OneStep method (Invitrogen Corporation) on total RNA isolated from either EO or SM (isolated as above). Thermal cycling conditions for all primer pairs were 55 ˚C (30 min), 94 ˚C (1min) followed by 25 cycles of 94 ˚C (15 sec), 60 ˚C (30 sec), 68 ˚C (1 min) and a final extension step of 68˚C (5 min). PCR products were resolved on a 1% agarose gel containing 1 μg /ml ethidium bromide. Results of each RT-PCR reaction are shown as negative gel images in Fig. 2-1.

Immunohistochemistry

Five additional *B. brachyistius* SM and EO tissues were sacrificed as described above. For each specimen, the caudal peduncle or ~1cm of axial muscle posterior to the operculum and dorsal to the lateral line was removed and flash frozen in liquid nitrogen-chilled isopentane (Cuellar et al., 2006), then mounted on a dry-ice chilled chuck using Cryo-M-Bed (Bright Instrument Company). Tissues were cut at 20μm using a cabinet cryostat onto freshly subbed slides and dried overnight at room temperature. Sections were ringed with PAP pens and washed 3 times using a 1x PBS wash buffer containing 0.3% Triton-X-100 (PBST). Sections were blocked in 5% goat serum at 4˚C for 1 hour, then washed 3 times for 30 seconds, and then 3 times for 10 minutes replacing the solution each time. Sections were incubated with primary antibodies (Table 2-3) diluted in wash buffer containing 5% normal goat serum for 1h at room temperature, in a humidified box. Sections were again washed as above, and then incubated with

Alexa-488 conjugated secondary antibodies (Invitrogen Corporation) diluted 1:200 in wash buffer containing 5% normal goat serum for 1h at room temperature in a humidified box. Sections were again washed as above, and then shaken dry. Slides were then mounted and coverslipped using VectaShield (Vector Laboratories, Inc.) and stored in the dark at -20˚C until analyzed. Slides were imaged on a Nikon Eclipse E600FN microscope equipped with a Diagnostic Instruments Camera and Spot 2.2 software (Diagnostic Instruments, Inc.). Fluorescent images were captured using the Nikon FITC-HYQ Filter Set (460-500nm excitation, 500nm dichromatic mirror and 510-560nm barrier filter). A DIC and fluorescent image was captured for each field of view. The two images were overlaid using the "Cover Overlay" function in Photoshop (Adobe Systems, Inc.; Macintosh version 10.0.1). Brightness and contrast were adjusted in the software to compensate for exposure differences.

Western Blotting

A single *B. brachyistius* was sacrificed and dissected as above to remove SM and EO tissues. Each tissue was frozen in liquid nitrogen, and then pulverized using a dry-ice chilled mortar and pestle. Tissues were then transferred to a glass homogenizer, and protein extractions were performed using a Total Protein Extraction Kit (Millipore). Proteins concentrations were quantified using a Bradford Assay Kit (Bio-Rad Laboratories, Inc.). Proteins samples were aliquoted and stored at -80˚C until use. 10µg of protein sample were combined 1:1 with Lammeli Buffer (BioRad Laboratories, Inc.) containing 5% β-mercaptoethanol and boiled at 95˚C for 3-5 min and directly applied to 8-15% gradient gels (BioRad Laboratories, Inc.) with the exception of preparations for Na^+/K^+ ATPase and Plasma Membrane Ca^{+2} ATPase proteins, were applied to gels without boiling. 30 µg of EO protein was loaded for western blotting of parvalbumin. Gels were run at 180V until bromothomol blue reached the end of the gel.

Polyvinylidene Fluoride (PVDF) membranes were wetted for 15 sec in methanol, and then submerged in ddH20 for 2 min. Proteins were transferred to a PVDF membrane using a Mini PROTEAN3 System (BioRad Laboratories, Inc.) for 1.5 hours at 100V in a cold room under constant circulation to prevent overheating, except parvalbumin, which because of its small size was transferred for only 45 min at 100V. Following transfer, PVDF membranes were blocked in 5% nonfat dried milk for 1h at room temperature on an orbital shaker. Following blocking, PVDF membranes were rinsed three times in PBS containing 0.05% Tween 20 (PBST) briefly. 5mL of primary antibody solution diluted in PBST containing 5% bovine serum albumin (BSA) was then directly applied the PVDF membrane, at room temperature for 1h with constant shaking for 1 hour. Membranes were then rinsed quickly three times in a large volume of PBST, followed by three 10-minute washes in PBST. HRP conjugated secondary antibodies (see Table 2-3 for concentrations) diluted in PBST containing 5% BSA was then applied to the membrane and incubated for 1h at room temperature. Membranes were again rinsed quickly three times in a large volume of PBST, followed by three 10 min washes in PBST. Membranes were then treated with Amersham ECL reagent (GE Healthcare, UK), then exposed to film for 1-10 min.

Myocyte Enhancing Factor 2 (MEF2) Cloning

A 3'UTR of the transcription factor MEF2A was differentially expressed in EO tissues (Table 2-1, Fig. 2-1). In fishes and other vertebrates, there are 4 known isoforms of the MEF2 gene, MEF2a-d. We attempted to obtain coding sequence of all MEF2 mRNAs expressed in EO and SM. Degenerate primers were developed to conserved sequences in fishes and other vertebrates for exons 1 (encoding amino acid sequence MGRKKIQI) and exon 6 (RKPDLRV) of MEF2a,c, and d. The forward primer was 5'-CCGAATTCATGGGRMGGAARAAGATWCAGATCA-3' and the reverse primer was 5'-CCAAGCTACTCTCARGTCTGGCTTGCG-3'. Additional degenerate

primers were generated for conserved residues in the more divergent MEF2B gene (EMQLKVK and KTDMQSWEEQSQGA). Degenerate primers for MEF2B were 5'-GAATTCGARATGCARYTSAAAGTVARA-3'and 5'- AAGCTCTCTGRTCCTCCCAGCTCTGCATG-3'. mRNA from EO and SM was reverse transcribed using an oligodT primer and the Superscript III Reverse Transcriptase protocol. The degenerate primer sets were used to amplify MEF2 cDNAs from SM or EO cDNA using the FailSafe PCR system. Cycling conditions for PCR were 94˚C (3 min) followed by 5 cycles of 95˚C (45 sec) 50˚C (45 sec) 72˚C (3min) and 35 cycles of 95˚C (45 sec) 55˚C (45 sec) 72˚C (3min), followed by a final extension step of 72˚C for 10 min.

The resulting amplified cDNAs were subcloned using the TOPO TA vector as described above. 10 colonies from SM and 10 colonies from EO were selected for sequencing using both the T7 forward and T3 reverse primers of the TOPO PCR2.1 vector. These sequences were edited by visual inspection, and then aligned using CLC Sequence Viewer (CLC Bio) to generate consensus sequences. Each MEF2 consensus sequence was then identified by BLASTn and BLASTx alignment to published *Danio rerio* MEF2 sequences. The edited consensus sequences were then deposited in the NCBI GenBank database. Lastly, MEF2a expression differences EO and SM were further evaluated between SM and EO by performing RT-PCR using primers generated to sequences conserved in all MEF2a transcripts detected in SM and EO. The forward primer was 5'-AGTACAACGAGCCACATGAGAGCA-3' and the reverse primer was 5'-TTGACAAAGCCGTTTCCTGCACTG-3'. Thermal cycling conditions for this primer pair was 94˚C (30 sec) followed by 35 cycles of 94˚C(30 sec), 55˚C (30 sec), 68˚C (1 min). PCR products were resolved on a 2% agarose gel containing 1 μg/ml ethidium bromide.

Results

Identification of Differentially Expressed Transcripts between EO and SM:

We obtained cDNA sequences from 152 of 166 selected clones after our subtractive hybridization efforts. Of these sequences, 117 were from EO and 35 were from skeletal muscle. The average length was 577 bp for all sequences. The cDNA sequence of each clone was given a unique identifier and submitted to dbEST maintained by the NCBI. The individual accession numbers for all sequences (HO702384-HO2394; HO702396-HO702414; HO702416-HO702420; HO702424-HO702463; HO702465-HO702542) are included as Appendix 1, accompanying this report. Of these sequences no *Danio rerio* matches were identified for 88 clones from EO and 9 clones from SM using either blastn and blastx search strategies, likely due to 3' UTR bias associated with the reverse-transcription priming strategy (Brooks et al. 1995). However, we were able to putatively identify 28 differentially expressed sequences: 19 were enriched in the EO library and 9 were enriched in the SM library. The matches of these identified EST sequences are summarized for EO (Table 2-1) and SM (Table 2-2) to *Danio rerio* entries in the NCBI databases.

To confirm differential expression of these identifiable ESTs, we performed RT-PCR using primers generated from each EST sequence (Table 2-1, Table 2-2). The results of each RT-PCR reaction, and the forward and reverse primers used are listed for each EST in Tables 2-1 and 2-2. Additionally, gel images of each RT-PCR reaction are presented in Figure 2-1. For the purposes of later discussion, we assigned putative functional roles based on known function of these genes in skeletal muscle: "Transcription Factors", "Ca^{+2} Binding", "Sarcomeric Proteins", "Ion Pump" and "Other" (Fig. 2-1). ESTs that were upregulated in EO are shown in blue, ESTs upregulated in SM are shown in grey.

Using the combination of a subtractive hybridization strategy and RT-PCR, we are able to demonstrate the differential expression of ESTs with different putative roles in the electric

organ. We detected the differential expression of 2 ESTs which matched *D. rerio* genes encoding transcription factors (MEF2a and Enhancer of Rudimentary Homolog), 6 genes encoding Ca^{+2} binding proteins (parvalbumins 1,2,9; S100, neurogranin, calcyclin), 4 ESTs matched *D. rerio* genes encoding sarcomeric proteins (myosin heavy chain, troponin T, Troponin I and arpc3), and 5 ESTs matched *D. rerio* genes encoding ion pump proteins (Na^{+}/K^{+} ATPase alpha 1b, 2a and Na^{+}/K^{+} ATPase beta 1a,1b, and plasma membrane Ca^{+2} ATPase 4). We also identified additional ESTs encoding prosaposin, cystatin B, myoglobin, creatine kinase, thymosin and dynein.

Spatial Distribution of Proteins is Similar but not Identical, between SM and EO

Cuellar et al (2006) described the existence of several mRNAs present in the EO of gymnotiforms, but their corresponding proteins were not found using both immunohistochemistry and western blotting, suggesting the existence of a post-transcriptional mechanism of regulating gene expression. Given the similar identities of the mRNAs detected by Cuellar et al. (2006) and the differentially expressed ESTs described in this study, we wished to determine if proteins products like those differentially expressed ESTs described above, were translated in mormyrid EO. We determined protein presence and distribution in the mormyrid EO and SM using widely cross reactive antibodies for a subset of 7 proteins: myosin heavy chain, Na^{+}/K^{+} ATPase, plasma-membrane Ca^{+2} ATPase, MEF2, troponin I, parvalbumin and tropomyosin (Table 2-3).

Because of the unique histology of the electric organ, we digress briefly to summarize the major anatomical features of the mormyrid electric organ. For a more detailed and thorough reviews of electric organs in a comparative context, we refer the reader to the excellent reviews of Bass (1986) and Bennett (1971). Shown in Fig. 2-2A are illustrations to orient the reader to

Table 2-1. Differentially Expressed Electric Organ EST sequences identified using NCBI BLAST.
A putative identification is assigned based on the top match to NCBI Blast searching against *Danio rerio* sequences (accession numbers and e-values are reported). N corresponds to the number of clones containing this sequence in our random sequencing of 166 total clones. For each sequence, a number is provided that corresponds to a RT-PCR reaction to confirm the differential expression of each EST. The results of this confirmation are summarized, and the forward and reverse primers are listed. The results of each RT-PCR reaction are labeled by number and putative identification in Fig. 2-1.

No.	Putative Identification	n	Matches	NCBI *Danio* Match	E	Differential?	RT-PCR Primer Set
2	3' end of the mef2a gene myocyte enhancer factor 2a	1	BBRACH_EO_6002	BX323877	3.0E-34	Yes	5'-TCATCCATGGCAACAAAGTCCAGC-3' 5'-TGTGCTGATACACACTCCTTGGGT-3'
3	enhancer of rudimentary homolog	1	BBRACH_EO_2003	NP_571303	7.0E-07	Yes	5'-AGCCCTACAACAAGGACTGGATCA-3' 5'-GGCCGAGGTACAATGTCAAACCAA-3'
6	parvalbumin 9	1	BBRACH_EO_2006	NP_891983	1.0E-23	Yes	5'-GAGGTACTGAGCAGAAGGCAGAAA-3' 5'-GCATTGACGATGATGACAGCGGTT-3'
7	S100 calcium binding protein, beta	3	BBRACH_EO_1020; BBRACH_EO_1021; BBRACH_2008	XP_002666278	2.0E-29	Yes	5'-TGCTTGCTTCACAGCAGCAGTTAG-3' 5'-AGGAGTTCATGACCTTCGTCACCA-3'
8	neurogranin	1	BBRACH_EO_6012	ACJ64077	9.0E-25	Yes	5'-CAACCTGATTGGGCCAAGAAGCAA-3' 5'-TAAGGACATCATGGACATCCCGCT-3'
9	calcyclin binding protein	1	BBRACH_EO_2012	CAQ14532	4.0E-44	Yes	5'-AATTATCCGACTGGTCCCATCCGT-3' 5'-ATTGGCGAACAGATCACCGAGCTA-3'
10	myosin, heavy polypeptide 6, cardiac muscle, alpha-like	1	BBRACH_EO_4028	XP_002667378	3.0E-50	Yes	5'-ACGTGAGCTGGAATCTGAGGTTGA-3' 5'-TCTTGGCTCTCAGCTTGTTGACCT-3'
13	troponin I, skeletal, fast 2b.1 isoform 1	1	BBRACH_EO_4017	NP_001129964	2.0E-40	Yes	5'-ATGAAGGGCAAGTTCAAGAAGCCG-3' 5'-AACTGAAACCAGGCAACATCCACC-3'
14	arpc3-like	1	BBRACH_EO_2011	AM422121	6.0E-06	Yes	5'-TGTGTGTGCGCGGCCATTCTTATT-3' 5'-GCCGAGGTACCAACTGTTCCATTT-3'
15	ATPase, Na+/K+ transporting, alpha 1b	2	BBRACH_EO_4019; BBRACH_EO_6034	CAQ13999	3.0E-19	Yes	5'-ATGCAGCCTTTGGAAGCTTTAGCG-3' 5'-TCTTCCAGCAACACCACATCTCCT-3'
16	ATPase, Na+/K+ transporting, alpha 2a	1	BBRACH_EO_4011	CAQ14308	5.0E-45	Yes	5'-AGGTCCGGAACAACAATGAACTGG-3' 5'-AGTCTCAGCGAAGAGGCCAAAGAT-3'
17	ATPase, Na+/K+ transporting, beta 1a	2	BBRACH_EO_6008; BBRACH_EO_1019	BC045376	1.0E-11	Yes	5'-ACTGCACTCCACGGAAACCTACTT-3' 5'-ACTGCACTCCACGGAAACCTACTT-3'
18	ATPase, Na+/K+ transporting, beta 1b	1	BBRACH_EO_4025	XP_002662295	5.0E-32	Yes	5'-TGTGCTATTTCTGAGAGCCGAGGT-3' 5'-ACAAACAAGAGGGATGAGGATGCC-3'
19	ATPAse, Ca++ transporting, 4	2	BBRACH_EO_1003; BBRACH_EO_1006	ACB45514	3.0E-30	Yes	5'-GGCAGGTACAGGAGCAGAAGTTT-3' 5'-GGGTCCTTATGCAGTGCTTT-3'
20	prosaposin	1	BBRACH_EO_6004	AAL54381	8.0E-13	Yes	5'-CCGAGGTACCCTGTAGAAATACCA-3' 5'-GCACTGCAAACGTCATGTGTGGAA-3'
21	cystatin B	2	BBRACH_EO_4014; BBRACH_EO_4016	NP_001096599	5.0E-32	Yes	5'-ATGCAGTTCAAGCTTTCTGCCAGC-3' 5'-AGTCACCATGTTATGCGGAGGACT-3'
22	myoglobin	2	BBRACH_EO_4013; BBRACH_EO_6027	NP_956880	2.0E-51	Yes	5'-AGCTGTTCCCTAAGTTTGTCGGGA-3' 5'-AACCGACTTCCTTGTAGACAGCGT-3'
24	thymosin, beta 4-like	1	BBRACH_EO_6035	XM_002665906	1.0E-05	Yes	5'-AGCCACGATTGGCTTGGATTAGAG-3' 5'-GGTACTTACTCTACCACTTCCACTCC-3'
25	dynein light chain roadblock-type 1	1	BBRACH_EO_4007	NP_957482	1.0E-40	Equivocal	5'-TCCAATGGATCCTGACCACGAAGA-3' 5'-ACACTGAAACGGATCCAGACCCAA-3'

Table 2-2: Differentially Expressed Skeletal Muscle EST sequences identified using NCBI BLAST.
A putative identification is assigned based on the top match to NCBI Blast searching against *Danio rerio* sequences (accession numbers and e-values are reported). N corresponds to the number of clones containing this sequence in our random sequencing of 166 total clones. For each sequence, a number is provided that corresponds to a RT-PCR reaction to confirm the differential expression of each EST. The results of this confirmation are summarized, and the forward and reverse primers are listed. The results of each RT-PCR reaction are labeled by number and putative identification in Fig. 2-1. * We were unable to synthesize primers to differentiate between this and other similar forms despite sequence differences. Myosin heavy chain 4 was not tested for differential expression due to an inability to obtain effective RT-PCR primers.

No.	Putative Identification	n	Matches	NCBI *Danio* Match	E	Differential?	RT-PCR Primer Set
1	3' end of the mef2a gene myocyte enhancer factor 2a	1	BBRACH_SM_3011	BX323877	1.00E-40	Yes	5'-GTCGCCTTGTAAACTTGGCGGTAA-3' 5'-GGCTAAGCTTGTGGAACACACACA-3'
4	parvalbumin isoform 1c	6	BBRACH_SM_3014; BBRACH_SM_3019; BBRACH_5001; BBRACH_SM_7002; BBRACH_SM_7008; BBRACH_SM_5002	NP_997948	2.00E-36	Yes	5'-TGGTTCCCATGGAGAGTCCAAAGT-3' 5'-AACCCAACATAATGGCCTTCGCTG-3'
4	parvalbumin isoform 1b	2	BBRACH_SM_3003; BBRACH_SM_3006	NP_956506	6.00E-19	Yes*	-
5	parvalbumin 2	8	BBRACH_SM_3001; BBRACH_SM_3010; BBRACH_SM_3012; BBRACH_SM_3013; BBRACH_SM_3015; BBRACH_SM_5005; BBRACH_SM_5007; BBRACH_SM_7006	NP_571591	1.00E-48	Yes	5'-AACCCAACATAATGGCCTTCGCTG-3' 5'-TGGTTCCCATGGAGAGTCCAAAGT-3'
11	myosin heavy chain b	4	BBRACH_SM_3016;BBRACH_SM_5006;BBRACH_7001; BBRACH_SM_7003	XP_001339206	4.00E-75	Yes	5'-AGACGTGGAGCCGATGCTGTTAAA-3' 5'-TCTTGGCTCTCAGCTTGTTGACCT-3'
11	myosin, heavy polypeptide 6, cardiac muscle, alpha-like	4	BBRACH_SM_3004;BBRACH_SM_5004; BBRACH_SM_3018; BBRACH_SM_XXXXX	XP_002667378	3.00E-50	Yes*	-
12	troponin T, skeletal, fast T3b	1	BBRACH_SM_7004	AAH65452	1.00E-26	Yes	5'-TCAGCTTTCTTCCTGACGTCTGCT-3' 5'-AGGGAGCTCACTTCTTTCAGCCTT-3'
23	creatine kinase b, Ckmb	2	BBRACH_SM_3002; BBRACH_SM_3020	NP_001099153	8.00E-53	Equivocal	5'-CACACGGTTGGCATGGTTACTTGT-3' 5'-TTCATGTGGAACGAGCACATTGGC-3'
	myosin heavy chain 4	1	BBRACH_SM_3007	CAM14143	5.00E-27	Not Tested	

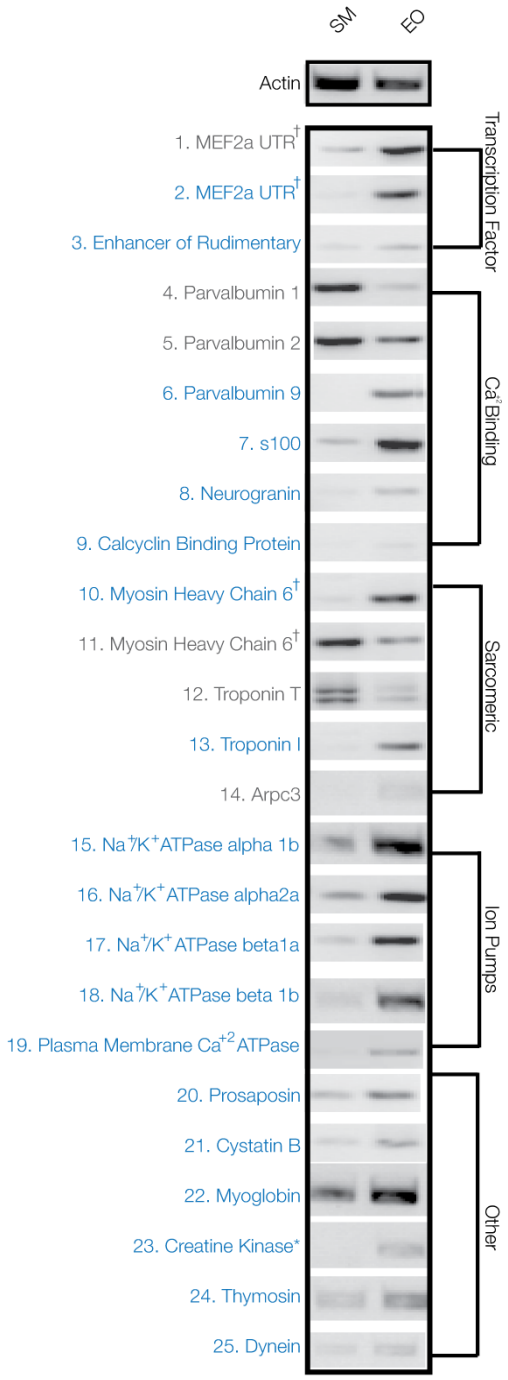

Figure 2-1: RT-PCR of ESTs Identified via Suppressive Subtractive Hybridization.
Negative gel images of 25 RT-PCR reactions performed confirm differential expression of ESTs detected by SSH (See Table 2-1, 2-2, Appendix 1). For each RT-PCR reaction, the number listed corresponds to primers and sequence information listed in Table 2-1 or Table 2-2. RT-PCR products are grouped by putative cell functions (explained in methods). Sequences labeled in blue are upregulated in EO, sequences in grey are upregulated in SM when compared to actin control. † indicates ESTs that matched different regions of the same *Danio rerio* sequence during BLAST searching (see methods). * indicates ESTs that SSH revealed as differentially expressed in one library that were later found via RT-PCR to be differentially expressed in the opposite library.

Antigen	Antibody Name	Host	Expected Size	WB Conc.	IHC Conc.
MEF2 (*Homo sapiens)*	C-21	Rabbit	40-65 kd	1:50	1:50
Myosin Heavy Chain (*Gallus gallus)*	MF20	Mouse	200 kd	1:5000	1:1000
Na/K+ ATPase alpha (*G. gallus)*	a5	Mouse	113 kd	1:100	1:10
Parvalbumin (Frog)	MAB1572	Mouse	12kd	1:1000	1:50
Tropomyosin (*Gallus gallus*)	CH1	Mouse	36 kd	1:200	1:100
Troponin I (*Bos Taurus*)	MAB1691	Mouse	27.6 kd	1:250	1:100
PMCA (*Homo sapiens*)	5F10	Mouse	150 kd	1:1000	1:500

Table 2-3: Antibodies for Immunohistochemistry and Western Blotting.
Antigen and antibody names are listed for each antibody used in this study, along with antibody host and expected size of protein detected, determined by NCBI entries for *D. rerio* proteins in NCBI databases. Concentrations of antibody used in western blotting (WB) and immunohistochemistry (IHC) are listed. MF20, a5 and CH1 were obtained from the DSHB (University of Iowa, USA). C-21 was obtained commercially (Santa Cruz Biotechnology, Santa Cruz, CA USA), as were MAB1691 and MAB1572 (Millipore, Billerica, MA USA). Antibody 5F10 was generously provided by E. Strehler and A. Filoeto (Mayo Clinic, USA).

the major anatomical features of the electric organ. The electrocytes of *Brienomyrus brachyistius*, are doubly penetrating with posterior innervation (DPp; see Sullivan et al. 2000; Hopkins, 1999b). The 7μm sagittal section in the center of Fig. 2-2A was made from a plastic embedded specimen and stained with toluidine blue (see Gallant et al. 2011) for detailed histological methods). After toluidine blue staining, each electrocyte appears as a blue stripe (**E**) surrounded by loose, pink-stained connective tissue, and is bounded from neighboring electrocytes by a connective tissue septum (**C**) on the anterior and posterior side. Each electrocyte face contains multiple nuclei (**Nu**), and the center of the electrocyte contains filamentous material (**F**) between the anterior and posterior membranes, which has been shown in greater detail using electron microscopy by Bass et al. (1986). Based on these micrographs, Bass et al. (1986) concluded that this was a disorganized layer of myofilaments, rather than the typical parallel arrangement of myofilaments found in SM. Another key feature of the mormyrid electrocyte is an elaborate stalk system: microstalklets (**M**) emerge from the posterior face of each electrocyte, fuse and pass through penetrations (**P**) to the anterior side. Further fusion into a larger diameter stalk (**S**) occurs on the anterior side. The stalk passes briefly posterior once more, where it is innervated (**Ne**).

We tested for 3 sarcomeric proteins found in our SSH screen using immunohistochemistry with antibodies listed in Table 2-3 to identify the composition of the central filamentous material found in the electrocyte. As expected, we found that myosin heavy chain (MHC, Fig. 2-2B) was uniformly distributed across SM muscle fibers. In the EO, expression of MHC was confined to a single vertical stripe between the anterior and posterior membranes of the electrocyte (F). We detected no MHC expression in the stalk system (S). Tropomyosin (Fig. 2-2B) staining was also widespread in SM tissues, but it was restricted to a

Figure 2-2: Anatomy of EO and sarcomeric protein localization in EO and SM.
A. This panel provides a brief overview of the major anatomical features of the electric organ. Shown on the left is a diagram of a single *Brienomyrus brachyistius* electrocyte, which have doubly penetrating stalks with posterior innervation (see Sullivan et al., 2000; Hopkins, 1999b). Shown in the center is a single 7µm sagittal section made from a plastic embedded specimen, stained with toluidine blue (see Gallant et al., 2011 for full method). On the right is an illustration of a single electrocyte as it appears in the toluidine blue stained electric organ, and in Fig. 2-2B. Boxes indicate comparable areas in each of the illustrations. **B.** Immunohistochemistry was performed using primary antibodies for 3 sarcomeric proteins: Myosin Heavy Chain, Troponin I and Tropomyosin, which are listed in Table 2-3. The images presented in this figure are overlays of DIC and fluorescent images (see methods). Illustrations are provided to summarize the localization of each protein. For all images, anterior is left, posterior is to the right. Abbreviations used are: **E** - electrocytes **C** - connective tissue septa **Nu** - nuclei, **F**- myofilament material between the anterior and posterior membranes, **M**- microstalklets **P**- penetrations **S** -stalk **Ne** – motor neuron.

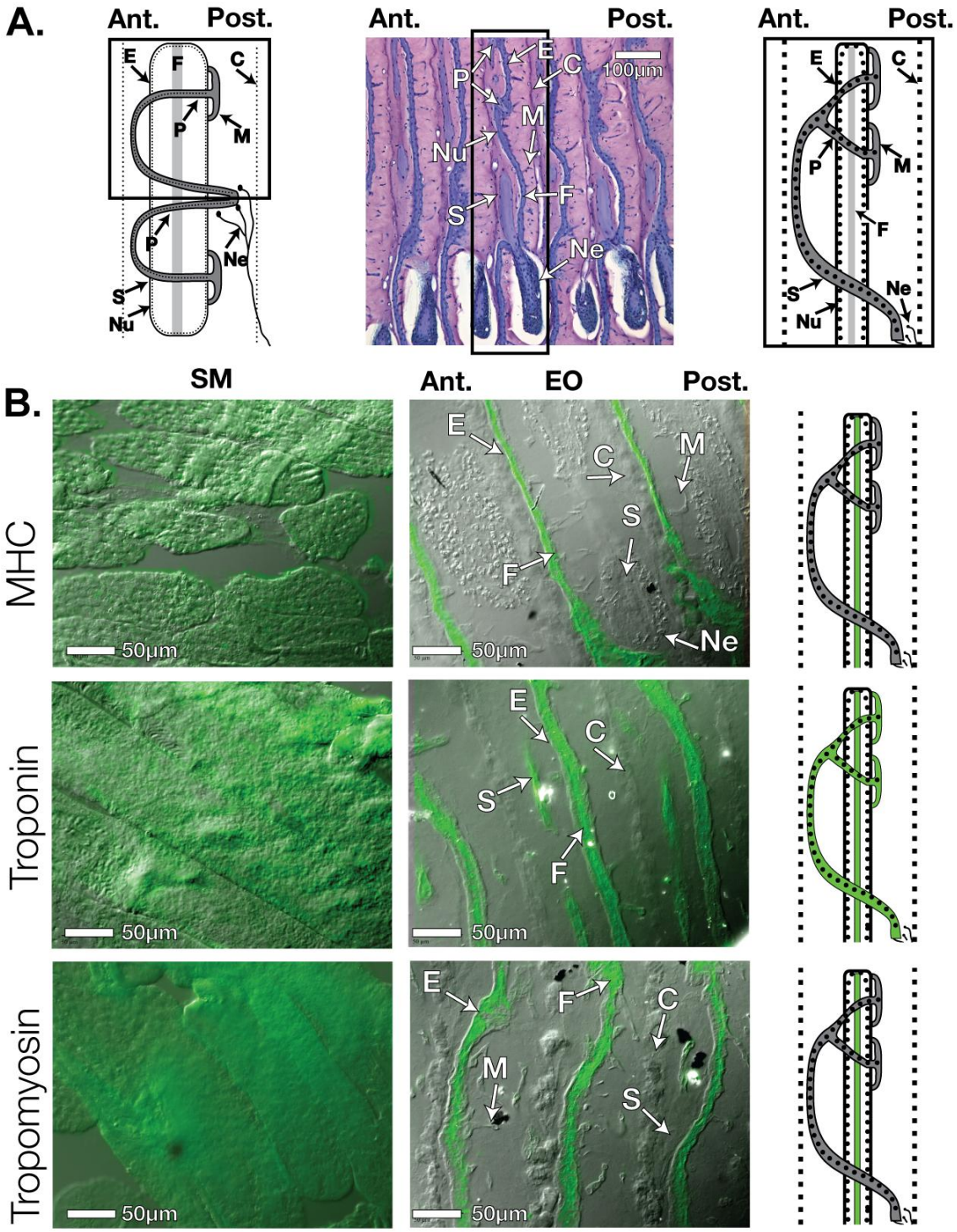
A.
Ant.
Post.
E
F
C
P
M
Nu
Ne
S
100µm
B.
SM
EO
MHC
Troponin
Tropomyosin
50µm

distribution to that of MHC, running in a longitudinal filament between the anterior and posterior faces. Contrasting with MHC, troponin I is also clearly visible in the stalk system.

We also performed IHC to localize additional proteins like those identified in our SSH screen. Plasma membrane Ca^{+2} ATPase (PMCA; Fig. 2-3) staining was visible in the sarcolemma of SM, but in EO, staining was present in both electrocyte faces *and* the stalk system. MEF2 (Fig. 2-3) staining was localized to nuclei (**Nu**) in both SM and EO tissues. An increased number of larger, more spherical nuclei (*vs.* SM) are visible in both the stalks and electrocytes in the EO. Na^{+}/K^{+} ATPase alpha (Fig. 2-3) staining was localized to the sarcoplasm in SM and to the anterior and posterior faces of the electrocyte. Again, no staining of the stalk system was visible. Parvalbumin staining (Fig. 2-3) is abundant in SM cytoplasm, as well as in EO electroplasm, stalks, and in motor neurons (**Ne**) innervating the electrocyte.

To summarize, we found evidence that proteins like the seven differentially expressed ESTs described above (myosin heavy chain, Na^{+}/K^{+} ATPase, plasma-membrane Ca^{+2} ATPase, MEF2, troponin I, tropomyosin, and parvalbumin) were translated in *both* EO and SM using immunohistochemistry (Figs. 2-2, 2-3). We emphasize that the antibodies utilized (Table 2-3) recognized highly conserved epitopes across a wide variety of species, and therefore antibodies were not selective for specific isoforms detected during SSH and RT-PCR above, and were not expected to exhibit differential presence in SM and EO. Our results therefore should be viewed as demonstrating the presence of all seven proteins in both EO and SM, as well as their spatial distribution in muscle fibers vs. electrocytes. The spatial distribution was generally quite similar

Figure 2-3: Protein localization in EO and SM.
Immunohistochemistry was performed using primary antibodies for 4 additional proteins: Plasma Membrane Ca^{+2} ATPase (PMCA), Myocyte Enhancing Factor 2 (MEF2), the α subunit of the Na^{+}/K^{+} ATPase, and parvalbumin, which are listed in Table 2-3. The images presented in this figure are overlays of DIC and fluorescent images (see methods). Illustrations are provided to summarize the localization of each protein. For all images, anterior is left, posterior is to the right. Abbreviations used are: **E -** electrocytes **C** - connective tissue septa **Nu** - nuclei, **F-** my filament material between the anterior and posterior membranes, **M**- microstalklets **P-** penetrations **S** -stalk **Ne** – motor neuron. See Fig. 2-2 for overview of anatomical features in the EO.

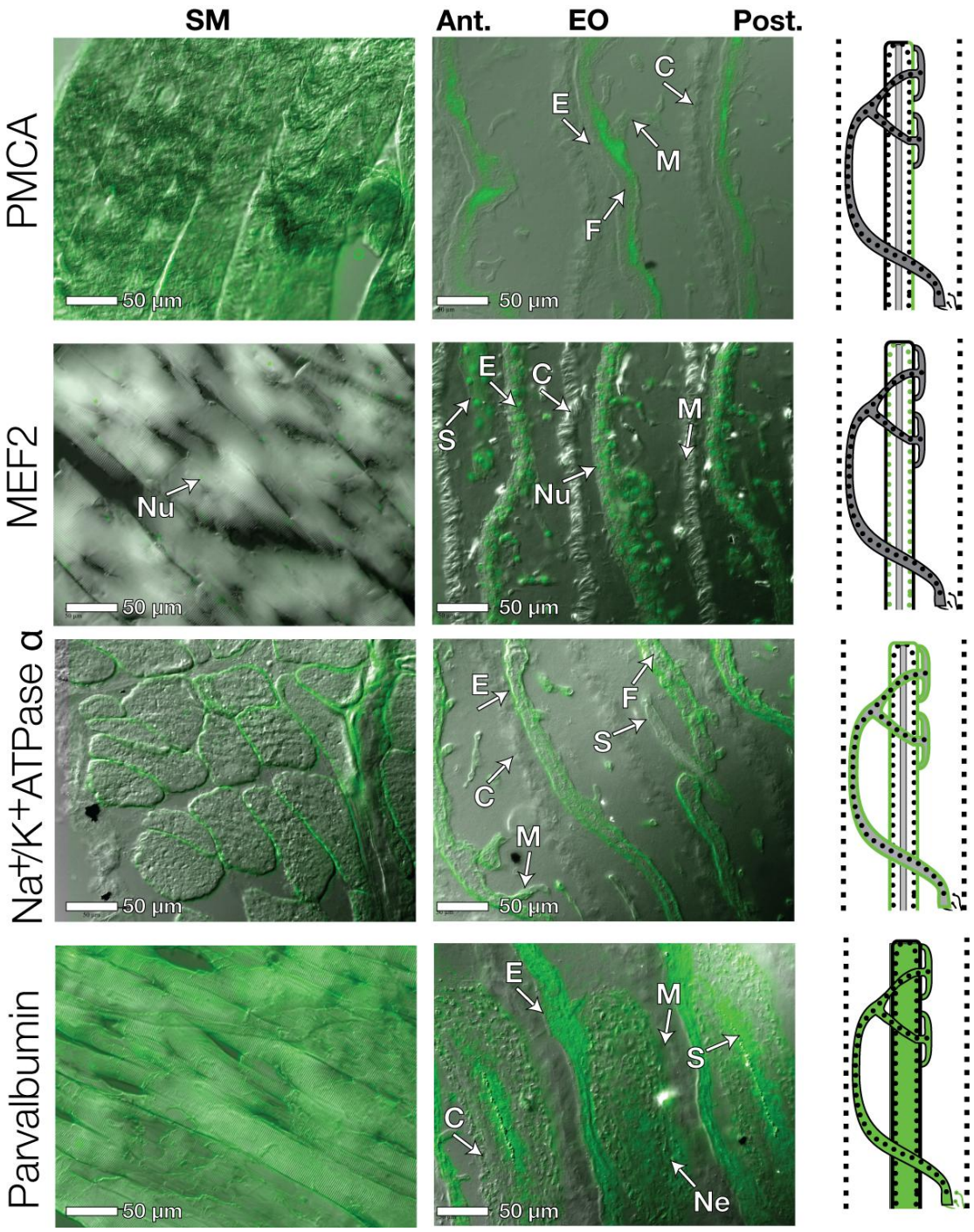
SM
Ant.
EO
Post.
PMCA
MEF2
Na+/K+ATPase α
Parvalbumin
50 µm
E
C
M
F
S
Nu
Ne

center filament between the anterior and posterior faces of the electrocyte, like that of MHC. No staining was observed in stalk materials. Troponin I (Fig. 2-2B) staining was abundant in myofibrils of the SM, and was present in a similar spatial between EO and SM (i.e. ion pumps were localized to plasma membrane, transcription factors in nuclei, etc.), with some notable exceptions in the distribution of proteins involved in SM contraction (i.e. MHC, troponin I and tropomyosin).

Western blotting reveals differences in abundance of some proteins between SM and EO

Western blots were also performed to confirm that the selected antibodies recognized proteins of the expected size. In addition, western blots allowed some insight into relative amounts of protein between tissues, presuming the epitope was equally well recognized in both tissue types. Overall, western blotting results (Fig. 2-4) indicate that proteins detected using IHC (Fig. 2-2, 2-3) recognized proteins of expected sizes (Table 2-1).

For all western blots, 10μg of protein homogenate was loaded for both SM and EO, except for parvalbumin, where 30μg of EO homogenate was required to detect a band, presuming that the antibodies recognized the epitopes with the same affinity, a 3-4 fold reduced concentration in the concentration of parvalbumin in the EO. Comparing the intensity of bands between tissues, myosin heavy chain, parvalbumin, and tropomyosin were also more concentrated in SM than in EO, whereas Na^+/K^+ ATPase α, plasma membrane Ca^{+2} ATPase, and MEF2 seemed to be in approximately equal concentrations in both tissues.

Finally, we note slight differences in the sizes of protein bands between Na^+/K^+ ATPase α and MEF2a. One band detected in SM for Na^+/K^+ ATPase α (90 kd), was not present in EO, and a second band (99 kd) was present in both EO and SM. Western blotting for MEF2 protein indicated the presence of a large (120kd) form in SM that was absent in EO, and a smaller form

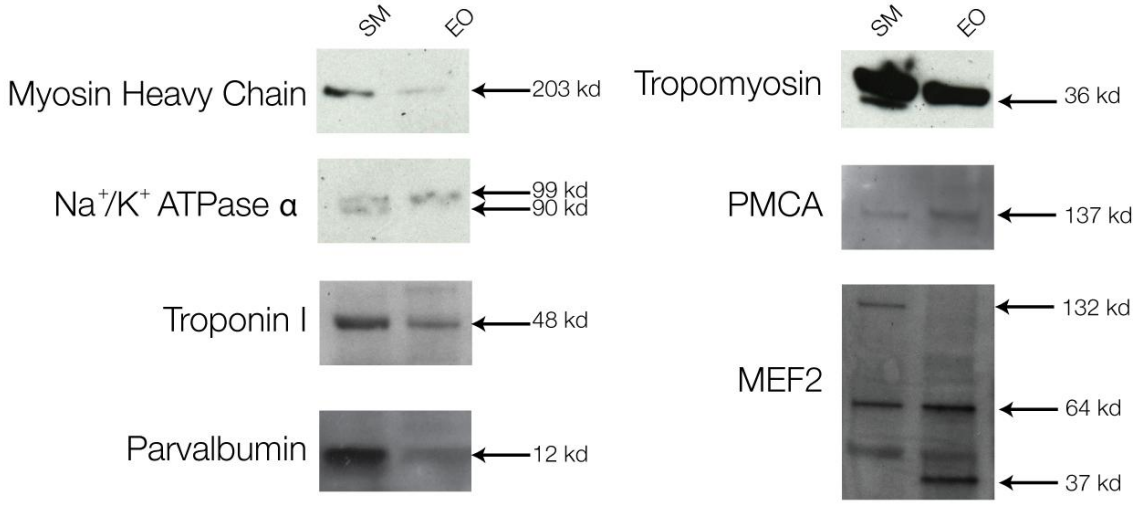

Figure 2-4: Western Blots of Proteins from Electric Organ and Skeletal Muscle.
For each of seven proteins, western blotting was also performed using 10µg SM and EO protein extracts (see Methods). For parvalbumin 3x the protein was loaded for EO than was for SM. Size markers are listed to the right, expected sizes for each antibody are listed in Table 2-3 along with primary antibody concentrations.

(36kd) that was absent in SM.

MEF2a is differentially expressed in EO vs. SM

MEF2 is an important transcription factor regulating the development of muscle fibers (Black and Olson 1998). In vertebrates, there are four MEF2 genes, designated MEF2a-d. The detection of differentially expressed, conserved 3'UTRs of the MEF2a transcription factor (Fig. 2-1), and evidence of potentially different MEF2 isoforms from western blotting (Fig. 2-4) prompted us to clone coding sequence of transcribed MEF2 genes to determine if this important transcription factor was differentially expressed between SM and EO.

We successfully cloned transcripts of MEF2 genes in EO and SM: based upon alignment to NCBI *Danio rerio* sequences, we determined that these sequences matched MEF2a (Fig 2-5), and MEF2c (Appendix 1, Figure A-1). We were unable to detect MEF2b or MEF2d expression in SM or EO. DNA sequencing revealed three different MEF2a transcripts: one unique MEF2a transcript was expressed in SM (*B.b.* MEF2a SM1), and three unique MEF2a transcripts were expressed in EO (*B.b.* MEF2a EO1, 2, or 3 Fig 2-4b). One of the forms (*B.b* MEF2a 3; Fig 2-5a) lacked an approximately 100 bp region, while *B.b.* MEF2a1 and *B.b.* MEF2a2 contained this region, but had divergent sequences over the region between 267-401bp. This region corresponds to exon 5 of the *Danio rerio* MEF2a gene. We have also identified three MEF2c transcripts, two that were expressed in SM (Appendix 2, *B.b.* MEF2c SM1, 2) and one expressed in EO (Appendix 2, *B.b.* MEF2c EO1). All MEF2 sequences detected have been uploaded to NCBI Genbank with the accession numbers JN107727-JN107733. To determine the relative abundance of the three MEF2a isoforms in EO, RT-PCR was performed using primers generated to conserved sequence of all MEF2a transcripts sequenced (primer locations shown Fig 2-5a, boxes).

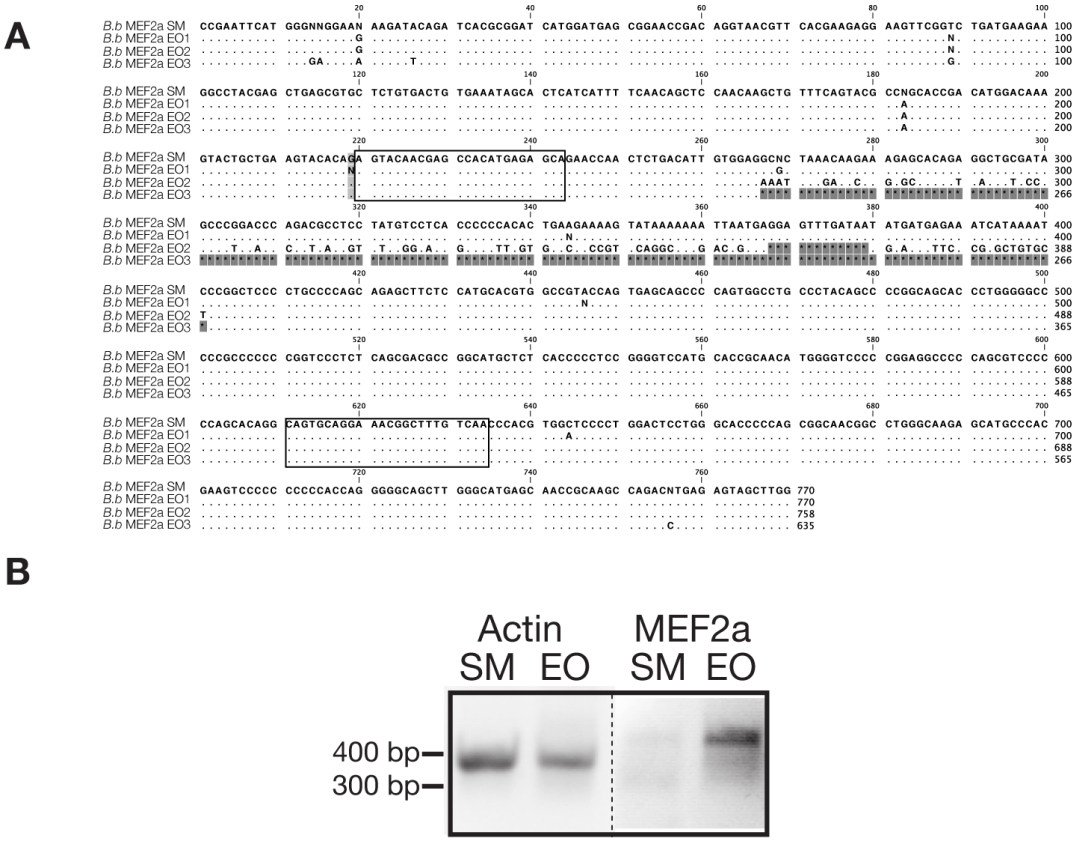

Figure 2-5: Differential Expression of MEF2A

The discovery a differentially expressed 3' MEF2a UTRs in EO prompted further subcloning and sequencing of all MEF2 genes expressed in EO and SM (see methods). **A)** Subcloning revealed multiple sequences of MEF2a expressed in SM (B.b MEF2a SM1) and EO (B.b. MEF2a EO1-3). These sequences were largely similar except for a region from 264-401bp that was variable, corresponding to Exon 5 of MEF2a in *D. rerio*. One of the transcripts (B.b. MEF2a EO3) completely lacked this region (grey squares indicate "missing" bases). Using MEF2a specific primers (open boxed regions) we amplified all MEF2a transcripts expressed in EO to determine which of these sequence variants were expressed in EO and SM. **B)** RT-PCR comparing actin and MEF2a expression reveals the upregulation of MEF2a in EO. The PCR products are consistent with *B.b.* MEF2a EO1 and EO2 and MEF2a SM1 from SM. Using the above primers, 35 cycles failed to produce an EO3 sized splice variant.

A smeared band between 420-400bp (Fig 2-5b) is consistent with *B.b.* MEF2a EO1 (expected size 414 bp) and *B.b.* MEF2a EO2 (expected size 402 bp), rather than *B.b.* MEF2a EO3 (expected size 280bp). Using the same cycling parameters, we detected a very faint band at this expected size range in SM (Fig 2-5b), indicating differential expression of MEF2a between the tissues.

Discussion

Subtractive Hybridization Results

In this study, we have shown evidence for the differential expression of 28 genes between mormyrid EO and SM. We suspect that these 28 genes represent only a fraction of the total number of differentially expressed genes between SM and EO. We base this conclusion on: 1) roughly the same proportion of new differentially expressed ESTs were found in each batch of randomly selected clones submitted for sequencing, and 2) that most transcripts (particularly in the EO) were represented only once.

Our strategy to identify these differentially expressed genes utilized a novel approach as applied to electric organ gene discovery, suppressive subtractive hybridization (SSH). Previous approaches to characterizing the molecular differences between SM and EO in gymnotiforms have largely relied on *a priori* assumptions regarding the identities of specific genes that might be differentially expressed (Patterson and Zakon 1996, 1997; Cuellar et al. 2006; Kim et al. 2008; Kim et al. 2009; Kim et al. 2004; Unguez and Zakon 1998a, b; Zakon and Unguez 1999). Unlike these prior approaches, our use of the SSH technique allows for the construction of a dataset for which fewer assumptions have been made. As such, our dataset contains evidence of differential expression in closely related genes (e.g. parvalbumin and myosin isoforms expressed in SM and EO), which may not have been detected using a candidate gene approach.

What types of genes are differentially expressed between EO and SM?

We consider some of the differentially expressed genes identified in *Brienomyrus brachyistius* in the context of what is known about their function in SM and EO tissues in other vertebrates. We conclude by briefly considering this data in terms of the growing molecular and developmental data that are becoming available for weakly electric fish.

Transcription Factors - Our subtractive hybridization revealed two differentially expressed transcription factors in the adult electric organ: enhancer of rudimentary homolog (ERH), and the 3'UTR of the MEF2a gene. ERH is a highly conserved gene among vertebrates (Gelsthorpe et al. 1997; Pogge von Strandmann et al. 2001). Studies have implicated its function in transcriptional regulation for pyridine biosynthesis (Wojcik et al. 1994) and cell cycle repression (Gelsthorpe et al. 1997). More recently, ERH was found to directly interact with a DNA replication factor (Lukasik et al. 2008), however little is ultimately known about the role of this gene in development.

Following the early specification of muscle progenitors, the combined actions of the muscle regulatory factors (MRFs) MyoD and MEF2 are responsible for the transcriptional activation of muscle specific genes (Black and Olson 1998). Indeed, MEF2a has been demonstrated to be critical in the development of posterior somites in fish, from which electric organs originate in mormyrid (Denizot et al. 1982). Knockdown of MEF2a in *D. rerio* induces apoptosis of posterior somites during development (Wang et al. 2006), whereas MEF2 c/d controls thick filament assembly (Hinits and Hughes 2007). Following muscle development, MEF2s continue to interact with signaling pathways (e.g. MAPK and Ca^{+2} signaling) to regulate gene expressions in response to changes in electrical activity (Black and Olson 1998). Differential expression of these transcription factors may therefore provide an attractive

hypothesis to explain physiological and morphological differences between electric organs and skeletal muscle. A series of studies (Kim et al. 2004: Kim, 2008; Kim et al. 2009) examined the transcriptional patterns and roles of several MRFs and their co-factors including *MyoD, myogenin, myf5, MRF4, MEF2C, Id1* and *Id2* in the gymnotiform *Sternopygus macurus.* These studies have found little differences in expression levels of between skeletal muscle and electric organ, and that several of the myogenic regulatory factors cloned from *S. macurus* retain their ability to induce normal muscle development in mouse cultured myoblasts (Kim et al. 2008; Kim et al. 2009).

We found no evidence of differential expression of any of these previously analyzed MRF genes in mormyrids, but did detect differential expression of the 3'UTR of the MEF2a gene in our subtractive hybridization screen (Table 2-1). Because of the aforementioned importance of MEF2 transcription factors in the regulation of muscle phenotype, we developed degenerate primers to clone a protein-coding portion of this gene from SM and EO. We determined that the MEF2a and MEF2c genes are expressed in EO and SM, and did not detect the expression of MEF2b or d. Remarkably, like in gymnotiforms, we see little evidence of differences in MEF2C transcription, but found evidence of MEF2a upregulation in EO tissues (Fig. 2-5a), as well as some potential evidence of alternative splicing in MEF2a between SM and EO tissues (Fig. 2-5b). Intriguingly, the MEF2A 3' untranslated region (UTR), detected as differentially expressed in EO and SM, (see Table 2-1, Fig. 2-1) may have a role in these expression differences between the two tissues: Black et al. (1997) demonstrated that the MEF2A 3'UTR (which is highly conserved among vertebrates) acts as a cis-acting translational repressor, and may confer tissue specific translational activity.

Na^+/K^+ ATPases- Given that EOs are electrically excitable tissues, there has been a great deal of

attention devoted to differentially expressed proteins involved in ion transport and permeability in EO vs. SM (i.e. Zakon, et al, 2006). In the present study, we did not detect any differentially expressed ion channels, however we did detect clear differential expression of transcripts for Na^+/K^+ ATPase subunits α1 and α2, two Na^+/K^+ ATPase β subunits, and a plasma membrane Ca^{+2} ATPase in EO when compared to SM (Fig. 2-1, Table 2-1; see discussion below). When examining the relative amounts of Na^+/K^+ ATPase α protein between SM and EO (Fig. 2-4), however, there is no clear difference in the relative amount of protein abundance, suggesting the two tissues express unique forms of Na^+/K^+ ATPase subunits.

The functional consequences of differential expression of Na^+/K^+ ATPase subunits are presently unclear. Lowe et al. (2004) demonstrated that Na^+/K^+ ATPase subunits α1 and α2 are heterogeneously distributed between the innervated and non-innervated faces of the EO of the strongly electric gymnotiform *Electrophorus electricus*, using both oubain sensitivity, western blotting, and immunohistochemistry. The two faces of *E. electricus* electrocytes are known to differ in terms of their specific resistance (Bennett, 1971), and therefore different alpha subunits may be associated with changes in Na^+ or K^+ permeability between these two faces. Bell et al. (1976) noted similar differences in the membrane resistivity of the anterior and posterior faces of mormyrid electrocytes. Along these lines, because specializations for current production have lead to a much lower specific resistance of electrocytes vs. skeletal muscle (Bennett 1971) we suspect that the differential expression of Na^+/K^+ ATPase are attributable to these specializations for current production, namely increased ion permeability.

Intriguingly, the amount of Na^+/K^+ ATPase α subunit protein did not appear to vary between SM and EO tissues (Figs. 2-3, 2-4), which suggest that there may be differences between the efficiency/kinetic properties of the Na^+/K^+ ATPase pumps between SM and EO,

specifically that EO pumps may be "faster" than their SM counterparts. This is of interest given that ion pumps impose significant demand on the metabolic resources of excitable tissues (Clausen et al. 1991). Several have considered the metabolic costs of electrical signaling in both gymnotiforms (Markham et al. 2009; Salazar and Stoddard 2008; Stoddard and Salazar 2011) and mormyrids (Bell et al. 1976; Hopkins 1999), of which cation pump activity is likely to be a large component. A variety of physiological estimates have estimated that metabolic expenditure of Na^+/K^+ ATPases at approximately 10% of the basal metabolic rate (BMR) at rest to 30-40% of the BMR during activity (Clausen et al. 1991). In gymnotiforms, diurnal fluctuation in electric organ discharge amplitude is mediated by hormonally regulated Na^+ channel trafficking (Markham et al. 2009). Such fluctuation in Na^+ currents in the EO would impose an estimated 30% increase in ATP consumed by electrocytes during period of maximum EOD amplitude, due to Na^+/K^+ ATPase demand (Markham et al. 2009).

Ca+2 ATPase and Ca+2 Binding Proteins- We also detected the upregulation of a plasma membrane Ca^{+2} ATPase (PMCA, Table 2-1; Fig. 2-1), as well as several other proteins involved in Ca^{+2} binding proteins, such as neurogranin, calcyclin binding protein and s100. IHC indicates that PMCA is localized only to the posterior (innervated) surface of the electrocyte and its stalk system, consistent with findings by Taffarel (1989) who reported Ca^{+2} ATPase activity was localized only to the innervated face of the *E. electricus* electrocyte. Western blotting suggests that PMCA concentration may be slightly increased in *Brienomyrus brachyistius* EO when compared to SM (Fig. 2-4).

Because electrocytes do not contract, and are postsynaptic membranes, the consequence of Ca^{+2} binding and transporting proteins in the EO is unclear. Bartels (1971) reported that *E. electricus* electrocytes, following a depolarizing current, remain depolarized in Ca^{+2} free

Ringer's solution and are repolarized upon the addition of Ca^{+2}. Bartels (1971) also demonstrated that electrocytes in a Ca^{+2} free Ringer's solution had diminished inward K^{+} currents, suggesting a possible Ca^{+2} mediated K^{+} current in the repolarization of the electrocyte. This does not, however seem to be a common feature in all gymnotiforms; studies in *Sternopygus macurus* provide no evidence of Ca^{+2} based currents contributing to EODs (Ferrari and Zakon 1993), even despite the (relatively) long duration of the EOD pulse compared to action potentials (Ferrari and Zakon 1993).

Related to the upregulation of plasma membrane Ca^{+2} ATPase is evidence for rather remarkable changes in expression of the Ca^{+2} binding protein parvalbumin in EO as compared to SM. Two parvalbumins, matches to *Danio rerio pvalb1* and *pvalb2* respectively, were absent or downregulated in EO (Fig. 2-1, Table 2-2), and one transcript that matched *D. rerio pvalb9*, was upregulated in EO (Fig. 2-1, Table 2-1). Intriguingly, this transcript lacked the normal transcriptional start site found in all other parvalbumins (see dbEST # HO702432). Parvalbumin (the major allergenic compound in fish), is typically present in very high concentrations in fish muscle (as great as 1.5 mM in some species (Gillis 1985)), but appears to be at least 3-4 fold lower in mormyrid electric organ vs. skeletal muscle (Fig. 2-4). This finding is consistent with studies by Childers and Siegel (1976), which examined parvalbumin concentrations in SM and EO of *E. electricus.* Parvalbumins are considered critical in excitation contraction coupling in muscle (Arif 2009; Wilwert et al. 2006). Typically, muscles with fast relaxation rates express higher levels of parvalbumins than more powerful, slow contracting muscles (Wilwert et al. 2006). Thus, the decreased expression of parvalbumins in EO is consistent with the fact that EOs is non-contractile. Taken together, our findings strongly indicate an important, but presently unknown role for Ca^{+2} in electric organ physiology in mormyrids.

Sarcomeric Proteins - SSH, IHC, and western blots are all consistent with the retention of sarcomeric proteins (i.e. myosin heavy chain, troponin, and tropomyosin) in the EO, which has been suggested by previous histological and ultrastructural studies in mormyrids (Bass et al. 1986). Because EOs are not contractile in mormyrids, the role of these proteins in EO physiology are not known. Sarcomeric proteins are clearly not necessary for EO function: in gymnotiforms, the transition between skeletal muscle and electric organ is associated with a profound down-regulation of sarcomeric proteins such as myosin heavy chain (MHC), troponin and tropomyosin, (Patterson and Zakon 1996).

In mormyrids, electrocytes comprising the EO are large cells, with numerous structural components. Our IHC data suggests that the distribution of these proteins is heterogeneous in the EO (Fig 2-2), with MHC, troponin and tropomyosin, contributing to a thick center layer between the two electrocyte faces. Intriguingly, stalks seem to be devoid of MHC and tropomyosin, but continue to express troponin. One hypothesis for the retention of sarcomeric proteins may be a need for additional cytoskeletal support associated with the large size and physical complexity of electrocyte cells to maintain structural integrity. This hypothesis is of considerable interest given that the structural features of the EO are critical in shaping the EOD waveforms. For example, structural alterations in the stalk system such as the absence or presence of penetrating stalks can create additional complexity in EOD signals (Gallant et al. 2011), In addition, electrocyte membrane structure can contribute to EOD waveform shape, particularly in duration (Bass et al., 1986). Both of these features may be a substrate for sexual selection on EOD signals (Arnegard et al. 2010a).

Preliminary Insights into EO Development in Mormyrids

Electric organs have evolved at least six times independently in the history of vertebrates

from skeletal muscle tissue. In addition, other specialized muscles, namely heater organs (Block 1994) and sonic muscles (Rome 2006) have also evolved in teleost fishes from skeletal muscle. In each of these cases, while some of the molecular mechanisms underlying these unique physiologies have been identified (Block 1994; Rome 2006; Zakon et al. 2006; Arnegard et al. 2010b), the developmental mechanisms that coordinate these transformations are poorly understood. In this sense, the highly convergent gymnotiforms and mormyrids provide a unique opportunity to take a comparative approach to better understanding how such novelty evolves.

In both mormyrids and gymnotiforms, adult EOs originate during development from a distinct group of fully differentiated SM myofibrils (Patterson and Zakon 1997). Thus SM-like progenitor electrocytes (cells that comprise the EO) undergo an additional process leading to a mature electrocyte phenotype. In mormyrids, this process is accompanied by transition from motoric organization of muscle fibers, to a continuous tube of electrocytes parallel to the spinal cord (Denizot et al. 1982). The transition between the muscle-like progenitors and electrocytes is additionally characterized by a substantial change in cell size (Unguez and Zakon 1998a, b), morphology (Denizot et al. 1982), and physiology (Westby and Kirschbaum 1977), ultimately leading to the retention of electrical excitability without generating contractile force. In gymnotiforms, sarcomeric proteins are down regulated, and EO-specific proteins, such as keratin, are upregulated (Patterson and Zakon 1997; Kim et al. ; Unguez and Zakon ; Zakon and Unguez 1999). In mormyrids, histological evidence suggests that sarcomeric proteins are retained in EOs (Bass 1986; Bass et al. 1986), and the present study has verified that at least myosin heavy chain, troponin and tropomyosin expression is maintained in mormyrid EOs.

Some attempts have been made to determine potential mechanisms that may be involved in this developmental transition. Several have hypothesized that motor neurons innervating the

electric organ facilitate the transition between skeletal muscle and electric organ during development (Patterson and Zakon 1997; Unguez and Zakon 1998b; Szabo and Kirschbaum 1983). Experimental manipulations of innervation in mormyrids and gymnotiforms have lead to opposing results: innervation appears to be essential in the development and maintenance of the ECs in gymnotiforms (Patterson and Zakon 1997; Unguez and Zakon 1998a, b; Zakon and Unguez 1999; Cuellar et al. 2006), but does not appear necessary for the development of ECs in mormyrids (Szabo and Kirschbaum 1983). A recent study has suggested that motor neuron activity in gymnotiform EO may suppress SM gene expression via through post-transcriptional regulation (Cuellar et al. 2006). Our data does not provide evidence of post-transcriptional regulation in mormyrids; we were able to detect both transcripts and proteins, several of which were found to be "suppressed" sarcomere mRNA transcripts detected by Cuellar et al. (2006). Considered in the light of previous denervation studies (Szabo and Kirschbaum 1983), these findings raise the possibility that EO development in mormyrids may not be initiated through the same developmental processes. This is especially intriguing given that the gymnotiform EO can be regenerated upon injury (Cuellar et al. 2006; Kim et al. 2008; Kim et al. 2009; Kim et al. 2004; Unguez and Zakon 1998a, b; Zakon and Unguez 1999; Patterson and Zakon 1996, 1997), whereas the mormyrid EO cannot.

In addition to the role of innervation in this transition, a variety of experiments have examined the role of several muscle regulatory transcription factors (Kim et al. 2008); intriguingly many are upregulated (e.g. *MyoD*, *myogenin*, *myf5*, and *MRF4*) whereas others (e.g. *MEF2c*, *Id1*, and *Id2*) are not (Kim et al. 2008). As found by Kim et al. (2008), we saw no differential expression of MEF2c, however we did detect up regulation of the muscle regulatory transcription factor MEF2a in mormyrid EO, which was not examined by Kim et al. (2008 18).

This is of considerable interest given the involvement of the role of MEF2a in SM development in posterior somites, the developmental source of electric organ (Wang et al. 2006).

To briefly conclude, we have summarized some of these major developmental and gene expression similarities and differences in Table 2-4. Our results indicate that the biochemical differences between SM and EO in mormyrid appears to be present on the transcriptional level. This contrasts strongly with the results of a comparable recent study by Cuellar et al. (2006), which demonstrates in gymnotiforms that many of the biochemical differences between tissues appeared post-transcriptionally. In mormyrids, biochemical differences seem to manifest mainly as expression of different isoforms of a common gene (e.g. parvalbumins, myosin heavy chain). Results by Zakon et al (2006) and Arnegard et al (2010b) have already demonstrated that paralogous sodium channel genes, resulting from ancient teleost gene duplication events, are capable of serving novel functions in the EO. Rather than building the novel EO by "switching off" genes as appears to occur in gymnotiforms (Cuellar et al. 2006), one could easily imagine an alternative process by which neofunctionalized gene duplicates (normally muscle specific) could lead to a functional EO as effectively. We find these possibilities a compelling motivation for future comparative work using high-throughput transcriptomics and genomics techniques, which will doubtlessly allow for a more satisfying and comprehensive view of these processes.

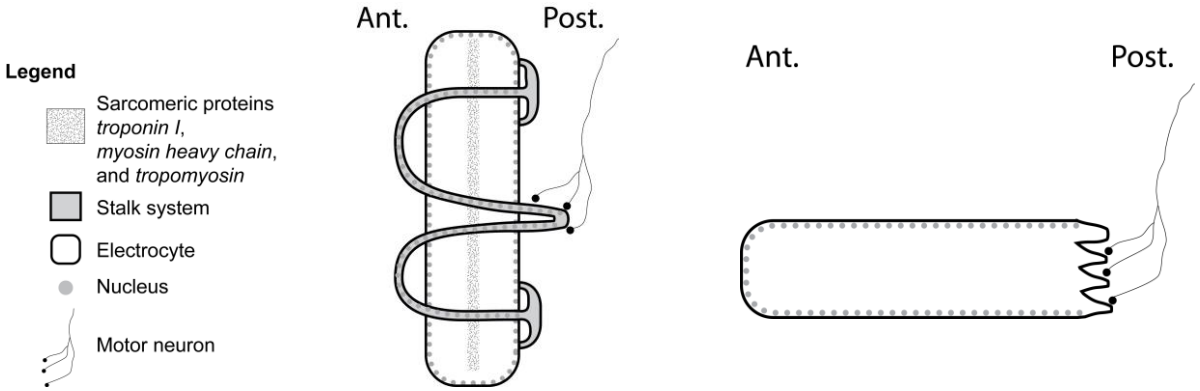

	Mormyrids ***e.g. Brienomyrus brachyistius***	**Gymnotiforms** **e.g. *Sternopygus macurus***
Transcription Factor Expression	MEF2a upregulated in EO* ERH upregulated in EO*	*MyoD myogenin myf5 MRF4* upregulated[1] *MEF2C*, *Id1*, *Id2* not differentially expressed[1]
Na^+/K^+ ATPase Expression	Multiple isoforms upregulated in EO*	No known evidence for differential expression Differential distribution of Na+/K+ Types [2]
$Ca+^2$ Proteins Expression	Parvalbumin 9 isoform downregulated in EO* *PMCA* isoform upregulated in EO*	Parvalbumin downregulated in *E. electricus* [3] Ca^{+2} Dependent Repolarization in *E. electricus* [4] No Ca^{+2} dependent changes in *S. macurus* [5];
Sarcomeric Protein Expression	Isoforms of troponin I, myosin heavy chain, tropomyosin upregulated in EO*	mRNAs present but no proteins [6]
Results of Denervation Experiments	Stays EO [7]	Reverts to SM [8]
Do EOs regenerate?	None observed	Observed in *S. macrurus* [8]

Table 2-4: Summary of gene expression and developmental differences between surveyed mormyrids and gymnotiforms.
Images above: Sketch summaries of major anatomical features of *Brienomyrus brachyistius* (mormyrid), and *Sternopygus macurus* (gymnotiform). Stalk system of mormyrids is shown in gray, which is absent in *Sternopygus macurus.* In both, oval shaped grey dots indicate location of nuclei. Hatched lines indicate presence of the sarcomeric proteins troponin I, myosin heavy chain, and tropomyosin, which are present in mormyrid EO and not expressed in gymnotiform EOs. Thin black line indicates presence of motor neurons, which innervate electrocytes. *Table below*: see text for detailed discussion. * Indicates results of present study. [1] Kim, 2008, [2] Lowe et al. 2004 , [3] Childers and Siegel, 1976. [4] Bartels, 1971, [5] Ferrari and Zakon, 1993, [6] Cuellar et al, 2006, [7] Szabo and Kirschbaum, 1983, [8] Cuellar et al., 2006; Patterson and Zakon, 1997; Unguez and Zakon, 1998a; Unguez and Zakon, 1998b, Zakon and Unguez, 1999.

References

Albert JS (2003) Family Apterontoidae. In: Reis RE, Kullander SO, Ferraris CJJ (eds) Checklist of the Freshwater Fishes of South and Central America. Edipucrs, Porto Alegre, pp 503-508

Arif S (2009) A Ca2+-binding protein with numerous roles and uses: parvalbumin in molecular biology and physiology. Bioessays 31 (4)

Arnegard M, McIntyre PB, Harmon LJ, Zelditch ML, Crampton WGR, Davis JK, Sullivan JP, Lavoué S, Hopkins C (2010a) Sexual signal evolution outpaces ecomorphological and trophic divergence during electric fish species radiation. Am Nat 176:335-356

Arnegard M, Zwickl D, Lu Y (2010b) Old gene duplication facilitates origin and diversification of an innovative communication system—twice. Proc Natl Acad Sci USA. doi:10.1073/pnas.1011803107

Bartels E (1971) Depolarization of electroplax membrane in calcium-free Ringer's solution. J Membr Biol 5 (2):121-&

Bass AH (1986) Electric organs revisited: evolution of a vertebrate communication and orientation organ. In: Bullock TH, Heiligenberg W (eds) Electroreception. Wiley, New York, pp 13-70

Bass AH, Denizot JP, Marchaterre M (1986) Ultrastructural features and hormone-dependent sex-differences of mormyrid electric organs. J Comp Neurol 254 (4):511-528

Bell CC, Bradbury J, Russell CJ (1976) The electric organ of a mormyrid as a current and voltage source. J Comp Physiol A 110:65-88

Bennett M (1971) Electric organs. In: Hoar WS, Randall DJ (eds) Fish Physiology, vol 5. Academic Press, New York, NY, pp 347-491

Black B, Lu J, Olson E (1997) The MEF2A 3' untranslated region functions as a cis-acting translational repressor. Mol Cell Biol 17 (5):2756

Black B, Olson E (1998) Transcriptional control of muscle development by myocyte enhancer factor-2 (MEF2) proteins. Annu Rev Cell Dev Biol 14:167-196

Block BA (1994) Thermogenesis in muscle. Annu Rev Phyiol 56:535-577

Brooks EM, Sheflin LG, Spaulding SW (1995) Secondary structure in the 3' UTR of EGF and the choice of reverse transcripatses affect the detection of message diversity by RT-PCR. BioTechniques 19:806-815

Clausen T, Van Hardeveld C, Everts ME (1991) Significance of cation transport in control of energy metabolisim and thermogenesis. Physiol Rev 71:733-773

Cuellar H, Kim JA, Unguez GA (2006) Evidence of post-transcriptional regulation in the maintenance of a partial muscle phenotype by electrogenic cells of *S. macrurus*. FASEB J 20 (14):2540

Darwin C (1859) The Origin of Species. Vol. XI: The Harvard Classics, vol XI. P.F. Collier & Sons, New York

Denizot JP, Kirschbaum F, Westby GW, Tsuji S (1982) On the development of the adult electric organ in the mormyrid fish *Pollimyrus isidori* (with special focus on the innervation). J Neurocytol 11 (6):913-934

Ferrari M, Zakon HH (1993) Conductances contributing to the action-potential of *Sternopygus* electrocytes. J Comp Physiol A 173 (3):281-292

Gallant JR, Arnegard ME, Sullivan JP, Carlson BA, Hopkins CD (2011) Signal variation and its

morphological correlates in *Paramormyrops kingsleyae* provide insight into evolution of electrogenic signal diversity in mormyrid fish. J Comp Physiol A. doi:10.1007/s00359-011-0643-8

Gelsthorpe M, Pulumati M, McCallum C, Dang-Vu-K., Tsubota SI (1997) The putative cell cycle gene, enhancer of rudimentary, encodes a highly conserved protein found in plants and animals. Gene 186

Gill TN (1862) On the West African genus *Hemichromis* and descriptions of new species in the museums of the Academy and Smithsonian Institution. Proc Acad Nat Sci Phila 14:134-139

Gillis J (1985) Relaxation of vertebrate skeletal muscle. A syntehsis of the biochemical and physiological approaches. Biochim Biophys Acta 811:98-145

Heiligenberg W (1986) Jamming avoidance responses: model systems for neuroethology. In: Bullock TH, Heiligenberg W (eds) Electroreception. John Wiley & Sons, Inc., New York,

Hinits Y, Hughes SM (2007) MEF2s are required for thick filament formation in nascent muscle fibres. Development 134 (13):2511-2519

Hopkins CD (1999a) Design features for electric communication. J Exp Biol 202:1217-1228

Hopkins, C.D. (1999b). Signal evolution in electric communication. In: Hauser, MD and Konishi, M (eds) The Design of Animal Communication. MIT Press, Cambridge, MA.

Kawasaki M (2005) Physiology of the tuberous electrosensory system. In: Bullock TH, Hopkins CD, Popper AN, Fay RR (eds) Electroreception. Springer, New York, pp 154-194

Kim HJ, Archer E, Escobedo N, Tapscott SJ, Unguez GA (2008) Inhibition of mammalian muscle differentiation by regeneration blastema extract of *Sternopygus macrurus*. Developmental dynamics : an official publication of the American Association of Anatomists 237 (10):2830-2843

Kim HJ, Güth R, Jonsson CB, Unguez GA (2009) *S. macrurus* myogenic regulatory factors (MRFs) induce mammalian skeletal muscle differentiation; evidence for functional conservation of MRFs. Dev Biol 53 (7):993-1002

Kim JA, Jonsson CB, Calderone T, Unguez GA (2004) Transcription of MyoD and myogenin in the non-contractile electrogenic cells of the weakly electric fish, Sternopygus macrurus. Dev Genes and Evol 214 (8):380-392

Kirschbaum F (1983) Myogenic electric organ precedes the neurogenic organ in apteronotid fish. Die Naturwissenschaften 70 (4):205-207. doi:10.1007/BF01047569

Lissmann H (1958) On the function and evolution of electric organs in fish. J Exp Biol 35 (1):156-191. doi:ISI:A1958WV57500013

Lissmann HW (1951) Continuous electrical signals from the tail of a fish, *Gymnarchus niloticus* Cuv. Nature 167 (4240):201-202. doi:10.1038/167201a0

Lissmann HW, Machin KE (1958) The mechanisim of object location of *Gymnarchus niloticus* and similar fish. J Exp Biol 35:451-486

Lowe J, Araujo GM, Pedrenho AR, Nunes-Tavares N, Ribeiro MG, Hassón-Voloch A (2004) Polarized distribution of Na+, K(+)-ATPase alpha-subunit isoforms in electrocyte membranes. Biochim Biophys Acta 1661 (1):40-46

Lukasik A, Uniewicz KA, Kulis M, Kozlowski P (2008) Ciz1, a p21Cip1/Waf1-interacting zinc finger protein and DNA replication factor, is a novel molecular partner for human enhancer of rudimentary homolog. FEBS Journal 275:332-340

Markham MR, McAnelly ML, Stoddard PK, Zakon HH (2009) Circadian and social cues

regulate ion channel trafficking. PLOS Biology 7:e1000203. doi:doi:10.1371/journal.pbio.1000203
Mörhes FP (1957) Elektrische entladungen im dienste der revierabgrenzung bel fischen. Naturwissenschaften 44
Patterson JM, Zakon HH (1996) Differential expression of proteins in muscle and electric organ, a muscle derivative. J Comp Neurol 370 (3):367-376
Patterson JM, Zakon HH (1997) Transdifferentiation of muscle to electric organ: Regulation of muscle-specific proteins is independent of patterned nerve activity. Dev Biol 186 (1):115-126
Pogge von Strandmann E, Senke. S, Ryffel GU (2001) ERH (enhancer of rudimentary homologue), a conserved factor identical between frog and human, is a transcriptional repressor. Biol Chem 382:1379-1385
Rebrikov DV (2003) Identification of differential genes by supression subtractive hybridizaiton. In: Dieffenback, Dveksler (eds) PCR Primer. 2nd Edition edn. Cold Spring Harbor Laboratory Press, Cold Spring Harbor, NY USA,
Rome LC (2006) Design and function of superfast muscles: new insights into the physiology of skeletal muscle. Annu Rev Phyiol 68:193-221
Salazar VL, Stoddard PK (2008) Sex differences in energetic costs explain sexual dimorphisim in the circadian rhythm modulation of the electrocommunication signal of the gymnotiform fish *Brachyhypopomus pinnicaudatus*. J Exp Biol 211:1012-1020
Stoddard PK, Salazar VL (2011) Energetic cost of communication. J Exp Biol 214:200-205
Sullivan JP, Lavoue S, Hopkins CD (2000) Molecular systematics of the African electric fishes (Mormyroidea: teleostei) and a model for the evolution of their electric organs. J Exp Biol 203 (Pt 4):665-683
Szabo T, Kirschbaum F (1983) On the differentiation of electric organs in the absence of central connections or peripheral innervation. In: The Physiology of Excitable Cells. Alan R. Liss, New York, pp 451-460
Taffarel M, TatianaCoelho S, Teixeira-Ferreira A, Somló C, Souza WD, Machado RD, Vieyra A (1989) Localization and cation dependence of a Ca or Mg -ATPase from electrocytes of *Electrophorus electricus* ,L. J Histochem Cytochem 37 (7):953-959
Unguez GA, Zakon HH (1998a) Phenotypic conversion of distinct muscle fiber populations to electrocytes in a weakly electric fish. J Comp Neurol 399 (1):20-34
Unguez GA, Zakon HH (1998b) Reexpression of myogenic proteins in mature electric organ after removal of neural input. J Neurosci 18 (23):9924-9935
Wang Y, Qian L, Dong Y, Jiang Q, Gui Y, Zhong TP, Song H (2006) Myocyte-specific enhancer factor 2A is essential for zebrafish posterior somite development. Mech Dev 123 (10):783-791
Westby GW, Kirschbaum F (1977) Emergence and development of the electric organ discharge in the mormyrid fish, *Pollimyrus isidori* I. The larval discharge. J Comp Physiol A 122:251-271
Wilwert JL, Madhoun NM, Coughlin DJ (2006) Parvalbumin correlates with relaxation rate in the swimming muscle of sheepshead and kingfish. J Exp Biol 209 (2):227
Wojcik E, Murphy AM, Fares H, Dang-Vu-K., Tsubota SI (1994) Enhancer of rudimentaryp1, e(r)p1, a highly conserved enhancer of the rudimentary gene. Genetics 138:1163-1170
Zakon HH (1986) The electroreceptive periphery. In: Bullock TH, Heiligenberg W (eds) Electroreception. Wiley, New York, pp 103-156

Zakon HH, Lu Y, Zwickl D, Hillis DM (2006) Sodium channel genes and the evolution of diversity in communication signals of electric fishes: convergent molecular evolution. Proc Natl Acad Sci U S A 103 (10):3675-3680. doi:10.1073/pnas.0600160103

Zakon HH, Unguez GA (1999) Development and regeneration of the electric organ.

Zupanc GKH, Bullock TH (2005) From electrogenesis to electroreception: an overview. In: Bullock TH, Hopkins CD, Popper AN, Fay RR (eds) Electroreception. Springer, New York, pp 5-46

CHAPTER 3. SIGNAL VARIATION AND ITS MORPHOLOGICAL CORRELATES IN PARAMORMYROPS KINGSLEYAE PROVIDE INSIGHT INTO THE EVOLUTION OF ELECTROGENIC SIGNAL DIVERSITY IN MORMYRID ELECTRIC FISH.*

Abstract

We describe patterns of geographic variation in electric signal waveforms among populations of the mormyrid electric fish species *Paramormyrops kingsleyae*. This analysis includes study of electric organs and electric organ discharge (EOD) signals from 553 specimens collected from 12 localities in Gabon, West-Central Africa from 1998-2009. We measured time, slope, and voltage values from nine defined EOD "landmarks" and determined peak spectral frequencies from each waveform; these data were subjected to principal components analysis. The majority of variation in EODs is explained by two factors: the first related to EOD duration, the second related to the magnitude of the weak head-negative pre-potential, P0. Both factors varied clinally across Gabon. EODs are shorter in eastern Gabon and longer in western Gabon. Peak P0 is slightly larger in northern Gabon and smaller in southern Gabon. P0 in the EOD is due to the presence of penetrating-stalked (*Pa*) electrocytes in the electric organ while absence is due to the presence of non-penetrating stalked electrocytes (*NPp)*. Across Gabon, the majority of *P. kingsleyae* populations surveyed have only individuals with P0-present EODs and *Pa* electrocytes. We discovered two geographically distinct populations, isolated from others by barriers to migration, where all individuals have P0-absent EODs with *NPp* electrocytes. At two sites along a boundary between P0-absent and P0-present populations, P0-absent and P0-present individuals were found in sympatry; specimens collected there had electric organs of intermediate morphology. This pattern of geographic variation in EODs is considered in the context of current phylogenetic work. Multiple independent paedomorphic losses of penetrating stalked electrocytes have occurred within five *Paramormyrops* species and seven genera of mormyrids. We suggest that this key anatomical feature in EOD signal evolution may be under a simple mechanism of genetic control, and may be easily influenced by selection or drift throughout the evolutionary history of mormyrids.

* Reprinted from *The Journal of Comparative Physiology A 2011:* Signal variation and its morphological correlates in *Paramormyrops kingsleyae* provide insight into the evolution of electrogenic signal diversity in mormyrid electric fish; by Gallant, J.R. Arnegard, M.E. Sullivan, J.P. , Carlson, B.A. and Hopkins, C.D.; © 2011; with permission from Springer, Inc.

Introduction

Diversity in courtship signaling behavior is a common component of the evolution of reproductive isolation between species (Mayr 1963). The task of identifying the evolutionary processes that act upon signals to generate such diversity is of considerable interest, and requires insights into the anatomical and physiological basis of signal variation that can be gained through comparative study. For several reasons, this endeavor is challenging. First, for many communication modalities, signals can be difficult to quantify, particularly in terms of salient aspects relevant to the nervous system and behavior of the organism. Second, it may be difficult to correlate these differences in signals with discrete physiological processes or anatomical differences between species. Third, many courtship signals are subject to a multitude of selective pressures in addition to sexual selection (Bradbury and Verencamp 1998) making it difficult to ascertain the effect of specific evolutionary pressures on communication systems.

We consider here a particularly amenable system for the study of communication signals and species divergence: a species flock of African weakly electric fish. Recent estimates have suggested 22 *Paramormyrops* species (Lavoué et al. 2008). In contrast to the low level of genetic divergence between these species that suggests the recency of their origin (Sullivan et al. 2002), *Paramormyrops* exhibit highly divergent electrical signals (Sullivan et al. 2002; Sullivan et al. 2004) termed electric organ discharges (EODs). EODs are species-specific, simple, stereotyped, easily quantified signals with a well-established morphological and neurophysiological basis (Hopkins 1986; Carlson 2002; Sullivan et al 2002; Caputi et al. 2005). The behaviorally salient features of these signals are known (Hopkins and Bass 1981; Carlson 2002), and the neural circuit encoding these features has been well characterized (Xu-Friedman and Hopkins 1999; Carlson 2009). Moreover, the ease with which EOD waveforms can be

quantified permitted a detailed demonstration that these electric signals evolve faster than feeding morphology, size, or trophic ecology implicating sexual selection as a potentially important driving force in mormyrid evolution (Arnegard et al. 2010). Indeed, this has been supported by several playback studies (Hopkins and Bass 1981; Machnik and Kramer 2008; Feulner et al. 2009). This work has motivated our interest in identifying additional evolutionary processes that may lead to the evolution of divergent signals, as well as the anatomical substrates and physiological processes that evolution acts upon to generate signal diversity. Our approach is to use patterns of intraspecific geographic variation as a tool (Foster et al. 1998; Mayr 1963; Lewontin 1974; Endler 1989; McPhail 1994; Verrell 1998) to (1) identify types of variation between populations that parallel signal differences between species and (2) to infer from geographic patterns of this variation, microevolutionary factors that might contribute to signal evolution. Patterns of geographic variation in communication signals (acoustic and electrical), genetics and external morphology have been previously examined for these reasons among the mormyrid genera *Marcusenius* (Lamml and Kramer 2007; Kramer et al. 2007); *Hippopotamyrus* (Kramer et al. 2004; Kramer and Swartz 2010) and *Pollimyrus* (Kramer et al. 2003; Lamml and Kramer 2006) and *Petrocephalus* (Kramer and van der Bank 2000).

The present study describes geographic patterns of EOD signal variation in *Paramormyrops kingsleyae* (Günther 1896), a geographically widespread species in West-Central Africa. EODs are produced by a myogenically derived electric organ, restricted to the caudal peduncle. The electric organ is comprised of four axially oriented columns, each consisting of approximately 20-100 disc-shaped electrocytes (Bass 1986b). Interspecific variation in EOD waveforms is explained, in part, by variation in the structure of these electrocytes (Fig. 1-1; for reviews see also Bennett and Grundfest 1961; Bennett 1971; Bass

1986c). Electrocyte morphology is typically homogeneous across the entire electric organ of an individual (Bass 1986b; Sullivan et al. 2000), and is usually species typical (Sullivan et al. 2000). EODs and electrocyte morphology are especially diverse within *Paramormyrops*; between species EODs may vary in duration (0.5-8 ms), in polarity, in the number of phases, and in the rates of voltage change over time (Sullivan et al. 2002). We focus here on the species *P. kingsleyae,* which exhibits intraspecific EOD diversity (Arnegard and Hopkins 2003; Arnegard et al. 2005; Sullivan et al. 2004). Each EOD type consists of two main peaks, a head-positive phase, P1, followed by a head negative phase, P2. P1 is usually preceded by a weak head negative phase, P0, which is absent in some specimens (Fig. 1-1). This intraspecific variation is of interest because variation in the presence of P0 presence vs. absence of P0 characterizes much of the diversity in mormyrid EODs, including *Paramormyrops*. In addition, this physiological character has a discrete morphological basis. Mormyrid electrocytes have protruding stalk systems that can originate on the posterior face, and pass through to the anterior face, where they are innervated (*P*enetrating with *a*nterior innervation or *Pa*; Fig 1-1c). Alternatively they can have stalks that remain on the posterior face, and are innervated on the posterior face (*N*on-*P*enetrating with *p*osterior innervation, or *NPp*; Fig 1-1c). The EOD waveform produced by these two electric organ types relates to the direction of current flow through the stalk and the relative order in which the anterior and posterior electrocyte faces depolarize (see Bennett 1971; Bass 1986b). P0-present EODs are associated with *Pa* type electric organs, and P0-absent EODs are associated with *NPp* type electric organs (Fig. 1-1c).

Our analysis begins with a detailed description of the nature of intraspecific variation in EOD signals of *P. kingsleyae*, followed by a description of the biogeographic patterns that this variation takes. We examine the morphology of electric organs of *P. kingsleyae* from several

independent populations, and demonstrate morphological correlates for the observed signal variation. One morphological correlate of signal variation parallels not only interspecific diversity in the *Paramormyrops* species flock, but also within several other genera of mormyrids. We discuss different hypotheses that could potentially explain this variation, and put forward the hypothesis that genetic drift might play an important role during the early stages of EOD evolution in some mormyrid species in certain geographical settings.

Methods

Specimen Collection and Electric Organ Discharge (EOD) recording:

Each of the 553 specimens considered in this analysis are identified as the species *Paramormyrops kingsleyae*[2] based upon the diagnosis of Hopkins et al. (2007). The Cornell University Museum of Vertebrates (CUMV) accession numbers (CU80230-95238) with individual voucher numbers (2004-6927), along with collection dates and collection coordinates are listed in tabular format in Appendix 3. We consider the specimens in this study to be the same species, based upon the following additional evidence: First, ten of the specimens, representing 10 collection localities listed in the present study, appear to form a monophyletic group within *Paramormyrops*, based on AFLP nuclear genetic markers (Sullivan et al. 2004). Second the habitat preference of all *Paramormyrops kingsleyae* specimens is largely for small

[2] *Paramormyrops kingsleyae* has been previously referred to using several operational taxonomic designators. ***Brienomyrus brachyistius (Long Biphasic or LBP)*** was used originally by Bass (1986a,b,c); Bass et al. (1986) Hopkins (1986), Hopkins (1980), and Hopkins and Bass (1981). As different regions of Gabon were explored, newly discovered allopatric populations were called ***Brienomyrus BN1, Brienomyrus BP1, Brienomyrus BX1, Brienomyrus LIB, Brienomyrus CAB*** by Sullivan et al. (2002), Arnegard and Hopkins (2003), Sullivan et al. (2004) and Arnegard et al. (2005). Eventually, all of the above populations were recognized as a single species *Paramormyrops kingsleyae*, on the basis of genetic similarity, similar morphology and ecology, and overall EOD similarity. The most current diagnosis of *Paramormyrops* (formerly "the Gabon-Clade *Brienomyrus") and P. kingsleyae* is summarized by Hopkins et al. (2007), and is provided for convenience as Appendix 2.

headwater streams vs. main river channels (Table 3-1). Third, the overall differences between EODs, when compared to intraspecific variation in EODs between other *Paramormyrops*, is quite small (Arnegard et al. 2003; Sullivan et al. 2004), which is the subject of the present study.

P. kingsleyae exhibit a sex-difference in their EODs which is evident during the wet-season breeding period with sexually mature males producing EODs approximately double the duration of female and dry season non-breeding males (Bass 1986a; Bass et al. 1986; Bass and Volman 1987). Because of the difficulty of collecting mormyrids from flooded rivers, insufficient samples of exaggerated male EODs have been collected outside of the Ivindo region (Table 3-1). Given this lack of male recordings, we restrict our analysis of electric signal variation to the species-typical female-like EOD exhibited by both breeding females and adult males outside the breeding season. Electrical playbacks to breeding male *Paramormyrops* spp. suggest that male mate choice targets variable features of these species-typical EODs (Hopkins and Bass 1981; Arnegard et al. 2006). Playbacks to mormyrids in other genera further suggest that females exhibit mating preferences for variable EOD features in males as well (Feulner et al. 2009; Machnik and Kramer 2008), reinforcing the case that EOD waveforms are an important component of species recognition and mate choice during courtship.

Our collections were made from 26 individual collection sites. For analysis, we grouped these 26 collection sites into 12 regional drainage basins, referred to herein as localities (Table 3-1). Fish were collected using a variety of methods, including fish traps baited with worms, hand nets and electric fish detectors, hook and line, damming and draining streams (a local fishing technique), and light rotenone applications (Table 3-1). Following any application of rotenone, fish were immediately transferred to fresh, aerated water, where they recovered completely. We saw no difference in the EODs of rotenone captured fish and those captured using other methods.

Table 3-1: Collections data for all sites and localities.
Each of the 26 collection sites is grouped into localities (italic). Major drainages are listed in bold for each of these localities. For each collection site, date visited, number of specimens (N), water temperature, conductivity, Latitude, Longitude, capture type and habitat type are listed. For capture: **N**=nets; **R**=rotenone; **S**= seine; **E**=fishing with detector; **D**= damming, **T**=traps. For habitat: **a**=rocky; **b**=sandy; **c**=muddy; **1**=slow water velocity; **2**=moderate water velocity; **3**=high water velocity. (**–)** indicates that data is not available

.

Northern Costal			Date	n	Temp ˚C	Cond. (µS/cm)	Lat	Long	Capture	Habitat
	Cocobeach									
		Small Creek	Mar-00	**23**	-	52	0˚ 55’ 57" N	9˚ 34’ 28" E	N, R	a, 3
		Small Creek	Mar-00	**7**	-	45.7	0˚ 52’ 14" N	9˚ 35’ 5" E	N, S	b, 1
	Libreville - Cape Estereas									
		Small Stream	Feb-98	**13**	-	71.6	0˚ 33’ 5" N	9˚ 20’ 48" E	R	b
		Small Stream	Aug-99	**2**	24.6	31.4	0˚ 35’ 5" N	9˚ 20’ 5" E	N, R	b
Ogooué River										
	Bambomo									
		Bambomo Creek	Jul-99 ; Aug-09	**159**	23	13.3-16.3	2˚ 9’ 49" S	11˚ 27’ 42" E	R, N	-
	Ivindo									
		Bale Creek	Feb-98	**6**	22.8	20.3	0˚ 31’ 11" N	12˚ 47’ 58" E	E, N, R	b
		Bialé Creek	Jan-98	**5**	-	-	0˚ 32’ 18" N	12˚ 49’ 32" E	N, E, D	-
		Nyamé Pendé	Jan-98; Aug-01	**4**	22.5	17.93	0˚ 30’ 8" N	12˚ 47’ 48" E	R	b
	Louétsi (Above Falls)									
		Louétsi River	Jul-99	**6**	-	-	2˚ 14’ 0" S	11˚ 27’ 0" E	-	-
		Banganda Creek	Jul-99	**6**	21.5	-	2˚ 12’ 10" S	11˚ 31’ 45" E	N	-
		Bikagala Creek	Jul-99; Aug-09	**35**	22.1	29.9	2˚ 11’ 43" S	11˚ 33’ 40" E	N	-
		Songou Creek	Jul-09	**11**	21.0	14.8	2˚ 16' 42"S	11˚ 36' 41" E		
		Bavelela Creek	Jul-09	**23**	23	14.4	2˚ 14' 33" S	11˚ 33' 22" E		
		Biroundou Creek	Jul-99; Jul-09	**7**	24.1	16.03	2˚ 12’ 47" S	11˚ 28’ 40" E	N	-
	Louétsi (Below Falls)									
		Moussabou Creek	Sep-98	**8**	-	-	2˚ 13’ 8" S	11˚ 27’ 50" E	D	-
		Apassa Creek	Aug-09	**31**	22.0	26.0	2˚ 12' 42" S	11˚ 27' 35" E		
		Louétsi River	Sep-98	**1**	-	-	2˚ 14’ 2" S	11˚ 27’ 42" E	H	-
	Mouvanga									
		Mouvanga Creek	Jul-99; Aug-09	**118**	21.2-23.8	18.34-23.1	2˚ 19’ 23" S	11˚ 41’ 18" E	R, D, N, T	c, a
	Ntem									
		Ngomo River	Sep-99	**4**	23.3	-	1˚ 42’ 8" N	11˚ 38’ 40" E	T, N	-
	Nyanga									
		Small Stream	Jul-01	**4**	22.8	-	3˚ 22’ 27" S	10˚ 47’ 22" E	-	-
	Ogooué									
		Small Stream	Sep-01	**4**	23.8	55.4	0˚ 34’ 6" S	10˚ 12’ 47" E	-	3
		Diengui River	Sep-99	**10**	25.5	-	0˚ 39’ 35" S	10˚ 19’ 29" E	N	2
		Mikouma River	Sep-99	**13**	26.1	-	0˚ 40’ 5" S	10˚ 20’ 12" E	R	a
Okano River										
	Okano									
		Okano River	Aug-01	**38**	22.8	21.3	0˚ 49’ 56" N	11˚ 39’ 2" E	-	-
Woleu River										
	Woleu									
		Minka Creek	Aug-99	**4**	24.2	14	1˚ 32’ 1" N	11˚ 34’ 48" E	-	c, 1
		Small Stream	Aug-99	**11**	22	21.3	1˚ 32’ 41" N	11˚ 45’ 56" E	R	c, 1

EODs of each specimen were originally recorded within hours of capture in 1- to 5 liter plastic boxes filled with water from the collection site. Signals were recorded with bipolar silver chloride coated silver wire electrodes, and amplified (bandwidth =0.0001-50 kHz) with a differential bioamplifier (CWE, Inc : Ardmore, PA), and digitized at a 100 kHz-1 MHz sampling rate, with head-positivity upward using a Daqbook or WaveBook (IOTECH: Cleveland, OH), or a USB-powered A-D Converter (National Instruments: Austin, TX). All EOD recordings were made at a vertical resolution of 16 bits per sample. After recording their EODs, individual specimens were euthanized with an overdose of MS-222. We classified obvious mature males based on the presence of an indentation of the body profile along the base of the anal fin (Iles 1960; Okedi 1969; Kirschbaum 1995; Scheffel and Kramer 1997; Pezzanite and Moller 1998). Individuals lacking such an indentation included juveniles and females. Standard lengths were measured from the tip of the snout to the fork of the tail between the two caudal fin lobes (Lévêque et al 1990). Each specimen was given a unique specimen identification tag, and fixed free-floating in 10% formalin (phosphate-buffered; pH 7.2) for at least 2 weeks. Specimens were then transferred to 70% ethanol, and deposited in the Cornell University Museum of Vertebrates. All methods conform to protocols approved by Cornell University's Center for Research Animal Resources and Education.

EOD Analysis

For each specimen, we analyzed a single EOD waveform recording using a custom written program in MATLAB (Mathworks, Inc.: Natick, MA), adapted from a previous study (Arnegard and Hopkins 2003). Each EOD waveform was normalized by its peak-to-peak amplitude, and by subtracting the mean amplitude of the first 100 points. Twenty-one measurements were made on each EOD recording; we measured amplitudes, times and slopes at

nine landmarks defined by peaks, zero crossings, first derivative peaks, and threshold crossings. All landmarks are indicated by red crosses in Fig. 3-2b and are defined in Table 3-2 along with a definition of each of the 21 metrics. Slopes at waveform peaks, being zero by definition, were omitted. The zero point of all time measurements was defined by the time of the first head-positive peak (Table 3-2). We calculated a power spectrum of each EOD waveform using the MATLAB *fft* function to determine the peak frequency and a low and high frequency 3 dB below the peak frequency for each EOD recording. Peak P0 was small in *P. kingsleyae* relative to background electrical noise in recordings, so to measure the magnitude of P0, we integrated the area under the curve between tZC1 and tZC1-0.5 ms (Fig. 3-2). To obtain a baseline measurement of the noise in each recording, expressed as area, we measured the area under the curve for the first 0.5 ms of each recording (where the EOD is absent). Using the MATLAB function *princomp*, we performed principal components analysis (PCA) on the set of all EOD measurements to quantify EOD signal variation.

Because we describe variation in signals between populations over large geographic areas, we considered differences in recording temperature as a potential confounding source of variation. Kramer and Westby (1985) demonstrated that the overall duration of pulse EODs varied in a manner consistent with a typical Q_{10} factor of 1.49. In our collections of *P. kingsleyae*, water temperatures at time of EOD recording varied between 21.0-26.7 ˚C. Because of incomplete temperature records, we were unable to perform a Q10 temperature correction for each EOD in our analysis. Instead, we evaluated the effect of temperature on a subset of 491 temperature-corrected EOD recordings; the full methodology and results of this analysis are included as Appendix 4. We concluded from this analysis that recording temperature was not a significant source of variation in our dataset, and therefore proceeded with our analysis on the

Landmarks		
	Name	*Definition*
	P0	Small negative pre-potential; assumed present in all waveforms
	P1	Largest head positive phase
	P2	Largest head negative phase
	S1	Point of maximum slope between T1 and P1
	S2	Point of maximum slope between P1 and P2
	T1	Waveform beginning; first point to deviate from baseline by 2% of peak to peak height
	T2	Waveform ending; last point to deviate from baseline by 2% of peak to peak height
	ZC1	Point voltage crosses baseline from P1-start of record; if exists
	ZC2	Point voltage crosses baseline between P1-P2
Variables		
	Name	*Definition*
	aP0	Area under curve between ZC1-0.5ms and ZC1
	aP1	Area under curve between ZC2-ZC1
	aP2	Area under curve between tT2-ZC2
	vP0	Minimum voltage between ZC1-0.5ms and ZC1
	vP1	Voltage of P1 (vP1-vP2=1)
	vS1	Voltage at S1
	vS2	Voltage at S2
	tP0	Time at P0
	tP2	Time at P2
	tS1	Time at S1
	tS2	Time at S2
	tZC1	Time at ZC1
	tZC2	Time at ZC2
	Duration	Total duration (T2-T1)
	sZC1	Slope at ZC1
	sZC2	Slope at ZC2
	sS1	Slope at S1
	sS2	Slope at S2
	fftmax	Peak frequency of FFT transform of EOD
	fftlo	Frequency below fftmax at -3dB
	ffthi	Frequency above fftmax at -3dB

Table 3-2: Landmark and variable definitions each of the landmarks used for EOD analysis.

All variables used in subsequent PCA are defined using these landmarks.

full (n=553) dataset without temperature correction.

Electric Organ Confocal Microscopy

We dissected individual electrocytes for whole-mount confocal imaging. Formalin fixation of field-captured specimens (see above) resulted in substantial membrane autofluorescence (λ=500-550 nm), and such autofluorescence was suitable for confocal imaging of superficial electrocyte structures without further histological processing. Individual electrocytes (approx. 1 mm in dorsal-ventral height) were imaged with a Zeiss LSM 510 META microscope using a motorized stage for data collection with optical slices of 6 µm. Laser excitation was at 488 nm; fluorescent emission was collected using a long-pass 505 nm filter and a 72 µm pinhole opening. Slice data from multiple fields of view were assembled for each electrocyte using Zeiss LSM 4.2 software (Carl Zeiss MicroImaging: Thornwood, NY). Resulting stacks were ray-tracer rendered using Volocity 4.5 (Improvision: Waltham, MA) on a white background (1-3% black level, 58% density, 50% brightness). Morphological measurements were performed upon bitmapped versions of electrocyte rendering using a custom-written MATLAB program or IMAGEJ (U. S. National Institutes of Health, Bethesda, Maryland, USA). We attempted to quantify variation in both the length of microstalklets and in the cross-sectional area of each electrocyte devoted to penetrations by performing image analysis on seven bitmapped 3D projections for which EOD recordings were available. We first determined the area of ellipsoid boundaries surrounding each observed penetration, summed these areas per electrocyte, and then standardized this sum by total electrocyte area. Second, we determined the boundary of each penetration's microstalklets, and then determined linear distances between each pixel in this region to the point of penetration, standardizing this value by the perimeter of the electrocyte.

Electric Organ Light Microscopy

We also made serial sections of electric organs for light-microscopy analysis. Electric organs were removed from fixed specimens and decalcified overnight using 100% CalEx-II solution (Fisher Chemicals: Fair Lawn, NJ). Next, tissue samples were dehydrated in a graded alcohol series up to 95%, then infiltrated and embedded in JB-4 glycol methacrylate resin (Polysciences, Inc.: Warrington, PA). We then made serial sagittal sections of the embedded samples 6 µm thick, mounted these sections on clean glass slides, and stained each slide with a 0.5% Toluidine blue solution for 30 sec. Sections were then imaged using a Leica Leitz DMRB microscope equipped with at SPOT Flex 15.2 64MP Shifting Pixel digital camera (Diagnostic Instruments: Sterling Heights, MI).

For each specimen, we reconstructed one of four columns of electrocytes from serial, sagittal 6 µm sections, cut from lateral to medial. As each column surrounds the spinal cord, we began our reconstruction at the lateral edge of the electric organ, and stopped counting when the spinal cord was clearly visible (approximately 250-650 µm depending on the size of the individual). For each section, the number of penetrations was counted for each electrocyte (27-72 electrocytes per section) from anterior to posterior. An electrocyte was scored with a penetration whenever a stalk was observed to pass through either or both faces of the electrocyte (Fig. 1-1 for example). For our analysis, we considered each 6 µm section to have an independent number of penetrations from all other sections to minimize the probability of underestimating the total number of penetrations.

Results

EOD Waveform Variation

Fig. 3-2 illustrates representative EODs recorded from 48 individuals from 12 different localities across Gabon. EODs vary in duration (e.g. Woleu vs. Cocobeach), in the position of inflection points on the rising phase of the first peak P1 (e.g. Ntem vs. Lower Louétsi) and in the presence or absence of a small head-negative pre-potential peak, P0, which can be seen on the vertically expanded traces (Fig. 3-2c). Our quantitative analysis of some aspects of EOD variation is summarized in Table 3-3 by collection locality. The first two principal components (Fig. 3-3) of the dataset account for 68.0% of variation in EOD waveform metrics. Principal component 1 describes 48.0% of the dataset variance, and principal component 2 describes an additional 20.0%. Factor loading coefficients for the first two principal components allowed us to determine the combinations of variables that contributed to the majority of variance between waveforms. Variables related primarily to the relative timing of landmarks in the EOD and duration of EOD waveform loaded most strongly on principal component 1, whereas variables related to the magnitude of P0 loaded most strongly on principal component 2 (Table 3-4).

Boundaries plotted in Fig. 3-3 illustrate that variation in EOD waveform is less within localities than between localities. Typically, variation in geographically adjacent localities is less than geographically distant ones, with the exception of Ntem and Woleu which are geographically proximate, but separate watersheds. To evaluate this relationship more stringently, we examined the correlation between principal components scores 1 and 2 each with latitude and longitude. PC scores are plotted

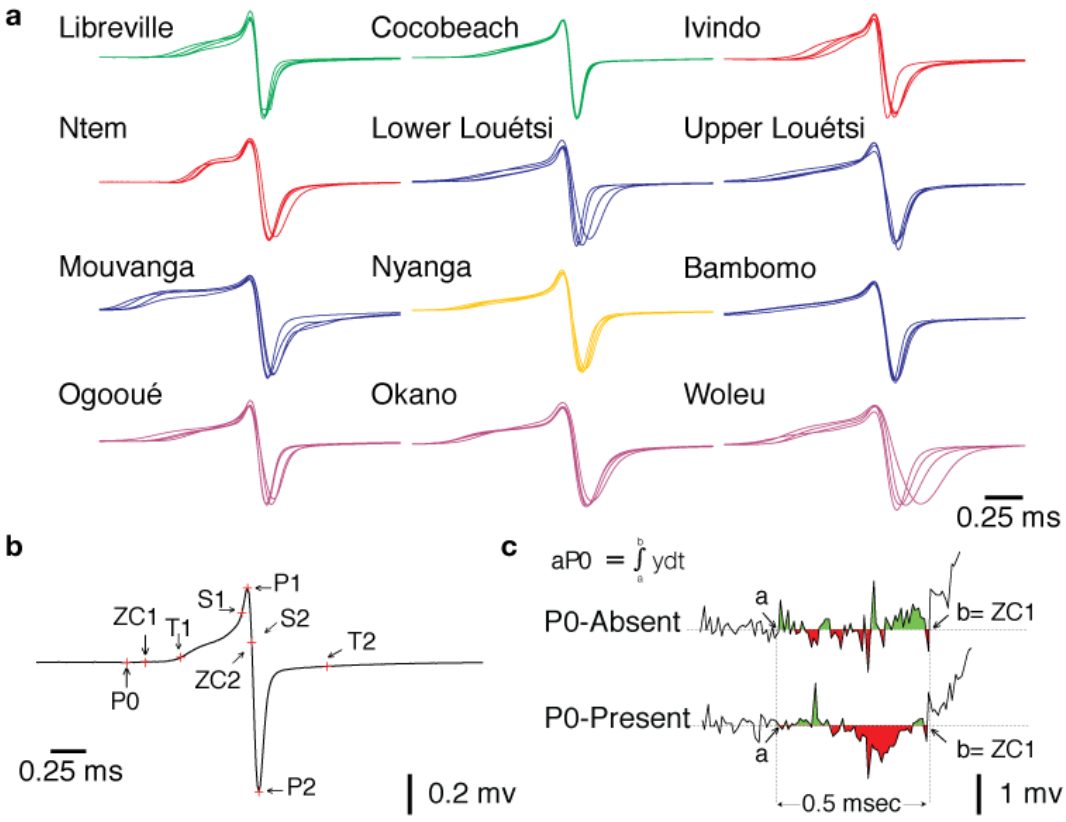

Figure 3-2: EOD waveform analysis of *Paramormyrops kingsleyae*.
a. Representative variation in EOD waveforms of *P. kingsleyae* from 12 localities (n=4 EODs for each locality). Waveforms vary principally in the duration and shape of initial P1 phase. **b.** Nine landmarks were determined for each of 544 EOD recordings (indicated by red crosses). For each landmark time and voltage relative to P1 were determined. See Table 3-2 for definitions of all landmarks used in this analysis. **c.** P0 is a small pre-potential observed in some waveforms. We determined a robust (even in noisy recordings, as indicated here) method of detection that searches backwards in time from P1 until ZC1 is reached (*b*). The area under the curve is computed for 0.5 ms prior to ZC1 (*a*) to determine P0 area. The time and voltage of the minimum over this interval is recorded as the peak of P0.

Locality	n	Duration (ms)	Peak FFT (Hz)	tP0 (ms)*	aP0 (mV x ms)†
Bambomo Ck	**159**	1.71 ± 0.35	676.98 ± 135.62	-1.56 ± 0.24	0 ± 0.09
Cocobeach	**30**	1.37 ± 0.28	957.03 ± 150.42	-1.14 ± 0.18	-0.04 ± 0.11
Ivindo	**15**	1.47 ± 0.48	917.97 ± 168.34	-0.78 ± 0.13	-0.79 ± 0.45
Libreville	**15**	1.18 ± 0.2	1074.22 ± 152.19	-0.79 ± 0.07	-0.2 ± 0.05
Lower Louétsi	**40**	1.41 ± 0.21	760.5 ± 112.7	-1.22 ± 0.12	-0.31 ± 0.13
Mouvanga	**119**	1.84 ± 0.22	649.21 ± 91.6	-1.42 ± 0.14	-0.35 ± 0.12
Ntem	**4**	1.06 ± 0.1	1074.22 ± 112.76	-0.51 ± 0.04	-0.56 ± 0.13
Nyanga	**4**	1.5 ± 0.18	756.84 ± 93.5	-1.21 ± 0.09	-0.37 ± 0.07
Ogooué	**27**	1.49 ± 0.3	788.48 ± 157.76	-1.16 ± 0.17	-0.29 ± 0.11
Okano	**38**	1.87 ± 0.17	601.36 ± 53.37	-1.32 ± 0.08	-0.43 ± 0.15
Upper Louétsi	**87**	1.5 ± 0.29	802.02 ± 133.75	-1.49 ± 0.22	0.04 ± 0.13
Woleu	**15**	1.4 ± 0.15	794.27 ± 103.53	-0.94 ± 0.07	-0.4 ± 0.35
Grand Total	**553**				

Table 3-3: Selected EOD Metric Values by Locality
Values for selected variables (see Table 3-2) are listed by Locality (see Table 3-1) ± SD. * denotes relative to tP1= 0 ms ; † denotes relative to vP1-vP2 =1.

Variable	PC1		Variable	PC2
ap2 *	0.3058		tZC1	0.4055
ap1 *	-0.2984		tP0 †	0.3952
ffthi *	0.2866		vP0 †	-0.3887
sZC2	-0.2811		sZC1	0.3761
duration *	-0.2793		ap0 †	-0.3578
sS2	-0.2777		vS1 †	0.2497
tP2 *	-0.2735		fftlo	0.2308
tZC2	-0.2668		fftmax	0.2015
tS2 *	-0.2630		vS2	0.1559
fftmax *	0.2516		tZC2	0.1337

Table 3-4: Top ten factor loading values for principal components 1 & 2.
The ten highest-magnitude loading scores for each PC1 and PC2 are shown with their associated variables. The magnitude of the loading score indicates the relative contribution of each individual variable to variation in this principal component. * Indicates factors for PC1 which are related to overall duration of EOD waveform, † indicates factors for PC2 which are related to overall magnitude of phase P0 (see Table 3-1).

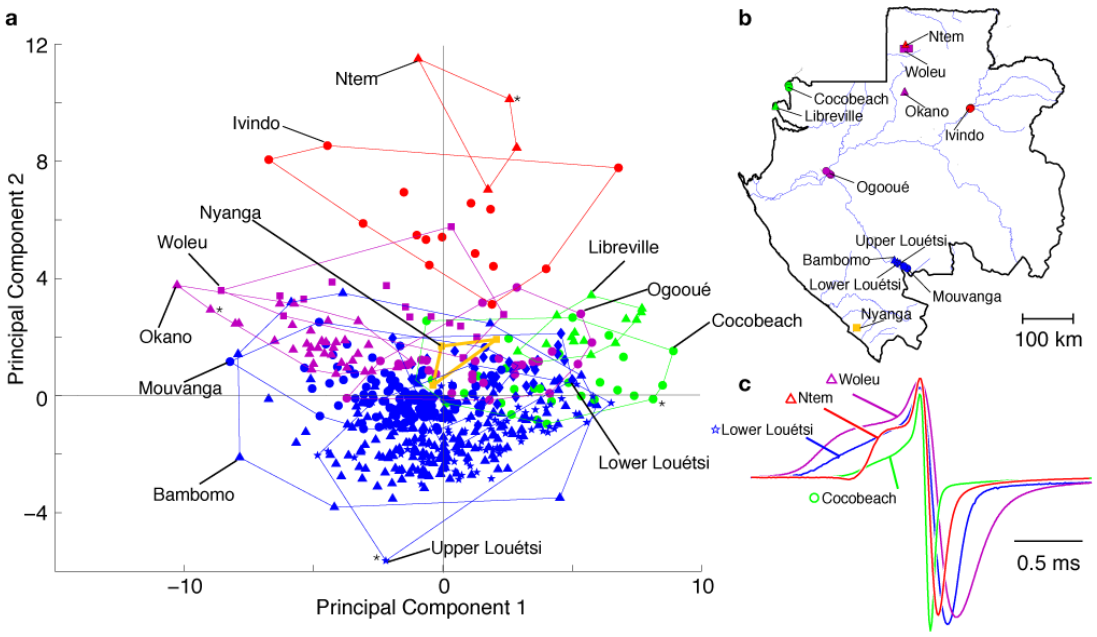

Figure 3-3 Principal components analysis of EOD waveform variation for the *Paramormyrops kingsleyae* dataset.

a. The first two principal components (n=553) describe variation across 21 variables. Each data point represented in principal component space has a representative shape and color corresponding to locality (see 2b). Each locality is bounded by a minimum polygon (colored line, labeled with locality). Asterisk symbols represent the EOD waveforms shown in 2c. **b.** Map of Gabon with major rivers; 12 collection localities are shown and shaded by geographic region (Green = West, Purple = N. Central, Red=N. East, Blue= Southern, Yellow=Nyanga). Shapes are assigned based on population. **C.** Overlay diagram of four EOD waveforms indicated by asterisks in 2a.

versus longitude and latitude in pairwise combinations in Fig. 3-4. Linear regression analysis indicated a significant linear relationship of principal component 1 to longitude (slope=-2.13; $F=143.98$, $df=552$, $r^2=0.21$, $p<0.001$) but not latitude, and principal component 2 with increasing latitude (slope=0.99; $F=387.77$, $df=552$, $r^2=0.41$, $p<0.001$) but not longitude.

P0 Signal Analysis

Figure 3-5a shows a histogram of all 553 measured P0 areas. Three example waveforms are shown as insets; the EOD on the far left has a P0 area of -0.79 mV x ms, the EOD on the left has a P0 area of -0.17 mV x ms, and the P0-absent EOD on the right has a P0 area of 0.03 mV x ms. The histogram of all individuals is bimodal with respect to their P0 magnitude, representing P0 present individuals (the left modal peak, -0.35 mV x ms), or P0 absent individuals (the right modal peak at 0.00 mV x ms). Because of noise in the recordings, some fish with no discernible P0 had a measureable P0 area when applying this metric. We wished to compare the magnitude of our measured P0s to the noise in our recordings, so we determined the mean value of the area under the curve during the first 0.5ms (see Methods) for all recordings (where no EOD is present). A histogram of these area measurements is shown in Figure 3-5b. Next, we classified waveforms as either P0-absent (green) or P0-present (red) using the threshold value 3 standard deviations from this mean value (-0.064 mV x ms). Thus EODs that had a P0 area significantly greater than the area under the curve in the recording noise ($p=0.01$) were considered P0-present. Those that had a P0 area less than 3 standard deviations from 0 mV x ms were considered P0-absent. Note that this threshold corresponds exactly to the "trough" between the two modes in the distribution of P0 area across all populations, generating two objectively defined classes of EOD waveforms in *P. kingsleyae*. Accordingly, 297 individuals were classified as P0-present; 256 individuals were classified as P0-absent.

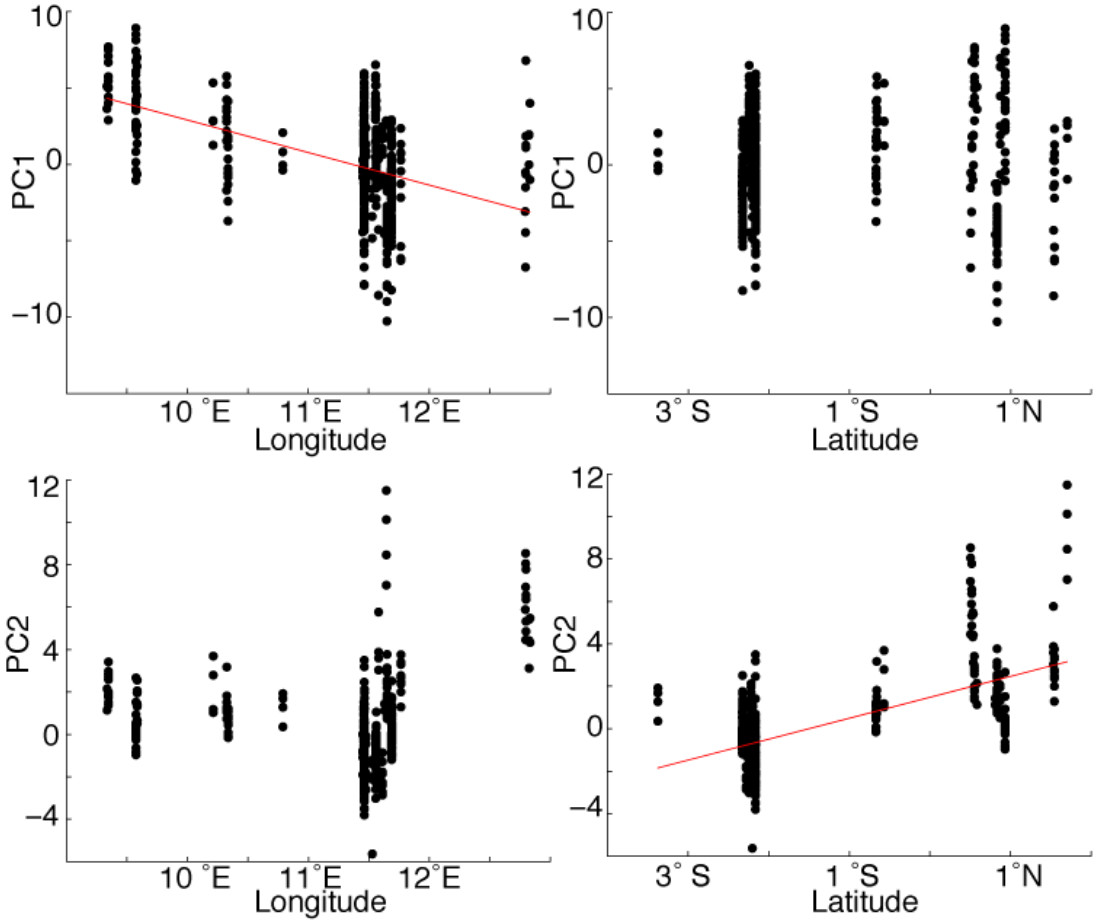

Figure 3-4: Clinal variation in EOD waveform.
Principal component 1 of all data has a negative linear relationship with Longitude (upper left; F=143.98; df=552 R^2=0.21; p<0.001) but not Latitude; principal component 2 of all data has a positive linear relationship with Latitude (lower right; F=387.77, df=552, r^2=0.41; p<0.001) but not Longitude.

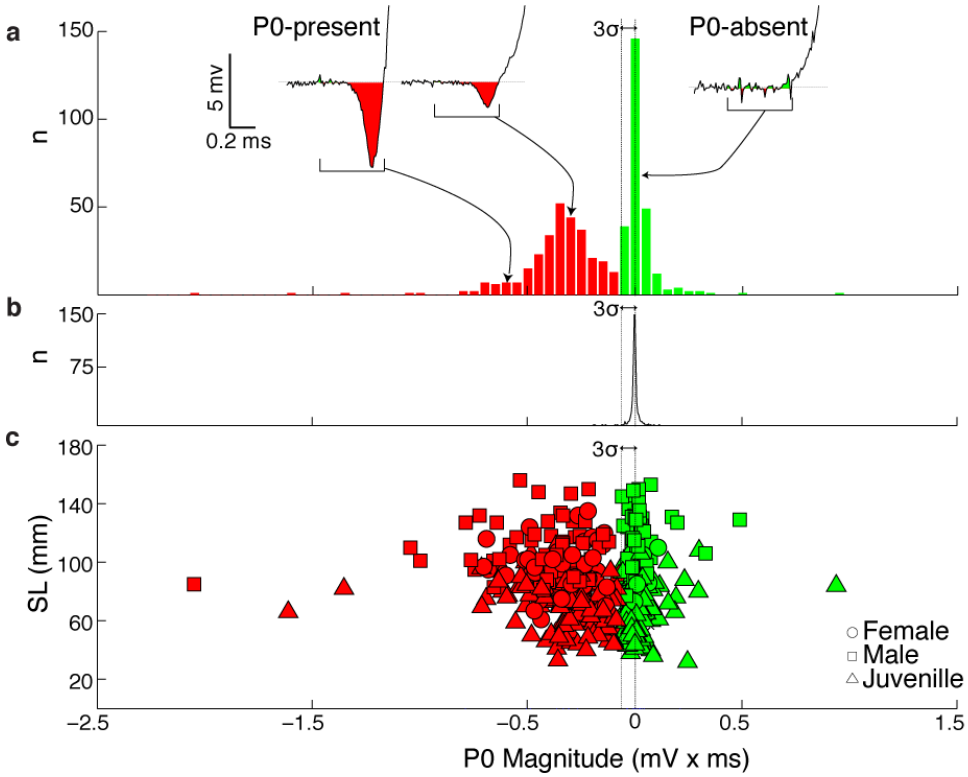

Figure 3-5: Distribution of P0 magnitude among collected *Paramormyrops kingsleyae* specimens. **a.** Histogram of P0 areas (n=553) indicates a bimodal distribution of P0 areas corresponding to P0-present waveforms and P0-absent waveforms. Modal P0 magnitude of P0-present waveforms is -0.35 mV x ms, modal value for P0-absent waveforms is 0.00 mV x ms. Insets show representative P0 waveforms; far left inset is P0-present (P0=-0.79 mV x ms), middle left is P0-present (P0=-0.17mV x ms), right inset is P0-absent (P0=0.03 mV x ms) **b.** Shown is a histogram of area measurements in the first 0.5ms of each recording, where no EOD is present, indicating the area under the curve due to electrical noise in the recordings (see Methods). We used the value (-0.064 mV x ms) 3 standard deviations smaller than the mean area of the recording noise (and thus significant at the p=0.01 level) as a threshold for classifying individuals as P0-absent or P0-present (green and red respectively). **c.** Individual P0 values plotted by sex and standard length (SL) indicate no relationship (see Results) between either variable (n=524; for 29 specimens sex or SL were not determined).

Fig. 3-5c shows P0 area plotted against standard length and sex. There is no significant difference in P0 magnitude between males and females (one-way ANOVA; F=0.01, df=524, p=0.9365). There is a weak but statistically significant linear correlation with standard length, a general indicator of specimen age in fish (slope=-0.0012; F=10.76; df=552; p=0.001, r^2=0.01). P0 area (one-way ANOVA; F=103.31, df=11 p<0.0001) and time of P0 (one-way ANOVA; F=72.44 df=11, p<0.0001) varied significantly among collection localities.

Fig. 3-6 illustrates the geographic distribution of our sampling efforts across Gabon. Pie charts for each collection locality represent the proportion of signal types at each collection site, and sample sizes are listed below. In the majority of localities, only P0-present individuals were captured. P0-absent individuals occurred only in two geographically distinct regions (Cocobeach, Fig. 3-6 circular inset, and in the Louétsi drainage basin, Fig. 3-6). Both signal types were observed at two collection sites: Apassa Creek (n=31: 30 P0-present, 1 P0 absent) and Bambomo creek (n=159: 14 P0-present, 145 P0-absent).

After the 1998 and 1999 collecting seasons, the combination of data from high-resolution topographic maps, GIS coordinates, and detailed signal analysis revealed that only P0-absent individuals were collected in rivers draining into the Louétsi river above Bongolo Falls (Fig. 3-6, gray area bounded by red dashed line), and that P0-present individuals were predominantly captured in rivers draining into the Louétsi and Ngounié rivers below Bongolo Falls. We hypothesized that Bongolo Falls acted as a barrier between the two signaling types, and tested this hypothesis with additional sampling in these and additional creeks in 2009. Table 3-5 summarizes the results of our collecting efforts. Our collections in 2009 were consistent with collections made in 1999; the same signaling types were collected at the same sites 10 years later in Biroundou, Bikagala, Bambomo and Mouvanga Creek. Above Bongolo Falls, only P0-absent

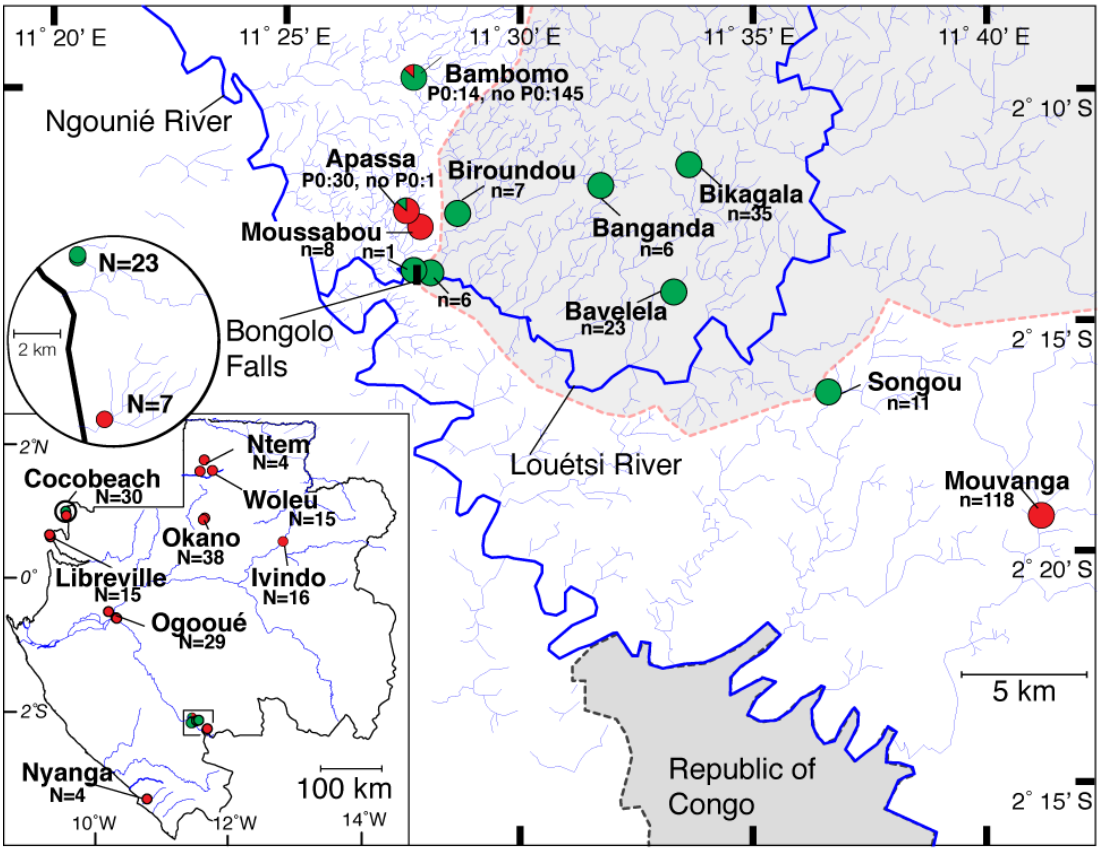

Figure 3-6: Geographic distribution of P0 absent and P0 present *Paramormyrops kingsleyae* collected 1998-2009.

We indicate the distribution of P0 absent and P0 present individuals in Gabon at a variety of geographic scales. Each sampled locality is displayed as a pie chart proportional to signaling types collected. Pie charts are shaded based on signal type; red indicates proportion of *P. kingsleyae* that are P0-present; green indicate proportions of *P. kingsleyae* that are P0-absent. Sample sizes for each population are indicated. The map of Gabon (lower left) represents our sampling efforts across Gabon; the circular inset is a detailed view of the area known as Cocobeach. The main figure is a detailed view of the area surrounding the confluence of the Louétsi and Ngounié rivers. Two populations (Bambomo and Apassa) were mixed for both P0-absent and P0-present signal types. The lightly shaded area, bounded by a red dashed line, corresponds to the Upper Louétsi watershed, which is isolated from the Lower Louétsi watershed by the presence of a 15m waterfall, Bongolo Falls. The grey shaded area, bounded by a grey dashed line, demarks the boundary of the Republic of the Congo

individuals were captured during these two field seasons. During 2009, we found an exceptional population, Songou creek, where the river drained into the Ngounié River, but had entirely P0-absent individuals (n=11). Two populations had individuals that had both P0-absent and P0-present EODs; Apassa Creek (Surveyed only in 2009) and Bambomo Creek (surveyed in 1999 and 2009).

Morphology of Electric Organs and Individual Electrocytes

Fig. 3-7 summarizes counts of stalk penetrations in 8 of the 12 electric organs surveyed, exemplifying the variation in electric organ anatomy we observed. Each section surveyed is represented as a square shaded based on the number of penetrations observed (gray= 0; orange=1; yellow=2; red=3; white=section missing/no data). Each column represents a single electrocyte; each row represents a single 6 μm section made from lateral to medial. For each specimen, the number of electrocytes analyzed for each individual is reported (n=27-72 electrocytes). Only partial organs were available for Cocobeach 4015 and 4025. In some electric organs, stalk penetrations were present only in a few electrocytes (nearly every column is gray from left to right, e.g. Cocobeach 4002). In others, penetrations are evident in almost every electrocyte (plot

has a colored pixel in nearly every column from left to right; e.g. Mouvanga 2627), indicative of *NPp* or *Pa* type morphology respectively. A third group of electric organs had penetrations in some electrocytes, but not others (plot has some columns containing color, and adjacent columns are lacking color in all 6μm sections). Our survey of all 12 electric organs is summarized in Table 3-6. For each electric organ, the number of penetrations was summed for each electrocyte across all sections. Six specimens examined with P0-present waveforms had predominantly *Pa*

Site Name	Drainage	1999	2009
Biroundou	Above	P0 Absent	P0 Absent
Banganda	Above	P0 Absent	-
Bikagala	Above	P0 Absent	P0 Absent
Bavelela	Above	-	P0 Absent
Louétsi River	Above	P0 Absent	-
Bambomo	Below	Mixed	Mixed
Moussabou	Below	P0 Present	-
Songou	Below	-	P0 Absent
Mouvanga	Below	P0 Present	P0 Present
Louétsi River	Below	P0 Absent	-
Apassa	Below	-	P0 Present

Table 3-5 Summary of Predominant Signaling Types in 1998-1999 and 2009 near Bongolo Falls.
Predominant signal types are noted for each collection locality visited in 1998-1999 and 2009. Sites are described as draining into the Louétsi River above and below Bongolo Falls. Sites that were not surveyed in that year are listed as (-).

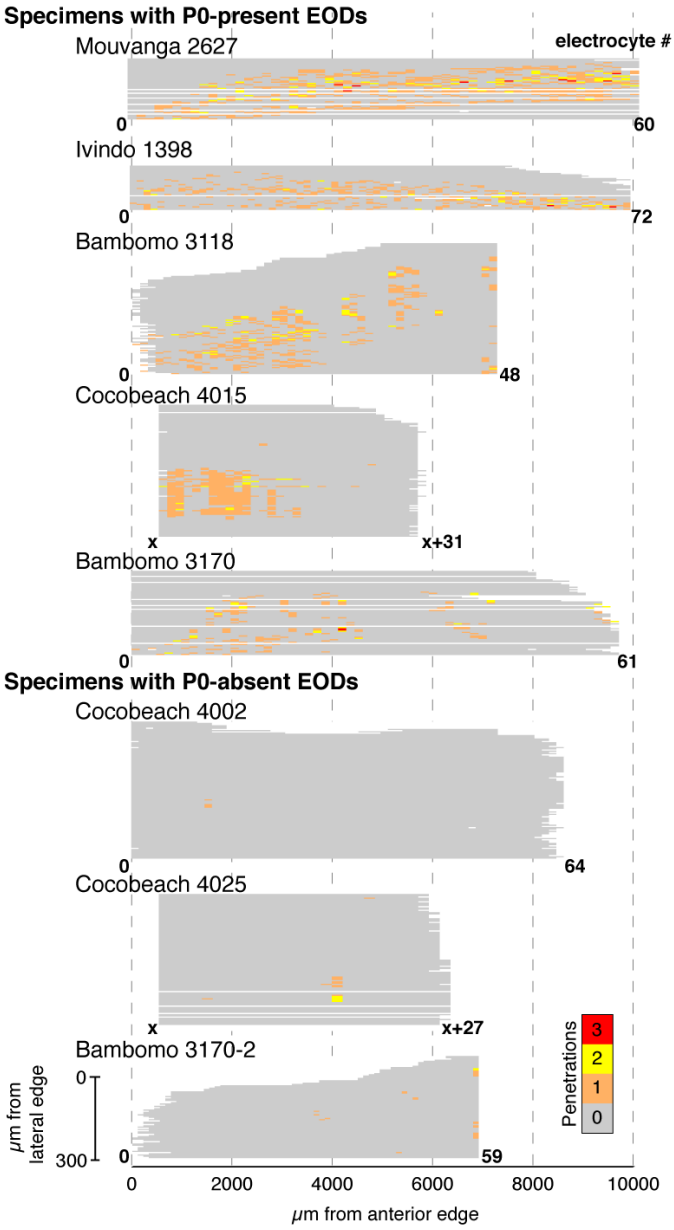

Figure 3-7: Heterogeneous and homogeneous electric organ morphology in *Paramormyrops kingsleyae*. We show here variation in electric organ morphology from 8 individuals, representing 3 major types of electric organs observed (mostly *Pa*, mostly *NPp* and mixed). Number of penetrations in individual section is indicated by color (gray= 0; orange=1; yellow=2; red=3; white=section missing/no data). For all plots, horizontal axis represents distance from the anterior edge of the electric organ, and the vertical axis represents distance from the lateral edge of the electric organ (top=lateral). Mouvanga 2627 and Ivindo 1398 represent "typical" patterns of penetration in P0-present type Mormyrids. *Pa* type morphology is present in each electrocyte, characterized by a colored box in each column from anterior to posterior. In Bambomo (3170; 3118) and Cocobeach (4015) P0-present specimens the electric organ is heterogeneous (both *Pa* and *NPp* electrocyte morphology). P0-absent specimens (Bambomo 3170-2; Cocobeach 4002, 4025) exhibit comparatively homogenous *NPp* morphology in the electric organ. Numbers of electrocytes are noted in bold on the ends of each plot; note the variability in the number of electrocytes between individuals. For Cocobeach 4025 and 4015 only a posterior portion each electric organ was available for analysis

type electrocytes, and six specimens examined with P0-absent waveforms had predominantly *NPp* type electrocytes. In six of twelve specimens, we observed both *Pa* and *NPp* electrocytes in the same electric organ.

We also used confocal microscopy to visualize the complex, three-dimensional morphology of an additional eight, individually dissected, electrocytes (see methods). Fig. 3-8a displays confocal 3D reconstruction of the anterior and posterior faces of two electrocytes dissected from one individual that had both electrocyte types, Bambomo specimen number 3118. One electrocyte (Fig. 3-8a; left) is *Pa*; the other (Fig. 3-8a; right) is *NPp*. Fig. 3-8b shows the anterior and posterior faces of electrocytes from additional localities. For each electrocyte, morphological features, number of penetrations, and specimen locality are indicated. In *Pa* type electrocytes the nerve and stalk system are visible on the anterior face, whereas microstalklets, the result of profuse stalk branching following a penetration, fuse over restricted regions of the posterior face ("territories"). In *NPp* type electrocytes, the nerve, microstalklets, and stalk system are only visible on the posterior face. We observed differences in the number of the stalk penetrations (4-16) between electrocytes, as well as in the length of microstalklets on the posterior face of *Pa* type electrocytes. Though these individual electrocytes were selected from electric organs composed of several hundred electrocytes, the number of penetrations detected by this method in each electrocyte appears consistent (among electrocytes with penetrations, indicated by width and color density of yellow-red bands; Fig. 3-7) with the individuals surveyed using serial histology (Fig. 3-7, Table 3-6).

We hypothesized that the number of penetrations is responsible for the magnitude of P0. Given that the discharge of the posterior face is responsible for P1 (Bennett 1971), we also

Specimen	Locality	Signal Type	# of Electrocytes	*Pa-type*	*NPp-type*
3217	Upper Louétsi	P0-Absent	49	0	49
3170-2	Bambomo	P0-Absent	59	3	56
4025	Cocoa Beach	P0-Absent	27	2	25
N.V. "A"	Cocoa Beach	P0-Absent	58	0	58
4002	Cocoa Beach	P0-Absent	64	1	63
4020	Cocoa Beach	P0-Absent	25	0	25
2429	Libreville	P0-Present	58	58	0
2627	Mouvanga	P0-Present	60	60	0
1398	Ivindo	P0-Present	73	73	0
3170	Bambomo	P0-Present	61	*39*	22
4015	Cocoa Beach	P0-Present	31	*21*	10
3118	Bambomo	P0-Present	48	*37*	11

Table 3-6: Summary of Histological Analysis.
Twelve electric organs were examined. Specimen numbers and localities are listed, with corresponding signal type (see Methods). Total numbers of electrocytes are listed, along with the number of those corresponding to *Pa* type anatomy and *NPp* type anatomy (see Methods).

Figure 3-8: Confocal reconstruction of within and between specimen variation in electrocyte morphology. For each electrocyte, anterior faces are shown on the left, posterior faces on the right. For each, the **N**erve, **S**talk, **M**icrostalklets, and **P**enetrations are shown. **a.** Two electrocytes were dissected from the electric organ of a single specimen. Eight penetrations can be observed (**P**) in the electrocyte on the left, none can be observed in the electrocyte on the right. The *NPp* electrocyte (right) is innervated on the posterior face and has microstalklets on the posterior face. No penetrations can be observed, and no stalk is observed on the anterior face. **b.** Variation in *Paramormyrops kingsleyae* electrocytes. Shown are six 3D projections of the anterior and posterior faces of electrocytes from various localities dissected from individual specimens. Cocobeach *NPp* has no penetrations; stalk is located only on posterior face. For all other electrocytes, penetrations are visible, and stalk is located on the anterior face.

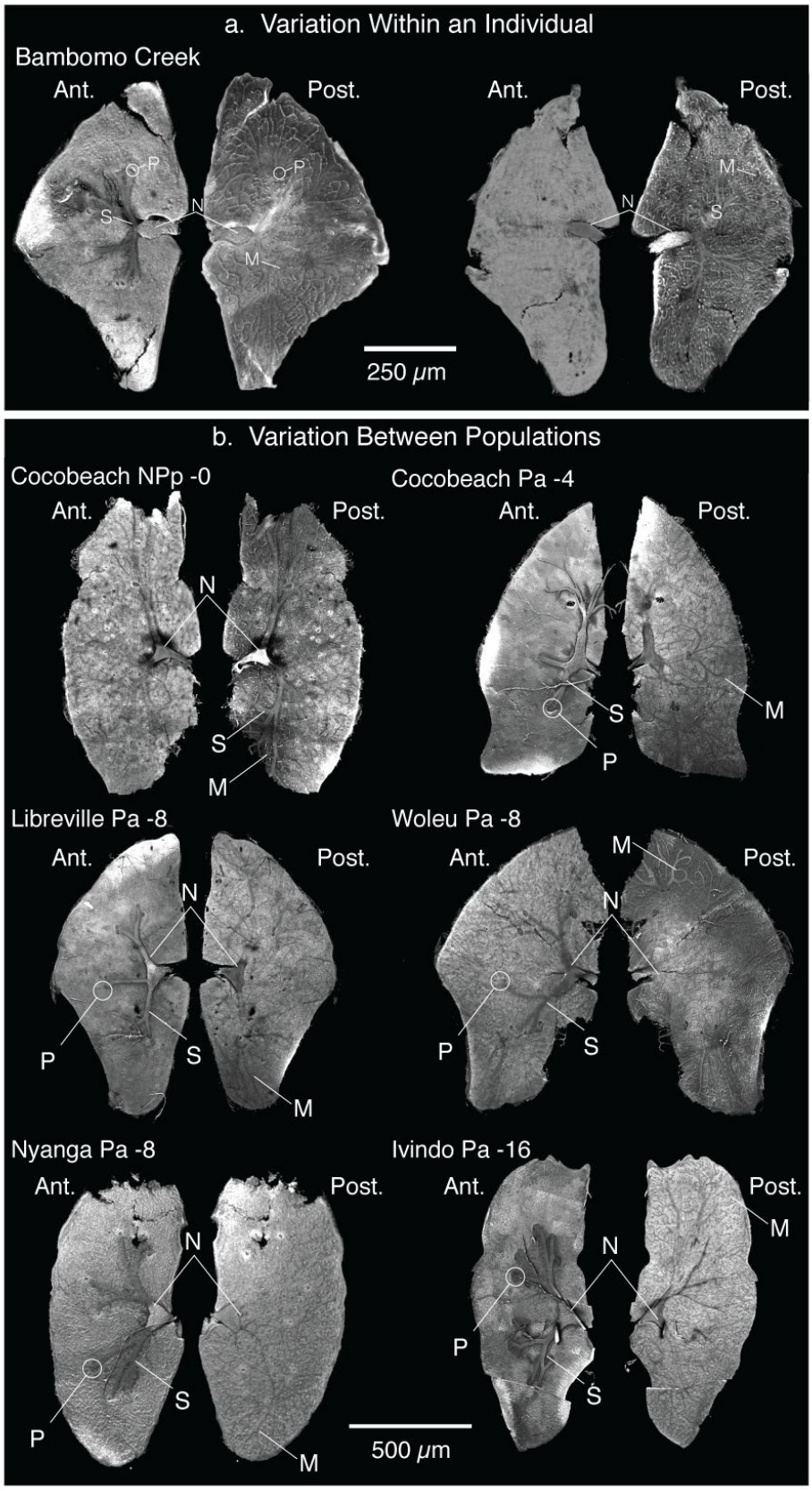
a. Variation Within an Individual
Bambomo Creek
Ant.
Post.
Ant.
Post.
P
P
S
N
M
N
M
S
250 μm
b. Variation Between Populations
Cocobeach NPp -0
Ant.
Post.
N
S
M
Cocobeach Pa -4
Ant.
Post.
S
M
P
Libreville Pa -8
Ant.
Post.
N
P
S
M
Woleu Pa -8
Ant.
M
Post.
N
P
S
Nyanga Pa -8
Ant.
Post.
N
S
P
M
Ivindo Pa -16
Ant.
Post.
M
N
P
S
500 μm

hypothesized that delay in electrical conduction along the stalk system, after it penetrates through the electrocyte, may be responsible for the timing of P0 relative to P1. Assuming that conduction velocity along microstalklets remained constant, a source of this variation might be microstalklet territory length. We were able to determine a linear relationship between the area of electrocyte face devoted to penetrations and the magnitude of P0 (Fig. 3-9; slope=-1.10; $p=0.008$; $r^2=0.78$). Though we observed differences in the territory size, we were unable to determine any meaningful relationship between territory size and delay of P0 relative to P1.

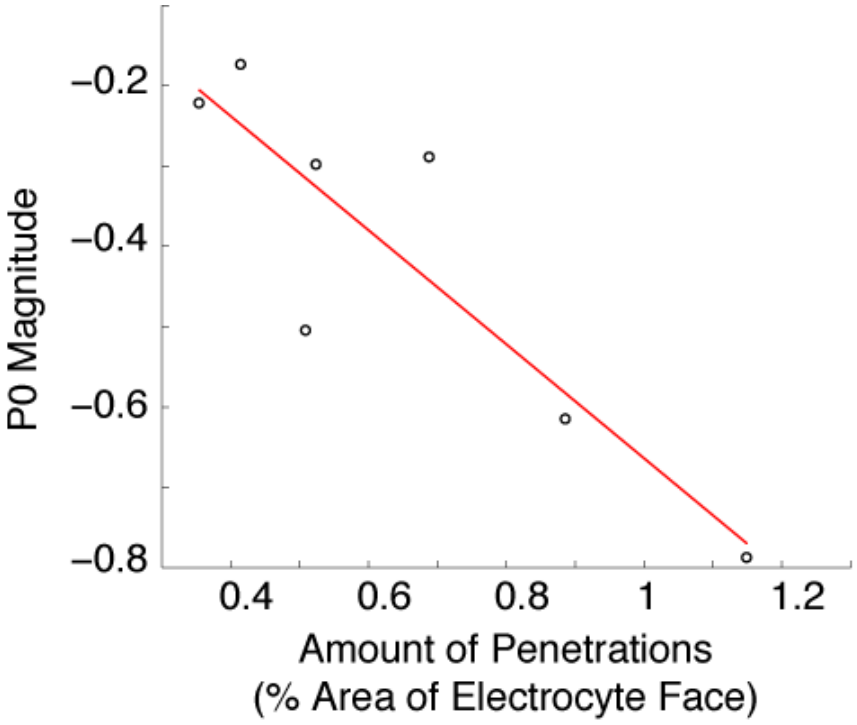

Figure 3-9: Morphological correlates of signal variation in *Paramormyrops kingsleyae* electrocytes.
There is a linear relationship between the percent area of electrocyte face devoted to penetrations and magnitude of P0 for seven individually dissected electrocytes ($p=0.008$; $R^2=0.78$).

Discussion

P. kingsleyae EODs are geographically variable

Principal components analysis of EODs (Fig. 3-3) indicates that EOD waveforms among *Paramormyrops kingsleyae* in Gabon are more similar across 21 variables (indicated by their degree of overlap) when compared to variation across these variables between other *Paramormyrops* species (Arnegard and Hopkins 2003). Despite this overall similarity, *P. kingsleyae* EOD waveforms do vary in two distinct aspects: duration and the magnitude of peak P0. Our analysis shows that this variation is clinal, and that those localities separated by the largest geographic distances are correspondingly the most divergent with respect to these two characters; EOD duration increases from East to West, while the magnitude of P0 decreases from North to South. EOD waveforms of *P. kingsleyae* are bimodally distributed with respect to the magnitude of peak P0, corresponding to P0-absent and P0-present signal types. In the majority of the populations sampled, the P0-present signaling type was collected (Fig. 3-6). P0-absent individuals were collected in only two localities, at Cocobeach, and near the confluence of the Louétsi and Ngounié rivers. Both populations occur less than 10 km from P0-present populations. P0-present and P0-absent individuals rarely co-occur; only in two collection sites (Bambomo and Apassa Creeks) were P0-absent and P0-present individuals captured together.

There are several potential explanations for the observed variation in *P. kingsleyae* EOD signals. Such variation may be caused primarily by: (1) the actions of natural and/or sexual selection, (2) phenotypic plasticity coupled with variation in environmental conditions among sites, or (3) genetic drift. We consider the plausibility of each of these alternative but non-exclusive, hypotheses in light of other mormyrid studies.

Hypothesis #1: Selection Drives EOD Divergence in P. kingsleyae

Electroreception - EOD production serves a dual role for both communication and active

electrolocation behaviors (von der Emde 1999; Hopkins 1999). The presence of an additional phase in P0-present individuals may enhance information content for electroreception because of wider frequency bandwidth per individual electric pulse, thus improving electroreceptive performance in certain conditions (Meyer 1982). We consider this an unlikely explanation since the magnitude of difference in P0 amplitude between P0-absent and P0-present waveform types is only, at maximum, 1% of the peak-to-peak amplitude of the entire EOD (Table 3-2). In addition, our analysis of FFT curves computed for each EOD was unable to detect a systematic relationship between the presence/absence of P0 and differences in frequency content (Table 3-2).

Cryptic Species - Variation in EOD signals might reflect the existence of two distinct species within *Paramormyrops kingsleyae.* Several lines of evidence suggest that this is unlikely: First, recent study of divergent EOD signaling in another *Paramormyrops* species has revealed, despite larger phenotypic EOD divergence in P0 magnitude, no overt evidence of reproductive isolation (Arnegard et al. 2005). Second, morphological and molecular evidence (Sullivan et al. 2002; Sullivan et al. 2004) suggest only a single *P. kingsleyae* species rather than two distinct groups. Finally, our data suggests that the morphological differences between P0-absent and P0-present *P. kingsleyae* electric organs are not maintained in sympatry, leading to individuals of mixed morphology (Fig. 3-9, Table 3-3). This may be evidence of potential hybridization between signal types in these localities, resulting from a lack of any pre-mating reproductive isolation between the co-occurring signal types. Behavioral, neurophysiological and genetic studies are needed to completely rule out this possibility, and are presently in progress.

Character Displacement - A final possibility is that of reproductive character displacement, a process of divergence which gives rise to greater courtship signal differences between co-

occurring taxi than between the same taxa in geographical isolation from one another (Pfenning and Pfenning 2009). Because our collecting methods did not permit exhaustive, systematic sampling of mormyrid assemblages at multiple sites (e.g., along river channel transects), we are presently unable to rule out this possibility. We are compelled to note, however, that our collections of *P. kingsleyae* at sites in Cocobeach and the Louétsi rivers rarely included other mormyrid species. The possibility of reproductive character displacement merits future studies on the relationship between intra- and interspecific species diversity among a variety of *Paramormyrops* assemblages.

Hypothesis #2: Developmental Plasticity in Response to Environmental Heterogeneity Underlie EOD Variation in P. kingsleyae

Development of EODs and electric organs has been observed in multiple species in the laboratory (Denizot et al. 1982; Werneyer and Kramer 2006; Baier et al. 2006; Hopkins unpublished). The P0 character emerges late in electric organ development, when larvae are approximately 2 cm in standard length, when stalk penetrations develop (Denizot et al. 1982). P0s and penetrations manifest regardless of the sex of the individual, and are retained until adulthood. Our data clearly supports that the presence or absence of P0 is not due to differences between juvenile and adult fishes, nor is it a sexually dimorphic character (Fig. 3-5).

Though few studies have demonstrated developmental responses of the electric organ to environmental heterogeneity (see Hopkins 1999), it is unlikely that P0 and the development of penetrations may be in response to environmental factors. Our data on *P. kingsleyae* collected from Gabon field sites 1998-2009 concerning variation in environmental variables, including water temperature, conductivity, and habitat vegetation do not predict the variation between EOD signal types. In addition, P0s (and penetrating stalks) have widespread phylogenetic

distribution (Sullivan et al. 2000; see also below), encompassing a wide variety of habitat types that have not been associated with the presence or absence of penetrating stalks. Finally, sympatric *Paramormyrops* assemblages (and other sympatric mormyrid assemblages) include P0-absent and P0-present species, presumably under the same or similar environmental influences, suggesting that the presence of P0s and penetrating stalks are more likely due to genetic differences between species.

Hypothesis #3: Genetic Drift within small, isolated populations Causes EOD Variation in P. kingsleyae

Principal components analysis revealed a strong geographic component in the described EOD variation. Because of no correlated variation in environmental conditions, and presumably few selective differences between collection localities, we consider the alternative hypothesis that distance between populations potentially explains this variation. As cartographic data were unavailable to determine river distances between many of our collection localities, we used Latitude and Longitude coordinates of our collection sites to estimate distances between populations. We found significant correlations between duration and Longitude and magnitude of P0 and Latitude (Fig. 3-4), indicative of clinal variation in EODs across Gabon, even among temperature corrected datasets (see Appendix 5 for more details). The clinal nature of this variation, particularly in the absence of systematic variation between populations in terms of selective or environmental factors (discussed above), leads us to favor the hypothesis that phenotypic differences may be the result of populations isolated by geographic distance. Qualitative and quantitative analysis of EODs support this (Figs. 3-2 and 3-3); localities separated by the largest geographic distances (i.e. Ivindo and Upper Louétsi) are correspondingly the most divergent with respect to PC1 and PC2, whereas nearby populations are often similar

(Nyanga vs. Upper Louétsi). These phenotypic differences are consistent with evidence of genetic differences between many of the same populations of *P. kingsleyae* (Sullivan et al. 2004; Arnegard et al. 2005).

We also detected spatial variation in EOD waveforms at finer geographic scales. Individuals across all populations were bimodally distributed with respect to the magnitude of peak P0, corresponding to P0-absent and P0-present signal types (Fig. 3-5). In the majority of the populations sampled, the P0-present signaling type was encountered (Fig. 3-6). P0-absent individuals were encountered in only two localities, at Cocobeach, and near the confluence of the Louétsi and Ngounié rivers, both of which occur less than 10km from P0-present populations. P0-present and P0-absent individuals rarely co-occur; only in two collection sites (Bambomo and Apassa Creeks) were P0-absent and P0-present individuals captured together.

Consistent with this, both populations of P0-absent *P. kingsleyae* signal types are associated with prominent physical barriers to migration. In Cocobeach, small adjacent creeks are isolated from each other by the Atlantic Ocean, whereas along the Louétsi River, a 15 m waterfall (Bongolo Falls; Fig. 3-6b) isolates the Upper Louétsi from the Lower Louétsi. The distribution of signal types in the Louétsi region is consistent with Bongolo Falls acting as a barrier between populations; only P0-absent fish were collected above the Bongolo Falls (N=94). Bambomo Creek was one of two sites that contained both signal types. Bambomo is a tributary of a small river that drains into the Ngounié River. Its headwaters, however, are within close proximity (<150 m) of streams that ultimately drain above Bongolo Falls (Fig. 3-6).

Our collections have suggested that *P. kingsleyae* selectively inhabit the shallow headwaters of small creeks in many areas; as such, *P. kingsleyae* habitat preferences may reduce opportunities for migration down main river channels. Our observations of this habitat

preference, taken with (1) prior evidence of genetic differences between populations over these scales (Sullivan et al. 2002; Sullivan et al. 2004; Arnegard et al. 2005) and (2) the lack of plausible selective or environmental factors that influence EOD evolution (discussed above), lead us to consider the hypothesis that divergent *P. kingsleyae* signals may have evolved as the result of reduced gene flow between populations. This may be due to large geographic distances separating some populations, across which migration is reduced, or due to more abrupt topographic changes preventing migration when prominent barriers are encountered. With such reduced gene flow, small populations of genetically isolated *P. kingsleyae,* such as those above Bongolo Falls, may have "lost" penetrating stalks and associated P0s (see below) through the effects of genetic drift over multiple generations, during isolation from P0-present populations. While is plausible given the lack of compelling selective pressures outlined above, we concede that more data is required concerning the population genetics of *P. kingsleyae* in this region. We are presently in the process of testing this hypothesis using microsatellite genotyping strategies among *P. kingsleyae* in the Louétsi drainage region. We note that such a mechanism has been implicated recently (via quantitative trait loci mapping) in the loss of pigmentation among the blind cave tetra *Astyanax mexicanus* (Protas et al. 2007).

Morphological Correlates of EOD Diversity

We reported two morphological features of electrocytes that are correlated with the physiological features of waveforms: the first is the presence or absence of anteriorly innervated, penetrating stalked electrocytes (*Pa*) that are associated with P0-present or P0-absent EOD waveforms, respectively. Our analysis of 12 *P. kingsleyae* electric organs (Fig. 3-7, Table 3-6) and three-dimensional reconstruction of individual electrocytes (Fig. 3-8) demonstrate that these two signal types have a morphological basis. P0-present specimens have predominantly *Pa* type

electrocytes whereas P0-absent specimens have electric organs with predominantly *NPp* type electrocytes. Second, we show that the presence and number of penetrating stalks (Fig. 3-9) is positively related to the magnitude of P0. Both findings are consistent with previous work in other mormyrid species (Bennett and Grundfest 1961; Bass 1986b).

Our analysis also detects heterogeneous electric organs, a phenomenon, to the authors' knowledge, that has not been previously described in mormyrids. This heterogeneous morphology results from the presence of both *NPp* and *Pa* type electrocytes within the same individuals (Fig. 3-7). This morphological heterogeneity was only observed in specimens collected from localities where signal types occurred in close proximity (i.e. Cocobeach and Bambomo Ck.). In localities where only one signal type was found, electric organs were comparatively homogeneous. Among P0-present individuals where significant heterogeneous morphology was observed, *NPp* type electrocytes occurred only in the posterior portion of the surveyed electric organ column. Morphological heterogeneity was observed predominantly among individuals with P0-present EODs; individuals examined with P0-absent signals had comparatively homogenous *NPp* type electric organs (Fig. 3-7, Table 3-6), with occasional penetrations. *NPp* type electrocytes in heterogeneous electric organs did not occur singly, but rather occurred in discrete groups of 7-10 (Fig. 3-7). Denizot and Kirschbaum (1982) observed that electric organs originate in *Pollimyrus* from tail myomeres during early ontogeny, and that each myomere contributes approximately 7-10 electrocytes to the final adult organ.

Electrocyte character optimization on mormyrid phylogeny suggests that *Pa* electrocytes evolved from *NPp*-type early in the history of Mormyridae, followed by several reversals to *NPp*-type (Sullivan et al. 2000). In *Paramormyrops*, *Pa*-type were likely ancestral and there have been minimally five reversals to *NPp* in this genus alone (Sullivan et al. 2004). Stalk

penetrations appear late in electrocyte ontogeny—*Pa*-type electrocytes pass through an *NPp* stage of development (Denizot et al. 1982; Hopkins unpublished; Szabo 1960). Thus, these reversals from adult *Pa*-type to *NPp*-type electrocytes have been interpreted as paedomorphic (Sullivan et al. 2004). The repeated evolutionary reversals from *Pa* to *NPp* in mormyrids and the evidence of heterogeneity in this character among and within populations of *P. kingsleyae* suggests that a simple genetic and developmental mechanism might underlie this character.

Concluding Remarks

Our analysis of fine-scale variation in *P. kingsleyae* EODs and electric organs provide two hypotheses concerning how EODs may evolve. First, the geographic pattern of EOD variation in *P. kingsleyae* suggest that electric signals may evolve through genetic drift, facilitated via isolation by distance, or by prominent barriers to dispersal. Second, the microevolutionary changes occurring in isolated populations of *P. kingsleyae* mirror a repeated pattern of electric organ and signal evolution in the Mormyridae as whole. The fact that the origin of the *NPp* electrocytes and P0-absent EODs from *Pa*/P0-present ancestors is inferred to have occurred multiple times in the history of mormyrids, and again among populations of *P. kingsleyae*, suggests that the genetic mechanism controlling the development of this character may be relatively simple. In *P. kingsleyae* we may be witness to the microevolutionary, population-level processes that have contributed to the macroevolutionary patterns of signal diversity among mormyrid electric fishes.

References

Alves-Gomes J, Hopkins CD (1997) Molecular insights into the phylogeny of mormyriform fishes and the evolution of their electric organs. Brain Behav Evol 49:324-351

Arnegard ME, Hopkins CD (2003) Electric signal variation among seven blunt-snouted *Brienomyrus* species (Teleostei: Mormyridae) from a riverine species flock in Gabon, Central Africa. Environ Biol Fishes 67:321-339

Arnegard ME, Jackson BS, Hopkins CD (2006) Time-domain signal divergence and discrimination without receptor modification in sympatric morphs of electric fishes. J Exp Biol 209:2182-2198

Arnegard ME, McIntyre PB, Harmon LJ, Zelditch ML, Crampton WGR, Davis JK, Sullivan JP, Lavoué S, Hopkins C (2010) Sexual signal evolution outpaces ecological divergence during electric fish species radiation. Am Nat 176:335-356.

Arnegard ME, Bogdanowicz SM, Hopkins CD (2005) Multiple cases of striking genetic similarity between alternate electric fish signal morphs in sympatry. Evolution 59:324-343

Baier B, Lamml M, Kramer B (2006) Ontogeny of the electric organ discharge in two parapatric species of the dwarf stonebasher, *Pollimyrus castelnaui* and *P. marianne* (Mormyridae, Teleostei). Acta Zool. 87:209-214

Bass AH (1986a) A hormone-sensitive communication-system in an electric fish. J Neurobiol 17:131-155

Bass AH (1986b) Electric organs revisited: evolution of a vertebrate communication and orientation organ. In: Bullock TH, Heiligenberg W (eds) Electroreception. Wiley, New York, pp 13-70

Bass AH (1986c) Species differences in electric organs of mormyrids: substrates for species-typical electric organ discharge waveforms. J Comp Neurol 244:313-330

Bass AH, Denizot JP, Marchaterre MA (1986) Ultrastructural features and hormone-dependent sex-differences of mormyrid electric organs. J Comp Neurol 254:511-528

Bass AH, Volman SF (1987) From behavior to membranes - testosterone-induced changes in action-potential duration in electric organs. Proc Natl Acad Sci USA 84:9295-9298

Bennett MV, Grundfest H (1961) Studies on morphology and electrophysiology of electric organs III. Electrophysiology of electric organs in mormyrids. In: Chagas C, Paes de Carvalho A (eds) Bioelectrogenesis. pp 113-135

Bennett MV (1971) Electric organs. In: Hoar, W, Randall D (eds) Fish Physiology, vol. 5, pp 347-491. New York: Academic

Bradbury JW, Verencamp SL (1998) Principles of Animal Communication. 1st edn. Sinauer Associates, New York

Carlson BA (2009) Temporal-pattern recognition by single neurons in a sensory pathway devoted to social communication behavior. J Neurosci 29:9417-9428

Carlson BA (2002) Neuroanatomy of the mormyrid electromotor control system. J Comp Neurol 454: 440-455

Caputi AA, Carlson BA, Macadar O (2005) Electric organs and their control. In: Bullock TH, Hopkins C, Popper A, Fay RR (eds) Electroreception. Springer, New York, pp 410-451

Denizot JP, Kirschbaum F, Max Westby GW, Tsuji S (1982) On the development of the adult electric organ in the mormyrid fish *Pollimyrus isidori* (with Special Focus on the Innervation). J Neurocytol 11:913-934

Endler JA (1989) Conceptual and other problems in speciation. In: Otte D, Endler JA (eds) Speciation and Its Consequences. Sinauer Associates, Sunderland, MA, pp 625-648
Feulner PG, Plath M, Engelmann J, Kirschbaum F, Tiedemann R (2009) Electrifying love: electric fish use species-specific discharge for mate recognition. Biol Lett 23:225-228
Foster SA, Scott RJ, Cresko WA (1998) Nested biological variation and speciation. Philos Trans R Soc B 353:207-218
Xu-Friedman MA, Hopkins C (1999) Central mechanisms of temporal analysis in the knollenorgan pathway of mormyrid electric fish. J Exp Biol 202:1311-1318
Günther A (1896) Report on a collection of reptiles and fishes made by Miss M.H. Kingsley during her travels on the Ogowe river and in Old Calabar. Ann Mag Nat Hist 100:261-285
Hopkins CD (1980) Evolution of electric communication channels of mormyrids. Behav Ecol Sociobiol 7:1-13
Hopkins CD (1986) Behavior of mormyridae. In: Bullock TH, Heiligenberg W (eds) Electroreception. John Wiley and Sons, New York, pp 527-576
Hopkins CD (1999) Signal evolution in electric communication. In: Hauser MD, Konishi M (eds) The Design of Animal Communication. M.I.T. Press, Cambridge, Massachusetts, pp 461-491
Hopkins CD, Bass AH (1981) Temporal coding of species recognition signals in an electric fish. Science 212 (4490):85-87
Hopkins CD, Lavoué S, Sullivan JP (2007) Mormyridae. In: Stiassny MLJ, Teugels GG, Hopkins CD (eds) Poissons D'eaux Douces Et Saumâtres De Basse Guinée: Ouest de l'Afrique Centrale' vol 1. Faune Et Flore Tropicales. IRD Éditions, Paris, pp 220-334
Iles RB (1960) External sexual differences and their significance in *Mormyrus kannume* (Forskal, 1775). Nature 188:516.
Kirschbaum F (1995) Reproduction and development in mormyriform and gymnotiform fishes. In: Moller P (ed) Electric Fishes: History and Behavior. Chapman & Hall, London, pp 267-301
Kramer B, Westby GWM (1985) No sex difference in the waveform of the pulse type electric fish, *Gnathonemus Petersii* (Mormyridae). J Comp Physiol A 145:399-403
Kramer B, van der Bank H (2000) The southern churchill, *Petrocephalus wesselsi*, a new species of mormyrid from South Africa defined by electric organ discharges, genetics, and morphology. Environ Biol Fish 59: 393–413
Kramer B, van der Bank H, Flint N, Sauer-Gürth H, Wink M (2003) Evidence for parapatric speciation in the mormyrid fish *Pollimyrus castelnaui* (Boulenger, 1911) from the Okavango-Upper Zambezi river systems: *P. marianne* sp. nov., defined by electric organ discharges, morphology and genetics. Environ Biol Fish 67:47-70
Kramer B, van der Bank H, Wink M (2004) *Hippopotamyrus ansorgii* Species Complex in the upper Zambezi River system with a description of a new species, *H. szaboi* (Mormyridae) Zool Scr 33:1-18
Kramer B, Skelton P, van der Bank H, Wink M (2007) Allopatric differentiation in the *Marcusenius macrolepidotus* species complex in Southern and Eastern Africa: the resurrection of *M. pongolensis* and *M. angolensis*, and the description of two new Species (Mormyridae, Teleostei) J Nat Hist 41:647-708
Kramer B, Swartz E (2010) *Hippopotamyrus ansorgii* complex from the Cunene river in southern Africa (Teleostei: Mormyriformes) J Nat Hist 44:2213-2242

Lamml M, Kramer B (2006) Differentiation of courtship songs in parapatric sibling species of dwarf stonebashers from southern Africa (Mormyridae, Teleostei) Behavior 143:783-810
Lamml M, Kramer B (2007) Allopatric differentiation in the acoustic communication of a weakly electric fish from southern Africa, *Marcusenius macrolepidotus* (Mormyridae, Teleostei) Behav Ecol Sociobiol
Lavoué S, Arnegard M, Sullivan JP, Hopkins C (2008) *Petrocephalus* of Odzala offer insights into evolutionary patterns of signal diversification in the Mormyridae, a family of weakly electrogenic fishes from Africa. J Physiol-Paris 102:322-339
Lévêque D, Paugy D, Teugels GG (1990) The Fresh and Brackish Water Fishes of West Africa (Vol. 1). Musée Royal de l'Afrique Centrale. Tervuren, Belgium.
Lewontin RC (1974) The Genetic Basis for Evolutionary Change. Columbia University Press, New York, NY
Machnik P, Kramer B (2008) Female choice by electric pulse duration: attractiveness of the males' communication signal assessed by female bulldog fish, *Marcusenius pongolensis* (Mormyridae, Teleostei). J Exp Biol. 211:1969-77
Mayr E (1963) Animal Species and Evolution. Belknap Press, Cambridge, MA
McPhail JD (1994) Speciation and the evolution of reproductive isolation in the sticklebacks (*Gasterosteus*) of southwestern British Columbia. In: Bell MA, Foster SA (eds) The Evolutionary Biology of the Threespine Stickleback. Oxford University Press, Oxford, UK
Meyer JH (1982) Behavioral responses of weakly electric fish to complex impedances. J Comp Physiol A 145:459-470
Pezzanite B, Moller P (1998) A sexually dimorphic basal anal-fin ray expansion in the weakly discharging electric fish *Gnathonemus petersii*. J Fish Biol 53:638-644
Pfenning KS, Pfenning DW (2009) Character displacement: ecological and reproductive responses to a common evolutionary problem. Q Rev Biol 84:253-276
Protas M, Conrad M, Gross JB, Tabin C, Borowsky R (2007) Regressive evolution in the Mexican cave tetra, *Astyanax mexicanus.* Curr Biol 17:452–454
Scheffel A, Kramer B (1997) Electrocommunication and social behavior in *Marcusenius senegalensis* (Mormyridae, Teleostei). Ethology 103:404-420.
Sullivan JP, Lavoué S, Arnegard ME, Hopkins CD (2004) AFLPs resolve phylogeny and reveal mitochondrial introgression within a species flock of African electric fish (Mormyroidea: Teleostei). Evolution 58:825-841
Sullivan JP, Lavoué S, Hopkins CD (2000) Molecular systematics of the African electric fishes (Mormyroidea : Teleostei) and a model for the evolution of their electric organs. J Exp Biol 203:665-683
Sullivan JP, Lavoué S, Hopkins CD (2002) Discovery and phylogenetic analysis of a riverine species flock of African electric fishes (Mormyridae: Teleostei). Evolution 56:597-616
Szabo T (1960) Development of the electric organ of Mormyridae. Nature 188:760-762
Teugels G, Hopkins CD (1998) Morphological and osteological evidence for the generic position of *Mormyrus kingsleyae* in the genus *Brienomyrus* (Teleostei: Mormyridae). Copeia 1998:199-204
Verrell PA (1998) Geographic variation in sexual behavior: sex signals and speciation. In: Foster SA, Endler JA (eds) The Evolution of Geographic Variation in Behavior. Oxford University Press, Oxford, UK,
von der Emde G (1999) Active electrolocation of objects in weakly electric fish. J Exp Biol

202:1205-1215
Werneyer M, Kramer B (2006) Ontogenetic development of electric-organ discharges in a mormyrid fish, the bulldog *Marcusenius macrolepidotus* (South African Form). J Fish Biol 69:1190-1201

CHAPTER 4. PHENOTYPIC VARIATION IN ELECTRIC SIGNALS AMONG *PARAMORMYORPS KINGSLEYAE* RESULTS FROM REDUCED GENE FLOW IMPOSED BY GEOGRAPHIC ISOLATION*

Abstract

Understanding the origins of phenotypic divergence is important for understanding processes of speciation. In this study, we extend a prior analysis of geographic variation in electric signals (EODs) emitted by the mormyrid electric fish *Paramormyrops kingsleyae*, by taking a population genetics approach to examine patterns of gene flow, population structure, electric organ anatomy, and signal diversity. We test the hypothesis that reduced gene flow, imposed by naturally occurring geographic barriers between populations of *P. kingsleyae*, has lead to the evolution of subtly divergent EOD signals.

We examined microsatellite genotypes at five loci and electric organ discharge signals from each of 338 specimens from nine populations from Gabon, West Central Africa, collected in 1999-2009. First, we examined patterns of gene flow using microsatellite genotyping at five loci. We determined statistically significant genetic differentiation between most populations, and that genetic differentiation between populations was significantly related to geographic distance between populations, as measured by distance along rivers. Second, we employed the Bayesian clustering algorithm STRUCTURE to classify genotyped individuals without *a priori* information, and found evidence of hierarchical population structure that related to geographic distances along watershed migration routes. A waterfall appears to act as a significant geographic barrier, additionally influencing gene flow. Third, we performed principal components analysis to examine patterns of EOD variation across populations. Patterns of EOD variation were reflected by patterns of spatial genetic structure described above, specifically in regards to signal duration, and in the presence or absence of a small head-negative phase, termed P0, that is present in some specimens and absent in others. Fourth, we utilized a dishabituation paradigm to assess the ability of *P. kingsleyae* to discriminate between divergent EOD forms. We were unable to demonstrate that *P. kingsleyae* could discriminate between EOD types. This is consistent with genetic evidence collected in two localities where divergent signal types occurred in sympatry. In these populations, there was little evidence of genetic differentiation between signal types, and histological evidence of some individuals supports the possibility of hybridization between divergent signal types.

The evidence presented in this analysis supports the overall hypothesis that patterns of signal variation in *P. kingsleyae* have resulted from reduced gene flow due to geographic isolation. As present evidence most likely indicates that changes in EOD waveforms result from the effects of genetic drift, this implicates a mechanism by which variation in an important component of electric signal diversity among the rapidly radiated *Paramormyrops* species flock could be generated, and upon which selection could later act in the speciation process.

* This work is currently a manuscript in preparation, authored by the following: Jason R. Gallant, Dr. Matthew Arnegard, Dr. Bruce Carlson, Joshua Sperling, Catherine Cheng, Jessica Thiesmeyer, Erica Sher and Dr. Carl Hopkins

Introduction

Understanding the causes of phenotypic divergence has been an important goal in evolutionary biology. Phenotypic variation may result from either developmental plasticity in response to the environment (West-Eberhard, 2003), or from the interaction between the homogenizing effects of gene flow and the actions of selection and/or genetic drift (Slatkin, 1987). There are two causal frameworks under which the interaction between gene flow and selection and/or drift could act to cause divergence in phenotypic characters. One possibility is that geographic barriers act to reduce the number of migrants between neighboring populations, thus reducing the effects of gene flow and enabling divergence to occur through the actions of selection or drift (Slatkin, 1987; Wright, 1943). Another possibility is that adaptive divergence in different ecological environments over a geographic range could result in selection against migrants between adjacent populations (Schluter, 2009; Wang and Summers, 2010), secondarily leading to the reduction of gene flow. It is important to note that these two frameworks are not exclusive, and could conceivably act in a positive feedback loop (Hendry et al., 2002). Delineation between these two frameworks is difficult, however, without knowledge regarding the role of the phenotype in reproductive isolation (Nosil and Crespi, 2003). Establishing whether reduced gene flow is either the cause or the effect of phenotypic divergence takes on special relevance in the efforts to understand the population level processes that contribute to the speciation process, given that divergent phenotypes and reproductive isolation are part-and-parcel to what defines a species (Mayr, 1963).

In this study, we use a combination of morphological, physiological and population genetic data to infer patterns of gene flow as they relate to patterns of previously described geographic variation in electric courtship signals (EODs) produced by the mormyrid electric fish *Paramormyrops kingsleyae* (Gallant et al., 2011). We then assess the likelihood that either (1)

reduced gene flow between populations has caused divergence in EOD signals or (2) divergence in EOD signals has reduced gene flow (i.e. reproductive isolation) by using behavioral playback experiments to determine whether EOD variation can be discriminated.

The Study System

P. kingsleyae is a member of a recently evolved, rapidly radiated species flock (Sullivan et al., 2002). *Paramormyrops* exhibit highly divergent electrical signals (Sullivan et al., 2004) termed electric organ discharges (EODs), which vary in their waveform duration (0.5-8 ms), the number of phases or peaks in the electric pulse, and in their polarity (Sullivan et al., 2000). A recent study by Arnegard et al. (2010) has shown compelling evidence that EOD divergence within *Paramormyrops* greatly outpaces rates of diversification in ecological and morphological characteristics, suggesting that sexual selection is an important driver of species divergence, rather than natural selection in this group. Arnegard et al. (2010) notes that species radiation in *Paramormyrops* may have arisen due to use of electric signaling; which is relatively "private" compared to other sensory modalities, thereby making *Paramormyrops* a sexual selection parallel of other cases of adaptive radiations arising after "key innovations" followed by the actions of natural selection (Grant and Grant, 2008; Losos, 2009; Seehausen, 2006). For these reasons, *Paramormyrops* have become an emerging model for the study of species diversification and the evolution of sexual signals.

We are interested in understanding how this broad, macroevolutionary pattern has resulted from processes that act among individual populations. Has sexual selection acted between populations of *P. kingsleyae* to drive EOD divergence, or have other process contributed to diversity, upon which sexual selection later acts? Recently characterized patterns of geographic variation among the geographically widespread *Paramormyrops* species, *P.*

kingsleyae, which presents a unique framework to explore some of these questions (Gallant et al. 2011).

P. kingsleyae exhibit clinal variation in EOD signals with regard to duration, and a small head-negative phase, termed P0. This subtle signal feature ranges from approximately 2% of the peak-to-peak magnitude of some EODs, or is altogether absent in some geographically isolated forms. While the majority of populations across Gabon have P0-present EODs, in two regions, isolated by major barriers to migration (a waterfall, Bongolo Falls in the South, or the Atlantic Ocean in a Northern Population), every individual possesses P0-absent EODs. Two populations, Apassa and Bambomo creek, occurr along a watershed boundary between which streams either drained above or below Bongolo Falls, and are the only locations known locations where individuals with P0-present and P0-absent waveforms co-occur, and may represent a possible hybrid zone.

Despite the subtle difference in EOD signals between these forms, the anatomical substrate for P0-present and P0-absent signals requires a considerable reorganization of the electric organ: in P0-present EODs individual electrocytes have penetrating stalks with anterior innervation (*Pa*) whereas in P0-absent EODs, electrocytes have non-penetrating stalks with posterior innervation (*NPp*). In the majority of specimens surveyed from populations across Gabon, individuals with P0-present EODs have electric organs with *Pa* type anatomy, whereas individuals with P0-absent EODs have electric organs with NPp type anatomy. However, in Bambomo creek, we discovered multiple individuals that contained both Pa type electrocyte and NPp type electrocytes in the electric organ.

The discovery of a species that is geographically variable in the presence or absence of P0 and its morphological correlate characterizes a major component of signal diversity for the

entire *Paramormyrops* species flock, as well as several other mormyrid genera: *NPp* type electric organs, together with their P0-absent EOD waveforms have independently evolved from *Pa* type electric organs at least five times in *Paramormyrops* and seven times within mormyrids (Sullivan et al., 2004; Sullivan et al., 2000; Sullivan et al., 2002). Therefore, insights into population level processes may provide insight into understanding how electric signals in other *Paramormyrops* species may have evolved, thus providing a connection between population divergence and processes of speciation.

These prior results have motivated the hypothesis that reductions in gene flow between geographically isolated populations of *P. kingsleyae* have caused geographic variation in electric signals (EODs). If this hypothesis is valid, we expect to find: (1) evidence of genetic structure associated with physical barriers or large distances between populations, which correlates detectable variation in EOD signals. (2) Evidence that *P. kingsleyae* individuals are incapable of discriminating between divergent EOD types (i.e. P0-absent vs. P0-present), and (3) Genetic, morphological, and/or physiological evidence that hybridization between signal forms occurs in populations where individuals occur sympatrically.

Materials and Methods

Specimen Collection and EOD Recording, and EOD Analysis

Collections of *Paramormyrops kingsleyae* were made during field trips to Gabon, West Central Africa in 1999, 2001 or 2009 from locations summarized in Table 4-1 and Figure 4-1. Fish were collected using a variety of methods, including fish traps baited with worms, hand nets and electric fish detectors, hook and line, and light rotenone applications. Following any application of rotenone, fish were immediately transferred to fresh, aerated water, where they recovered completely. We saw no difference in the EODs of rotenone captured fish and those captured using other methods.

EODs of each specimen were originally recorded within hours of capture in 1- to 5 liter plastic boxes filled with water from the collection site. Signals were recorded with bipolar silver chloride coated silver wire electrodes, and amplified (bandwidth =0.0001-50 kHz) with a differential bio amplifier (CWE, Inc : Ardmore, PA), and digitized at a 100 kHz-1 MHz sampling rate, with head-positivity upward using a Daqbook or WaveBook (IOTECH: Cleveland, OH), or a USB-powered A-D Converter (National Instruments: Austin, TX). All EOD recordings were made at a vertical resolution of 16 bits per sample. After recording their EODs, individual specimens were euthanized with an overdose of MS-222. We removed one or more paired fins from specimens and preserved these tissues in 95% ethanol. Each specimen was given a unique specimen identification tag, and fixed free-floating in 10% formalin (phosphate-buffered; pH 7.2) for at least 2 weeks. Specimens were then transferred to 70% ethanol, and deposited in the Cornell University Museum of Vertebrates. All methods conform to protocols approved by Cornell University's Center for Research Animal Resources and Education.

Following the methods described by Gallant et al. (2011), we made 21 measurements from a single recorded EOD waveform using a custom written program in MATLAB (Mathworks, Inc.: Natick, MA). For each waveform, amplitudes, times and slopes at nine landmarks defined by peaks, zero crossings, first derivative peaks, and threshold crossings were calculated. In addition, we performed a power spectrum analysis of each EOD waveform using the MATLAB *fft* function to determine the peak frequency and a low and high frequency 3 dB below the peak frequency for each EOD recording. Variation across these 21 measurements (normalized by using the MATLAB function *zscore*) was quantified by performing principal components analysis (PCA) with the MATLAB function *princomp*.

Microsatellite Genotyping

We extracted DNA from fin clips using DNeasy Tissue Kits (Qiagen, Inc.) for 1998-1999 samples or AgenCourt DNAadvance kits (Beckman-Coulter, Inc) for 2009 samples. We

Pop	Year	Lat.	Long.	N	Genotype	Ne	Structure	IBD	EOD	EO	Behavior.
Apassa	2009	2° 12' 42" S	11° 27' 50" E	28	**X**		**X**	**X**	**X**	**X (4)**	
Balé	1999	0°31' 7 "N	12° 48' 2"E	11	**X**		**X**		**X**		
Bambomo	2009	2° 9' 49" S	11° 27' 42" E	109	**X**	**X**	**X**	**X**	**X**	**X (7)**	**X (10)***
Bambomo	1999	2° 9' 49" S	11° 27' 42" E	27	**X**	**X**	**X**	**X**	**X**		
Bavavela	2009	2°14' 33"S	11° 33' 22" E	24	**X**		**X**	**X**	**X**		
Bikagala	2009	2° 11' 43" S	11° 33' 40" E	29	**X**		**X**	**X**	**X**		
Mouvanga	2009	2° 19' 23" S	11° 41' 18" E	32	**X**	**X**	**X**	**X**	**X**	**X (6)**	**X (10)***
Mouvanga	1999	2° 19' 23" S	11° 41' 18" E	19	**X**	**X**	**X**	**X**	**X**		
Nyamé Pendé	1999	0°30' 2" N	12° 47' 48" E	12	**X**		**X**		**X**		
Okano	2001	0°48' 56" N	11°42' 4" E	38	**X**		**X**		**X**		
Songou	2009	2° 16' 42" S	11° 36' 41" E	9	**X**		**X**	**X**	**X**	**X (4)**	

Table 4-1: Summary of locations and years of population samples, and analyses performed on each population.
* Indicates additional individuals were sampled from these populations to perform these analyses. Numbers in parentheses indicate sample sizes, if no sample size is reported, the entire population reported (N) was analyzed. Genotype= microsatellite genotyping, Ne= effective population size, Structure= Bayesian Clustering Analysis, IBD= analysis of genotypic variation with geographic distance (Southern populations only), EOD= electric signal analysis, EO= electric organ histology, Behavior= subjects for dishabituation paradigm.

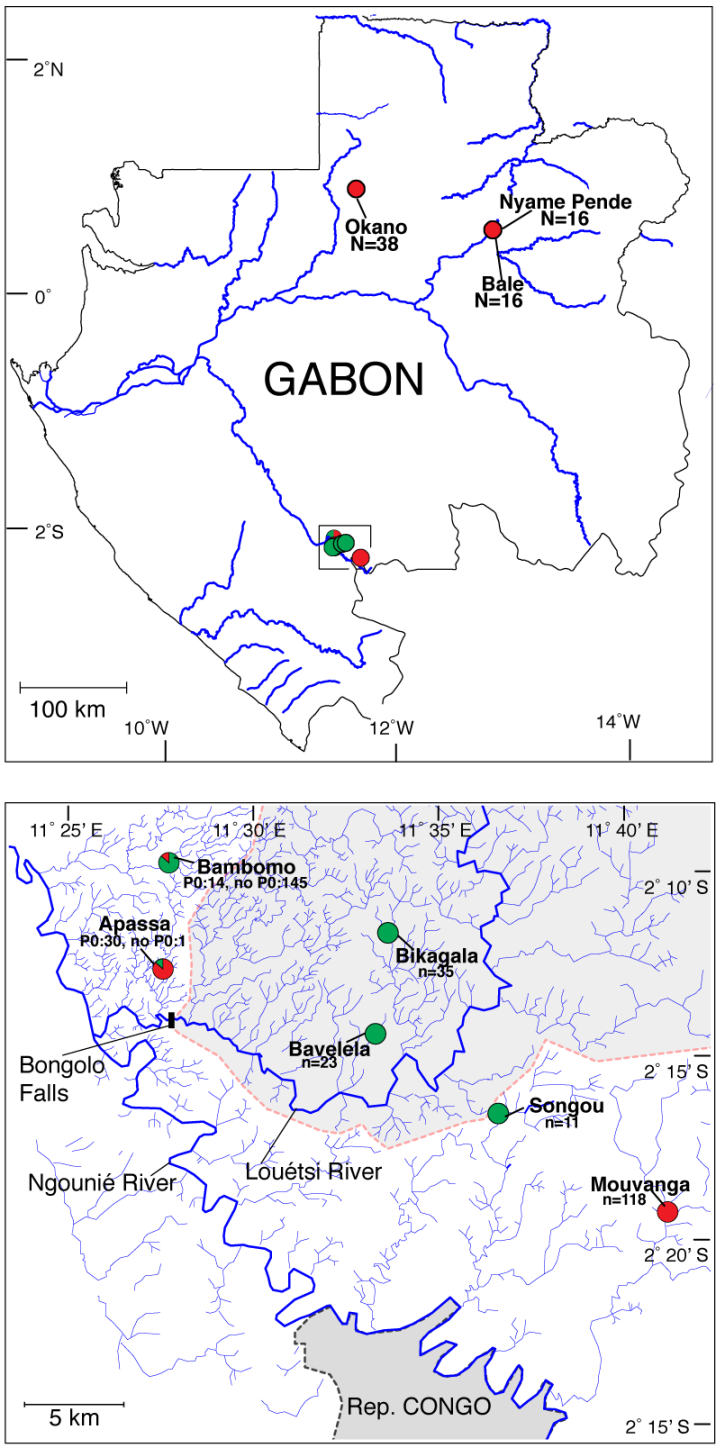

Figure 4-1 Map of study populations.
Top map shows relationship between populations across Gabon. Box in the south indicates the location of the lower detail map, which indicates the relationship of Southern populations near the confluence of the Louétsi and Ngounié rivers. For all maps, populations are indicated by pie charts, as reported in Gallant et al. 2011. Red indicates proportion of individuals P0-present, green indicates proportion of individuals that were P0-absent. Bongolo falls is indicated in the map of southern populations, and a grey region bounded by a red dotted line indicates the small streams and creeks that drain into the Louétsi River above Bongolo Falls.

amplified DNA at each of five microsatellite loci (NBB01-NBB05) previously described by Arnegard et al. (2005) using the Qiagen Type-It multiplex PCR System (Qiagen, Inc.). Reaction volumes were 15µl, consisting of 1µl template DNA, 7.5µl Type-it Multiplex Master Mix (containing HotStarTaq Plus DNA Polymerase and PCR buffer with 3 mM $MgCl_2$), and 2 pmol of each primer (5' primers labeled with Applied Biosystems fluorescent dyes FAM, HEX or NED). Thermal cycling (under mineral oil) was 5 min at 95˚C (initial activation) followed by 28 cycles of 95˚ for 30 sec, 60˚C for 90 sec and 72˚C for 30 sec. Each individual reaction (containing PCR products for all 5 loci) was resolved by electrophoresis on an ABI 3100 automated sequencer (Applied Biosystems). Under these initial thermal conditions, reactions for locus NBB04 failed for the Bambomo, Nyame Pende, and Bale Creek populations. For these populations, an additional PCR reaction was performed as above using primers only for the NBB04 locus, with thermal cycling (under mineral oil) for 5 min at 95˚C (initial activation) followed by 35 cycles of 95˚ for 30 sec, 50˚C for 90 sec and 72˚C for 30 sec.
Following genotyping, individual fragment lengths were analyzed and binned according to size by visual inspection, using Genemapper 4.1 software (Applied Biosystems).

Genotyping Data Analysis

For each microsatellite locus (NBB001-NBB005), we examined possible deviations from expected Hardy-Weinberg equilibrium within populations using the two-tailed exact test (Weir, 1990) as implemented by GENEPOP v4.1 (Rousset, 2008). Next, we performed exact tests of linkage disequilibrium between all pairs of loci (within and between populations), to test the independent assortment of loci. Statistical significance in both sets of tests was evaluated using Markov chain methods (10,000 dememorization steps; 1000 batches; 5000 iterations per batch). We additionally calculated observed and expected heterozygosity under Hardy-Weinberg equilibrium for each population at each allele using the software Arlequin 3.5 (Excoffier, 2010).

The significance of each was evaluated at the p=0.05 level and the Bonferoni corrected level of p=0.001.

Genetic differentiation between pairs of populations was assessed as variance in allele frequencies between subpopulations (s) over total variance in allele frequencies between populations (t) expressed by the standardized measure of genetic differentiation, F_{st} (Weir, 1984), and was estimated using Arlequin v 3.5 (Excoffier and Lischer, 2010). F_{st} significance was evaluated by permuting genotypes between populations 50,000 times, and using a threshold of p=0.05 or the Bonferoni corrected level of p=0.001. Pairwise genetic comparisons were complimented by evaluation of pairwise geographic distances between populations, in order to determine any patterns of genetic differentiation with distance. Pairwise distances between all study populations were computed using digitized topographic maps, which were superimposed over satellite imagery provided in Google Earth software (Google, Inc. v.6.0.1). For each pair of populations, the distance between was defined as the shortest river path between populations, following the flow of water ("as the fish swims" distance). For some pairwise comparisons, these distances traversed a known major waterfall, Bongolo Falls (Fig. 4-1).

The correlations between pairwise distance the pairwise distance matrix and pairwise F_{st} matrix was assessed by performing a Mantel test computed using the program IBD v.1.5.2 (Bohonak, 2002). Significance was calculated by permuting the matrix 1000 times. A reduced major axis regression technique was employed to estimate the slope and intercept of the relationship between genetic differentiation and geographic distance. Confidence intervals for this relationship were computed by one-delete jackknifing over all populations (Bohonak, 2002).

Effective Population Size

Repeated sampling in Bambomo and Moving Creek in 1999 and 2009 enabled us to attempt to estimate contemporary effective population size using the two-sample method of

Waples (1989). Change in allele frequency over the 10-year period was calculated at each locus using Pollack's (1983) F_k statistic (as expressed by Waples 1989, equation 9). In addition, we calculated an average Fk value for each population, weighted by number of alleles at each locus. Using formula (11) and formula (16) from Waples (1989), we calculated the effective population size and their 95% confidence intervals respectively.

Bayesian Clustering Analysis

We examined genotyping data for evidence of population structure among *P. kingsleyae* without making *a priori* categorizations by EOD waveform or collection locality. To do so, we used the program *Structure* 2.3 (Falush et al., 2003; Pritchard et al., 2000), which employs a model-based Bayesian clustering algorithm to determine the most probable number of genetic clusters of populations (K), and the probability of each individual's membership in each cluster. All simulations were run under an admixture model, allowing for separate alpha values (a model parameter expressing the degree of admixture) for each population. Otherwise, default parameters were used. Simulations were run with 5 replicates each for each K value from K=1 to K=14, with a 25000 MCMC iteration burnin followed by 250000 MCMC iterations for each run, and were completed using a parallel computing version of *Structure* 2.3, provided by the Biopics Web Computing Resources, via the Cornell University Computational Biology Service Unit.

To determine the appropriate number of clusters (K) we used a method described by Evanno et al. (2005), which detects the uppermost level of population structure in a given sample. Our initial run detected two clusters, of which, we wished to detect further population substructuring. Following the methods of Evanno et al. (2005), we used each individual's highest probability of membership to each cluster to assign individuals to subgroups. Each subgroup was subsequently analyzed with STRUCTURE to determine the number of clusters

within each subgroup. This process was repeated until no further clusters could be determined for a subgroup (i.e. highest ΔK was for K=1). Following each STRUCTURE analysis, we used the software *Clumpp* (Jakobsson and Rosenberg, 2007) to align outputs and determine a mean permuted matrix of individual cluster membership across replicates. This matrix was then visualized using the cluster visualization program *Distruct* (Rosenberg, 2004).

Electric Organ Histology & Analysis

Serial sections of electric organs from selected individuals were made for light-microscopy analysis following the methods described by Gallant et al. (2011). Briefly, electric organs were removed from fixed specimens, decalcified overnight, dehydrated in a graded alcohol series then infiltrated in glycol methacrylate resin (JB-4, Polysciences, Inc.). Serial sagittal sections of the embedded electric organs were made at 6 μm thickness, mounted on glass slides, and stained each slide with a 0.5% Toluidine blue solution for 30 sec.

For each specimen, we reconstructed one of four columns of electrocytes from serial, sagittal 6 μm sections, cut from lateral to medial. As each column surrounds the spinal cord, we began our reconstruction at the lateral edge of the electric organ, and stopped counting when the spinal cord was clearly visible (approximately 234-648 μm depending on the size of the individual). For each section, the number of penetrations was counted for each electrocyte (50-70 electrocytes per section) from anterior to posterior. An electrocyte was scored with a penetration whenever a stalk was observed to pass through either or both faces of the electrocyte (Fig. 1-1; 4-6 for examples). For our analysis, we considered each 6-μm section to have an independent number of penetrations from all other sections to minimize the probability of underestimating the total number of penetrations.

Behavioral Playback Experiments

We performed electrical playbacks on 20 individual *P. kingsleyae*, ten were captured

from Mouvanga Creek (where EODs are all P0-present; see Gallant et al., 2011), and ten were captured from Bambomo Creek (where EODs are mixed, most are P0-absent, some are P0-present; see Gallant et al., 2011). We assessed behavioral discrimination of EOD waveforms using dishabituation paradigm described in detail by Carlson et al. (2011b).

Briefly, fish were placed in a tank with a rectangular PVC enclosure containing both Ag/AgCl stimulus electrodes and Ag/AgCl recording electrodes oriented orthogonally (Fig. 4-7). Each fish was administered control and experimental stimulus trains consisting of 10 bursts of 10 EOD pulses each, with an intra-burst interval of 30 ms, and inter-burst interval of 10 s, with a peak-to-peak intensity of 145 mV/cm. For control stimulation, all 100 pulses were an identical sympatric EOD waveform: in playbacks to Mouvanga Creek specimens, this was a P0-present EOD recorded previously from Mouvanga Creek, and in playbacks to Bambomo Creek subjects, this was a P0-absent EOD recorded from Bambomo Creek. For experimental stimuli the 10 pulses in the 9th burst were substituted with either (1) a 90˚ phase-shifted (Carlson et al., 2011b; Heiligenberg and Altes, 1978; Hopkins and Bass, 1981) version of the same conspecific waveform (2) an allopatric P0-present EOD waveform (3) an allopatric P0-absent waveform or (4) a sympatric P0-present waveform. Mouvanga Creek subjects received control and stimuli trains 1, 2, and 3, and Bambomo Creek subjects received control and stimuli trains 1, 3, and 4. The experimental design is summarized in Fig. 1-7. The response of each subject was recorded as the maximum discharge rate of the subject in response to each of the 10 bursts. We report the change in the response between the 8^{th} and 9^{th} bursts as dishabituation, and therefore evidence of discrimination between waveforms for control and experimental waveforms.

Results

Table 4-1 and Fig 4-1 presents a summary of microsatellite genotypes at 5 loci of 338 individuals of *Paramormyrops kingsleyae*, collected at 11 localities. In this first part of our analysis, we address the question of how similar populations of *P. kingsleyae* are, as a means of assessing gene flow between populations.

Loci Attributes, Linkage Equilibrium and Hardy-Weinberg Proportions

We were able to amplify fragments without any failed reactions for all 338 individuals genotyped in this study (i.e. possible null homozygotes). Total number of alleles detected at each of 5 loci over all populations ranged from 2-21 (Table 4-1). For each population, locus-specific expected heterozygosities ranged from 0.11-0.88 (Table 4-2). Exact tests produced no evidence of linked loci across all populations ($p > 0.17$). Only in a few populations did observed heterozygosity deviate significantly from Hardy-Weinberg expected heterozygosity at the $p=0.05$ level; the exceptions were NBB02: Balé ($p=0.015$) and Nyamé Pendé ($p=0.019$); NBB03: Bambomo 1999 ($p=0.003$); NBB04 (Bambomo 1999, Bambomo 2009 and Nyamé Pendé; all $p<0.0001$); NBB05 (Bikagala $p=0.038$). After Bonferoni adjustment for multiple comparisons, only NBB04 (Bambomo 1999, Bambomo 2009 and Nyamé Pendé; all $p<0.0001$) remain significant.

Small changes in allele frequencies over time suggest large contemporary effective population sizes of P. kingsleyae

Fig. 4-2 shows the allele frequency histograms at each of 5 loci for each of the 338 individuals genotyped in this study, grouped by population. Two populations at Mouvanga and Bambomo Creeks were sampled in 1999-2001 and again in 2009. Allele frequencies appeared to change little over this 10 year period between sampling (discussed in detail below). Between populations, there are apparent differences between the distribution of alleles; of particular note

	NBB01				NBB02				NBB03				NBB04				NBB05			
Pop.	***k***	***Ho***	***He***	***p***	***k***	***Ho***	***He***	***p***	***k***	***Ho***	***He***	***p***	***k***	***Ho***	***He***	***p***	***k***	***Ho***	***He***	***p***
Apassa	6	0.71	0.67	0.955	4	0.79	0.71	0.393	6	0.75	0.68	0.212	4	0.64	0.75	0.276	17	0.75	0.92	0.184
Bale	5	0.55	0.63	0.552	10	0.64	0.87	0.015	10	0.82	0.88	0.422	6	0.55	0.58	0.143	9	0.73	0.88	0.445
Bambomo09	6	0.38	0.35	0.963	11	0.82	0.75	0.114	7	0.69	0.69	0.393	11	0.37	0.62	0.000	21	0.72	0.78	0.174
Bavavela	6	0.67	0.60	0.693	6	0.58	0.59	0.184	6	0.83	0.81	0.546	4	0.83	0.73	0.059	6	0.71	0.71	0.584
Bambomo99	5	0.41	0.38	0.537	5	0.67	0.77	0.251	4	0.44	0.63	0.003	4	0.22	0.69	0.000	4	0.78	0.81	0.455
Bikagala	2	0.69	0.64	0.485	3	0.52	0.53	0.120	5	0.52	0.59	0.437	6	0.34	0.33	0.373	3	0.55	0.54	0.038
Mouvanga09	4	0.09	0.09	1.000	7	0.16	0.15	1.000	5	0.44	0.42	0.811	8	0.44	0.43	0.445	13	0.44	0.51	0.576
Mouvanga99	2	0.05	0.05	1.000	3	0.16	0.15	1.000	5	0.32	0.37	0.147	6	0.37	0.48	0.228	4	0.63	0.56	0.644
Nyam. Pend.	4	0.17	0.31	0.090	11	0.58	0.88	0.019	8	1.00	0.85	0.173	4	0.08	0.60	0.000	13	1.00	0.93	1.000
Okano	8	0.53	0.55	0.271	2	0.24	0.25	0.569	7	0.42	0.37	1.000	9	0.45	0.43	0.489	16	0.82	0.90	0.197
Songou	3	0.33	0.52	0.202	2	0.11	0.11	1.000	4	0.33	0.65	0.090	2	0.22	0.52	0.172	2	0.22	0.21	1.000

Table 4-2: Summary of loci attributes.
For each locus and population, the number of alleles (k) at each locus (NBB01-NBB05), the observed (H_o) and expected heterozygosity (H_e) are reported. Probabilities of deviation from Hardy-Weinberg equilibrium are reported as p.

Figure 4-2 Allele frequency histograms for each population and microsatellite locus.
Microsatellite loci genotyped are denoted as NBB01-NBB05. For each population, sample sizes are reported as number of individuals genotyped

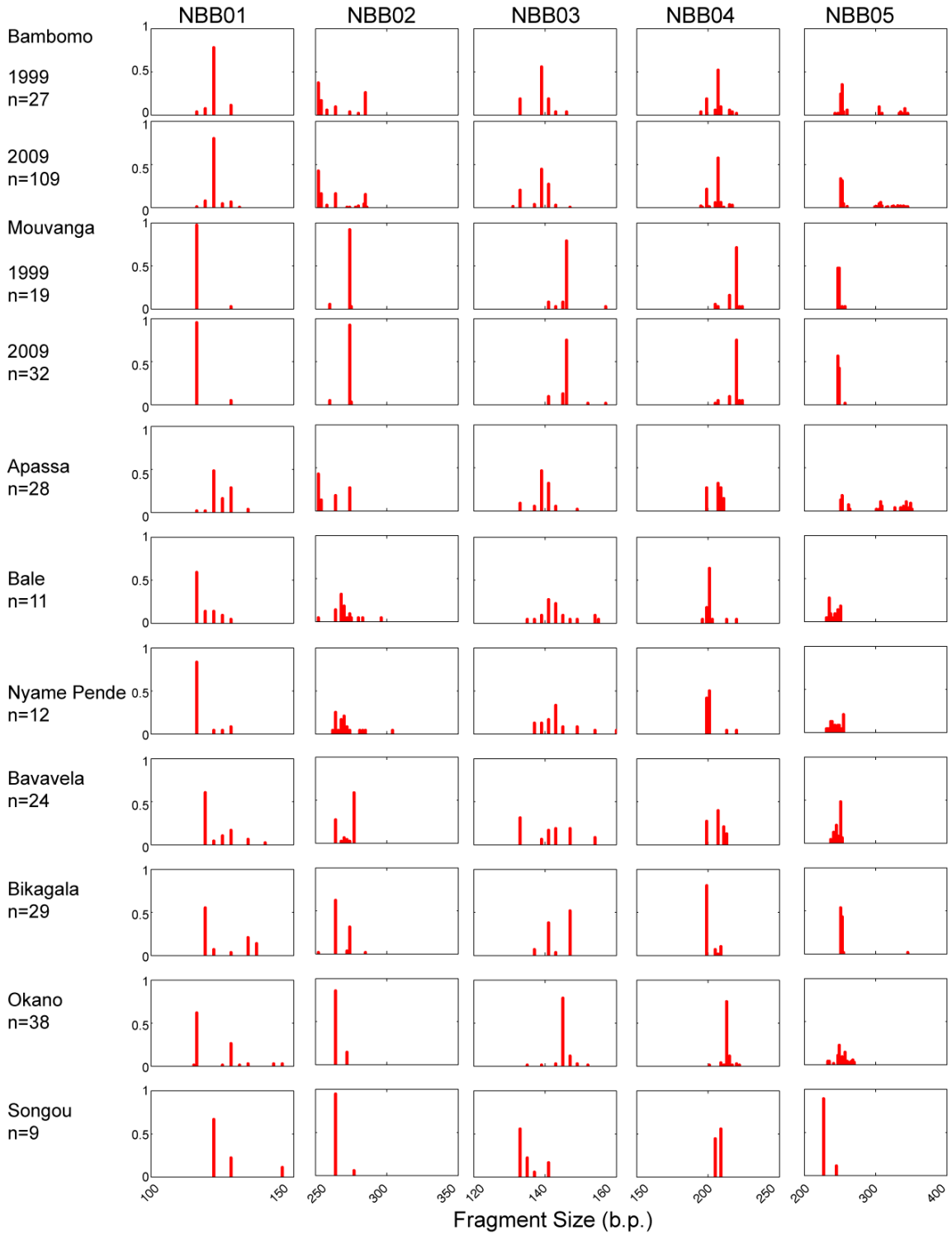
NBB01
NBB02
NBB03
NBB04
NBB05
Bambomo
1999
n=27
2009
n=109
Mouvanga
1999
n=19
2009
n=32
Apassa
n=28
Bale
n=11
Nyame Pende
n=12
Bavavela
n=24
Bikagala
n=29
Okano
n=38
Songou
n=9
0
0.5
1
100
150
250
300
350
120
140
160
150
200
250
200
300
400
Fragment Size (b.p.)

10 year sampling in Bambomo and Mouvanga creeks using the method of Pollack (1983). These values ranged per locus between <0.01 to 0.03, with a weighted average of 0.02 for Bambomo creek and 0.02 for Mouvanga Creek (Table 4-3). This corresponds to very little evidence of genetic drift in either population affecting allele frequency distribution between these 10-year periods. As change in allele frequency over multiple generations provide an indication of effective population size, we utilized the two-sample method of Waples (1989) to estimate effective population sizes and their associated 95% confidence intervals (Table 4-3). If the estimated temporal variance of allele frequencies, F_k, is smaller than expected based on sampling error alone, the temporal method can produce negative estimates of effective population size. Such cases represent no evidence for finite effective population size, which is common for large population sizes (Waples, 1989). Assuming 10 generations between samples, we estimated the effective population size in Bambomo Creek to be 1125 individuals (95% CI 272-∞), and found no evidence for finite population size in Mouvanga Creek (95% CI 1261-∞). Based on these calculations, we see little evidence to suggest small effective population sizes in either population.

Differences in allele frequencies suggest strong genetic differentiation between most populations of P. kingsleyae

Fig. 4-3 summarizes F_{st} values of all pairwise comparisons between *P. kingsleyae* populations surveyed. All populations were all significantly differentiated from one another at the p=0.05 and Bonferoni corrected thresholds, with the exceptional pairwise comparisons of Bambomo Creek 1999 vs. 2009, Mouvanga Creek 1999 vs. 2009, and Nyame Pende vs. Bale Creek. The degree of significant genetic differentiation, based on F_{st} value, varied between populations from 0.06-0.65.

Pop.	Locus	k	S_{1999}	S_{2009}	F_k	Ne	95% CI
Bambomo							
	NBB001	6	27	111	0.0321	558	29 - ∞
	NBB002	10	27	111	0.0280	1027	79 - ∞
	NBB003	12	27	111	0.0350	421	41 - ∞
	NBB004	12	27	111	0.0122	∞	416 - ∞
	NBB005	24	27	111	0.0315	598	128 - ∞
	All Loci	**64**	**27**	**111**	**0.0276**	**1125**	**272 - ∞**
Mouvanga							
	NBB001	3	18	32	0.0120	∞	1- ∞
	NBB002	4	18	32	0.0008	∞	∞
	NBB003	9	18	32	0.0229	∞	52- ∞
	NBB004	9	18	32	0.0219	∞	55 - ∞
	NBB005	7	18	32	0.0264	∞	15 - ∞
	All Loci	**32**	**18**	**32**	**0.0198**	∞	**1261-∞**

Table 4-3: Effective populations size using the "two-sample" method described by Waples, 1989.
Changes in allele frequencies and effective population sizes were estimated for Bambomo and Mouvanga Creek. k = number of independently assorting loci, $S_{1999 \text{ or } 2009}$ = sample size in each respective year, and F_k= Pollack's (1983) standardized measure of allele frequency change (see text). A weighted mean of all locus specific F_k values is calculated. For each locus, and the weighted mean of F_k values for each population, effective population size (Ne +/- 95% CI) is calculated as described in the text assuming 10 generations between 1999-2010.

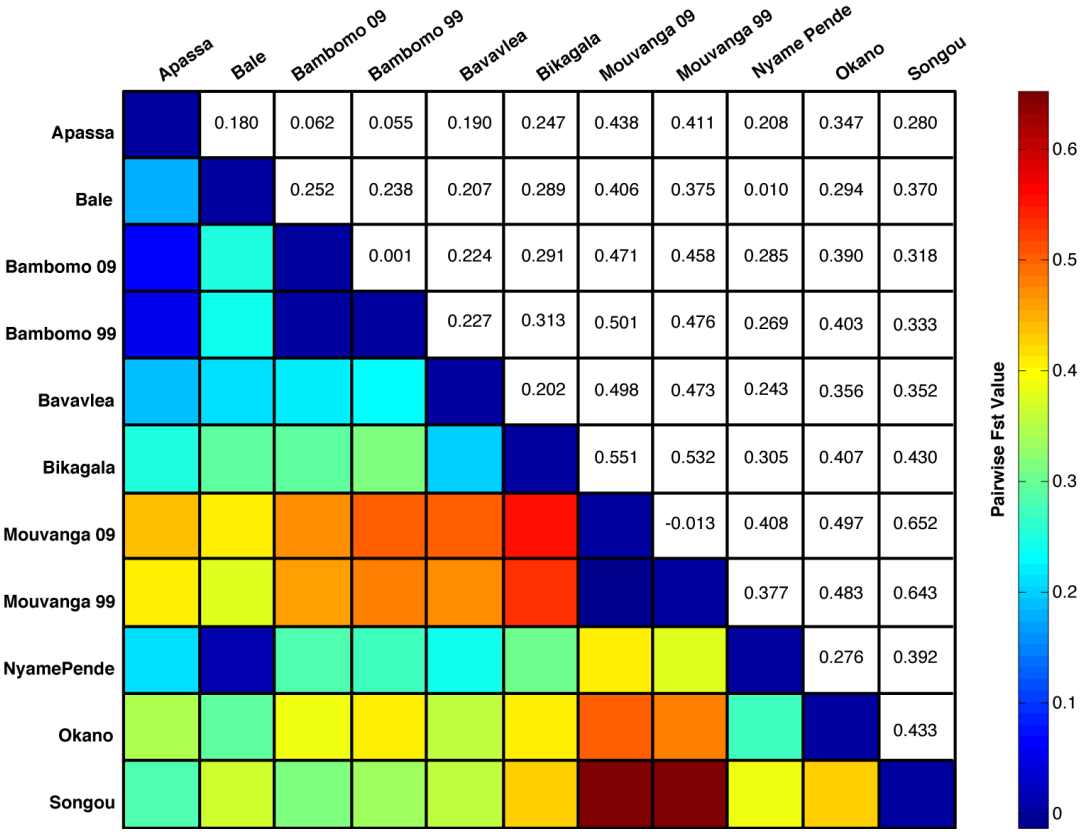

Figure 4-3 F_{st} values for each pairwise comparison of populations.
Lower half of the matrix codes F_{st} value by color, the upper half of the matrix reports the individual F_{st} values. All pairwise comparisons of F_{st} values were significant, with the exception of Mouvanga Creek (1999 vs. 2009), Bambomo Creek (1999 vs. 2009), and Bale Creek and Nyame Pende Creek.

are the presence of several alleles (NBB02, ~250 bp, NBB05 several alleles between 300-400 bp), which are present in Bambomo and Apassa creeks but absent in other populations.

We utilized this allele frequency data to compute change in allele frequency over

Pairwise genetic differentiation between population is related to geographic distance

Next, we investigated the relationship between genetic differentiation (F_{st}) and geographic distance. Pairwise F_{st} values between *P. kingsleyae* populations increased linearly with river distances between populations <120 km, however over greater distances F_{st} varied considerably. As such a single pattern of genetic differentiation and geographic distance may not hold across the entire geographic range considered in this study. Given that we undertook more comprehensive sampling among Southern populations, and that pairwise distances in this region never exceed 120 km, we focused this part of the analysis only on population comparisons within the South of Gabon. Results of these comparisons are shown in Fig. 4-4. As described above, we calculated the shortest river distance between each pair of populations; in some pairs this distance traversed Bongolo Falls, and in others it did not. We have indicated these populations in Fig. 4-4 as closed circles and open circles respectively. There was a significant relationship between pairwise genetic distance and pairwise geographic distance (Mantel Test $Z=720090.47$, $p<0.001$; $R^2=0.60$). We were unable to resolve any differences between population comparisons that traversed the waterfall and those that did not. Two comparisons (Mouvanga Creek 1999 vs. Songou Creek and Mouvanga Creek 2009 vs. Songou Creek) exceeded the 95%CI of this linear regression; in both cases genetic differentiation greatly exceeded the predicted relationship based upon the river distance between these two populations.

Bayesian clustering analysis suggests hierarchical population structure that corresponds to geographic barriers and distance

Hierarchical analysis of population structure for all 338 individuals was performed using

Figure 4-4: Comparison of pairwise F_{st} values and geographic distances in Southern Populations.
Geographic distance was measured as the shortest river distance between two populations. In some pairwise comparisons, this distance traversed Bongolo Falls, and in others it did not. The two types of distances are indicated as closed and open circles respectively. RMA regression was computed for the relationship between genetic and geographic distance, and the significance of the relationship between geographic and genetic distance was evaluated using a Mantel test (see results). 95% confidence intervals, computed by jackknifing across populations are shown as dashed lines.

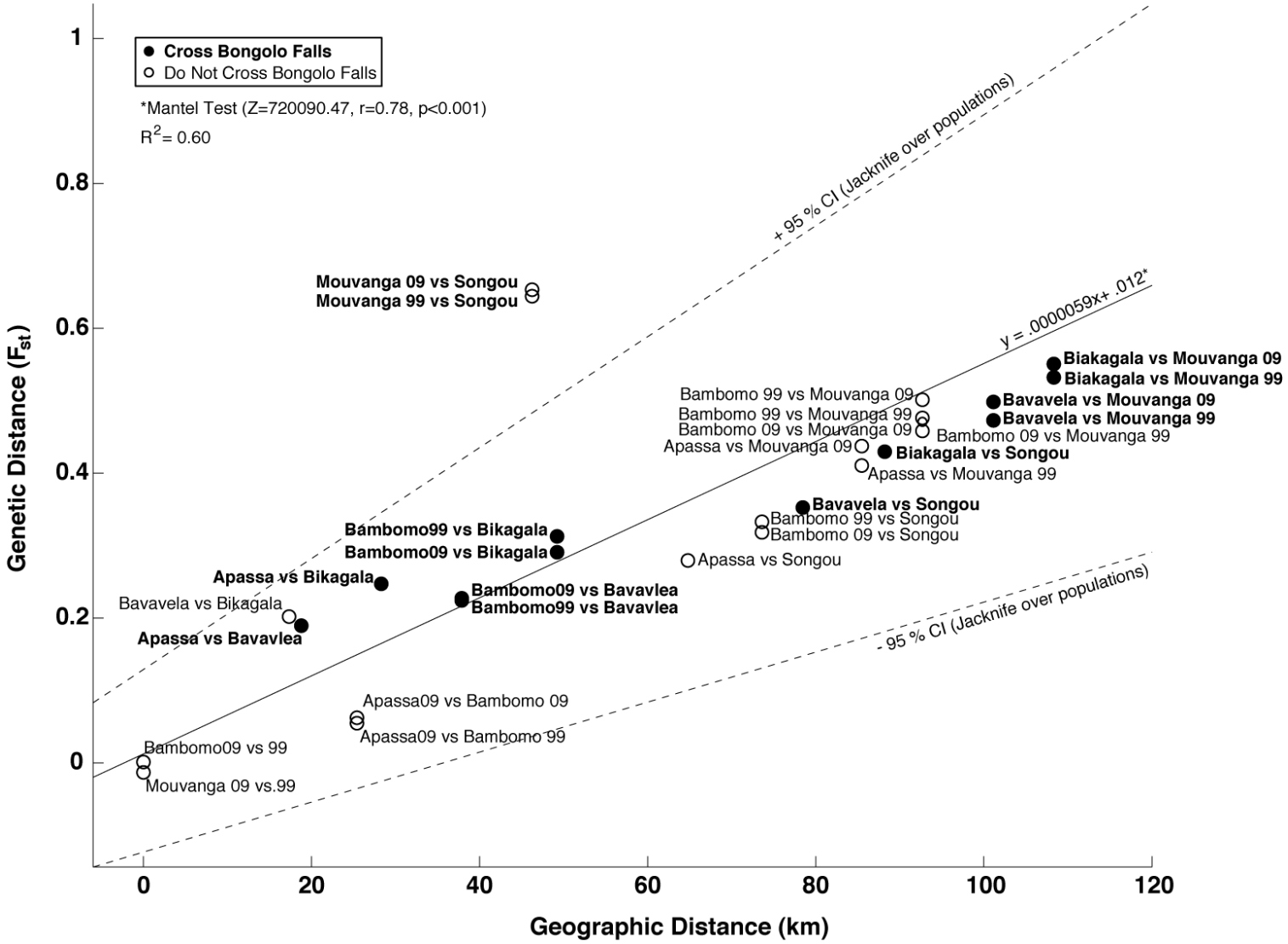
Cross Bongolo Falls
Do Not Cross Bongolo Falls
*Mantel Test (Z=720090.47, r=0.78, p<0.001)
R2= 0.60
+ 95 % CI (Jacknife over populations)
y = .0000059x+ .012*
- 95 % CI (Jacknife over populations)
Mouvanga 09 vs Songou
Mouvanga 99 vs Songou
Biakagala vs Mouvanga 09
Biakagala vs Mouvanga 99
Bambomo 99 vs Mouvanga 09
Bavavela vs Mouvanga 09
Bambomo 99 vs Mouvanga 99
Bavavela vs Mouvanga 99
Bambomo 09 vs Mouvanga 09
Bambomo 09 vs Mouvanga 99
Apassa vs Mouvanga 09
Biakagala vs Songou
Apassa vs Mouvanga 99
Bavavela vs Songou
Bambomo 99 vs Songou
Bambomo 09 vs Songou
Bambomo99 vs Bikagala
Bambomo09 vs Bikagala
Apassa vs Songou
Apassa vs Bikagala
Bambomo09 vs Bavavlea
Bambomo99 vs Bavavlea
Bavavela vs Bikagala
Apassa vs Bavavlea
Apassa09 vs Bambomo 09
Apassa09 vs Bambomo 99
Bambomo09 vs 99
Mouvanga 09 vs.99
Genetic Distance (Fst)
Geographic Distance (km)
0
0.2
0.4
0.6
0.8
1
0
20
40
60
80
100
120

Structure 2.3 (Falush et al., 2003; Pritchard et al., 2000), following the method of Evanno et al. (2005). We employed the ΔK statistic to determine the lowest hierarchical level of population structure in the dataset containing all populations (K=2). To determine structure of subpopulations, we divided the whole dataset into 2 subpopulations (G1 and G2) based on the most probable assignment of each individual to either group. We then ran STRUCTURE again independently on each subgroup to determine the most likely number of subpopulations in each group. In G1 there were two subgroups (G1.A and G1.B), and in G2, there were three subgroups (G2.A, G2.B, and G2.C). We repeated this procedure of splitting groups and performing structure analysis for each subpopulation until no further structure could be detected (largest ΔK was for K=1). This resulted in the splitting of G1.B into three more groups (G3.A, G3.B, and G3.C). Using this method, we detected 3 hierarchical levels of population structure in the total dataset, with 8 distinguishable clusters.

Fig. 4-5a shows the probability of membership in each cluster of each of the 338 individuals genotyped shown as a bar chart, organized by collection locality over each of the detected hierarchical levels. Considering the highest level of population structure for each group, most individuals were assigned with high confidence to a cluster. With few exceptions, at the highest hierarchical level of population structure (i.e. G2.A-C, G3.A-C), individuals were assigned to clusters that corresponded to their source population with the exception of Bambomo and Apassa (G1.A), which were not further divisible. The lowest levels of hierarchical organization corresponded to major geographic groups (Fig 4-5 c,d); G1 was composed of all Southern populations, whereas G2 corresponded to Northern populations and Mouvanga Creek. On the intermediate hierarchical level, G2 G1 was subdivided into G1.A, which corresponded to populations below Bongolo Falls, and G1.B corresponded to populations above Bongolo Falls

Figure 4-5: Genetic structure and signal variation.
STRUCTURE analysis was performed hierarchically using the methods of Evanno et al. (2005), see text. (A) Individuals are represented on a bar chart with the probability of membership to each group (below) indicated by the color of each bar. G1 and G2 were subdivided and analyzed for population substructure, and individuals are shown with their probability of membership in each subgroup. Subgroup G1.B. was further analyzed, and found to subdivide into 3 distinct subgroups. Note the correspondence between sampling populations and genetic grouping, except for Bambomo and Apassa Creek, which are indistinguishable genetically. (B) Variation in EOD signals was quantified using Principal Components Analysis (see Gallant et al., 2011 and text for further details). Principal component 1 strongly loaded duration, whereas principal component 2 strongly loaded P0 magnitude and some with duration (see Table 4-4). Top left shows correspondence between G1 and G2 and EOD signal types (P0 absent and P0 present). Top right shows correspondence among genetic and signal differences between G1 and variation in duration and P0 magnitude. Lower left, representing G1A shows considerable variation in both duration and P0 magnitude. Lower right, representing G1B populations shows correspondence of genetic clustering and duration, but not P0 magnitude. (C+D) Hierarchical genetic clusters are shown by geographic location on map of Gabon, and detail of the confluence of the Ngounié and Louétsi rivers in the South of Gabon. In D streams of capture are highlighted to show overlap in drainage. Colors correspond to genetic cluster assignments in A.

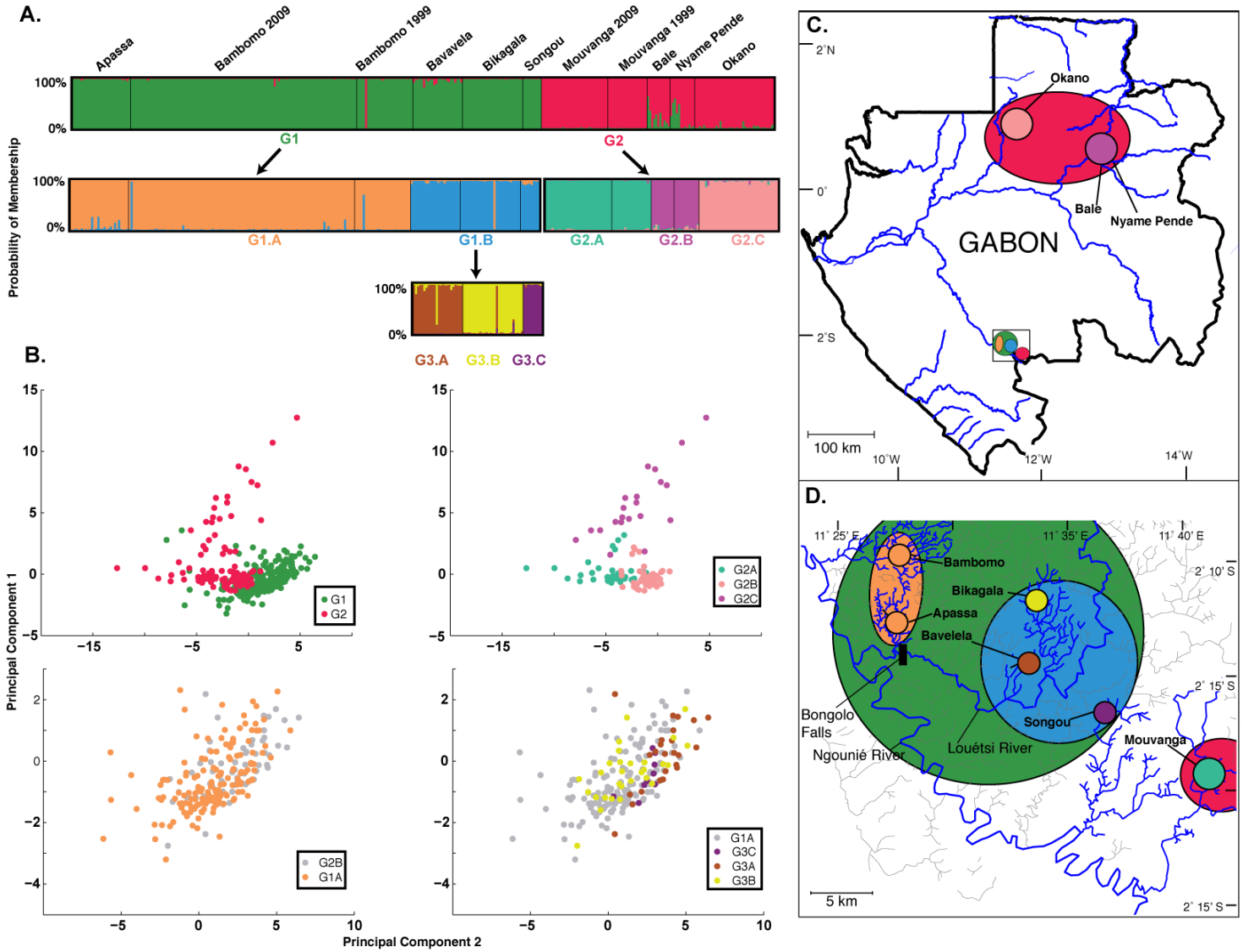
A.
Apassa
Bambomo 2009
Bambomo 1999
Bavavela
Bikagala
Songou
Mouvanga 2009
Mouvanga 1999
Bale
Nyame Pende
Okano
100%
0%
G1
G2
Probability of Membership
G1.A
G1.B
G2.A
G2.B
G2.C
G3.A
G3.B
G3.C
B.
Principal Component 1
Principal Component 2
G1
G2
G2A
G2B
G2C
G1A
G3C
G3A
G3B
C.
2°N
0°
2°S
Okano
Bale
Nyame Pende
GABON
100 km
10°W
12°W
14°W
D.
11° 25' E
11° 35' E
11° 40' E
2° 10' S
2° 15' S
Bambomo
Bikagala
Apassa
Bavelela
Songou
Mouvanga
Bongolo Falls
Ngounié River
Louétsi River
5 km

and Songou Creek.

Patterns of EOD variation relate to signatures of populations structure

We assessed variation in EOD signals using principal components analysis for each of the 338 individuals in this study, following the method of Gallant et al., 2011. The first principal component related strongly to duration, and correspondingly explained 41.02% of the variation between individuals. The second factor related strongly to the magnitude of the small, head negative phase P0, and partly to duration, and comprised approximately 17.97% of the variation between electric signals. Factor loadings for these two principal components are summarized in Table 4-4.

We compared the grouping assignments of each individual from Bayesian clustering analysis described above, to patterns of variation in EOD signals in Fig 4-5b. Over the lowest hierarchical level of population structure (Fig. 4-5b, *upper left*), groups were clearly differentiated in terms of their signals. G1 individuals (Fig. 4-5b, *upper left, green*) were primarily P0-absent or had small P0s (Apassa Creek) over a range of longer durations, whereas G2 individuals were entirely large magnitude P0-present, over a range of shorter durations. Within G2 individuals, EOD signals could further be separated into distinct groups based upon duration and P0 magnitude (Fig. 4-5b, *upper right*), which corresponded to G2.A subgrouping. G1.A individuals (Fig 4-5b, lower left, *orange*) overlapped with individuals from G1.B (Fig. 4-5b, *lower left*, *grey*), individuals within G1.A had EODs that had small P0's (primarily from Apassa Creek) as well as EODs that had no P0's (primarily from Bambomo Creek) and varied widely in their duration. G1.B individuals all lacked P0-present EODs, however could be resolved weakly from each in terms of duration (Fig. 4-5b, *lower right*), however each population overlapped with G1.A (Fig. 4-5b, *lower right, grey*).

Variable	PC1	PC2
Duration	-0.231039624	-0.154355104
tS0	9.15E-17	-2.43E-17
vs0	4.99E-18	-5.12E-17
sS0	8.92E-19	-2.06E-17
tP0	0.007062138	0.215129534
vP0	0.154756171	-0.388112877
tZC1	-0.000420046	0.217966522
sZC1	-0.12366472	0.029885385
tS1	0.195135682	0.186615757
vS1	-0.269027139	0.127344811
sS1	0.186298317	-0.265371541
tS2	-0.303830145	-0.033700684
vS2	-0.008076105	0.061480219
sS2	-0.203426695	0.312642581
tZC2	-0.314780611	-0.003276516
sZC2	-0.20730134	0.310600964
tP2	-0.312460562	-0.014781453
F_Low	0.166464022	0.37268552
F_Max	0.164288193	0.394851868
F_High	0.320361843	0.07724885
ap0	0.11934371	-0.292851849
ap1	-0.327003105	-0.128118623
ap2	0.331976479	0.084177515

Table 4-4: Summary of Factor Loadings for Principal Components Analysis.
Variables measured in this analysis were described in detail in detail in Table 3-2

Analysis of electric organ anatomy identifies an additional individual with intermediate anatomy in Apassa creek

Our analysis of 21 electric organs collected in 2009 complements an earlier analysis of electric organs by Gallant et al. (2011), which demonstrated that the morphological correlates of *P. kingsleyae* EOD signal types (P0-absent and P0-present) are related to the presence and absence of penetrating stalked electrocytes respectively (referred to as *Pa* and *NPp* morphology). In this original analysis, most individuals had electric organs that were entirely composed of electrocytes of either *Pa* or *NPp* anatomy, and some individuals from Bambomo creek exhibited "mixed" electric organ morphology. Our present analysis supports the existence of these morphological types. In Fig. 4-6 we show 4 examples of electric organs surveyed in Bambomo, Apassa, Mouvanga, and Songou Creeks, and summarize our analysis of all 21 individuals in Table 4-6. In Apassa and Mouvanga all individuals were of the Pa morphology type, with one exceptional individual in Apassa exhibiting mixed morphology (*NPp* + *Pa* morphology in the same individual). In Bambomo Creek and Songou creek, we detected individuals that had entirely NPp type morphology, with one exceptional individual in Bambomo creek that had entirely *Pa* type morphology.

Electrical playback experiments provide no evidence of discrimination between P. kingsleyae waveforms

We utilized a dishabituation paradigm described above and by Carlson et al. (2011b) to determine whether individual *P. kingsleyae* were capable of discriminating between sympatric and allopatric *P. kingsleyae* EOD waveforms that were either P0-absent or P0-present. We performed two experiments to assess this: the first experiment

Figure 4-6 Summary of histological survey of electric organs.
A. Individual *P. kingsleyae* were sectioned sagittal from lateral to medial, following one column of electrocytes of the 4 that comprise the electric organ. The electric organ is restricted to the caudal peduncle in mormyrids. **B.** Example histology showing the two basic types of anatomical configuration in the electric organ *Pa* (penetrating with anterior innervation) and NPp (nonpenetrating with posterior innervation). Stalks can be seen clearly passing through the electrocyte in Pa but not in NPp type electrocytes. **C.** Pa type electrocytes result in EOD signals that have a small head negative phase P0, which is absent in individuals with electrocytes that are NPp (see Gallant et al., 2011). **D.** Examples of histological analysis of 4 electric organs from each population. Each pixel represents an individual electrocyte in an individual section that was scored for number of penetrations. In Apassa creek, most individuals are Pa type (yellow-red) observed in each electrocyte from anterior to posterior, whereas one individual had NPp type and Pa type electrocytes (patches of yellow in mostly grey background). In Bambomo, most individuals were NPp with one individual exhibiting all Pa type electrocytes. Songou was entirely comprised of individuals with NPp type electrocytes, and Mouvanga was comprised of individuals with entirely Pa type electrocytes. Full analysis is summarized in Table 4-5.

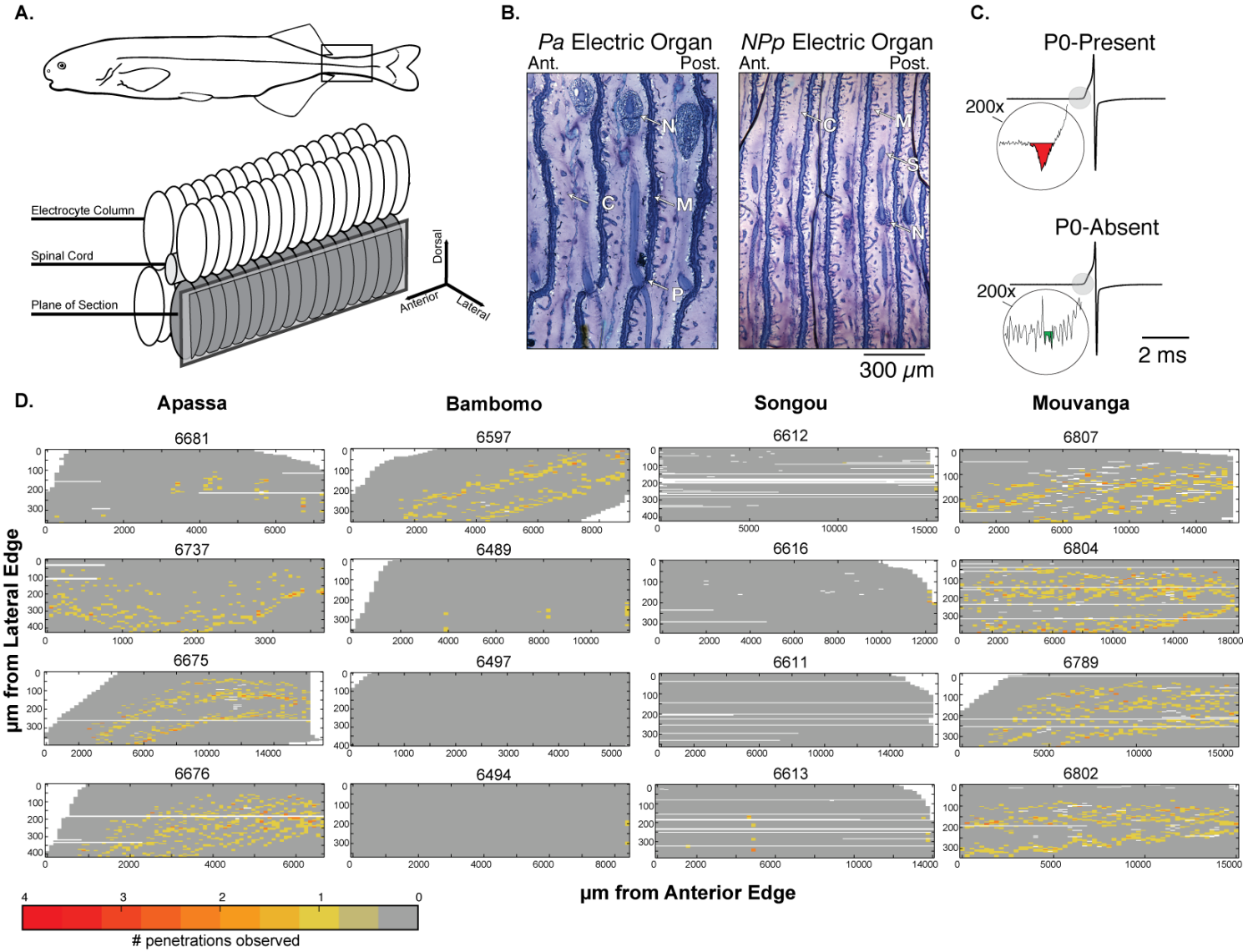
A.
Electrocyte Column
Spinal Cord
Plane of Section
Dorsal
Anterior
Lateral
B.
Pa Electric Organ
Ant.
Post.
N
C
M
P
NPp Electric Organ
Ant.
Post.
C
M
S
N
300 μm
C.
P0-Present
200x
P0-Absent
200x
2 ms
D.
Apassa
Bambomo
Songou
Mouvanga
6681
6597
6612
6807
6737
6489
6616
6804
6675
6497
6611
6789
6676
6494
6613
6802
μm from Lateral Edge
μm from Anterior Edge
4
3
2
1
0
penetrations observed

Population	Specimen No.	µm Surveyed	No. Sections	No. Electrocytes	No. *Pa*	No. *NPp*	Morphology
Apassa	6681	420	70	60	15	45	Mixed
Apassa	6675	648	108	64	50	14	Pa
Apassa	6676	366	61	69	58	11	Pa
Apassa	6637	258	43	70	65	5	Pa
Bambomo	6489	240	40	60	10	50	NPp
Bambomo	6494	384	64	61	1	60	NPp
Bambomo	6497	276	46	67	0	67	NPp
Bambomo	6500	270	45	59	1	58	NPp
Bambomo	6547	378	63	52	1	51	NPp
Bambomo	6549	186	31	60	5	55	NPp
Bambomo	6597	438	73	58	43	15	Pa
Mouvanga	6789	516	86	58	53	5	Pa
Mouvanga	6811	342	57	62	55	7	Pa
Mouvanga	6807	582	97	50	49	1	Pa
Mouvanga	6810	390	65	66	61	5	Pa
Mouvanga	6804	570	95	65	65	0	Pa
Mouvanga	6802	570	95	57	57	0	Pa
Songou	6611	252	42	59	0	59	NPp
Songou	6612	564	94	70	4	66	NPp
Songou	6613	234	39	64	5	59	NPp
Songou	6616	480	80	57	2	55	NPp

Table 4-5: Summary of electric organ histological survey, performed on 21 specimens of *Paramormyrops kingsleyae*.
For each individual, the collection locality and specimen number are provided. For each specimen, one column of the entire electric organ was surveyed for the specified depth (µm) from lateral to medial (see Fig. 4-6). Total number of electrocytes, and the number of those exhibiting *Pa* type morphology and *NPp* type morphology are provided. Finally, the assessment of the overall EO morphology is specified as either Pa (nearly all electrocytes Pa) NPP (nearly all electrocytes NPp) or mixed (some electrocytes Pa others NPp)

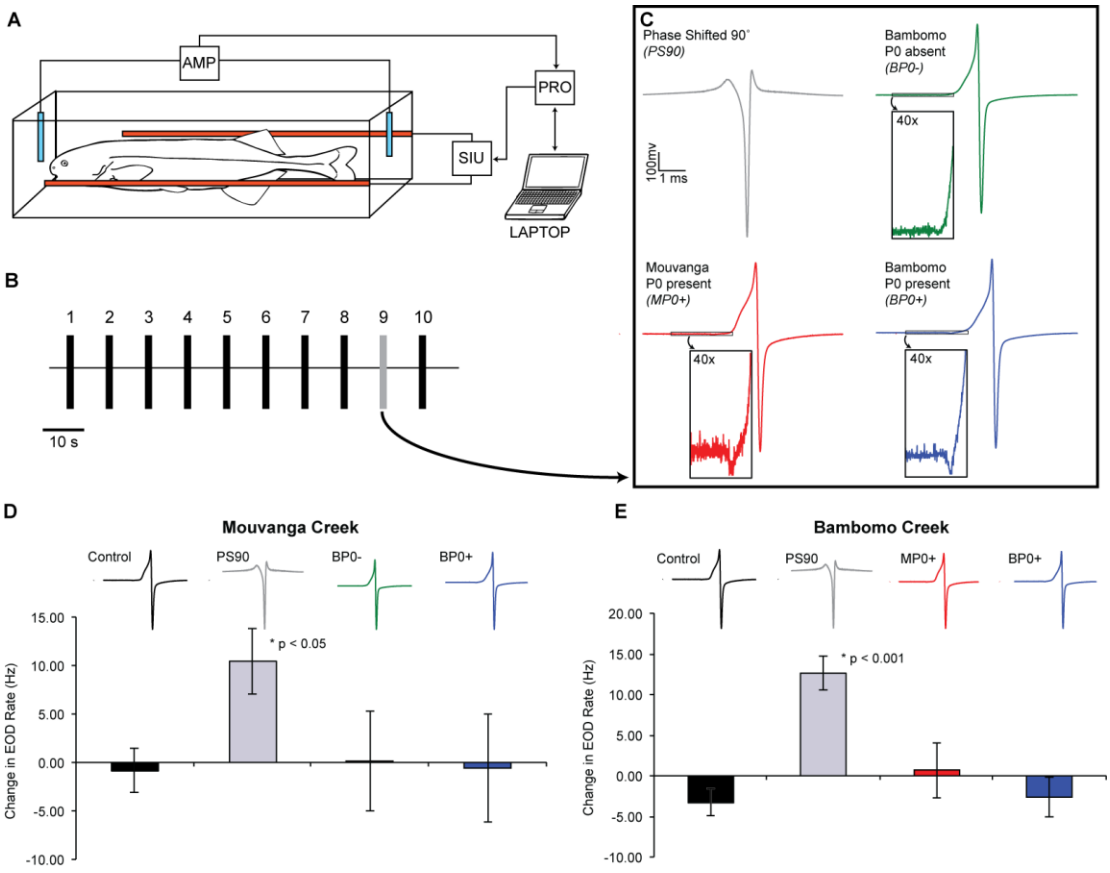

Figure 4-7: Playback experiments performed on *P. kingsleyae*. See text for details. **A.** Represents the recording setup, AMP= amplifier, SIU= stimulus isolation unit, PRO= mobile processor. Orange represents playback electrodes, blue represents recording electrodes. **B, C.** Overview of stimulus paradigm, see text for explanation. **D.** ***Left.*** Presentations of stimuli showed that *P. kingsleyae* from Mouvanga creek showed no evidence of behavioral discrimination between sympatric P0 present waveforms and either P0 absent waveforms or allopatric P0 present waveforms. ***Right.*** Presentations of stimuli showed that *P. kingsleyae* from Bambomo creek showed no evidence of behavioral discrimination between sympatric P0-absent EOD waveforms and allopatric P0 present waveforms or sympatric P0 present waveforms. Both groups could discriminate a 90˚ phase shifted-EOD

.
was a playback to 10 individuals from Mouvanga creek, where either 10 bursts of Mouvanga P0-present EODs were presented (control) or a similar train of bursts, but with the 9th burst replaced by (1) a burst of EODs substituted with either a phase-shifted EOD, (2) a burst of P0 absent EODs from Bambomo Creek, or (3) a burst of P0 present EODs from Bambomo Creek (Fig. 4-7d, *left*). Averaged across individuals, there was a significant increase in the EOD rate in response to phase-shifted EODs presented against P0-present EODs from Mouvanga Creek ($p< 0.05$), but not in response to Bambomo P0-absent EODs or Bambomo P0-present EODs. In the second experiment, 10 bursts of Bambomo P0-absent EODs were presented (control) or a similar train of bursts, but with the 9th burst replaced by a (1) a burst of EODs containing a phase-shifted EOD, (2) a burst of P0 present EODs from Bambomo Creek, or (3) a burst of P0 present EODs from Mouvanga Creek (Fig. 4-7d, *right*). Averaged over individuals, subjects from Bambomo Creek significantly increased their EOD rate in response to phase-shifted P0-absent EODs presented against P0-absent EODs ($p<0.001$), but not in response to Mouvanga P0-present EODs, or Bambomo P0-present EODs.

Discussion

The previous analysis by Gallant et al. (2011) analyzed geographic patterns of *P. kingsleyae* EODs, which motivated the present study and the hypothesis that divergent EODs were the result of reduced gene flow between populations. We made three predictions from this hypothesis: (1) evidence of genetic structure, which is associated with physical barriers or large distances between populations, which correlates with detectable variation in EOD signals. (2) Evidence that *P. kingsleyae* individuals are incapable of discriminating between divergent EOD types (i.e. P0-absent vs. P0-present), and (3) Genetic, morphological, and/or physiological evidence that, in populations where individuals occur sympatrically, that hybridization between

signal forms occurs. We consider our evidence for each in turn. We conclude our discussion by briefly discussing evidence for potential evolutionary mechanisms that may underlie this pattern of divergence.

Genetic structure is associated with physical barriers and large distances between populations

We detected significant signatures of pairwise differentiation between all 9 of populations compared using F_{st}. The magnitude of this differentiation was variable, reflecting populations such as Bambomo and Apassa, which were weakly differentiated (Fst < 0.07) to populations that were strongly differentiated, such as Mouvanga and Songou creeks (F_{st} >0.6). As noted in Table 4-2, locus specific heterozygosities were variable among populations of *P. kingsleyae*. As F_{st} is a ratio of variation between subpopulations to total variation, some of the pairwise comparisons of F_{st} (i.e. Mouvanga Creek vs. Songou Creek) may have been larger than others due to comparisons between two low-heterozygosity populations (discussed in detail below; see also Hedrick, 2005).

Overall variation in F_{st} led us to suspect that differences in genetic variation between populations corresponded to reduced gene flow between populations, as would be predicted by "isolation-by-distance" models (Wright, 1943). Over relatively short (<120 km) distances in the South of Gabon, where sampling was high, we were able to determine a significant relationship between genetic differentiation (i.e. F_{st}) and geographic distance (i.e. river distances between populations). In our analysis, we incorporated measurements that included pairwise distances that traversed waterfalls, as well as pairwise distances that did not traverse waterfalls. We would expect that waterfalls, if they acted as barriers between populations should increase genetic distance for a given geographic distance. From Fig. 4-4, we can see no apparent differences in populations that traversed waterfalls vs. those that did not. Only two comparisons were more

differentiated genetically than would have been expected by our regression model, given their geographic proximity: Mouvanga and Songou Creek. Our overall analysis of pairwise F_{st} presents a fairly robust and important conclusion: namely that most allopatric populations of *P. kingsleyae* are strongly genetically differentiated from each other, suggesting overall very low levels of gene flow between populations. Over distances less than 120 km, the amount of gene flow between populations is proportional to the distance between them, consistent with a classic isolation-by-distance pattern of dispersal between populations.

We noted in the results, however, that this relationship was not apparent over distances greater than 120 km. This is a common phenomenon related to the balance between mutational processes within populations and gene flow between them (Hutchison and Templeton, 1999). This issue was not limited to geographical distance: some F_{st} values determined in this analysis exceeded previously reported F_{st} values between nominal *Paramormyrops* species by Arnegard et al. (2005), which, measured in sympatry were equal to 0.3 or lower. In either case as the "distance" (geographic or genetic) between two populations increase, signal related to gene flow (i.e. similarity by descent) decreases relative to the signatures of genetic drift facilitated by mutational processes in genetic markers. This ends up a "double edged sword" when using microsatellites, which have very high mutation rates and unique mutational processes (Selkoe and Toonen, 2006), making them ideal for assessing the degree of gene flow between populations when gene flow is high relative to the influences of genetic drift in differentiation. However, as gene flow decreases with distance (as would be expected under IBD models or between two reproductively isolated species), mutational processes contribute a much larger effect to differentiation than does gene flow; as such the desired signal of similarity by descent becomes confounded by genetic drift. Genetic drift might confound our estimates of Fst as a

measure of gene flow in two ways: (1) mutations in different populations to the same alleles (i.e. homeoplasy) would reduce F_{st} or (2) decreases in heterozygosity through the fixation of alleles due through random genetic sampling would increase estimates of F_{st} (Hedrick, 2005). For these reasons, F_{st} based estimation of population structure by itself seems less than ideal, particularly because it appears to perform poorly at estimating differentiation between populations that are near complete reproductive isolation (i.e. at non-equlibrium states; Hutchison and Templeton, 1999), or between populations that have very low heterozygosity.

To circumvent these problems with the F_{st} method of assessing population structure, we employed Bayesian clustering analysis of population structure using the program STRUCTURE, which gives an independent, but complimentary picture of population structure by calculating the probability of membership of individuals to a pre-selected number of clusters, assuming loci within clusters are at Hardy-Weinberg equilibrium and exhibit linkage equilibrium (Pritchard et al., 2000). By using the method of Evanno et al. (2005), we could extend this analysis of population structure to gather additional information about hierarchical population structuring that might have resulted from geographic barriers to migration over various regional scales.

Overall, STRUCTURE results were consistent with F_{st} measures of population structure. All populations that had significant F_{st} values were detected as independent structure "clusters" at the highest level of hierarchical organization with nearly 100% probability (Fig. 4-5), with the exception of Bambomo and Apassa creeks which STRUCTURE could not sort into two distinct groups. Pairwise F_{st} between Bambomo and Apassa was, relative to other populations, very low (< 0.06), but was statistically significant at the $p=0.05$ and Bonferoni corrected thresholds.

In addition, the hierarchical method of Evanno et al. (2005) revealed that *P. kingsleyae* populations are more similar to genetically within watersheds than between them, which extends

from the regional level (e.g. Northern vs. Southern populations; Fig. 4-5 G1 vs. G2), down to the local levels (above vs. below Bongolo Falls G1.A vs. G1B). This is overall consistent with the pattern of isolation by distance observed by comparing F_{st} values with geographic distance in Southern populations, albeit over larger geographic scales. These analyses together strongly indicate that gene flow between populations is limited by dispersal between geographically distant populations. While isolation by distance plots showed little effect of the waterfall on gene flow (Fig. 4-4), the barrier to gene flow caused by Bongolo Falls was visible through STRUCTURE results.

Genetic and geographic structure correlates with detectable patterns of variation in EOD signals.

A key prediction of our hypothesis and previous results (Gallant et al., 2011) was that geographic isolation was responsible for patterns of signal divergence. As such, we predicted that patterns of signal diversity are related to signatures of genetic structure. We assessed signal variation as was performed by Gallant et al. (2011) using principal components analysis of 21 variables derived from 9 EOD landmarks. As in the previous analysis, principal component 1 corresponded primarily to duration and principal component 2 corresponded primarily to the magnitude of peak P0, which is absent in many of the southern populations.

Using only these two components of signal variation (which explain ~ 60% of the total variation among EOD waveforms, we examined how genetic structure (as assessed through Bayesian clustering analysis discussed above) and signal differentiation corresponded.

We found the lowest hierarchical groups (G1 and G2; corresponding mainly to populations in the South and North, respectively) corresponded to EODs that were mainly P0 absent (G1) and EODs that were entirely P0 present (G2) (Fig. 4-5, *upper left*). Among G2

individuals could further be subdivided genetically and on the basis EOD signal duration and magnitude of peak P0 (Fig. 4-5B, *upper right*). G1 individuals were distinguishable genetically, but were more overlapping in EOD signals. G1.A (Fig 4-5B, *lower left*) overlapped almost completely in regard to duration and P0 magnitude with populations belonging to G1.B, with the exception of individuals from Apassa and Bambomo creek with P0 present EODs (Fig. 4-5, *lower right*). Individuals in G1.B were further divisible both genetically, and by EOD duration, however they were not separable by P0 magnitude, as all EODs were P0-absent in this group.

Together, our use of the F_{st}, STRUCTURE, and principal component analysis of EOD signals present a consistent picture of genetic and phenotypic differentiation of *P. kingsleyae* EOD waveforms that corresponds strongly to distances between populations, and the presence of waterfall barriers. Over the lowest level of hierarchical analysis, both genotypes and EOD phenotypes were the most divergent. Over the highest levels of hierarchical analysis (i.e. populations in G3.A-C), EODs were more overlapping, but still distinguishable.

Behavioral and genetic evidence suggest P. kingsleyae signal types are not reproductively isolated

In playback experiments, we were unable to find evidence that *P. kingsleyae* can discriminate between P0-present and P0-absent EODs (Fig. 4-7) in either direction. Based on several studies that have characterized the neural encoding of EOD waveforms (Amagai et al., 1998; Carlson, 2009; Carlson et al., 2011a; Friedman and Hopkins, 1998; Xu-Friedman and Hopkins, 1999a), we predicted that *P. kingsleyae* are incapable of encoding EOD waveform differences related to P0 even at the first step of sensory encoding, the peripheral knollenorgan.

We note that these playback studies should be interpreted with a great deal of caution for several reasons. First, there was considerable variation in the responses of individual fishes to

stimuli during this playback experiment, suggesting the possibility that some fish may be capable of discriminating between EOD types, whereas others were not. This variation could be for two reasons: (1) some fish in this, and other ongoing studies briefly silence their discharges in response to novel electrical stimuli (Carlson et al., 2010b), or (2) fish may be variable in their ability to detect differences in signals. Second, given the small number of individuals sampled, only large changes in EOD rates were detectable as a significant response (low effect size, therefore low statistical power). Despite these limitations, our data does not show evidence to support the alternative hypothesis that fish, on average, are able to discriminate between signal types. Additional studies are needed to establish whether P0 present and P0 absent EODs are detectable to *P. kingsleyae* and are presently ongoing.

A second piece of evidence that supports the lack of mating isolation between signal types are the rather exceptional populations in Bambomo and Apassa creek, where both signal types occur in sympatry. Despite their relative proximity (25 km of river distance), the populations were fixed anatomically for two separate configurations of their electric organs and their corresponding signals: *Pa* electric organs with P0-present EODs are predominantly in Apassa, whereas *NPp* type electric organs with P0-absent EODs are predominantly in Bamboo. Despite these phenotypic differences, F_{st} values indicated that the populations are weakly, but significantly differentiated, and STRUCTURE analysis was unable to differentiate between the two populations. Individuals with mixed morphology have now been discovered in Apassa creek, in addition to those found in Bambomo Creek (Gallant et al., 2011). Also notable is that Bambomo creek and Apassa creek exhibit a so-called "rare alleles" phenomenon: both populations have additional alleles that are absent from all other populations genotyped, which been demonstrated as a signature of hybrid zones in other taxa (Barton, 1985; Golding, 1983;

Hoffman and Brown, 1995). Finally, as can be seen in Figures 4-1 and 4-5, Bambomo creek comes within very close proximity to streams that drain above Bongolo Falls, and Apassa Creek's headwaters come within very close proximity to other headwater branches of Bambomo, making it plausible that seasonal fluctuations in water level due to rainy season (Arnegard et al., 2006) might connect these waterways periodically, allowing migration to occur between these otherwise geographically isolated populations.

These lines of evidence, together with a tentative lack of evidence for the ability to detect these waveform differences in *P. kingsleyae*, specifically from Bambomo creek, suggest the possibility of potential hybridization between divergent signal forms within these populations. This favors the hypothesis that the observed patterns of genetic structure did not result from selection against migrants, and rather reductions in gene flow contributed to current patterns of EOD variation.

A role for genetic drift in the early divergence of EOD signals?

The analysis of Arnegard et al. (2010) strongly implicated the role of sexual selection in speciation of the *Paramormyrops* species flock, due to the increased rates of divergence between species when compared to morphological or ecological characters. In this paper, we have examined the role of gene flow between local populations and their relationship to the evolution of novel EOD signals. While our conclusions suggest that divergent EOD forms have likely evolved as a result of reduced gene flow between isolated populations, this has not strongly implicated any particular evolutionary mechanism in influencing this divergence. The original description of signal variation in *P. kingsleyae* considered several alternative hypotheses for potential mechanisms that could have contributed to the observed patterns of variation including various selective pressures (conspicuity to predators, reproductive character displacement, and

effects on electrolocation performance), as well as the possibility of reproductive isolation between *P. kingsleyae* signal types (Gallant et al., 2011). Many of these explanations were deemed unlikely, given the small difference in EOD signal between P0-absent and P0-present waveforms, despite the considerable anatomical reorganization. Behavioral evidence in the present analysis further emphasizes the subtlety of this difference between signals, causing us to move toward the null hypothesis that genetic drift between populations that were geographically isolated may have contributed to this divergence.

Under such a "neutral" hypothesis, we predict that the divergence of EODs may have resulted from the interaction of reduced gene flow between populations and the effects of small effective population sizes, such as those resulting from so called "founder events", that would have permitted the rapid fixation of new phenotypes in isolated populations. Reduced gene flow between populations may be a result of either (1) habitat preferences of *P. kingsleyae* for small headwater streams and (2) barriers to migration, such as distance or the presence of waterfall barriers between potential pathways for migration.

We have discussed at length the evidence of substantial population structure and the evidence for reduced gene flow above. We attempted to estimate contemporary effective population size using the so-called "two-sample" approach: changes in allele frequency across a population are directly related to the effective size of that population (Waples, 1989). The rationale behind this approach is that when effective populations size are small, variation in allele frequency will be great over successive samples due to the effects of genetic drift. Like other methods of assessing effective population size, the accuracy of this method in estimating the "true" effective population size relies on the conformity of the population to a number of assumptions; of the most direct relevance to the present study is the assumption that successive

generations are non-overlapping (Waples, 1989), or if they are overlapping, that a sufficient number of generations has passed between generations (Jorde and Ryman, 1995; Waples, 1989).

Given that mormyrids are iteroparous, this was of some concern; however overlapping generations tends to underestimate effective population size; thus we would interpret any estimates of effective population size as minimum effective population size. As the number of generations increases between samples, estimated effective population size approaches the actual effective population size in modeling studies, even with overlapping generations (Jorde and Ryman, 1995). Our study includes two populations (Mouvanga and Bambomo Creeks), which were sampled two times over a 10-year period. In both populations, we estimated a maximum of 10 generations per year to calculate effective population sizes.

Given the caveats outlined, we found very little evidence that genetic drift effects the distribution of allele frequencies over 10 years of sampling in Bambomo Creek and Mouvanga Creek (Pollack's Fk = 0.02 in Bambomo Creek and 0.019 in Mouvanga Creek). Estimates of effective population size were in the thousands of individuals in both creeks, though when including 95% confidence intervals, neither population had significant evidence beyond statistical noise of allele frequency change due to genetic drift, thus leading to estimates including infinite population size (Waples, 1989).

Bearing in mind that overlapping generations typically underestimates effective population size calculations using the two-sample method, we conclude that contemporary effective population sizes of *Paramormyrops kingsleyae* are quite large, and therefore, we have little evidence to suggest that genetic drift may have influenced signal evolution in *P. kingsleyae* beyond the absence of evidence for alternative hypotheses. We note, however our failure to detect small contemporary effective population sizes should not be interpreted as evidence that

effective population sizes were not historically small, as might be predicted during so-called "founder events" or "bottlenecks" (Mayr, 1942). One potential genetic signature of possible founder events may be the considerable variation in the heterozygosity at several loci among some populations (Table 4-2). The role of genetic drift in speciation or the evolution of divergence is considered unlikely by many (Coyne and Orr, 2004), however this idea has recently witnessed resurgence in interest from both a theoretical and empirical standpoint as it may work in tandem with sexual selection (Bush and Schul, 2010; Runemark et al., 2010; Tazzyman and Iwasa, 2009; Uyeda et al., 2009).

Conclusion

In this analysis we have demonstrated that patterns of geographic diversity, and divergence in EOD signals are caused by geographic isolation, and therefore reduced gene flow between populations of *Paramormyrops kingsleyae*.

Because the major components of EOD variation within *P. kingsleyae* are the same components of variation within *Paramormyrops*, namely duration and in the presence or absence of phase P0, populations of *P. kingsleyae* represent a "microcosm" of signal diversity within the *Paramormyrops*. Our data suggests that divergence in both duration and in the presence or absence of P0 (which is accompanied by a major anatomical reorganization of the electric organ) can quickly change at the population level. As present evidence most likely indicates that changes in EOD waveforms result from the effects of genetic drift, this implicates a mechanism by which electric signal diversity among *Paramormyrops* could be generated, and upon which sexual selection could later act. In this sense processes that lead to divergence in EOD waveforms in *Paramormyrops kingsleyae* may illuminate processes involved early stages of EOD signal divergence in other *Paramormyrops*, and insight into how substrates for sexual

selection might appear.

References

Amagai S, Friedman M, Hopkins C (1998) Time coding in the midbrain of mormyrid electric fish. I. Physiology and anatomy of cells in the nucleus exterolateralis pars anterior. JOURNAL OF COMPARATIVE PHYSIOLOGY A-NEUROETHOLOGY SENSORY NEURAL AND BEHAVIORAL PHYSIOLOGY 182:115-130

Arnegard M, McIntyre PB, Harmon LJ, Zelditch ML, Crampton WGR, Davis JK, Sullivan JP, Lavoué S, Hopkins C (2010) Sexual signal evolution outpaces ecomorphological and trophic divergence during electric fish species radiation. Am Nat 176:335-356

Arnegard ME, Bogdanowicz SM, Hopkins CD (2005) Multiple cases of striking genetic similarity between alternate electric fish signal morphs in sympatry. Evolution 59:324-343

Arnegard ME, Jackson BS, Hopkins CD (2006) Time-domain signal divergence and discrimination without receptor modification in sympatric morphs of electric fishes. J Exp Biol 209:2182-2198

Barton N (1985) Analysis of hybrid zones. Annual Review of Ecology and Systematics

Bohonak AJ (2002) IBD (Isolation by Distance): a program for analyses of isolation by distance. Journal of Heredity 93:153-154

Bush SL, Schul J (2010) Evolution of novel signal traits in the absence of female preferences in *Neoconocephalus* katydids (Orthoptera, Tettigoniidae). PLOS One 5:e12457

Carlson BA (2009) Temporal-Pattern Recognition by Single Neurons in a Sensory Pathway Devoted to Social Communication Behavior. J Neurosci 29:9417-9428

Carlson BA, Hasan SM, Hollmann M, Miller DB, Harmon LJ, Arnegard ME (2011a) Brain Evolution Triggers Increased Diversification of Electric Fishes. Science (New York, NY) 332:583-586

Carlson BA, Hasan SM, Hollmann M, Miller DB, Harmon LJ, Arnegard ME (2011b) Brain evolution triggers increased diversification of electric fishes. Science 332:583-586

Coyne JA, Orr HA (2004) Speciation. Sinauer Associates, Sunderland, MA

Evanno G, Regnaut S, Goudet J (2005) Detecting the number of clusters of individuals using the software STRUCTURE: a simulation study. Molecular Ecology 14:2611-2620

Excoffier L, Lischer HEL (2010) Arlequin suite ver 3.5: a new series of programs to perform population genetics analyses under Linux and Windows. Molecular Ecology Resources 10:564-567

Falush D, Stephens M, Pritchard JK (2003) Inference of population structure: extensions to linked loci and correlated allele frequencies. Genetics 164:1567-1587

Friedman MA, Hopkins CD (1998) Neural substrates for species recognition in the time-coding electrosensory pathway of mormyrid electric fish. The Journal of neuroscience : the official journal of the Society for Neuroscience 18:1171-1185

Gallant JR, Arnegard ME, Sullivan JP, Carlson BA, Hopkins CD (2011) Signal variation and its morphological correlates in *Paramormyrops kingsleyae* provide insight into evolution of electrogenic signal diversity in mormyrid fish. J Comp Physiol A

Golding G (1983) Increased number of alleles found in hybrid populations due to intragenic recombination. Evolution; international journal of organic evolution

Grant PR, Grant BR (2008) How and why species multiply. The radiation of Darwin's finches. Princeton University Press, Princeton, New Jersey

Hedrick PW (2005) A standardized genetic differentiation measure. Evolution 59:1633-1638
Heiligenberg W, Altes RA (1978) Phase sensitivity in electroreception. Science 199:1001-1004
Hendry AP, Taylor EB, McPhail JD (2002) Adaptive divergence and the balance between selection and gene flow: lake and stream stickleback in the misty system. Evolution 56:1199-1216
Hoffman SMG, Brown WM (1995) The molecular mechanism underlying the "rare allele phenomenon" in a subspecific hybrid zone of the California field mouse, *Peromyscus californicus*. Journal of Molecular Evolution 41
Hopkins CD, Bass A (1981) Temporal coding of species recognition signals in an electric fish. Science 212:85-87
Hutchison D, Templeton A (1999) Correlation of pairwise genetic and geographic distance measures: inferring the relative influences of gene flow and drift on the distribution of genetic variability. Evolution:1898-1914
Jakobsson M, Rosenberg NA (2007) CLUMPP: a cluster matching and permutation program for dealing with label switching and multimodality in analysis of population structure. Bioinformatics 23:1801-1806
Jorde PE, Ryman N (1995) Temporal allele frequency change and estimation of effective size in populations with overlapping generations. Genetics 139:1077-1090
Losos JB (2009) Lizards in an evolutionary tree: ecology and adaptive radiation of anoles. University of California Press, Berkeley
Mayr E (1942) Systematics and the origin of species: from the viewpoint of a zoologist. Columbia University Press, New York
Nosil P, Crespi BJ (2003) Does gene flow constrain adaptive divergence or vice versa? A test using ecomorphology and sexual isolation in *Timema cristinae* walking-sticks. Evolution 58:102-112
Pollack E (1983) A new method for estimating the effective population size from allele frequency changes. Genetics 95:1055
Pritchard JK, Stephens M, Donnelly P (2000) Inference of population structure using multilocus genotype data. Genetics 155:945-959
Rosenberg NA (2004) DISTRUCT: a program for the graphical display of population structure. Molecular Ecology Notes 4:137-138
Rousset F (2008) GENEPOP'007: a complete re-implmentation of the GENEPOP software for windows and linux. Molecular Ecology Resources 8:103-106
Runemark A, Hansson B, Pafilis P, Valakos ED, Svensson EI (2010) Isalnd biology and morphological divergence of the Skyros wall lizard *Podarcis gaigeae*: a combined role for local selection and genetic drift on color morph frequency divergence? BMC Evolutionary Biology 10
Schluter D (2009) Evidence for ecological speciation and its alternative. Science 323:737-741
Seehausen O (2006) African cichlid fish: a model system in adaptive radiation research. Proceedings of the Royal Soceity B: Biological Sciences 273:1987-1998
Selkoe KA, Toonen RJ (2006) Microsatellites for ecologists: a practical guide to using and evaluating microsatellite markers. Ecology Letters 9:615-629
Slatkin M (1987) Gene flow and the geographic structure of natural populations. Science 236:787-792
Sullivan JP, Lavoué S, Arnegard ME, Hopkins CD (2004) AFLPs resolve phylogeny and reveal mitochondrial introgression within a species flock of African electric fish (Mormyroidea:

Teleostei). Evolution 58:825-841
Sullivan JP, Lavoue S, Hopkins CD (2000) Molecular systematics of the African electric fishes (Mormyroidea: teleostei) and a model for the evolution of their electric organs. J Exp Biol 203:665-683
Sullivan JP, Lavoué S, Hopkins CD (2002) Discovery and phylogenetic analysis of a riverine species flock of African electric fishes (Mormyridae: Teleostei). Evolution 56:597-616
Tazzyman SJ, Iwasa Y (2009) Sexual selection can increase the effect of random genetic drift-- a quantitative genetic model of polymorphisim in *Oophaga pumilio*, the strawberry poison-dart frog. Evolution 64:1719-1728
Uyeda JC, Arnold SJ, Hohenlohe PA, Mead LS (2009) Drift promotes speciation by sexual selection. Evolution 63:583-594
Wang IJ, Summers K (2010) Genetic structure is correlated with phenotypic divergence rather than geographic isolation in the highly polymorphic strawberry poison-dart frog. Molecular Ecology 19:447-458
Waples RS (1989) A generalized approach for estimating effective population size from temporal changes in allele frequency. Genetics 121:379-391
Weir BS (1990) Genetic data analysis: methods for discrete population genetic data. Sinauer, Sunderland, MA
West-Eberhard MJ (2003) Developmental Plasticity and Evolution. Oxford University Press, New York, NY
Wright S (1943) Isolation by distance. Genetics 28:114-138
Xu-Friedman M, Hopkins C (1999) Central mechanisms of temporal analysis in the knollenorgan pathway of mormyrid electric fish. J Exp Biol 202:1311

APPENDIX 1: TABLE OF ALL ESTS IDENTIFIED USING SSH

Tabulated list of all ESTs sequenced in Chapter 2. For each, the internal identifier used (EST_ID) is listed, along with the NCBI best Accession Number, and Genbank Accession Number. For each EST, the Library is indicated (EO denotes that the sequence was from a library where EO was used as tester, and SM was used as driver; SM denotes that the sequence was from a library where SM was used as tester and EO was used as driver. If a match to a *Danio rerio* sequence was found using NCBI blast, the accession number of the best match, and E-value for this match are listed. Finally, the size of the EST cloned is listed in basepairs.

EST_ID	dbEST_Id	GenBank	Library	Putative Identification	Hit_Acc	Evalue	Sequence Size
BBRACH_EO_1001	71170942	HO702384	EO	None			778
BBRACH_EO_1002	71170943	HO702385	EO	None			396
BBRACH_EO_1003	71170944	HO702386	EO	ATPAse, Ca++ transporting, 4	ACB45514	3.00E-30	265
BBRACH_EO_1004	71170945	HO702387	EO	None			565
BBRACH_EO_1005	71170946	HO702388	EO	None			566
BBRACH_EO_1006	71170947	HO702389	EO	None			566
BBRACH_EO_1007	71170948	HO702390	EO	None			285
BBRACH_EO_1008	71170949	HO702391	EO	None			547
BBRACH_EO_1009	71170950	HO702392	EO	None			500
BBRACH_EO_1010	71170951	HO702393	EO	None			667
BBRACH_EO_1011	71170952	HO702394	EO	None			500
BBRACH_EO_1013	71170954	HO702396	EO	None			615
BBRACH_EO_1014	71170955	HO702397	EO	None			166
BBRACH_EO_1015	71170956	HO702398	EO	None			1163
BBRACH_EO_1016	71170957	HO702399	EO	None			517
BBRACH_EO_1017	71170958	HO702400	EO	None			507
BBRACH_EO_1018	71170959	HO702401	EO	None			507
BBRACH_EO_1019	71170960	HO702402	EO	ATPase, Na+/K+ transporting, beta 1a	**BC045376**	**1.00E-11**	443
BBRACH_EO_1020	71170961	HO702403	EO	S100 calcium binding protein, beta	XP_002666278	2.00E-29	713
BBRACH_EO_1021	71170962	HO702404	EO	S100 calcium binding protein, beta	XP_002666278	2.00E-29	713
BBRACH_EO_1022	71170963	HO702405	EO	None			501
BBRACH_EO_1023	71170964	HO702406	EO	None			517
BBRACH_EO_1025	71170965	HO702407	EO	None			500
BBRACH_EO_1026	71170966	HO702408	EO	ATPAse, Ca++ transporting, 4	ACB45514	3.00E-30	265
BBRACH_EO_1027	71170967	HO702409	EO	hypothetical protein	XP_002665943	9.00E-07	921
BBRACH_EO_1028	71170968	HO702410	EO	None			446
BBRACH_EO_1029	71170969	HO702411	EO	None			824
BBRACH_EO_1030	71170970	HO702412	EO	*B. brachyistius* cyochrome c oxidase subunit	NP_059334	2.00E-10	271
BBRACH_EO_1031	71170971	HO702413	EO	None			582
BBRACH_EO_1032	71170972	HO702414	EO	None			618
BBRACH_EO_1034	71170974	HO702416	EO	None			744
BBRACH_EO_1035	71170975	HO702417	EO	None			327
BBRACH_EO_1036	71170976	HO702418	EO	None			494

EST_ID	dbEST_Id	GenBank	Library	Putative Identification	Hit_Acc	Evalue	Sequence Size
BBRACH_EO_1037	71170977	HO702419	EO	None			500
BBRACH_EO_1038	71170978	HO702420	EO	None			476
BBRACH_EO_1042	71170982	HO702424	EO	None			433
BBRACH_EO_1043	71170983	HO702425	EO	None			501
BBRACH_EO_1044	71170984	HO702426	EO	None			577
BBRACH_EO_1045	71170985	HO702427	EO	None			494
BBRACH_EO_1046	71170986	HO702428	EO	None			457
BBRACH_EO_2001	71170987	HO702429	EO	None			552
BBRACH_EO_2003	71170988	HO702430	EO	enhancer of rudimentary homolog	NP_571303	7.00E-07	329
BBRACH_EO_2005	71170989	HO702431	EO	None			463
BBRACH_EO_2006	71170990	HO702432	EO	parvalbumin 9	NP_891983	1.00E-23	555
BBRACH_EO_2008	71170991	HO702433	EO	S100 calcium binding protein, beta	XP_002666278	2.00E-17	797
BBRACH_EO_2009	71170992	HO702434	EO	None			655
BBRACH_EO_2010	71170993	HO702435	EO	None			500
BBRACH_EO_2011	71170994	HO702436	EO	arpc3-like	**AM422121**	**6.00E-06**	288
BBRACH_EO_2012	71170995	HO702437	EO	calcyclin binding protein	CAQ14532	4.00E-44	479
BBRACH_EO_2013	71170996	HO702438	EO	None			1129
BBRACH_EO_2014	71170997	HO702439	EO	None			548
BBRACH_EO_2015	71170998	HO702440	EO	None			369
BBRACH_EO_4001	71170999	HO702441	EO	annexin a11b	NP_861431	7.00E-30	800
BBRACH_EO_4002	71171000	HO702442	EO	None			456
BBRACH_EO_4003	71171001	HO702443	EO	None			491
BBRACH_EO_4004	71171002	HO702444	EO	None			711
BBRACH_EO_4005	71171003	HO702445	EO	None			608
BBRACH_EO_4006	71171004	HO702446	EO	None			615
BBRACH_EO_4007	71171005	HO702447	EO	dynein light chain roadblock-type 1	NP_957482	1.00E-40	756
BBRACH_EO_4008	71171006	HO702448	EO	None			768
BBRACH_EO_4010	71171007	HO702449	EO	programmed cell death protein 6	NP_957244	2.00E-16	327
BBRACH_EO_4011	71171008	HO702450	EO	ATPase, Na+/K+ transporting, alpha 2a	CAQ14308	5.00E-45	308
BBRACH_EO_4012	71171009	HO702451	EO	None			367
BBRACH_EO_4013	71171010	HO702452	EO	myoglobin	NP_956880	2.00E-51	884
BBRACH_EO_4014	71171011	HO702453	EO	cystatin B	NP_001096599	5.00E-32	672
BBRACH_EO_4016	71171012	HO702454	EO	cystatin B	NP_001096599	2.00E-12	676
BBRACH_EO_4017	71171013	HO702455	EO	troponin I, skeletal, fast 2b.1 isoform	NP_001129964	2.00E-40	468

EST_ID	dbEST_Id	GenBank	Library	Putative Identification	Hit_Acc	Evalue	Sequence Size
				1			
BBRACH_EO_4018	71171014	HO702456	EO	retinoic acid receptor responder (tazarotene induced) 3-like isoform 1	XP_002664516	2.00E-09	537
BBRACH_EO_4019	71171015	HO702457	EO	ATPase, Na+/K+ transporting, alpha 1b	CAQ13999	3.00E-19	711
BBRACH_EO_4020	71171016	HO702458	EO	None			453
BBRACH_EO_4021	71171017	HO702459	EO	None			593
BBRACH_EO_4022	71171018	HO702460	EO	None			299
BBRACH_EO_4023	71171019	HO702461	EO	None			381
BBRACH_EO_4024	71171020	HO702462	EO	None			501
BBRACH_EO_4025	71171021	HO702463	EO	ATPase, Na+/K+ transporting, beta 1b	XP_002662295	5.00E-32	389
BBRACH_EO_4027	71171023	HO702465	EO	None			763
BBRACH_EO_4028	71171024	HO702466	EO	myosin, heavy polypeptide 6, cardiac muscle, alpha-like	XP_002667378	2.00E-49	503
BBRACH_EO_4029	71171025	HO702467	EO	None			1123
BBRACH_EO_4030	71171026	HO702468	EO	None			573
BBRACH_EO_4032	71171027	HO702469	EO	None			1163
BBRACH_EO_4033	71171028	HO702470	EO	None			453
BBRACH_EO_4034	71171029	HO702471	EO	None			538
BBRACH_EO_6001	71171030	HO702472	EO	None			285
BBRACH_EO_6002	71171031	HO702473	EO	3' end of the mef2a gene myocyte enhancer factor 2a	**BX323877**	**3.00E-34**	558
BBRACH_EO_6003	71171032	HO702474	EO	None			656
BBRACH_EO_6004	71171033	HO702475	EO	prosaposin	AAL54381	8.00E-13	323
BBRACH_EO_6006	71171034	HO702476	EO	None			656
BBRACH_EO_6008	71171035	HO702477	EO	ATPase, Na+/K+ transporting, beta 1a	**BC045376**	**3.00E-13**	734
BBRACH_EO_6009	71171036	HO702478	EO	None			552
BBRACH_EO_6010	71171037	HO702479	EO	None			896
BBRACH_EO_6011	71171038	HO702480	EO	None			389
BBRACH_EO_6012	71171039	HO702481	EO	neurogranin	ACJ64077	9.00E-25	602
BBRACH_EO_6014	71171040	HO702482	EO	None			527
BBRACH_EO_6016	71171041	HO702483	EO	None			335
BBRACH_EO_6019	71171042	HO702484	EO	None			513

EST_ID	dbEST_Id	GenBank	Library	Putative Identification	Hit_Acc	Evalue	Sequence Size
BBRACH_EO_6021	71171043	HO702485	EO	None			517
BBRACH_EO_6022	71171044	HO702486	EO	None			383
BBRACH_EO_6023	71171045	HO702487	EO	None			501
BBRACH_EO_6024	71171046	HO702488	EO	None			272
BBRACH_EO_6026	71171047	HO702489	EO	None			437
BBRACH_EO_6027	71171048	HO702490	EO	myoglobin	NP_956880	1.00E-52	664
BBRACH_EO_6029	71171049	HO702491	EO	homologus to novel protein similar to PRR18	CAX14053	1.00E-10	767
BBRACH_EO_6031	71171050	HO702492	EO	None			442
BBRACH_EO_6033	71171051	HO702493	EO	None			396
BBRACH_EO_6034	71171052	HO702494	EO	ATPase, Na+/K+ transporting, alpha 1b	CAQ13999	3.00E-19	710
BBRACH_EO_6035	71171053	HO702495	EO	thymosin, beta 4-like	**XM_002665906**	**1.00E-05**	493
BBRACH_EO_6036	71171054	HO702496	EO	None			445
BBRACH_EO_6038	71171055	HO702497	EO	None			692
BBRACH_EO_6039	71171056	HO702498	EO	None			484
BBRACH_EO_6040	71171057	HO702499	EO	None			442
BBRACH_EO_6041	71171058	HO702500	EO	None			334
BBRACH_EO_6043	71171059	HO702501	EO	None			367
BBRACH_EO_6045	**71171060**	**HO702502**	EO	***B. brachyistius* mitochondrial genomic DNA**			776
BBRACH_EO_6046	71171061	HO702503	EO	None			427
BBRACH_EO_6047	71171062	HO702504	EO	None			859
BBRACH_EO_6049	71171063	HO702505	EO	None			360
BBRACH_EO_6050	71171064	HO702506	EO	None			628
BBRACH_SM_3001	71171065	HO702507	SM	parvalbumin 2	NP_571591	1.00E-48	617
BBRACH_SM_3002	71171066	HO702508	SM	creatine kinase b, Ckmb	NP_001099153	8.00E-53	713
BBRACH_SM_3003	71171067	HO702509	SM	parvalbumin isoform 1b	NP_956506	6.00E-19	496
BBRACH_SM_3004	71171068	HO702510	SM	myosin, heavy polypeptide 6, cardiac muscle, alpha-like	XP_002667378	3.00E-50	505
BBRACH_SM_3006	71171069	HO702511	SM	parvalbumin isoform 1b	NP_956506	6.00E-27	547
BBRACH_SM_3007	71171070	HO702512	SM	myosin heavy chain 4	CAM14143	5.00E-27	302
BBRACH_SM_3008	71171071	HO702513	SM	None			939
BBRACH_SM_3010	71171072	HO702514	SM	parvalbumin 2	NP_571591	6.00E-48	729
BBRACH_SM_3011	71171073	HO702515	SM	3' end of the mef2a gene myocyte	**BX323877**	**1.00E-40**	691

EST_ID	dbEST_Id	GenBank	Library	Putative Identification	Hit_Acc	Evalue	Sequence Size
				enhancer factor 2a			
BBRACH_SM_3012	71171074	HO702516	SM	parvalbumin 2	NP_571591	1.00E-48	641
BBRACH_SM_3013	71171075	HO702517	SM	parvalbumin 2	NP_571591	1.00E-48	641
BBRACH_SM_3014	71171076	HO702518	SM	parvalbumin isoform 1c	NP_997948	2.00E-36	548
BBRACH_SM_3015	71171077	HO702519	SM	parvalbumin 2	NP_571591	1.00E-48	647
BBRACH_SM_3016	71171078	HO702520	SM	myosin heavy chain b	XP_001339206	4.00E-75	613
BBRACH_SM_3017	71171079	HO702521	SM	None			244
BBRACH_SM_3018	71171080	HO702522	SM	myosin, heavy polypeptide 6, cardiac muscle, alpha-like	XP_002667378	9.00E-41	450
BBRACH_SM_3019	71171081	HO702523	SM	parvalbumin isoform 1c	NP_997948	2.00E-36	547
BBRACH_SM_3020	71171082	HO702524	SM	creatine kinase b, Ckmb	NP_001099153	8.00E-53	713
BBRACH_SM_5001	71171083	HO702525	SM	parvalbumin isoform 1c	NP_997948	2.00E-47	502
BBRACH_SM_5002	71171084	HO702526	SM	parvalbumin isoform 1c	NP_997948	5.00E-47	480
BBRACH_SM_5003	71171085	HO702527	SM	None			631
BBRACH_SM_5004	71171086	HO702528	SM	myosin, heavy polypeptide 6, cardiac muscle, alpha-like	XP_002667378	3.00E-50	491
BBRACH_SM_5005	71171087	HO702529	SM	parvalbumin 2	NP_571591	5.00E-48	630
BBRACH_SM_5006	71171088	HO702530	SM	myosin heavy chain b	XP_001339206	4.00E-56	505
BBRACH_SM_5007	71171089	HO702531	SM	parvalbumin 2	NP_571591	5.00E-48	630
BBRACH_SM_7001	71171090	HO702532	SM	myosin heavy chain b	XP_001339206	4.00E-56	514
BBRACH_SM_7002	71171091	HO702533	SM	parvalbumin isoform 1c	NP_997948	2.00E-47	504
BBRACH_SM_7003	71171092	HO702534	SM	myosin heavy chain b	XP_001339206	4.00E-56	498
BBRACH_SM_7004	71171093	HO702535	SM	troponin T, skeletal, fast T3b	AAH65452	1.00E-26	480
BBRACH_SM_7005	71171094	HO702536	SM	None			640
BBRACH_SM_7006	71171095	HO702537	SM	parvalbumin 2	NP_571591	1.00E-48	627
BBRACH_SM_7007	71171096	HO702538	SM	None			518
BBRACH_SM_7008	71171097	HO702539	SM	parvalbumin isoform 1c	NP_997948	8.00E-35	519
BBRACH_SM_7009	71171098	HO702540	SM	None			668
BBRACH_SM_7010	71171099	HO702541	SM	None			1104
BBRACH_SM_xxxxx	71171100	HO702542	SM	myosin, heavy polypeptide 6, cardiac muscle, alpha-like	XP_002667378	9.00E-41	450

APPENDIX 2: ALIGNMENT OF MEF2C SEQUENCES FROM *B. BRACHYISTIUS* ELECTRIC ORGAN AND SKELETAL MUSCLE

APPENDIX 3: DESCRIPTION OF GENUS *PARAMORMYROPS* AND *P. KINGSLEYAE*

For the convenience of the reader, the following material is provided as a direct quote, available from:

Hopkins CD, Lavoué S, Sullivan JP (2007) Mormyridae. In: Stiassny MLJ, Teugels GG, Hopkins CD (eds) Poissons D'eaux Douces Et Saumâtres De Basse Guinée: ouest de l'Afrique Central vol 1. Faune Et Flore Tropicales. IRD Éditions, Paris, pp 220-334.

Ordering information for this volume is available at the following website
http://www.ird.fr/editions/catalogue/ouvrage.php?livre=534

Genus *Paramormyrops* Taverne,

Thys van den Audenaerde & Heymer, 1977

Brienomyrus (*Brienomyrus*) Taverne, 1971 partim

A new diagnosis and key is provided for Paramormyrops so that taxonomic nomenclature is consistent with recent molecular phylogenetic results (Alves-Gomes & Hopkins, 1997; Lavoué et al., 2000; Lavoué et al., 2003; Sullivan et al., 2000; Sullivan et al., 2002).

Body moderately elongate, somewhat compressed laterally, dorsal and ventral profiles parallel for much of the length; body depth, 15-25% SL. Head length approximately equal to or slightly greater than the body depth, snout non-tubular, often bluntly rounded or tapering to a gently pointed snout, snout profile blunt (U-shaped) or sharp (V-shaped) when viewed from above. Mouth small and terminal to subterminal; teeth bicuspid and pincer-like, 5-7 in upper jaw, 6-8 in lower. Chin fleshy, somewhat bulbous, covered with electroreceptors, not forward protruding. Dorsal and anal fins originating well posterior to mid-body length; anal fin equal or slightly longer than dorsal and containing an equal number or a few additional rays. Origins of last anal and last dorsal fin rays are vertically aligned. Base of last anal and dorsal fin rays vertically aligned. Nostrils well separated and positioned approximately half-way between eye and tip of snout. Circumpeduncular scales, 12-20. Electrocytes, type Pa (Penetrating stalks with anterior innervation) or NPp (Non-penetrating stalks with posterior innervation). Lateral ethmoid reduced or absent.

The distal tips of the last anal and last dorsal fin rays are aligned in *Paramormyrops* rather than offset as they are in *Brienomyrus* (Mamonekene & Teugels, 1993). The same is true for the origins of these last fin rays. Paramormyrops have U- or V-shaped head profiles when viewed from above while *Brienomyrus* and *Brevimyrus* all have rounded head profiles that appear U-shaped from above. There are eight species of *Paramormyrops* of which seven are known from Lower Guinea. Previously known as the 'Gabon-clade *Brienomyrus'*, this newly diagnosed genus has a number of undescribed taxa from Lower Guinea (see Sullivan et al., 2000, 2002, 2004). The centre of diversity appears to be in the Ogowe River of Gabon.

1 Teeth notched, seven in upper jaw, eight in lower .....***Paramormyrops hopkinsi***

Teeth notched, five in upper jaw, six in lower **2**

2 16 or more scales around caudal peduncle **3**

Fewer than 16 scales (typically 12) around the caudal peduncle **4**

3 Caudal peduncle length more than 24.5% SL; lateral line scales 73 or more ……..... ***Paramormyrops longicaudatus***

Caudal peduncle less than 24.5% SL; lateral line scales fewer than 73 ..... ***Paramormyrops batesii***

4 Head profile U-shaped when viewed from above ……. ……..... **5**

Head profile V-shaped when viewed from above ……..... **6**

5 Upper profile of head slightly concave; HL 24.9-27.6% of SL; caudal peduncle slender, its depth 3.7-4.7% SL; interorbital distance short, 110-133% of snout length .....***Paramormyrops gabonensis***

Upper profile of head rounded; HL 19.5-28.7% SL; caudal peduncle depth 4.1-7.5% SL; interorbital distance 121-212% of snout length ……..... ***Paramormyrops kingsleyae***

6 Upper profile of head slightly concave; mouth subterminal; HL 21.13% SL or greater ……..... ***Paramormyrops curvifrons***

Upper profile of head rounded; mouth inferior; HL 22.2% SL or less ……..... ***Paramormyrops sphekodes***

Paramormyrops kingsleyae

(Günther 1896)

Brienomyrus kingsleyae (Günther, 1896)

Description: a medium-sized Paramormyrops with five teeth in the upper jaw, six in the lower, 12 circumpeduncular scales and a U-shaped head when viewed from above. The dorsal profile of head is rounded, not concave. Head short, 19.5-28.7% SL. Caudal peduncle moderately thick, its depth 4.1-7.5% SL. Interorbital distance large, 121-212% of snout length. Body depth 14.8-24.9% SL. Head length 19.5-28.7% SL, head depth 13.5-20.2% SL. Eye diameter 7.4-16.3% HL, 27.8-79.7% of snout length. Snout 18-29% HL. Interorbital distance 121-212% of snout length, 40-67% of postorbital length. Postorbital length 54-82% HL; 202-385% of snout length. Mouth width 14.2-22.2% HL. Internarine distance 18-41% of snout length. Dorsal fin 15-21% SL with 15-19 rays including an initial single unbranched, unsegmented ray. Anal fin 18-28% SL with 21-26 rays including a single unbranched, unsegmented initial ray. Pectoral 13-20% SL. Pelvic fin 9-14% SL with six rays. Caudal peduncle moderately short and thick, its length 14-22% SL, its depth 4.1-7.5% SL, 21-43% of caudal peduncle length. Predorsal distance 64-74% SL, preanal distance 58-70% SL. Lateral line with 55-62 scales total; 9-10 scales above lateral line, 9-12 below.

Maximum size: 160 mm SL.

Colour: the fish varies from dark chocolate-brown to lighter brown with violet spots above, lighter brown to yellow-gold on the underside. EOD: figure 12.66 has two main peaks, P1 and

P2, sometimes preceded by a very small initial P0 peak. The overall duration is 1.93 msec ± 0.57 (std. dev.). The mean height of the initial peak, P0, is only 2% of the peak to peak height. The height of peak P1 is 37% of the peak to peak height. The peak of the power spectrum is at 675 Hz ± 125. The electric organ is variable in form.

Those specimens with no P0 have electrocytes that are all Type NPp, those with a small P0 have some or all of the electrocytes of type Pa.

Distribution: a Lower Guinea endemic with a widespread distribution throughout the Ogowe River basin including the Ivindo, the Woleu, the Nyanga and coastal drainages

of southern Gabon. The types of *Marcusenius cabrae* Boulenger from Mayumbe Chiloango River extend its range south of the Gabon border.

Remark: Teugels & Hopkins (1998) have analyzed the morphology of the haplotype of *Mormyrus kingsleyae* Gunther, 1896, with the stated type locality of 'Old Calabar' near the mouth of the Cross River (present-day Nigeria) and concluded that the type locality may have been reported in error because no P*aramormyrops kingsleyae*-like specimens have since been recovered from this area. These authors concluded that it is more likely that the holotype originates from Gabon, where Mary Kingsley travelled in 1895 after her visit to Old Calabar in May 1895 (Kingsley,1897). This fish has been referred to as *Brienomyrus* bp1 and B. bn1 and as B. cab. in previous publications (Sullivan et al., 2002, 2004; Arnegard 2005).

APPENDIX 4: TABULAR LIST OF ALL SPECIMENS USED IN THIS DISSERTATION

Tabulated list of all specimens included in this dissertation. Their date of collection, collection coordinates, assigned locality, standard length (SL), sex, Cornell University Museum of Vertebrates accession numbers, and individual voucher numbers are included. (-) indicates no data available for sex and (ND) indicates no data available for standard length.

CUMV #	Voucher #	Locality #	Date	Locality	SL	Sex	Lat.	Long.
CU80812	2004	1998-007	11-Jan-1998	Ivindo	101	male	0.519722222	12.79958333
CU80812	2006	1998-007	11-Jan-1998	Ivindo	75	juvenile	0.519722222	12.79958333
CU80812	2014	1998-007	11-Jan-1998	Ivindo	82	juvenile	0.519722222	12.79958333
CU80812	2116	1998-030-A	18-Jan-1998	Ivindo	-	male	0.538333333	12.82566667
CU80816	2118	1998-030-A	18-Jan-1998	Ivindo	91	female	0.538333333	12.82566667
CU80816	2119	1998-030-A	18-Jan-1998	Ivindo	85	juvenile	0.538333333	12.82566667
CU80811	2215	1998-054	23-Jan-1998	Ivindo	95	male	0.532608333	12.83333333
CU80811	2216	1998-054	23-Jan-1998	Ivindo	66	male	0.532608333	12.83333333
CU80853	2287	1998-083	30-Jan-1998	Ivindo	101	male	0.50225	12.79666667
CU80896	2311	1998-095	31-Jan-1998	Ivindo	95	female	0.519722222	12.79875
CU80896	2313	1998-095	31-Jan-1998	Ivindo	70	juvenile	0.519722222	12.79875
CU80855	2317	1998-100	02-Feb-1998	Ivindo	95	male	0.516111111	12.79388889
CU80867	2426	1998-115	12-Feb-1998	Libreville	150	male	0.551305556	9.346666667
CU80867	2427	1998-115	12-Feb-1998	Libreville	58	juvenile	0.551305556	9.346666667
CU80867	2428	1998-115	12-Feb-1998	Libreville	132	female	0.551305556	9.346666667
CU80867	2429	1998-115	12-Feb-1998	Libreville	128	male	0.551305556	9.346666667
CU80867	2430	1998-115	12-Feb-1998	Libreville	112	female	0.551305556	9.346666667
CU80867	2431	1998-115	12-Feb-1998	Libreville	114	female	0.551305556	9.346666667
CU80867	2432	1998-115	12-Feb-1998	Libreville	117	female	0.551305556	9.346666667
CU80867	2433	1998-115	12-Feb-1998	Libreville	115	female	0.551305556	9.346666667
CU80867	2434	1998-115	12-Feb-1998	Libreville	120	female	0.551305556	9.346666667
CU80867	2435	1998-115	12-Feb-1998	Libreville	74	juvenile	0.551305556	9.346666667
CU80867	2436	1998-115	12-Feb-1998	Libreville	110	male	0.551305556	9.346666667
CU80867	2437	1998-115	12-Feb-1998	Libreville	135	female	0.551305556	9.346666667
CU80867	2438	1998-115	12-Feb-1998	Libreville	67	juvenile	0.551305556	9.346666667
CU84663	2570	1998B-019	09-Sep-1998	Mouvanga	116	female	-2.323194444	11.68836111
CU84663	2572	1998B-019	09-Sep-1998	Mouvanga	112	male	-2.323194444	11.68836111
CU84663	2573	1998B-019	09-Sep-1998	Mouvanga	105	female	-2.323194444	11.68836111
CU84663	2574	1998B-019	09-Sep-1998	Mouvanga	95	female	-2.323194444	11.68836111
CU84663	2575	1998B-019	09-Sep-1998	Mouvanga	132	male	-2.323194444	11.68836111

CUMV #	Voucher #	Locality #	Date	Locality	SL	Sex	Lat.	Long.
CU84663	2578	1998B-019	09-Sep-1998	Mouvanga	78	juvenile	-2.323194444	11.68836111
CU84663	2579	1998B-019	09-Sep-1998	Mouvanga	105	male	-2.323194444	11.68836111
CU84663	2580	1998B-019	09-Sep-1998	Mouvanga	86	juvenile	-2.323194444	11.68836111
CU84663	2582	1998B-019	09-Sep-1998	Mouvanga	87	male	-2.323194444	11.68836111
CU84663	2584	1998B-019	09-Sep-1998	Mouvanga	98	female	-2.323194444	11.68836111
CU84663	2586	1998B-019	09-Sep-1998	Mouvanga	93	male	-2.323194444	11.68836111
CU84663	2587	1998B-019	09-Sep-1998	Mouvanga	83	male	-2.323194444	11.68836111
CU84663	2588	1998B-019	09-Sep-1998	Mouvanga	95	male	-2.323194444	11.68836111
CU84663	2589	1998B-019	09-Sep-1998	Mouvanga	88	female	-2.323194444	11.68836111
CU84663	2590	1998B-019	09-Sep-1998	Mouvanga	90	male	-2.323194444	11.68836111
CU84663	2609	1998B-019	09-Sep-1998	Mouvanga	87	female	-2.323194444	11.68836111
CU84663	2610	1998B-019	09-Sep-1998	Mouvanga	85	male	-2.323194444	11.68836111
CU84663	2611	1998B-019	09-Sep-1998	Mouvanga	74	male	-2.323194444	11.68836111
CU84663	2612	1998B-019	09-Sep-1998	Mouvanga	84	female	-2.323194444	11.68836111
CU84663	2613	1998B-019	09-Sep-1998	Mouvanga	79	male	-2.323194444	11.68836111
CU84663	2614	1998B-019	09-Sep-1998	Mouvanga	89	female	-2.323194444	11.68836111
CU84663	2615	1998B-019	09-Sep-1998	Mouvanga	83	female	-2.323194444	11.68836111
CU84663	2616	1998B-019	09-Sep-1998	Mouvanga	83	juvenile	-2.323194444	11.68836111
CU84663	2617	1998B-019	09-Sep-1998	Mouvanga	87	male	-2.323194444	11.68836111
CU84663	2618	1998B-019	09-Sep-1998	Mouvanga	47	juvenile	-2.323194444	11.68836111
CU84663	2627	1998B-019	09-Sep-1998	Mouvanga	96	female	-2.323194444	11.68836111
CU84663	2631	1998B-019	09-Sep-1998	Mouvanga	95	male	-2.323194444	11.68836111
CU84663	2632	1998B-019	09-Sep-1998	Mouvanga	86	male	-2.323194444	11.68836111
CU84663	2633	1998B-019	09-Sep-1998	Mouvanga	95	male	-2.323194444	11.68836111
CU84663	2634	1998B-019	09-Sep-1998	Mouvanga	88	female	-2.323194444	11.68836111
CU84663	2635	1998B-019	09-Sep-1998	Mouvanga	88	male	-2.323194444	11.68836111
CU84663	2636	1998B-019	09-Sep-1998	Mouvanga	92	male	-2.323194444	11.68836111
CU84663	2637	1998B-019	09-Sep-1998	Mouvanga	78	juvenile	-2.323194444	11.68836111
CU84581	2639	1998B-023	11-Sep-1998	Mouvanga	108	male	-2.323194444	11.68836111
CU84581	2640	1998B-023	11-Sep-1998	Mouvanga	102	male	-2.323194444	11.68836111

CUMV #	Voucher #	Locality #	Date	Locality	SL	Sex	Lat.	Long.
CU84581	2641	1998B-023	11-Sep-1998	Mouvanga	103	male	-2.323194444	11.68836111
CU84659	2684	1998B-032	15-Sep-1998	LowerLouetsi	118	male	-2.21875	11.46391667
CU84659	2685	1998B-032	15-Sep-1998	LowerLouetsi	76	female	-2.21875	11.46391667
CU84659	2686	1998B-032	15-Sep-1998	LowerLouetsi	95	male	-2.21875	11.46391667
CU84659	2687	1998B-032	15-Sep-1998	LowerLouetsi	77	female	-2.21875	11.46391667
CU84659	2688	1998B-032	15-Sep-1998	LowerLouetsi	78	female	-2.21875	11.46391667
CU84659	2689	1998B-032	15-Sep-1998	LowerLouetsi	71	juvenile	-2.21875	11.46391667
CU84659	2690	1998B-032	15-Sep-1998	LowerLouetsi	59	juvenile	-2.21875	11.46391667
CU84659	2691	1998B-032	15-Sep-1998	LowerLouetsi	54	juvenile	-2.21875	11.46391667
CU84581	2694	1998B-023	11-Sep-1998	Mouvanga	98	male	-2.323194444	11.68836111
CU84581	2695	1998B-023	11-Sep-1998	Mouvanga	114	male	-2.323194444	11.68836111
CU84581	2696	1998B-023	11-Sep-1998	Mouvanga	100	male	-2.323194444	11.68836111
CU84581	2697	1998B-023	11-Sep-1998	Mouvanga	113	male	-2.323194444	11.68836111
CU84581	2698	1998B-023	11-Sep-1998	Mouvanga	95	female	-2.323194444	11.68836111
CU84581	2699	1998B-023	11-Sep-1998	Mouvanga	97	male	-2.323194444	11.68836111
CU84581	2700	1998B-023	11-Sep-1998	Mouvanga	95	male	-2.323194444	11.68836111
CU84581	2701	1998B-023	11-Sep-1998	Mouvanga	87	female	-2.323194444	11.68836111
CU84581	2702	1998B-023	11-Sep-1998	Mouvanga	77	male	-2.323194444	11.68836111
CU84581	2703	1998B-023	11-Sep-1998	Mouvanga	84	female	-2.323194444	11.68836111
CU84581	2704	1998B-023	11-Sep-1998	Mouvanga	40	juvenile	-2.323194444	11.68836111
CU84566	2718	1998B-033	16-Sep-1998	LowerLouetsi	124	male	-2.233805556	11.46175
CU80230	2817	1999-007	05-Jul-1999	Oogoue	107	female	-0.659833333	10.32475
CU80230	2818	1999-007	05-Jul-1999	Oogoue	115	male	-0.659833333	10.32475
CU80230	2819	1999-007	05-Jul-1999	Oogoue	85	juvenile	-0.659833333	10.32475
CU80230	2820	1999-007	05-Jul-1999	Oogoue	76	juvenile	-0.659833333	10.32475
CU80230	2821	1999-007	05-Jul-1999	Oogoue	66	juvenile	-0.659833333	10.32475
CU80230	2822	1999-007	05-Jul-1999	Oogoue	71	juvenile	-0.659833333	10.32475
CU80230	2825	1999-007	05-Jul-1999	Oogoue	63	juvenile	-0.659833333	10.32475
CU80230	2826	1999-007	05-Jul-1999	Oogoue	77	juvenile	-0.659833333	10.32475
CU80230	2842	1999-007	05-Jul-1999	Oogoue	63	juvenile	-0.659833333	10.32475

CUMV #	Voucher #	Locality #	Date	Locality	SL	Sex	Lat.	Long.
CU80230	2843	1999-007	05-Jul-1999	Oogoue	61	juvenile	-0.659833333	10.32475
CU80232	2846	1999-010	07-Jul-1999	Oogoue	105	male	-0.668111111	10.33663889
CU80232	2847	1999-010	07-Jul-1999	Oogoue	91	juvenile	-0.668111111	10.33663889
CU80232	2848	1999-010	07-Jul-1999	Oogoue	91	juvenile	-0.668111111	10.33663889
CU80232	2849	1999-010	07-Jul-1999	Oogoue	93	female	-0.668111111	10.33663889
CU80232	2850	1999-010	07-Jul-1999	Oogoue	96	female	-0.668111111	10.33663889
CU80232	2852	1999-010	07-Jul-1999	Oogoue	134	male	-0.668111111	10.33663889
CU80232	2853	1999-010	07-Jul-1999	Oogoue	132	male	-0.668111111	10.33663889
CU80232	2854	1999-010	07-Jul-1999	Oogoue	101	male	-0.668111111	10.33663889
CU80232	2855	1999-010	07-Jul-1999	Oogoue	67	juvenile	-0.668111111	10.33663889
CU80232	2856	1999-010	07-Jul-1999	Oogoue	156	male	-0.668111111	10.33663889
CU80232	2857	1999-010	07-Jul-1999	Oogoue	113	male	-0.668111111	10.33663889
CU80232	2858	1999-010	07-Jul-1999	Oogoue	148	male	-0.668111111	10.33663889
CU80232	2859	1999-010	07-Jul-1999	Oogoue	147	male	-0.668111111	10.33663889
CU80355	3016	1999-044	22-Jul-1999	Mouvanga	102	male	-2.323194444	11.68836111
CU80355	3020	1999-044	22-Jul-1999	Mouvanga	83	juvenile	-2.323194444	11.68836111
CU80323	3040	1999-043	22-Jul-1999	Mouvanga	76	juvenile	-2.323194444	11.68836111
CU80323	3041	1999-043	22-Jul-1999	Mouvanga	65	juvenile	-2.323194444	11.68836111
CU80323	3042	1999-043	22-Jul-1999	Mouvanga	60	juvenile	-2.323194444	11.68836111
CU80323	3043	1999-043	22-Jul-1999	Mouvanga	66	juvenile	-2.323194444	11.68836111
CU80343	3118	1999-047	23-Jul-1999	Bambomo	80	juvenile	-2.163555556	11.46177778
CU80343	3119	1999-047	23-Jul-1999	Bambomo	82	juvenile	-2.163555556	11.46177778
CU80343	3120	1999-047	23-Jul-1999	Bambomo	88	juvenile	-2.163555556	11.46177778
CU80343	3121	1999-047	23-Jul-1999	Bambomo	103	male	-2.163555556	11.46177778
CU80343	3122	1999-047	23-Jul-1999	Bambomo	114	male	-2.163555556	11.46177778
CU80521	3125	1999-048	23-Jul-1999	UpperLouetsi	125	male	-2.233333333	11.45
CU81318	3126	1999-049	24-Jul-1999	Bambomo	100	juvenile	-2.163555556	11.46177778
CU81318	3127	1999-049	24-Jul-1999	Bambomo	118	male	-2.163555556	11.46177778
CU81318	3128	1999-049	24-Jul-1999	Bambomo	153	male	-2.163555556	11.46177778
CU81318	3129	1999-049	24-Jul-1999	Bambomo	130	male	-2.163555556	11.46177778

CUMV #	Voucher #	Locality #	Date	Locality	SL	Sex	Lat.	Long.
CU81318	3130	1999-049	24-Jul-1999	Bambomo	104	male	-2.163555556	11.46177778
CU81318	3141	1999-049	24-Jul-1999	Bambomo	131	male	-2.163555556	11.46177778
CU81318	3142	1999-049	24-Jul-1999	Bambomo	114	male	-2.163555556	11.46177778
CU81318	3143	1999-049	24-Jul-1999	Bambomo	94	juvenile	-2.163555556	11.46177778
CU81319	3144	1999-049	24-Jul-1999	Bambomo	103	male	-2.163555556	11.46177778
CU81318	3145	1999-049	24-Jul-1999	Bambomo	73	juvenile	-2.163555556	11.46177778
CU81318	3146	1999-049	24-Jul-1999	Bambomo	71	juvenile	-2.163555556	11.46177778
CU81318	3147	1999-049	24-Jul-1999	Bambomo	84	juvenile	-2.163555556	11.46177778
CU81318	3148	1999-049	24-Jul-1999	Bambomo	81	juvenile	-2.163555556	11.46177778
CU81318	3149	1999-049	24-Jul-1999	Bambomo	81	juvenile	-2.163555556	11.46177778
CU81318	3150	1999-049	24-Jul-1999	Bambomo	80	juvenile	-2.163555556	11.46177778
CU81318	3151	1999-049	24-Jul-1999	Bambomo	76	juvenile	-2.163555556	11.46177778
CU81318	3152	1999-049	24-Jul-1999	Bambomo	106	juvenile	-2.163555556	11.46177778
CU81318	3153	1999-049	24-Jul-1999	Bambomo	-	juvenile	-2.163555556	11.46177778
CU81318	3154	1999-049	24-Jul-1999	Bambomo	-	juvenile	-2.163555556	11.46177778
CU81318	3155	1999-049	24-Jul-1999	Bambomo	88	juvenile	-2.163555556	11.46177778
CU81318	3156	1999-049	24-Jul-1999	Bambomo	83	juvenile	-2.163555556	11.46177778
CU81318	3157	1999-049	24-Jul-1999	Bambomo	87	juvenile	-2.163555556	11.46177778
CU81318	3158	1999-049	24-Jul-1999	Bambomo	80	juvenile	-2.163555556	11.46177778
CU81318	3159	1999-049	24-Jul-1999	Bambomo	-	juvenile	-2.163555556	11.46177778
CU81318	3160	1999-049	24-Jul-1999	Bambomo	87	juvenile	-2.163555556	11.46177778
CU81318	3161	1999-049	24-Jul-1999	Bambomo	86	juvenile	-2.163555556	11.46177778
CU81318	3162	1999-049	24-Jul-1999	Bambomo	78	juvenile	-2.163555556	11.46177778
CU81318	3164	1999-049	24-Jul-1999	Bambomo	82	juvenile	-2.163555556	11.46177778
CU81318	3165	1999-049	24-Jul-1999	Bambomo	-	juvenile	-2.163555556	11.46177778
CU81318	3167	1999-049	24-Jul-1999	Bambomo	60	juvenile	-2.163555556	11.46177778
CU81318	3168	1999-049	24-Jul-1999	Bambomo	77	juvenile	-2.163555556	11.46177778
CU81318	3169	1999-049	24-Jul-1999	Bambomo	69	juvenile	-2.163555556	11.46177778
CU80521	3192	1999-048	23-Jul-1999	UpperLouetsi	91	juvenile	-2.233333333	11.45
CU80521	3196	1999-048	23-Jul-1999	UpperLouetsi	106	female	-2.233333333	11.45

CUMV #	Voucher #	Locality #	Date	Locality	SL	Sex	Lat.	Long.
CU80521	3197	1999-048	23-Jul-1999	UpperLouetsi	110	male	-2.233333333	11.45
CU80521	3198	1999-048	23-Jul-1999	UpperLouetsi	86	juvenile	-2.233333333	11.45
CU80521	3199	1999-048	23-Jul-1999	UpperLouetsi	98	male	-2.233333333	11.45
CU80348	3210	1999-052	26-Jul-1999	UpperLouetsi	108	juvenile	-2.195333333	11.56113889
CU80348	3211	1999-052	26-Jul-1999	UpperLouetsi	88	juvenile	-2.195333333	11.56113889
CU80348	3212	1999-052	26-Jul-1999	UpperLouetsi	66	juvenile	-2.195333333	11.56113889
CU80348	3213	1999-052	26-Jul-1999	UpperLouetsi	69	juvenile	-2.195333333	11.56113889
CU80342	3214	1999-054	26-Jul-1999	UpperLouetsi	127	male	-2.213111111	11.47766667
CU80527	3220	1999-051	26-Jul-1999	UpperLouetsi	150	male	-2.202888889	11.52925
CU80527	3221	1999-051	26-Jul-1999	UpperLouetsi	129	male	-2.202888889	11.52925
CU80527	3222	1999-051	26-Jul-1999	UpperLouetsi	84	juvenile	-2.202888889	11.52925
CU80527	3223	1999-051	26-Jul-1999	UpperLouetsi	106	male	-2.202888889	11.52925
CU80527	3224	1999-051	26-Jul-1999	UpperLouetsi	100	juvenile	-2.202888889	11.52925
CU80527	3225	1999-051	26-Jul-1999	UpperLouetsi	72	juvenile	-2.202888889	11.52925
CU80506	3273	1999-060	28-Jul-1999	Mouvanga	78	juvenile	-2.323194444	11.68836111
CU80506	3274	1999-060	28-Jul-1999	Mouvanga	86	juvenile	-2.323194444	11.68836111
CU80506	3276	1999-060	28-Jul-1999	Mouvanga	86	juvenile	-2.323194444	11.68836111
CU80506	3278	1999-060	28-Jul-1999	Mouvanga	93	male	-2.323194444	11.68836111
CU80506	3279	1999-060	28-Jul-1999	Mouvanga	90	juvenile	-2.323194444	11.68836111
CU80506	3280	1999-060	28-Jul-1999	Mouvanga	87	juvenile	-2.323194444	11.68836111
CU80506	3281	1999-060	28-Jul-1999	Mouvanga	100	juvenile	-2.323194444	11.68836111
CU80506	3282	1999-060	28-Jul-1999	Mouvanga	96	juvenile	-2.323194444	11.68836111
CU80506	3283	1999-060	28-Jul-1999	Mouvanga	94	juvenile	-2.323194444	11.68836111
CU80506	3284	1999-060	28-Jul-1999	Mouvanga	111	juvenile	-2.323194444	11.68836111
CU80506	3286	1999-060	28-Jul-1999	Mouvanga	96	juvenile	-2.323194444	11.68836111
CU80506	3287	1999-060	28-Jul-1999	Mouvanga	72	juvenile	-2.323194444	11.68836111
CU80506	3288	1999-060	28-Jul-1999	Mouvanga	70	juvenile	-2.323194444	11.68836111
CU80506	3289	1999-060	28-Jul-1999	Mouvanga	92	juvenile	-2.323194444	11.68836111
CU80506	3290	1999-060	28-Jul-1999	Mouvanga	78	juvenile	-2.323194444	11.68836111
CU80506	3291	1999-060	28-Jul-1999	Mouvanga	73	juvenile	-2.323194444	11.68836111

CUMV #	Voucher #	Locality #	Date	Locality	SL	Sex	Lat.	Long.
CU80506	3292	1999-060	28-Jul-1999	Mouvanga	70	juvenile	-2.323194444	11.68836111
CU80506	3318	1999-060	28-Jul-1999	Mouvanga	106	juvenile	-2.323194444	11.68836111
CU80506	3319	1999-060	28-Jul-1999	Mouvanga	96	juvenile	-2.323194444	11.68836111
CU80506	3320	1999-060	28-Jul-1999	Mouvanga	90	juvenile	-2.323194444	11.68836111
CU80506	3321	1999-060	28-Jul-1999	Mouvanga	93	juvenile	-2.323194444	11.68836111
CU80506	3322	1999-060	28-Jul-1999	Mouvanga	-	juvenile	-2.323194444	11.68836111
CU80506	3323	1999-060	28-Jul-1999	Mouvanga	94	juvenile	-2.323194444	11.68836111
CU80506	3325	1999-060	28-Jul-1999	Mouvanga	95	juvenile	-2.323194444	11.68836111
CU80506	3326	1999-060	28-Jul-1999	Mouvanga	99	juvenile	-2.323194444	11.68836111
CU80506	3327	1999-060	28-Jul-1999	Mouvanga	97	male	-2.323194444	11.68836111
CU80506	3328	1999-060	28-Jul-1999	Mouvanga	102	female	-2.323194444	11.68836111
CU80506	3329	1999-060	28-Jul-1999	Mouvanga	84	juvenile	-2.323194444	11.68836111
CU80506	3333	1999-060	28-Jul-1999	Mouvanga	77	juvenile	-2.323194444	11.68836111
CU80506	3334	1999-060	28-Jul-1999	Mouvanga	70	juvenile	-2.323194444	11.68836111
CU80506	3335	1999-060	28-Jul-1999	Mouvanga	88	male	-2.323194444	11.68836111
CU80506	3336	1999-060	28-Jul-1999	Mouvanga	72	juvenile	-2.323194444	11.68836111
CU80506	3338	1999-060	28-Jul-1999	Mouvanga	79	juvenile	-2.323194444	11.68836111
CU80506	3339	1999-060	28-Jul-1999	Mouvanga	105	male	-2.323194444	11.68836111
CU80804	3766	1999-094	22-Aug-1999	Libreville	90	female	0.58475	9.334777778
CU80804	3767	1999-094	22-Aug-1999	Libreville	90	female	0.58475	9.334777778
CU95191	3774	1999-095	25-Aug-1999	Woleu	105	male	1.533666667	11.58011111
CU95191	3777	1999-095	25-Aug-1999	Woleu	102	male	1.533666667	11.58011111
CU95191	3779	1999-095	25-Aug-1999	Woleu	119	male	1.533666667	11.58011111
CU95191	3783	1999-095	25-Aug-1999	Woleu	66	juvenile	1.533666667	11.58011111
CU95191	3799	1999-099	27-Aug-1999	Woleu	128	male	1.544777778	11.76541667
CU95191	3800	1999-099	27-Aug-1999	Woleu	124	female	1.544777778	11.76541667
CU95191	3802	1999-099	27-Aug-1999	Woleu	105	female	1.544777778	11.76541667
CU95191	3803	1999-099	27-Aug-1999	Woleu	103	female	1.544777778	11.76541667
CU95191	3804	1999-099	27-Aug-1999	Woleu	85	female	1.544777778	11.76541667
CU95191	3807	1999-099	27-Aug-1999	Woleu	119	male	1.544777778	11.76541667

CUMV #	Voucher #	Locality #	Date	Locality	SL	Sex	Lat.	Long.
CU95191	3808	1999-099	27-Aug-1999	Woleu	75	female	1.544777778	11.76541667
CU95191	3809	1999-099	27-Aug-1999	Woleu	83	female	1.544777778	11.76541667
CU95191	3810	1999-099	27-Aug-1999	Woleu	102	female	1.544777778	11.76541667
CU95191	3812	1999-099	27-Aug-1999	Woleu	87	male	1.544777778	11.76541667
CU95191	3813	1999-099	27-Aug-1999	Woleu	90	male	1.544777778	11.76541667
CU80926	3943	1999-105	01-Sep-1999	Ntem	91	female	1.702138889	11.6445
CU80926	3944	1999-105	01-Sep-1999	Ntem	97	female	1.702138889	11.6445
CU80926	3950	1999-105	01-Sep-1999	Ntem	86	male	1.702138889	11.6445
CU80926	3951	1999-105	01-Sep-1999	Ntem	83	juvenile	1.702138889	11.6445
CU81263	4001	2000-001	26-Mar-2000	Cocobeach	94	female	0.932583333	9.574316667
CU81263	4002	2000-001	26-Mar-2000	Cocobeach	72	male	0.932583333	9.574316667
CU81263	4003	2000-001	26-Mar-2000	Cocobeach	94	female	0.932583333	9.574316667
CU81263	4004	2000-001	26-Mar-2000	Cocobeach	83	male	0.932583333	9.574316667
CU81263	4005	2000-001	26-Mar-2000	Cocobeach	75	female	0.932583333	9.574316667
CU81263	4006	2000-001	26-Mar-2000	Cocobeach	77	female	0.932583333	9.574316667
CU81263	4007	2000-001	26-Mar-2000	Cocobeach	71	female	0.932583333	9.574316667
CU81263	4008	2000-001	26-Mar-2000	Cocobeach	68	juvenile	0.932583333	9.574316667
CU81263	4009	2000-001	26-Mar-2000	Cocobeach	54	juvenile	0.932583333	9.574316667
CU81263	4010	2000-001	26-Mar-2000	Cocobeach	51	juvenile	0.932583333	9.574316667
CU81263	4011	2000-001	26-Mar-2000	Cocobeach	45	juvenile	0.932583333	9.574316667
CU81263	4012	2000-001	26-Mar-2000	Cocobeach	42	juvenile	0.932583333	9.574316667
CU81264	4013	2000-004	27-Mar-2000	Cocobeach	85	juvenile	0.870483333	9.584616667
CU81264	4014	2000-004	27-Mar-2000	Cocobeach	117	male	0.870483333	9.584616667
CU81264	4015	2000-004	27-Mar-2000	Cocobeach	94	female	0.870483333	9.584616667
CU81264	4016	2000-004	27-Mar-2000	Cocobeach	86	female	0.870483333	9.584616667
CU81264	4017	2000-004	27-Mar-2000	Cocobeach	72	male	0.870483333	9.584616667
CU81264	4018	2000-004	27-Mar-2000	Cocobeach	118	male	0.870483333	9.584616667
CU81264	4019	2000-004	27-Mar-2000	Cocobeach	128	male	0.870483333	9.584616667
CU81260	4020	2000-002	27-Mar-2000	Cocobeach	103	male	0.93365	9.574316667
CU81260	4021	2000-002	27-Mar-2000	Cocobeach	132	male	0.93365	9.574316667

CUMV #	Voucher #	Locality #	Date	Locality	SL	Sex	Lat.	Long.
CU81260	4022	2000-002	27-Mar-2000	Cocobeach	105	male	0.93365	9.574316667
CU81260	4023	2000-002	27-Mar-2000	Cocobeach	142	male	0.93365	9.574316667
CU81260	4024	2000-002	27-Mar-2000	Cocobeach	125	male	0.93365	9.574316667
CU81260	4025	2000-002	27-Mar-2000	Cocobeach	96	female	0.93365	9.574316667
CU81260	4026	2000-002	27-Mar-2000	Cocobeach	107	female	0.93365	9.574316667
CU81260	4027	2000-002	27-Mar-2000	Cocobeach	131	male	0.93365	9.574316667
CU81260	4028	2000-002	27-Mar-2000	Cocobeach	121	male	0.93365	9.574316667
CU81260	4029	2000-002	27-Mar-2000	Cocobeach	93	female	0.93365	9.574316667
CU81260	4030	2000-002	27-Mar-2000	Cocobeach	105	female	0.93365	9.574316667
CU83330	4341	2001B-048	24-Jul-2001	Nyanga	81	female	-3.374166667	10.7895
CU83330	4343	2001B-048	24-Jul-2001	Nyanga	67	female	-3.374166667	10.7895
CU83330	4344	2001B-048	24-Jul-2001	Nyanga	49	juvenile	-3.374166667	10.7895
CU83330	4345	2001B-048	24-Jul-2001	Nyanga	74	female	-3.374166667	10.7895
CU83083	4601	2001C-001	13-Aug-2001	Okano	76	juvenile	0.83235	11.65045
CU83083	4602	2001C-001	13-Aug-2001	Okano	88.5	female	0.83235	11.65045
CU83083	4628	2001C-001	13-Aug-2001	Okano	97	male	0.83235	11.65045
CU83083	4630	2001C-001	13-Aug-2001	Okano	83	male	0.83235	11.65045
CU83083	4632	2001C-001	13-Aug-2001	Okano	86.5	male	0.83235	11.65045
CU83083	4634	2001C-001	13-Aug-2001	Okano	95.5	female	0.83235	11.65045
CU83083	4636	2001C-001	13-Aug-2001	Okano	82	female	0.83235	11.65045
CU83083	4637	2001C-001	13-Aug-2001	Okano	101.5	male	0.83235	11.65045
CU83083	4638	2001C-001	13-Aug-2001	Okano	89	male	0.83235	11.65045
CU83083	4640	2001C-001	13-Aug-2001	Okano	93.5	male	0.83235	11.65045
CU83083	4641	2001C-001	13-Aug-2001	Okano	82.5	male	0.83235	11.65045
CU83083	4642	2001C-001	13-Aug-2001	Okano	92	male	0.83235	11.65045
CU83083	4643	2001C-001	13-Aug-2001	Okano	90	juvenile	0.83235	11.65045
CU83083	4644	2001C-001	13-Aug-2001	Okano	76	juvenile	0.83235	11.65045
CU83083	4645	2001C-001	13-Aug-2001	Okano	87	juvenile	0.83235	11.65045
CU83083	4646	2001C-001	13-Aug-2001	Okano	101.5	female	0.83235	11.65045
CU83083	4647	2001C-001	13-Aug-2001	Okano	93	female	0.83235	11.65045

CUMV #	Voucher #	Locality #	Date	Locality	SL	Sex	Lat.	Long.
CU83083	4648	2001C-001	13-Aug-2001	Okano	102	male	0.83235	11.65045
CU83083	4649	2001C-001	13-Aug-2001	Okano	127	male	0.83235	11.65045
CU83083	4650	2001C-001	13-Aug-2001	Okano	99	female	0.83235	11.65045
CU83083	4651	2001C-001	13-Aug-2001	Okano	127	male	0.83235	11.65045
CU83083	4652	2001C-001	13-Aug-2001	Okano	112	male	0.83235	11.65045
CU83083	4653	2001C-001	13-Aug-2001	Okano	102	female	0.83235	11.65045
CU83083	4654	2001C-001	13-Aug-2001	Okano	82.5	juvenile	0.83235	11.65045
CU83083	4655	2001C-001	13-Aug-2001	Okano	69.5	juvenile	0.83235	11.65045
CU83083	4656	2001C-001	13-Aug-2001	Okano	98.5	female	0.83235	11.65045
CU83083	4657	2001C-001	13-Aug-2001	Okano	117	male	0.83235	11.65045
CU83083	4658	2001C-001	13-Aug-2001	Okano	114	male	0.83235	11.65045
CU83083	4659	2001C-001	13-Aug-2001	Okano	84.5	juvenile	0.83235	11.65045
CU83083	4660	2001C-001	13-Aug-2001	Okano	88	male	0.83235	11.65045
CU83083	4663	2001C-001	13-Aug-2001	Okano	89.9	female	0.83235	11.65045
CU83083	4665	2001C-001	13-Aug-2001	Okano	88	male	0.83235	11.65045
CU83083	4666	2001C-001	13-Aug-2001	Okano	73	juvenile	0.83235	11.65045
CU83083	4668	2001C-001	13-Aug-2001	Okano	81	male	0.83235	11.65045
CU83083	4671	2001C-001	13-Aug-2001	Okano	96.5	female	0.83235	11.65045
CU83083	4672	2001C-001	13-Aug-2001	Okano	75	male	0.83235	11.65045
CU83068	4720	2001C-007	17-Aug-2001	Okano	86.5	juvenile	0.809783333	11.63
CU83068	4727	2001C-007	17-Aug-2001	Okano	73	juvenile	0.809783333	11.63
CU83098	4863	2001C-016	25-Aug-2001	Ivindo	110	male	0.5045	12.79683333
CU83098	4864	2001C-016	25-Aug-2001	Ivindo	85	male	0.5045	12.79683333
CU83098	4870	2001C-016	25-Aug-2001	Ivindo	69.5	juvenile	0.5045	12.79683333
CU83114	4939	2001C-021	02-Sep-2001	Oogoue	70	female	-0.568277778	10.21302778
CU83114	4942	2001C-021	02-Sep-2001	Oogoue	62.5	juvenile	-0.568277778	10.21302778
CU83114	4943	2001C-021	02-Sep-2001	Oogoue	67	juvenile	-0.568277778	10.21302778
CU83114	4944	2001C-021	02-Sep-2001	Oogoue	60.5	juvenile	-0.568277778	10.21302778
CU95191	6487	2009-001	25-Jul-2009	Bambomo	70.5	juvenile	-2.163416667	11.46185
CU95191	6488	2009-001	25-Jul-2009	Bambomo	84	juvenile	-2.163416667	11.46185

CUMV #	Voucher #	Locality #	Date	Locality	SL	Sex	Lat.	Long.
CU95191	6489	2009-001	25-Jul-2009	Bambomo	74.5	juvenile	-2.163416667	11.46185
CU95191	6490	2009-001	25-Jul-2009	Bambomo	72	juvenile	-2.163416667	11.46185
CU95187	6491	2009-002	25-Jul-2009	UpperLouetsi	68	juvenile	-2.21305	11.47751667
CU95191	6493	2009-001	25-Jul-2009	Bambomo	61.5	juvenile	-2.163416667	11.46185
CU95191	6494	2009-001	25-Jul-2009	Bambomo	69.5	juvenile	-2.163416667	11.46185
CU95191	6495	2009-001	25-Jul-2009	Bambomo	46.5	juvenile	-2.163416667	11.46185
CU95191	6496	2009-001	25-Jul-2009	Bambomo	62	juvenile	-2.163416667	11.46185
CU95191	6497	2009-001	25-Jul-2009	Bambomo	46	juvenile	-2.163416667	11.46185
CU95191	6498	2009-001	25-Jul-2009	Bambomo	44	juvenile	-2.163416667	11.46185
CU95191	6499	2009-001	25-Jul-2009	Bambomo	43	juvenile	-2.163416667	11.46185
CU95191	6500	2009-001	25-Jul-2009	Bambomo	44.5	juvenile	-2.163416667	11.46185
CU95191	6502	2009-001	25-Jul-2009	Bambomo	40	juvenile	-2.163416667	11.46185
CU95191	6504	2009-001	25-Jul-2009	Bambomo	42	juvenile	-2.163416667	11.46185
CU95191	6506	2009-001	25-Jul-2009	Bambomo	44	juvenile	-2.163416667	11.46185
CU95191	6509	2009-001	25-Jul-2009	Bambomo	32	juvenile	-2.163416667	11.46185
CU95191	6510	2009-001	25-Jul-2009	Bambomo	38	juvenile	-2.163416667	11.46185
CU95187	6514	2009-002	25-Jul-2009	UpperLouetsi	58	ND	-2.21305	11.47751667
CU95187	6515	2009-002	25-Jul-2009	UpperLouetsi	55	ND	-2.21305	11.47751667
CU95187	6516	2009-002	25-Jul-2009	UpperLouetsi	48	ND	-2.21305	11.47751667
CU95187	6517	2009-002	25-Jul-2009	UpperLouetsi	48	ND	-2.21305	11.47751667
CU95187	6518	2009-002	25-Jul-2009	UpperLouetsi	51.5	ND	-2.21305	11.47751667
CU95186	6527	2009-004	27-Jul-2009	Bambomo	84	female	-2.1634167	11.46185
CU95186	6531	2009-004	27-Jul-2009	Bambomo	98	female	-2.1634167	11.46185
CU95186	6532	2009-004	27-Jul-2009	Bambomo	107	male	-2.1634167	11.46185
CU95186	6533	2009-004	27-Jul-2009	Bambomo	110	female	-2.1634167	11.46185
CU95192	6534	2009-004	27-Jul-2009	Bambomo	75	juvenile	-2.1634167	11.46185
CU95192	6535	2009-004	27-Jul-2009	Bambomo	143	male	-2.1634167	11.46185
CU95192	6536	2009-004	27-Jul-2009	Bambomo	136.5	male	-2.1634167	11.46185
CU95192	6537	2009-004	27-Jul-2009	Bambomo	97	female	-2.1634167	11.46185
CU95192	6538	2009-004	27-Jul-2009	Bambomo	128	male	-2.1634167	11.46185

CUMV #	Voucher #	Locality #	Date	Locality	SL	Sex	Lat.	Long.
CU95192	6539	2009-004	27-Jul-2009	Bambomo	97	female	-2.1634167	11.46185
CU95192	6540	2009-004	27-Jul-2009	Bambomo	76	juvenile	-2.1634167	11.46185
CU95192	6541	2009-004	27-Jul-2009	Bambomo	84	juvenile	-2.1634167	11.46185
CU95192	6542	2009-004	27-Jul-2009	Bambomo	87	male	-2.1634167	11.46185
CU95192	6543	2009-004	27-Jul-2009	Bambomo	98	juvenile	-2.1634167	11.46185
CU95192	6544	2009-004	27-Jul-2009	Bambomo	68.5	juvenile	-2.1634167	11.46185
CU95192	6545	2009-004	27-Jul-2009	Bambomo	89.5	juvenile	-2.1634167	11.46185
CU95192	6546	2009-004	27-Jul-2009	Bambomo	61	juvenile	-2.1634167	11.46185
CU95192	6547	2009-004	27-Jul-2009	Bambomo	79.5	juvenile	-2.1634167	11.46185
CU95192	6548	2009-004	27-Jul-2009	Bambomo	73	male	-2.1634167	11.46185
CU95192	6549	2009-004	27-Jul-2009	Bambomo	91	juvenile	-2.1634167	11.46185
CU95192	6550	2009-004	27-Jul-2009	Bambomo	70.5	juvenile	-2.1634167	11.46185
CU95192	6551	2009-004	27-Jul-2009	Bambomo	64.5	juvenile	-2.1634167	11.46185
CU95192	6552	2009-004	27-Jul-2009	Bambomo	76	juvenile	-2.1634167	11.46185
CU95192	6553	2009-004	27-Jul-2009	Bambomo	75	juvenile	-2.1634167	11.46185
CU95192	6554	2009-004	27-Jul-2009	Bambomo	67	juvenile	-2.1634167	11.46185
CU95192	6555	2009-004	27-Jul-2009	Bambomo	83	female	-2.1634167	11.46185
CU95192	6556	2009-004	27-Jul-2009	Bambomo	64	male	-2.1634167	11.46185
CU95192	6557	2009-004	27-Jul-2009	Bambomo	66	juvenile	-2.1634167	11.46185
CU95192	6558	2009-004	27-Jul-2009	Bambomo	74	juvenile	-2.1634167	11.46185
CU95192	6559	2009-004	27-Jul-2009	Bambomo	85	juvenile	-2.1634167	11.46185
CU95192	6560	2009-004	27-Jul-2009	Bambomo	69	juvenile	-2.1634167	11.46185
CU95192	6561	2009-004	27-Jul-2009	Bambomo	61	juvenile	-2.1634167	11.46185
CU95192	6562	2009-004	27-Jul-2009	Bambomo	72	juvenile	-2.1634167	11.46185
CU95192	6563	2009-004	27-Jul-2009	Bambomo	77	juvenile	-2.1634167	11.46185
CU95192	6564	2009-004	27-Jul-2009	Bambomo	71	juvenile	-2.1634167	11.46185
CU95192	6565	2009-004	27-Jul-2009	Bambomo	85	juvenile	-2.1634167	11.46185
CU95192	6566	2009-004	27-Jul-2009	Bambomo	-	ND	-2.1634167	11.46185
CU95192	6567	2009-004	27-Jul-2009	Bambomo	-	ND	-2.1634167	11.46185
CU95192	6568	2009-004	27-Jul-2009	Bambomo	79	juvenile	-2.1634167	11.46185

CUMV #	Voucher #	Locality #	Date	Locality	SL	Sex	Lat.	Long.
CU95192	6569	2009-004	27-Jul-2009	Bambomo	68	juvenile	-2.1634167	11.46185
CU95192	6570	2009-004	27-Jul-2009	Bambomo	76	juvenile	-2.1634167	11.46185
CU95192	6571	2009-004	27-Jul-2009	Bambomo	75	juvenile	-2.1634167	11.46185
CU95192	6589	2009-004	27-Jul-2009	Bambomo	59	juvenile	-2.1634167	11.46185
CU95192	6595	2009-004	27-Jul-2009	Bambomo	51	juvenile	-2.1634167	11.46185
CU95192	6596	2009-004	27-Jul-2009	Bambomo	49	juvenile	-2.1634167	11.46185
CU95192	6597	2009-004	27-Jul-2009	Bambomo	59	juvenile	-2.1634167	11.46185
CU95192	6598	2009-004	27-Jul-2009	Bambomo	42.5	juvenile	-2.1634167	11.46185
CU95192	6599	2009-004	27-Jul-2009	Bambomo	47	juvenile	-2.1634167	11.46185
CU95192	6600	2009-004	27-Jul-2009	Bambomo	45.5	juvenile	-2.1634167	11.46185
CU95192	6601	2009-004	27-Jul-2009	Bambomo	41	juvenile	-2.1634167	11.46185
CU95192	6602	2009-004	27-Jul-2009	Bambomo	52	juvenile	-2.1634167	11.46185
CU95192	6603	2009-004	27-Jul-2009	Bambomo	47	juvenile	-2.1634167	11.46185
CU95192	6604	2009-004	27-Jul-2009	Bambomo	44	juvenile	-2.1634167	11.46185
CU95192	6605	2009-004	27-Jul-2009	Bambomo	51	juvenile	-2.1634167	11.46185
CU95235	6606	2009-011	30-Jul-2009	UpperLouetsi	57	juvenile	-2.27845	11.6114
CU95235	6607	2009-011	30-Jul-2009	UpperLouetsi	65	juvenile	-2.27845	11.6114
CU95235	6608	2009-011	30-Jul-2009	UpperLouetsi	50	juvenile	-2.27845	11.6114
CU95235	6609	2009-011	30-Jul-2009	UpperLouetsi	48	juvenile	-2.27845	11.6114
CU95235	6610	2009-011	30-Jul-2009	UpperLouetsi	59	juvenile	-2.27845	11.6114
CU95235	6611	2009-011	30-Jul-2009	UpperLouetsi	87	male	-2.27845	11.6114
CU95235	6612	2009-011	30-Jul-2009	UpperLouetsi	85	female	-2.27845	11.6114
CU95235	6613	2009-011	30-Jul-2009	UpperLouetsi	73	female	-2.27845	11.6114
CU95235	6614	2009-011	30-Jul-2009	UpperLouetsi	56	juvenile	-2.27845	11.6114
CU95235	6615	2009-011	30-Jul-2009	UpperLouetsi	54	juvenile	-2.27845	11.6114
CU95235	6616	2009-011	30-Jul-2009	UpperLouetsi	77	male	-2.27845	11.6114
CU95236	6619	2009-013	30-Jul-2009	UpperLouetsi	50	juvenile	-2.242483333	11.556
CU95236	6620	2009-013	30-Jul-2009	UpperLouetsi	58	juvenile	-2.242483333	11.556
CU95236	6621	2009-013	30-Jul-2009	UpperLouetsi	49	juvenile	-2.242483333	11.556
CU95236	6622	2009-013	30-Jul-2009	UpperLouetsi	56	juvenile	-2.242483333	11.556

CUMV #	Voucher #	Locality #	Date	Locality	SL	Sex	Lat.	Long.
CU95236	6623	2009-013	30-Jul-2009	UpperLouetsi	64	juvenile	-2.242483333	11.556
CU95236	6624	2009-013	30-Jul-2009	UpperLouetsi	60	juvenile	-2.242483333	11.556
CU95236	6625	2009-013	30-Jul-2009	UpperLouetsi	55	juvenile	-2.242483333	11.556
CU95236	6626	2009-013	30-Jul-2009	UpperLouetsi	53	juvenile	-2.242483333	11.556
CU95236	6627	2009-013	30-Jul-2009	UpperLouetsi	53	juvenile	-2.242483333	11.556
CU95236	6628	2009-013	30-Jul-2009	UpperLouetsi	50	juvenile	-2.242483333	11.556
CU95236	6629	2009-013	30-Jul-2009	UpperLouetsi	44	juvenile	-2.242483333	11.556
CU95188	6675	2009-018	5-Aug-2009	LowerLouetsi	89	male	-2.211633333	11.45966667
CU95188	6676	2009-018	5-Aug-2009	LowerLouetsi	58	male?	-2.211633333	11.45966667
CU95188	6677	2009-018	5-Aug-2009	LowerLouetsi	55	female	-2.211633333	11.45966667
CU95188	6678	2009-018	5-Aug-2009	LowerLouetsi	61	female	-2.211633333	11.45966667
CU95188	6679	2009-018	5-Aug-2009	LowerLouetsi	51	juvenile	-2.211633333	11.45966667
CU95188	6680	2009-018	5-Aug-2009	LowerLouetsi	52	juvenile	-2.211633333	11.45966667
CU95188	6681	2009-018	5-Aug-2009	LowerLouetsi	50	juvenile	-2.211633333	11.45966667
CU95188	6682	2009-018	5-Aug-2009	LowerLouetsi	84	male?	-2.211633333	11.45966667
CU95188	6683	2009-018	5-Aug-2009	LowerLouetsi	49	juvenile	-2.211633333	11.45966667
CU95188	6684	2009-018	5-Aug-2009	LowerLouetsi	46	juvenile	-2.211633333	11.45966667
CU95188	6685	2009-018	5-Aug-2009	LowerLouetsi	69	female?	-2.211633333	11.45966667
CU95188	6686	2009-018	5-Aug-2009	LowerLouetsi	82	male	-2.211633333	11.45966667
CU95188	6687	2009-018	5-Aug-2009	LowerLouetsi	51	juvenile	-2.211633333	11.45966667
CU95188	6707	2009-018	5-Aug-2009	LowerLouetsi	50	juvenile	-2.211633333	11.45966667
CU95188	6708	2009-018	5-Aug-2009	LowerLouetsi	41	juvenile	-2.211633333	11.45966667
CU95188	6709	2009-018	5-Aug-2009	LowerLouetsi	64	juvenile	-2.211633333	11.45966667
CU95188	6710	2009-018	5-Aug-2009	LowerLouetsi	-	ND	-2.211633333	11.45966667
CU95188	6711	2009-018	5-Aug-2009	LowerLouetsi	59	juvenile	-2.211633333	11.45966667
CU95188	6712	2009-018	5-Aug-2009	LowerLouetsi	77	juvenile	-2.211633333	11.45966667
CU95188	6713	2009-018	5-Aug-2009	LowerLouetsi	55	juvenile	-2.211633333	11.45966667
CU95188	6714	2009-018	5-Aug-2009	LowerLouetsi	45	juvenile	-2.211633333	11.45966667
CU95188	6715	2009-018	5-Aug-2009	LowerLouetsi	61	juvenile	-2.211633333	11.45966667
CU95183	6716	2009-022	7-Aug-2009	Mouvanga	92.5	juvenile	-2.328033333	11.68583333

CUMV #	Voucher #	Locality #	Date	Locality	SL	Sex	Lat.	Long.
CU95183	6717	2009-022	7-Aug-2009	Mouvanga	94	juvenile	-2.328033333	11.68583333
CU95183	6718	2009-022	7-Aug-2009	Mouvanga	91	juvenile	-2.328033333	11.68583333
CU95183	6719	2009-022	7-Aug-2009	Mouvanga	86.5	juvenile	-2.328033333	11.68583333
CU95183	6720	2009-022	7-Aug-2009	Mouvanga	102	juvenile	-2.328033333	11.68583333
CU95183	6721	2009-022	7-Aug-2009	Mouvanga	85	juvenile	-2.328033333	11.68583333
CU95183	6722	2009-022	7-Aug-2009	Mouvanga	89	juvenile	-2.328033333	11.68583333
CU95183	6723	2009-022	7-Aug-2009	Mouvanga	100	juvenile	-2.328033333	11.68583333
CU95183	6724	2009-022	7-Aug-2009	Mouvanga	100	juvenile	-2.328033333	11.68583333
CU95183	6725	2009-022	7-Aug-2009	Mouvanga	103	male	-2.328033333	11.68583333
CU95188	6729	2009-018	5-Aug-2009	LowerLouetsi	49	Juv/male	-2.211633333	11.45966667
CU95188	6730	2009-018	5-Aug-2009	LowerLouetsi	52	juvenile	-2.211633333	11.45966667
CU95188	6731	2009-018	5-Aug-2009	LowerLouetsi	44	juvenile	-2.211633333	11.45966667
CU95188	6732	2009-018	5-Aug-2009	LowerLouetsi	64	Juv/male	-2.211633333	11.45966667
CU95188	6733	2009-018	5-Aug-2009	LowerLouetsi	49	juvenile	-2.211633333	11.45966667
CU95188	6734	2009-018	5-Aug-2009	LowerLouetsi	50	juvenile	-2.211633333	11.45966667
CU95188	6735	2009-018	5-Aug-2009	LowerLouetsi	-	male?	-2.211633333	11.45966667
CU95188	6736	2009-018	5-Aug-2009	LowerLouetsi	33	juvenile	-2.211633333	11.45966667
CU95188	6737	2009-018	5-Aug-2009	LowerLouetsi	48.5	juvenile	-2.211633333	11.45966667
CU95183	6788	2009-022	7-Aug-2009	Mouvanga	-	ND	-2.328033333	11.68583333
CU95183	6789	2009-022	7-Aug-2009	Mouvanga	-	ND	-2.328033333	11.68583333
CU95183	6790	2009-022	7-Aug-2009	Mouvanga	79	juvenile	-2.328033333	11.68583333
CU95183	6791	2009-022	7-Aug-2009	Mouvanga	75	male	-2.328033333	11.68583333
CU95183	6792	2009-022	7-Aug-2009	Mouvanga	79	juvenile	-2.328033333	11.68583333
CU95183	6793	2009-022	7-Aug-2009	Mouvanga	74	female	-2.328033333	11.68583333
CU95183	6794	2009-022	7-Aug-2009	Mouvanga	71.5	juvenile	-2.328033333	11.68583333
CU95183	6795	2009-022	7-Aug-2009	Mouvanga	71	juvenile	-2.328033333	11.68583333
CU95183	6796	2009-022	7-Aug-2009	Mouvanga	61	male	-2.328033333	11.68583333
CU95183	6797	2009-022	7-Aug-2009	Mouvanga	57.5	juvenile	-2.328033333	11.68583333
CU95183	6798	2009-022	7-Aug-2009	Mouvanga	-	ND	-2.328033333	11.68583333
CU95183	6799	2009-022	7-Aug-2009	Mouvanga	-	ND	-2.328033333	11.68583333

CUMV #	Voucher #	Locality #	Date	Locality	SL	Sex	Lat.	Long.
CU95183	6802	2009-022	7-Aug-2009	Mouvanga	-	ND	-2.328033333	11.68583333
CU95183	6803	2009-022	7-Aug-2009	Mouvanga	64	juvenile	-2.328033333	11.68583333
CU95183	6804	2009-022	7-Aug-2009	Mouvanga	92	male	-2.328033333	11.68583333
CU95183	6805	2009-022	7-Aug-2009	Mouvanga	72	juvenile	-2.328033333	11.68583333
CU95183	6806	2009-022	7-Aug-2009	Mouvanga	77.5	juvenile	-2.328033333	11.68583333
CU95183	6807	2009-022	7-Aug-2009	Mouvanga	84	juvenile	-2.328033333	11.68583333
CU95183	6808	2009-022	7-Aug-2009	Mouvanga	82	juvenile	-2.328033333	11.68583333
CU95183	6809	2009-022	7-Aug-2009	Mouvanga	81	juvenile	-2.328033333	11.68583333
CU95183	6810	2009-022	7-Aug-2009	Mouvanga	59.5	juvenile	-2.328033333	11.68583333
CU95183	6811	2009-022	7-Aug-2009	Mouvanga	56.5	juvenile	-2.328033333	11.68583333
CU95237	6823	2009-025	12-Aug-2009	Bambomo	92	male	-2.163333333	11.462
CU95237	6824	2009-025	12-Aug-2009	Bambomo	85	juvenile	-2.163333333	11.462
CU95237	6825	2009-025	12-Aug-2009	Bambomo	96.5	male	-2.163333333	11.462
CU95237	6826	2009-025	12-Aug-2009	Bambomo	86	female	-2.163333333	11.462
CU95237	6827	2009-025	12-Aug-2009	Bambomo	88	juvenile	-2.163333333	11.462
CU95237	6828	2009-025	12-Aug-2009	Bambomo	88	juvenile	-2.163333333	11.462
CU95237	6829	2009-025	12-Aug-2009	Bambomo	91	juvenile	-2.163333333	11.462
CU95237	6830	2009-025	12-Aug-2009	Bambomo	93	juvenile	-2.163333333	11.462
CU95237	6831	2009-025	12-Aug-2009	Bambomo	97	female	-2.163333333	11.462
CU95237	6832	2009-025	12-Aug-2009	Bambomo	98	male	-2.163333333	11.462
CU95237	6833	2009-025	12-Aug-2009	Bambomo	45	juvenile	-2.163333333	11.462
CU95237	6834	2009-025	12-Aug-2009	Bambomo	65	juvenile	-2.163333333	11.462
CU95237	6835	2009-025	12-Aug-2009	Bambomo	75	juvenile	-2.163333333	11.462
CU95237	6836	2009-025	12-Aug-2009	Bambomo	106	male	-2.163333333	11.462
CU95237	6837	2009-025	12-Aug-2009	Bambomo	51	juvenile	-2.163333333	11.462
CU95237	6838	2009-025	12-Aug-2009	Bambomo	87	male	-2.163333333	11.462
CU95237	6839	2009-025	12-Aug-2009	Bambomo	-	ND	-2.163333333	11.462
CU95237	6840	2009-025	12-Aug-2009	Bambomo	86	juvenile	-2.163333333	11.462
CU95237	6841	2009-025	12-Aug-2009	Bambomo	79	juvenile	-2.163333333	11.462
CU95237	6842	2009-025	12-Aug-2009	Bambomo	75	juvenile	-2.163333333	11.462

CUMV #	Voucher #	Locality #	Date	Locality	SL	Sex	Lat.	Long.
CU95237	6843	2009-025	12-Aug-2009	Bambomo	70	juvenile	-2.163333333	11.462
CU95237	6844	2009-025	12-Aug-2009	Bambomo	80	male	-2.163333333	11.462
CU95237	6845	2009-025	12-Aug-2009	Bambomo	63.5	juvenile	-2.163333333	11.462
CU95237	6846	2009-025	12-Aug-2009	Bambomo	101	juvenile	-2.163333333	11.462
CU95237	6847	2009-025	12-Aug-2009	Bambomo	88.5	male	-2.163333333	11.462
CU95237	6848	2009-025	12-Aug-2009	Bambomo	107.5	female	-2.163333333	11.462
CU95237	6849	2009-025	12-Aug-2009	Bambomo	-	ND	-2.163333333	11.462
CU95237	6850	2009-025	12-Aug-2009	Bambomo	69	female	-2.163333333	11.462
CU95237	6851	2009-025	12-Aug-2009	Bambomo	48.5	juvenile	-2.163333333	11.462
CU95237	6852	2009-025	12-Aug-2009	Bambomo	69	juvenile	-2.163333333	11.462
CU95237	6853	2009-025	12-Aug-2009	Bambomo	93	male	-2.163333333	11.462
CU95237	6854	2009-025	12-Aug-2009	Bambomo	61	juvenile	-2.163333333	11.462
CU95237	6855	2009-025	12-Aug-2009	Bambomo	64	juvenile	-2.163333333	11.462
CU95237	6856	2009-025	12-Aug-2009	Bambomo	-	ND	-2.163333333	11.462
CU95237	6864	2009-025	12-Aug-2009	Bambomo	-	ND	-2.163333333	11.462
CU95237	6865	2009-025	12-Aug-2009	Bambomo	78	juvenile	-2.163333333	11.462
CU95237	6866	2009-025	12-Aug-2009	Bambomo	70	juvenile	-2.163333333	11.462
CU95237	6867	2009-025	12-Aug-2009	Bambomo	75	juvenile	-2.163333333	11.462
CU95237	6868	2009-025	12-Aug-2009	Bambomo	82	juvenile	-2.163333333	11.462
CU95237	6869	2009-025	12-Aug-2009	Bambomo	50	juvenile	-2.163333333	11.462
CU95237	6870	2009-025	12-Aug-2009	Bambomo	74	juvenile	-2.163333333	11.462
CU95237	6871	2009-025	12-Aug-2009	Bambomo	74	juvenile	-2.163333333	11.462
CU95237	6872	2009-025	12-Aug-2009	Bambomo	72	juvenile	-2.163333333	11.462
CU95237	6873	2009-025	12-Aug-2009	Bambomo	73	juvenile	-2.163333333	11.462
CU95237	6874	2009-025	12-Aug-2009	Bambomo	80	juvenile	-2.163333333	11.462
CU95237	6875	2009-025	12-Aug-2009	Bambomo	68	juvenile	-2.163333333	11.462
CU95237	6876	2009-025	12-Aug-2009	Bambomo	65	juvenile	-2.163333333	11.462
CU95237	6877	2009-025	12-Aug-2009	Bambomo	89	juvenile	-2.163333333	11.462
CU95237	6878	2009-025	12-Aug-2009	Bambomo	74	male	-2.163333333	11.462
CU95237	6879	2009-025	12-Aug-2009	Bambomo	74	juvenile	-2.163333333	11.462

CUMV #	Voucher #	Locality #	Date	Locality	SL	Sex	Lat.	Long.
CU95237	6880	2009-025	12-Aug-2009	Bambomo	100	female	-2.163333333	11.462
CU95238	6881	2009-028	13-Aug-2009	UpperLouetsi	-	ND	-2.242483333	11.556
CU95238	6882	2009-028	13-Aug-2009	UpperLouetsi	41	juvenile	-2.242483333	11.556
CU95238	6883	2009-028	13-Aug-2009	UpperLouetsi	71	juvenile	-2.242483333	11.556
CU95238	6884	2009-028	13-Aug-2009	UpperLouetsi	68	juvenile	-2.242483333	11.556
CU95238	6885	2009-028	13-Aug-2009	UpperLouetsi	49	juvenile	-2.242483333	11.556
CU95238	6886	2009-028	13-Aug-2009	UpperLouetsi	49.5	juvenile	-2.242483333	11.556
CU95238	6887	2009-028	13-Aug-2009	UpperLouetsi	47	juvenile	-2.242483333	11.556
CU95238	6888	2009-028	13-Aug-2009	UpperLouetsi	68	juvenile	-2.242483333	11.556
CU95238	6889	2009-028	13-Aug-2009	UpperLouetsi	55	juvenile	-2.242483333	11.556
CU95238	6891	2009-028	13-Aug-2009	UpperLouetsi	68	juvenile	-2.242483333	11.556
CU95238	6892	2009-028	13-Aug-2009	UpperLouetsi	78	juvenile	-2.242483333	11.556
CU95238	6893	2009-028	13-Aug-2009	UpperLouetsi	36	juvenile	-2.242483333	11.556
CU95191	6898	2009-031	15-Aug-2009	UpperLouetsi	131	male	-2.195633333	11.56141667
CU95191	6899	2009-031	15-Aug-2009	UpperLouetsi	102.5	male	-2.195633333	11.56141667
CU95191	6900	2009-031	15-Aug-2009	UpperLouetsi	145	male	-2.195633333	11.56141667
CU95191	6901	2009-031	15-Aug-2009	UpperLouetsi	149	male	-2.195633333	11.56141667
CU95191	6902	2009-031	15-Aug-2009	UpperLouetsi	130	male	-2.195633333	11.56141667
CU95191	6903	2009-031	15-Aug-2009	UpperLouetsi	106	juvenile	-2.195633333	11.56141667
CU95191	6904	2009-031	15-Aug-2009	UpperLouetsi	111	male	-2.195633333	11.56141667
CU95191	6905	2009-031	15-Aug-2009	UpperLouetsi	116.5	male	-2.195633333	11.56141667
CU95191	6906	2009-031	15-Aug-2009	UpperLouetsi	135.5	male	-2.195633333	11.56141667
CU95191	6907	2009-031	15-Aug-2009	UpperLouetsi	129	male	-2.195633333	11.56141667
CU95191	6908	2009-031	16-Aug-2009	UpperLouetsi	101	juvenile	-2.195633333	11.56141667
CU95191	6909	2009-031	15-Aug-2009	UpperLouetsi	76	juvenile	-2.195633333	11.56141667
CU95191	6910	2009-031	15-Aug-2009	UpperLouetsi	63	juvenile	-2.195633333	11.56141667
CU95191	6911	2009-031	15-Aug-2009	UpperLouetsi	43	juvenile	-2.195633333	11.56141667
CU95191	6912	2009-031	15-Aug-2009	UpperLouetsi	91	juvenile	-2.195633333	11.56141667
CU95191	6913	2009-031	15-Aug-2009	UpperLouetsi	-	ND	-2.195633333	11.56141667
CU95191	6914	2009-031	15-Aug-2009	UpperLouetsi	67	juvenile	-2.195633333	11.56141667

CUMV #	Voucher #	Locality #	Date	Locality	SL	Sex	Lat.	Long.
CU95191	6915	2009-031	15-Aug-2009	UpperLouetsi	69	juvenile	-2.195633333	11.56141667
CU95191	6916	2009-031	15-Aug-2009	UpperLouetsi	-	ND	-2.195633333	11.56141667
CU95191	6917	2009-031	15-Aug-2009	UpperLouetsi	60	juvenile	-2.195633333	11.56141667
CU95191	6918	2009-031	15-Aug-2009	UpperLouetsi	93	juvenile	-2.195633333	11.56141667
CU95191	6919	2009-031	15-Aug-2009	UpperLouetsi	68	juvenile	-2.195633333	11.56141667
CU95191	6920	2009-031	15-Aug-2009	UpperLouetsi	80	juvenile	-2.195633333	11.56141667
CU95191	6921	2009-031	15-Aug-2009	UpperLouetsi	115	male	-2.195633333	11.56141667
CU95191	6922	2009-031	15-Aug-2009	UpperLouetsi	90	male	-2.195633333	11.56141667
CU95191	6923	2009-031	15-Aug-2009	UpperLouetsi	74	juvenile	-2.195633333	11.56141667
CU95191	6924	2009-031	15-Aug-2009	UpperLouetsi	49	juvenile	-2.195633333	11.56141667
CU95191	6925	2009-031	15-Aug-2009	UpperLouetsi	92	male	-2.195633333	11.56141667
CU95191	6926	2009-031	15-Aug-2009	UpperLouetsi	89	juvenile	-2.195633333	11.56141667
CU95191	6927	2009-031	15-Aug-2009	UpperLouetsi	96.5	male	-2.195633333	11.56141667

APPENDIX 5: TEMPERATURE CORRECTION METHOD

Kramer and Westby (1985) determined in the mormyrid *Gnathonemus Petersen* that EODs durations are stretched and compressed due to temperature-dependent processes with a Q10 factor of 1.49. For all of our collections, water temperatures in the EOD recording chamber varied between 21.0-26.7˚C. Regrettably, a subset of our data (n=63) did not have valid temperature data at the time of recording. Because these specimens represented key localities in Gabon, we wished to include them in the present study. To justify their inclusion, we include here the description of a test to measure the effect of Q10 temperature correction on variation in the 21 variables measured. To accomplish this, we compare the principal component scores before and after Q10 temperature correction of a subset (n=491) of data for which temperature data was available.

We began by applying a the Q10 correction in the time measurements of these X EODs to the mean observed temperature (23.31˚C), using this Q_{10} value 1.49 (Kramer and Westby, 1985). We adjusted the EOD time base in each recording by multiplying the A/D digitizer's sampling rate by factor f, using the following equation:

$$f = 10^{\frac{25^{\circ}C - T_{obs}}{10}\log(Q_{10})}$$

Where Q_{10}=1.49 and T_{obs} corresponds to the temperature in the recording chamber at the time of EOD recording. Fig. A5a illustrates the effect of Q10 correction on EOD waveform shape to 23.31˚C (blue) from 26.1˚C (red), resulting in a perceivable compression of the EOD at the higher (corrected) temperature.

For each of the 491 temperature corrected EODs, we analyzed each using the methods described in the main text, extracting a vector of twenty-one measurements (see Table 3-2).

Again, using the MATLAB function *princomp*, we performed principal components analysis (PCA) on this set of temperature corrected EODs. The PCA resulted in a 21x21 factor-loading matrix, which was used to transform each of the 21 variable vectors (corresponding to each of the temperature corrected EODs) into principal component scores. We plotted the resulting 1st and 2nd principal component scores for this "temperature corrected" dataset as filled symbols, coloring each according to its collection locality and geographic region (Fig. A5 b). In order to compare the effect of Q10 temperature correction, the factor-loading matrix derived from PCA of temperature-corrected EODs was applied to the 21 variable vectors describing each of the 553 uncorrected EOD waveforms ("uncorrected data"). These transformed data are plotted as open symbols (Fig. A5b). A thin black line is plotted to aid in visualizing corresponding principal component scores between each dataset. Minimum area polygon boundaries enclose *the uncorrected* data plotted for individual localities, referred to by their local geographic name on the map in Fig S3b.

The shift of points in principal components space (Fig A5b) between uncorrected and corrected datasets is primarily along the horizontal axis (PC1), with little shift along the vertical axis (PC2). This corresponds to the compression or expansion of the waveform due to Q10 correction (and provides a good test that PC1, in fact, represents primarily duration). As can be observed in the figure, the length of the thin black lines, representing the displacement of each EOD in PCA space as a result of Q10 temperature correction, is small when compared to distances between individual points and between polygons enclosing populations.

To further emphasize this point, Euclidean distances were computed between all pairwise combinations of PCA points (1) in the uncorrected dataset, and (2) the corrected dataset. Euclidean distances between corresponding points in (1) and (2) were also calculated

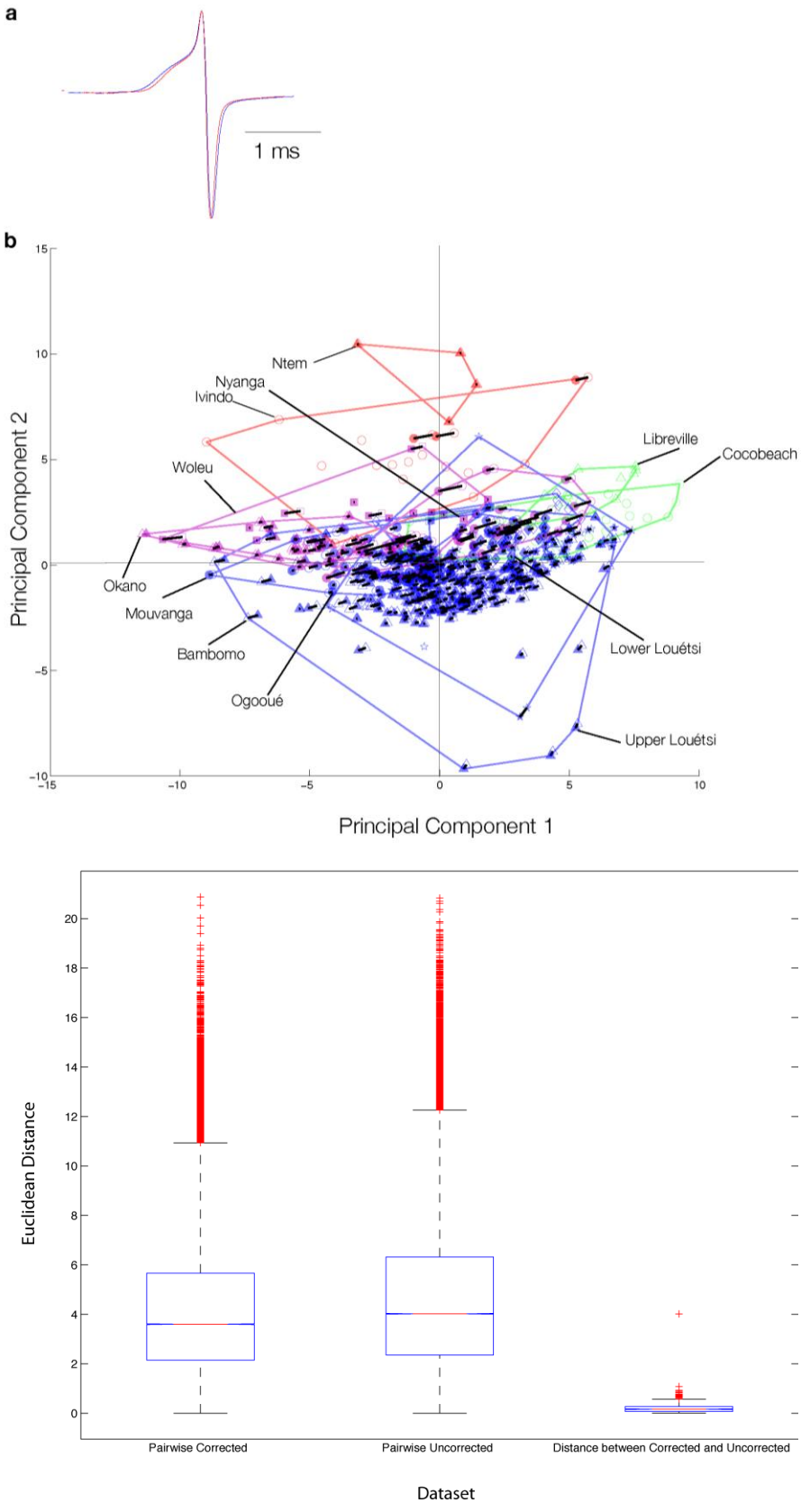
a
1 ms
b
Principal Component 2
Principal Component 1
Ntem
Nyanga
Ivindo
Woleu
Okano
Mouvanga
Bambomo
Ogooué
Libreville
Cocobeach
Lower Louétsi
Upper Louétsi
Euclidean Distance
Pairwise Corrected
Pairwise Uncorrected
Distance between Corrected and Uncorrected
Dataset

cc

(corresponding to the lengths of thin black lines in Fig S3b). The distribution of these distances is summarized in Fig A5c as box-and-whisker plots. This figure shows both that the distribution of pairwise distances between points did not change following temperature correction (distance 2 vs. 1, as described above), and that the displacement in PCA space due to temperature correction (distance 3, as described above) was much smaller than the differences between individuals (distances 3 vs. 1 and 2, as described above).

We conclude from these analyses that, while temperature correction does have a detectable effect on the duration of EODs in our PCA, this effect is negligible compared to the variation between individuals and localities sampled. We therefore, in the interests of including as much of our sampling efforts in Gabon in the present analysis, chose to proceed with our analysis of all EODs in this study without any temperature correction.